TUM School of Life Sciences

Trapping multiple dual mode liquid-liquid chromatography for the separation of intermediately-eluting components: A model-based design approach

Raena Jeanne Morley

Vollständiger Abdruck der von der
TUM School of Life Sciences
der Technischen Universität München zur Erlangung
einer Doktorin der Ingenieurwissenschaften (Dr.-Ing.)
genehmigten Dissertation.

Vorsitzende/-r: Prof. Dr. Michael Rychlik

Prüfende/-r der Dissertation:

1. Prof. Dr. Mirjana Minceva

2. Prof. Dr. Sonja Berensmeier

3. Prof. Dr.-Ing. Gerhard Schembecker

Die Dissertation wurde am 01.02.2021 bei der Technischen Universität München
eingereicht und durch die
TUM School of Life Sciences am 14.02.2022 angenommen.

Table of contents

Acknowledgements

Abstract

Solid support-free liquid-liquid chromatography (LLC) uses the two phases of a biphasic solvent system as the mobile and stationary phases, granting this preparative separation technique advantageous characteristics of both conventional chromatography (high selectivity) and liquid-liquid extraction (high sample loading) in addition to high process flexibility. The ability to switch the roles of the mobile and stationary phases during a separation run has allowed the development of a variety of operating modes unique to LLC. One such operating mode, trapping multiple dual mode (trapping MDM), can be used as an alternative to standard batch injections for ternary separations of intermediately-eluting target components. Such separations are regularly encountered in the expanding natural products sector in which LLC has found its niche. Despite its advantages, the use of a biphasic system as the mobile and stationary phases in LLC poses several design challenges as well. Changes to the thermodynamic or hydrodynamic equilibrium of the two phases in the column, caused by feed introduction or alterations in the process conditions, can affect both process stability and separation performance. Additionally, complex operating modes such as trapping MDM require rational approaches for the selection of multiple interdependent operating parameters.

To address these challenges, this thesis establishes a model-based design approach for trapping MDM separations under maximized-throughput conditions. Special focus is placed on the use of simple preliminary experiments (shake flask, phase volume ratio, settling time, and stationary phase retention measurements) to determine the limiting feed concentration and mobile phase flow rate for stable operation, as well as on process modeling approaches for rational selection of the set of five interdependent trapping MDM operating parameters (step durations during the Loading and Separation stages in the two elution modes, number of cycles). The process modeling approaches vary in complexity and involve a linear, ideal short-cut model for initial identification of the valid operating parameter space, followed by determination of the parameter set resulting in maximized throughput. Separation performance predictions are made using either the short-cut model or the more detailed equilibrium stage model, which takes non-ideal band broadening effects into account.

The model-based design approach was successfully applied to experimental trapping MDM separations of ternary mixtures of model components as well as to a complex natural product mixture obtained from an industrial side stream. The approach was also implemented in a thorough comparison study of trapping MDM and batch injection performance, resulting in helpful guidelines for operating mode selection. The investigations performed in this thesis demonstrate the high potential of trapping MDM for difficult ($\alpha \leq 1.3$) high-throughput separations of intermediately-eluting components. More broadly, the proven model-based design approach aids in lowering the barrier to the acceptance and implementation of LLC as a downstream processing technique in the natural products field and beyond.

Kurzzusammenfassung

In der Flüssig-Flüssig Chromatographie („liquid-liquid chromatography", LLC) werden beide Phasen eines zweiphasigen Lösungsmittelsystems als mobile und stationäre Phase verwendet. Dadurch werden die vorteilhaften Eigenschaften der konventionellen Chromatographie (hohe Selektivität) und der Flüssig-Flüssig-Extraktion (hohes Probenaufkommen) kombiniert. Die Möglichkeit, während des Betriebs die Rollen der mobilen und der stationären Phase zu wechseln, hat zu der Entwicklung einer Vielfalt an LLC-spezifischen Betriebsmodi geführt. Ein solches Beispiel ist der „trapping multiple dual mode" („trapping MDM"), der eine Alternative zu der standardmäßigen Verwendung von „batch injections" (chargenweisen Probeninjektionen) für die Auftrennung intermediär eluierender Zielkomponenten darstellt. Trotz vieler Vorteile bringt die Verwendung zwei flüssiger Phasen in LLC auch Herausforderungen in der Prozessauslegung mit sich. Eine Änderung des thermodynamischen oder hydrodynamischen Gleichgewichtes zwischen den zwei Phasen in der Säule, die durch das Einspeisen der Feedlösung oder Änderungen der Prozessbedingungen verursacht wird, kann sich auf die Stabilität des Prozesses und die Trennleistung auswirken. Zudem fordern komplexe Betriebsmodi wie „trapping MDM" rationale Vorgehensweisen für die Auswahl von mehreren zusammenhängenden Betriebsparametern.

Um diese Herausforderung zu bewältigen, wurde in dieser Arbeit ein modellbasierter Ansatz für Trennungen mit Hilfe von „trapping MDM" unter maximalen Durchsatzbedingungen entwickelt. In einfachen Vorversuchen wurden die limitierende Feedkonzentration und Durchflussrate der mobilen Phase für einen stabilen Betrieb bestimmt. Um die fünf voneinander abhängigen „trapping MDM"-Betriebsparameter auszuwählen, wurde ein zweistufiger Prozessmodellierungsansatz verwendet. Hierbei wurden zuerst die möglichen Parametersätze mit dem „short-cut" (Kurzverfahren) Modell, das auf den Annahmen der linearen und idealen Chromatographie basiert, identifiziert. Danach wurde der Parametersatz, der zum maximalen Durchsatz führt, entweder mit Hilfe des „short-cut" Modells oder des detaillierteren Gleichgewichtsstufenmodells, welches nicht-ideale Bandverbreiterungseffekte berücksichtigt, festgelegt.

Der modellbasierte Ansatz wurde erfolgreich auf die experimentelle Trennung ternärer Mischungen von Modellkomponenten mittels „trapping MDM" angewendet sowie auf ein komplexes Naturstoffgemisch gewonnen aus einem industriellen Nebenstrom. Dieser Ansatz wurde auch in einer umfassenden Vergleichsstudie über die Leistung von "trapping MDM" und „batch injections" angewendet. Die durchgeführten Untersuchungen dieser Arbeit zeigen das große Potential von „trapping MDM" bei schwierigen Trennungen ($\alpha \leq 1.3$). Darüber hinaus trägt die bewährte modellbasierte Vorgehensweise dazu bei, die Hürde für die Akzeptanz und Implementierung von LLC als Weiterverarbeitungstechnik zu senken.

1. Introduction

Solid-support free liquid-liquid chromatography (LLC), encompassing both countercurrent chromatography (CCC) and centrifugal partition chromatography (CPC), is a preparative separation technique combining characteristics of conventional liquid-solid chromatography and liquid-liquid extraction [1]. The result is a versatile and highly adaptable unit operation that can simultaneously exhibit high selectivity and high feed loadings. In LLC, the mobile and stationary phases are the two phases of a liquid-liquid biphasic system. Separation of a feed mixture is achieved owing to differences in feed solute partitioning between the two phases, which affect the propagation velocities of the solutes through the column. Either of the two phases of the biphasic system may be used as the stationary phase, which is held in place during operation in a specially-designed column by the application of centrifugal force. The other phase, used as the mobile phase, is pumped through the stationary phase. The roles of the two phases and the mobile phase flow direction may be simultaneously switched during operation, leading to a reversal of the elution order of feed solutes [2]. This unique characteristic of LLC has allowed for the development of several operating modes without a liquid-solid chromatography equivalent [3-6].

The use of the two phases of a liquid-liquid biphasic system as the mobile and stationary phases imposes several design challenges concerning their hydrodynamic and thermodynamic equilibria within the column during operation. At hydrodynamic equilibrium, the flow patterns of the two phases and the stationary phase volume retained in the column remain constant, leading to a constant degree of band broadening during the chromatographic process (i.e., efficiency). The hydrodynamic conditions in the column are dependent on the properties of the selected biphasic solvent system [7, 8], the column geometry [9, 10], and the operating parameters (e.g., mobile phase flow rate, column rotational speed [7], temperature [11]). Additionally, the mobile and stationary phases are subject to the thermodynamics of liquid-liquid equilibria, with the implication that a change in composition in one phase induces a change in the other. Compositional changes brought about by feed introduction or a change in the process conditions may be accompanied by alterations in the physical properties (e.g., density, viscosity, interfacial tension) and volume ratio of the phases, leading to altered flow patterns that impact the hydrodynamic equilibrium. This can cause operational instability, observed as stationary phase loss, as well as deviations from predicted solute retention and band broadening behavior, all of which can negatively impact separation performance [12-15]. Such unwanted effects are rarely reported, however, as they are generally part of the development phase and not included with the successful final results [14]. Mitigating disruptions of the thermodynamic and hydrodynamic equilibria is especially critical in the design of high-throughput preparative LLC separations, which are conducted at high flow rates and feed loadings of high volume and concentration. Since it is not yet possible to fully describe

9

the complex interplay of the operating parameters, the system thermodynamics and hydrodynamics, and their effects on stability and performance, preliminary experimental measurements must be used to determine practical operating parameter limits.

LLC is primarily used for the isolation of natural product compounds obtained from plant extracts [16, 17]. Given their natural origin, these crude or pre-purified extracts are often complex mixtures containing molecules of both similar and different sizes, structures, polarities, and degrees of hydrophobicity. The target component to be isolated commonly has an intermediate elution velocity relative to the other solutes in the mixture. This results in the need for a ternary separation strategy, i.e., separation of the earlier- and later-eluting components from the intermediately-eluting target. When using the standard batch injection operating mode with feed injection followed by isocratic elution with the mobile phase, overlap of neighboring impurities with the target component peak is often encountered, leading to reduced target purities and yields. An alternative LLC operating mode for difficult ternary separations in which the target and impurities exhibit low separation factors (α<1.5) is trapping multiple dual mode (trapping MDM). Trapping MDM takes advantage of the possibility to switch the roles of the mobile and stationary phases during operation. The intermediately-eluting target remains "trapped" on the column while becoming increasingly separated from its neighboring impurities during successive cycles of phase role switching and mobile phase flow direction reversal. Although trapping MDM can offer improvements in separation performance over batch injections, its increased complexity introduces several additional, interdependent operating parameters, complicating separation design. Using the inefficient design approaches based on user experience and trial-and-error that have long been the norm in LLC, it is nearly guaranteed that separation performance will be sub-optimal, if a successful separation is achieved at all.

Separation design in LLC is currently moving away from heuristic and trial-and-error based approaches toward more structured, rational strategies for operating parameter selection [17]. The development and implementation of thorough, model-based design approaches considering the particularities of LLC processes (i.e., the effects of the hydrodynamics and thermodynamics of the biphasic system on separation performance) are needed. Model-based design strategies have been applied for sequential centrifugal partition chromatography (sCPC), a continuous binary separation process, in [18, 19] and specifically for maximized throughput in [20]. By coupling preliminary experiments for determination of operating parameter limits with process models of varying degrees of complexity, model-based design approaches allow for streamlined operating parameter selection, prediction and optimization of separation performance, and the ability to perform comparison studies with process alternatives. The required level of model complexity will depend on the implementation. Simple short-cut models based on linear, ideal chromatography assumptions

10

are useful for identification of valid combinations of interdependent operating parameters and rudimentary predictions of process performance, whereas more detailed models taking band broadening effects into account [21] can provide a more accurate description of the separation. The implementation of advanced LLC operating modes with several interdependent parameters, such as trapping MDM, can greatly benefit from these model-based design approaches. The establishment and demonstrated effectiveness of such approaches will help further industrial acceptance of the LLC technique, for which demands of high process stability must be met under high-throughput conditions to ensure economic feasibility and consistent product quality.

This thesis focuses on the rational design of trapping MDM separations for the separation task most frequently encountered in natural product isolation: difficult ternary separations involving an intermediately-eluting target component under requirements of high throughput and high purity and yield. The objectives of this thesis are (1) to develop and validate a model-based design approach for trapping MDM operating parameter selection and (2) to further demonstrate the effectiveness and flexibility of this approach through its implementation in varying contexts, including throughput maximization and operating mode comparison studies. The relevant theory and background information is presented in Section 2, followed by the thesis results in the form of four publications in Section 3. A comprehensive discussion of the paper findings is conducted in Section 4. Overall conclusions are made in Section 5, followed by an outlook for related future investigations in Section 6.

2. Theory and background

This section includes an introduction to the principles of liquid-liquid chromatography (LLC) (Section 2.1) and the key characteristics of centrifugal partition chromatography (CPC) (Section 2.2). The LLC operating modes for ternary separations, batch injections and trapping MDM, are then described (Section 2.3). A presentation of the importance of considering the thermodynamics and hydrodynamics of the two-phase system during separation design follows (Section 2.4). Next, the LLC process modeling approaches relevant for this thesis are detailed (Section 2.5). Lastly, the model-based approach for the design of high throughput separations is described (Section 2.6).

2.1 Fundamentals of liquid-liquid chromatography

The equipment set-ups for conventional liquid-solid chromatography and LLC share the same basic elements: a pump system, an automated or manual feed injection port, a chromatography column, an online detection unit (e.g., UV-Vis), and a fraction collection unit. Different from liquid-solid chromatography, in place of a solid stationary phase and a liquid mobile phase that can be selected independently, the mobile and stationary phases in LLC are the two phases of a liquid-liquid biphasic system and are therefore chosen simultaneously. During an LLC separation, the total column volume, V_C, is occupied by the mobile and stationary phase volumes, V^M and V^S, respectively (Equation (1)).

$$V_C = V^M + V^S \tag{1}$$

The biphasic systems used in LLC are typically composed of three to four organic solvents. Solvent system families such as HEMWat (*n*-hexane/ethyl acetate/methanol/water) [22] and ARIZONA (*n*-heptane/ethyl acetate/methanol/water) [23] are widely used, as they generally provide sufficient stationary phase retention and offer a wide polarity range that can be tuned by altering the volumetric ratios of the four solvents according to published tables.

The stationary phase is held in place by the application of centrifugal force through column rotation while the mobile phase is pumped through it. Under conditions of hydrodynamic equilibrium, the flow patterns and stationary phase volume in the column remain constant. The stationary phase volume retained during operation is described by the stationary phase retention or stationary phase fraction, S_f (Equation (2)).

$$S_f = \frac{V^S}{V_C} \tag{2}$$

S_f is dependent on the column geometry, the physical properties of the mobile and stationary phases, and the operating parameters (e.g., mobile phase flow rate, rotational speed). This is a key difference to liquid-solid chromatography, in which the surface area of

the solid stationary phase available for interaction with the feed solutes is determined at the time of column packing and generally remains independent of the process conditions. Although an S_f of approximately 0.5 or higher is recommended to achieve satisfactory resolution, lower values may also be acceptable, depending on the difficulty of the separation [24].

In LLC, separation of a feed mixture is achieved due to the differing partitioning behavior of the feed solutes between the two liquid phases, resulting in different velocities with which they travel through the column with the mobile phase and arrive at the outlet. The affinity of a component k to the stationary phase is quantified by the partition coefficient (distribution constant), K_k, defined as the ratio of the concentrations in the stationary and mobile phases, c_k^S and c_k^M, at thermodynamic equilibrium (Equation (3)). At thermodynamic equilibrium, the temperature, pressure, and chemical potential of all chemical species (i.e., the solvents and feed solutes) are uniform throughout the two-phase system, meaning that the compositions of the two phases on a solute-free basis and the solute concentrations in the two phases remain unchanged with respect to time [25]. Consequently, the physical properties of the two phases (e.g., density, viscosity, interfacial tension) remain constant as well.

$$K_k = \frac{c_k^S}{c_k^M} \tag{3}$$

Next to high feed mixture solubility and satisfactory stationary phase retention, the partition coefficient serves as a key screening parameter in solvent system selection. Target compound partition coefficients in the so-called sweet spot range between 0.4 and 2.5 [22] are preferred when using the standard batch injection operating mode, as this provides a compromise between high resolution and fast separation. Up to a certain concentration, known as the linear range of the partition isotherm, a plot of c_k^S vs. c_k^M yields a linear curve. Within this range, solute partitioning can be considered independent of concentration and constant. As further discussed in Section 2.4.1, operation within the linear range is preferred in LLC, differing from preparative liquid-solid chromatography separations typically conducted in the non-linear range.

Either phase of the biphasic system, the less-dense upper phase or denser lower phase, may be used as the stationary phase. This results in two possible elution modes. In the ascending (As) elution mode, the lower phase is stationary and the upper phase mobile; in the descending (Des) elution mode, the upper phase is kept stationary and the lower phase is used as the mobile phase. When switching from one elution mode to the other, the mobile phase flow direction must be reversed. The partition coefficient definitions with respect to the stationary and mobile phases of the Des and As modes are given by Equation (4), with the superscripts U and L referring to the upper and lower phases.

$$K_{Des,k} = \frac{c_k^U}{c_k^L} = \frac{1}{K_{As,k}} \tag{4}$$

It is seen that the partition coefficient values for a component k in the two elution modes are inversely related. Therefore, for two components A and B with $K_{Des,A} < K_{Des,B}$ in Des mode, switching to As mode results in $K_{As,A} > K_{As,B}$. Accordingly, A has the highest velocity and elutes first in Des mode; in As mode, B moves fastest and elutes first from the opposite end of the column, as the mobile phase flow direction is reversed as well.

The difficulty of a separation can be quantified by the separation factor (selectivity), $\alpha_{k,l}$, where $K_k \geq K_l$ (Equation (5)). The greater the separation factor, the easier the separation, i.e., it can be achieved at lower theoretical stage numbers (further described below). A separation is no longer thermodynamically possible at a separation factor of unity.

$$\alpha_{k,l} = \frac{K_k}{K_l} \tag{5}$$

In LLC, solute retention is often described using retention volumes, $V_{R,k}$, instead of retention times, $t_{R,k}$. Both terms are used in this thesis. Under linear (i.e., K_k independent of solute concentration), ideal chromatography conditions (i.e., neglecting band broadening due to axial dispersion and mass transfer resistance, instantaneous partition equilibrium), and with F as the mobile phase flow rate, $V_{R,k}$ and $t_{R,k}$ can be calculated using Equation (6). A detailed derivation of $V_{R,k}$ is found in Appendix A.

$$V_{R,k} = F t_{R,k} = V^M + K_k V^S \tag{6}$$

The propagation velocity of solute k, v_k, is given by Equation (7).

$$v_k = \frac{F}{V_{R,k}} \tag{7}$$

The position of the band front (front of solute concentration profile inside the column) of solute k as a fraction of the column "length", x_k, is related to the velocity, v_k, and elapsed time since injection, t, according to Equation (8).

$$v_k t = x_k \tag{8}$$

The band front positions and propagation velocities calculated for linear, ideal LLC play an integral role in the derivation of the short-cut models described in Section 2.5.1.

The retention volume equation (Equation (6)) can be alternatively expressed in terms of the stationary phase fraction (Equation (9)).

$$V_{R,k} = V_C \left[1 + S_f (K_k - 1) \right] \tag{9}$$

From inspection of Equation (9), it is seen that an increase in S_f leads to an increase in $V_{R,k}$ when $K_k > 1$, and a decrease when $K_k < 1$. When $K_k = 1$, the retention volume is equal to the column volume, V_C, and independent of S_f. Therefore, an increase in S_f cannot be generalized as resulting in an improved separation.

Under the non-ideal conditions of a real separation, band broadening resulting from axial dispersion and mass transfer resistance occurs, resulting in dispersed elution profiles. The degree of band broadening undergone by a solute k can be described by the efficiency, N_k, also known as the number of theoretical plates or stages. N_k is the equivalent number of hypothetical stages at which the thermodynamic partition equilibrium of the solute between the two phases is obtained during a separation run. High column efficiencies are preferred, corresponding to narrow, less dispersed elution profiles and, as a result, less detrimental overlap of target and impurities at the outlet. Whereas N_k values in the thousands are common in liquid–solid chromatography, only hundreds of theoretical plates are typically encountered in LLC. Satisfactory separations are nevertheless possible due to the extremely high ratio of stationary phase available for solute interaction to mobile phase compared to that of liquid-solid chromatography [26].

N_k is experimentally determined from elution profiles obtained from pulse injections performed at low feed concentrations (i.e., in the linear range of the partition isotherm) and low injection volumes. When $N_k>100$ and dispersion attributed to off-column volumes is negligible, pulse injections are expected to result in Gaussian elution profiles (peaks) [27]. N_k is then related to the variance, σ_k, and the retention time, $t_{R,k}$, which is equivalent to the peak maximum, by Equation (10).

$$N_k = \left(\frac{t_{R,k}}{\sigma_k}\right)^2 \qquad (10)$$

2.2 Centrifugal partition chromatography

There exist two main column types in LLC: countercurrent chromatography (CCC) and centrifugal partition chromatography (CPC) columns. All experimental trapping MDM separations in this thesis were performed using CPC. CPC columns have a single axis of rotation, subjecting the mobile and stationary phases to a constant, time-independent centrifugal field. Mixing and mass transfer between the two phases takes place within small geometrical volumes referred to as cells. The cells are connected in series by narrow channels through which the mobile phase flows. A CPC column, also called a rotor, consists of a set of stacked stainless-steel disks from which the cells and channels have been cut. Disks are separated by Teflon sheets. Each disk contains an inlet and outlet aligned with corresponding perforations in the Teflon sheets to allow flow of the mobile phase from one disk to the next. A representative illustration of the CPC disks and sheets is found in Figure 1. Figure 2 depicts a fully assembled CPC rotor.

16
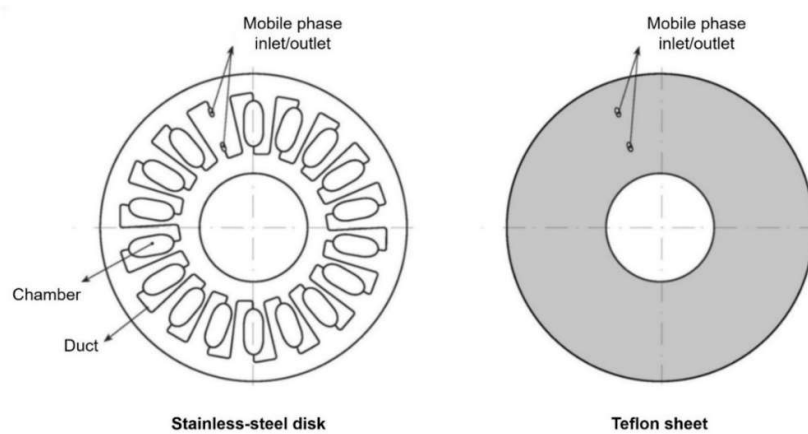
Figure 1. Disks and sheets of a centrifugal partition chromatography column.
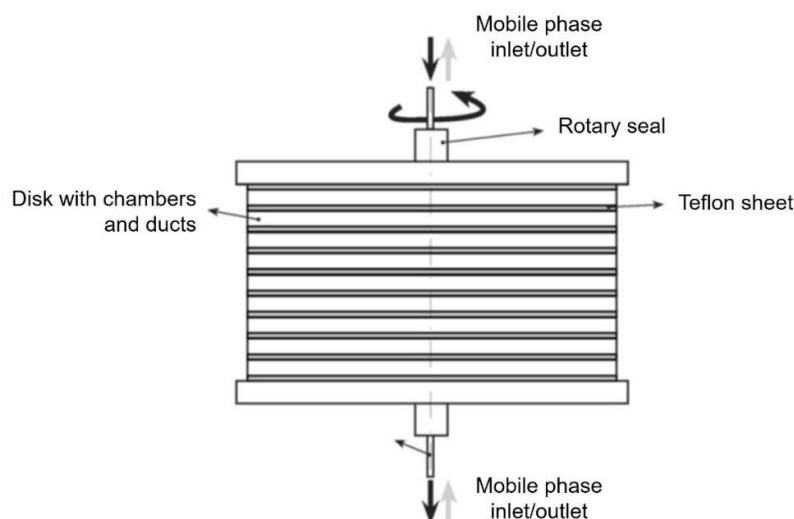
Figure 2. Assembled centrifugal partition chromatography column (rotor).

The CPC design was first reported in the early 1980s following the development of reliable rotary seal joints [28], which ensure leak-proof connection of the mobile phase inlet and outlet tubes to the column at high rotational speeds. CPC columns with volumes between 25 ml and 18 l are currently available [29, 30]. Larger CPC columns up to 25 l consisting of cartridge-like cells with the ability to process kilograms of crude extract per day have also recently entered the market [31].

The two LLC elution modes, ascending (As) mode and descending (Des) mode, are depicted for CPC in Figure 3. In As mode, the mobile upper phase is pumped through the lower stationary phase in the cells in the radial direction, toward the axis of rotation. The opposite is the case in Des mode, in which the lower phase is used as the mobile phase and is pumped through the less dense stationary upper phase, away from the axis of rotation.
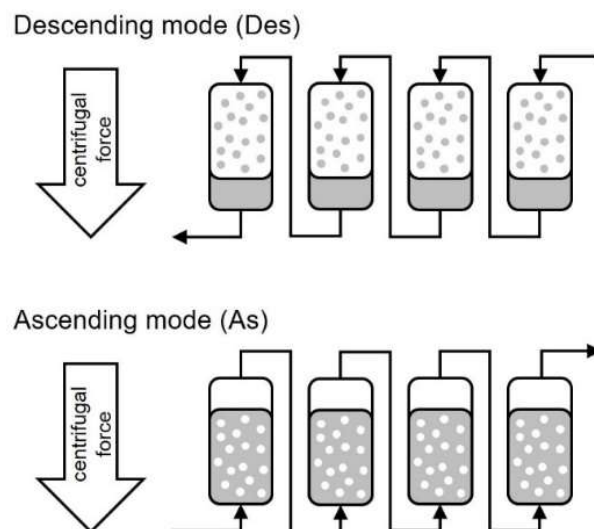
Figure 3. Descending and ascending elution modes in centrifugal partition chromatography. White shading: upper phase. Gray shading: lower phase.

2.3 Operating modes for ternary separations

The preparative separation of natural products from complex starting mixtures often involves the isolation of an intermediately-eluting compound. Such a target has an intermediate partition coefficient and may exit the column between potentially hundreds of earlier- and later-eluting compounds. To simplify the description and design of the separation process, it is often sufficient to represent the mixture by two or three solutes of interest: the target component and main impurities. This reduces the complex mixture to a pseudo-ternary one (see depiction in Figure 4).
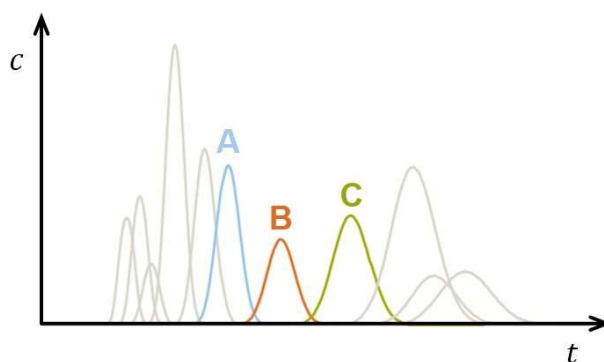
Figure 4. Representation of a complex multi-component mixture as a pseudo-ternary mixture of target component B and neighboring impurities A and C.

The two operating modes for ternary separations in LLC, batch injections (Section 2.3.1) and trapping MDM (Section 2.3.2) are described for simplified mixtures of three

components, A, B, and C, with relative partition coefficient values $K_{Des,A} < K_{Des,B} < K_{Des,C}$ in Des mode and $K_{As,A} > K_{As,B} > K_{As,C}$ in As mode. B is the intermediately-eluting target.

2.3.1 Batch injections

Batch injections consist of a single, discontinuous injection of the feed followed by isocratic elution with the mobile phase in As or Des mode. The feed is typically dissolved in the corresponding mobile phase of the elution mode. The batch injection operating mode is depicted in Figure 5.

A minimum separation factor of 1.5 between the target and nearest-eluting impurities is recommended for successful batch injection separations [24]. Although batch injections have the advantage of being easy to implement and typically possible on all CPC units, elution profile overlap often occurs under the high feed volume loading conditions desired for preparative separations. When high purities are required, low injection volumes or heart-cutting of the target fraction becomes necessary, to the detriment of the throughput and the product yield, respectively.
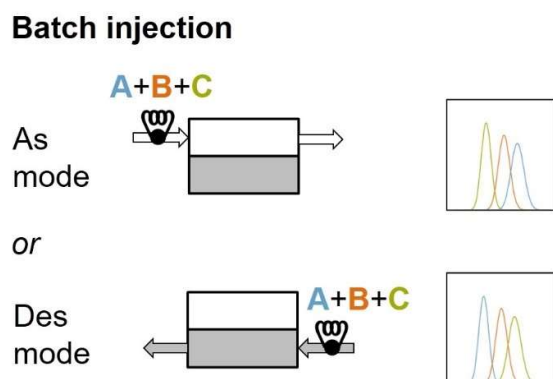
Figure 5. Batch injection operating mode. White shading: upper phase. Gray shading: lower phase.

Column hardware permitting, several process options can be implemented to help overcome the performance limitations of batch injections, such as elution extrusion mode [32-34], narrowly-timed stacked injections [35-37], closed-loop recycling of the mobile phase effluent [38-40], and reinjection of the heart-cut fraction with the same [41-43] or a different solvent system [44-46]. All of these have certain limitations and drawbacks, however, and are not particularly well-suited to the tandem goals of high feed loading and fast separation. Trapping MDM can be a useful alternative to these batch injection variations when faced with difficult ternary separations of complex mixtures.

2.3.2 Trapping multiple dual mode

Trapping MDM is a discontinuous operating mode for the separation of intermediately-eluting target compounds from (pseudo-)ternary mixtures. High throughput separations at low selectivities are made possible by a virtual "lengthening" of the column achieved by performing multiple cycles of alternating As and Des steps. Trapping MDM is performed on a CPC set-up consisting of two identical columns mounted on separate rotors and connected in series. The set-up also includes two mobile phase pumps, two feed solution pumps, two UV-Vis detectors, and two fraction collectors. One of each pair of pumps, detectors, and fraction collectors is active at a time, depending on the elution mode (As or Des). In trapping MDM, the feed pumps introduce the feed between the two columns in the flow direction corresponding to the elution mode. Additional details regarding the CPC set-up used in the investigations of this thesis are found in Appendix B.

The trapping MDM process consists of three stages, as depicted in Figure 6: Loading, Separation, and Recovery. During the Loading stage, pre-determined volumes of the feed solutions dissolved in the upper and lower phases are introduced between the two columns in the corresponding elution mode during a single cycle. The As and Des feed solutions are prepared by allowing the starting mixture to mix with and equilibrate between the two phasesin a single vessel, before being split into separate reservoirs. In the second stage, Separation, multiple cycles are performed, each consisting of one As and one Des step. Pure mobile phase (upper phase in As mode; lower phase in Des mode) is pumped from the corresponding inlet at one end of the two-column unit. The Separation stage step durations are selected with respect to those of the Loading stage to prevent the target B from reaching either outlet. Meanwhile, with each cycle components A and C experience a net movement toward the Des and As mode outlets, respectively, increasing their degree of separation from B. During Separation, A and C may elute from the column outlets completely, partially, or not at all. Once a satisfactory degree of separation of A and C from B is reached, the Recovery stage is started. A single elution mode step performed in As or Des mode allows B to be collected in purified form and any remaining portions of the A and C solute bands to leave the column completely.

Trapping multiple dual mode (trapping MDM)

(1) Loading

A+B+C

As mode

Des mode

A+B+C

(2) Separation

C

A

(3) Recovery

B
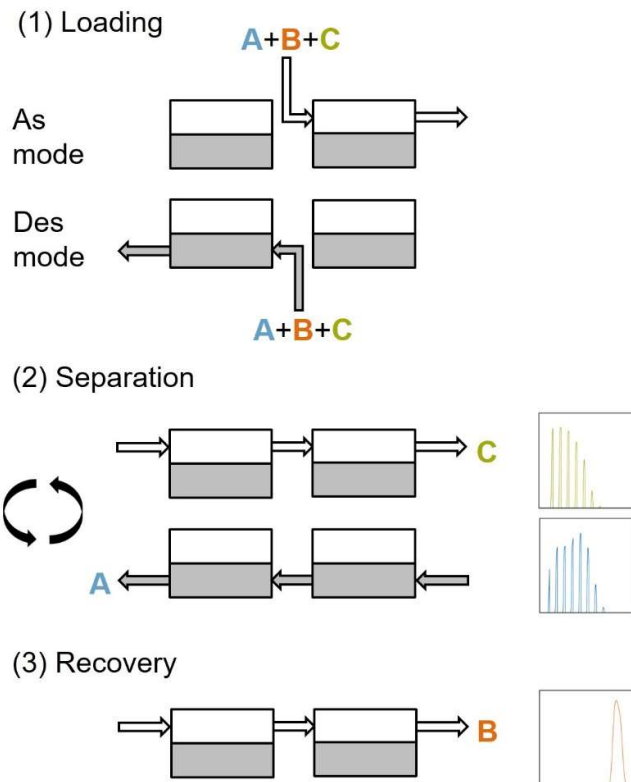
Figure 6. Trapping multiple dual mode process for the separation of an intermediately-eluting target (B) from a ternary feed mixture (A, B, and C). White shading: upper phase. Gray shading: lower phase.

As in other flow reversal operating modes (e.g., sCPC), a solvent system in which the target has a partition coefficient close to unity is preferred. This allows for selection of As and Des steps of similar duration, leading to similar solvent consumption in both elution modes [19, 47]. A pre-set 50/50 ratio of the upper and lower phases is also recommended, as this corresponds to an S_f of 0.5 [48] and similar column efficiency in both elution modes when the mobile phase flow rates are the same [19]. Step durations should additionally be as long as possible to avoid excessive valve wear and to subject the feed solutes to a high number of theoretical stages in each cycle [19]. Achievement of a successful trapping MDM separation hinges on appropriate selection of the Loading and Separation stage step durations, as well as the number of Separation stage cycles. Given the interdependent nature of these parameters, it is unlikely that a trial-and-error selection approach will produce a viable separation.

2.4 Considerations for preparative separation design

Viewed as a preparative separation technique for use in industrial settings, the design of LLC separations aims to maximize throughput, i.e., the amount of feed processed per unit time, while simultaneously ensuring stable, predictable operation. These objectives lay in opposition to each other, since high feed loading and fast separation conditions can adversely affect performance, whereas conservative parameter selection prioritizing stable operation is not conducive to obtaining high throughput. The goal is therefore to identify the maximum feed concentration and flow rate at which the process stability and predictability are not compromised by, e.g., stationary phase loss. This requires consideration of the interdependent effects of multiple parameters on the system thermodynamics and hydrodynamics, described in Section 2.4.1 and Section 2.4.2, respectively. These interdependencies are illustrated by the flow diagram in Figure 7.
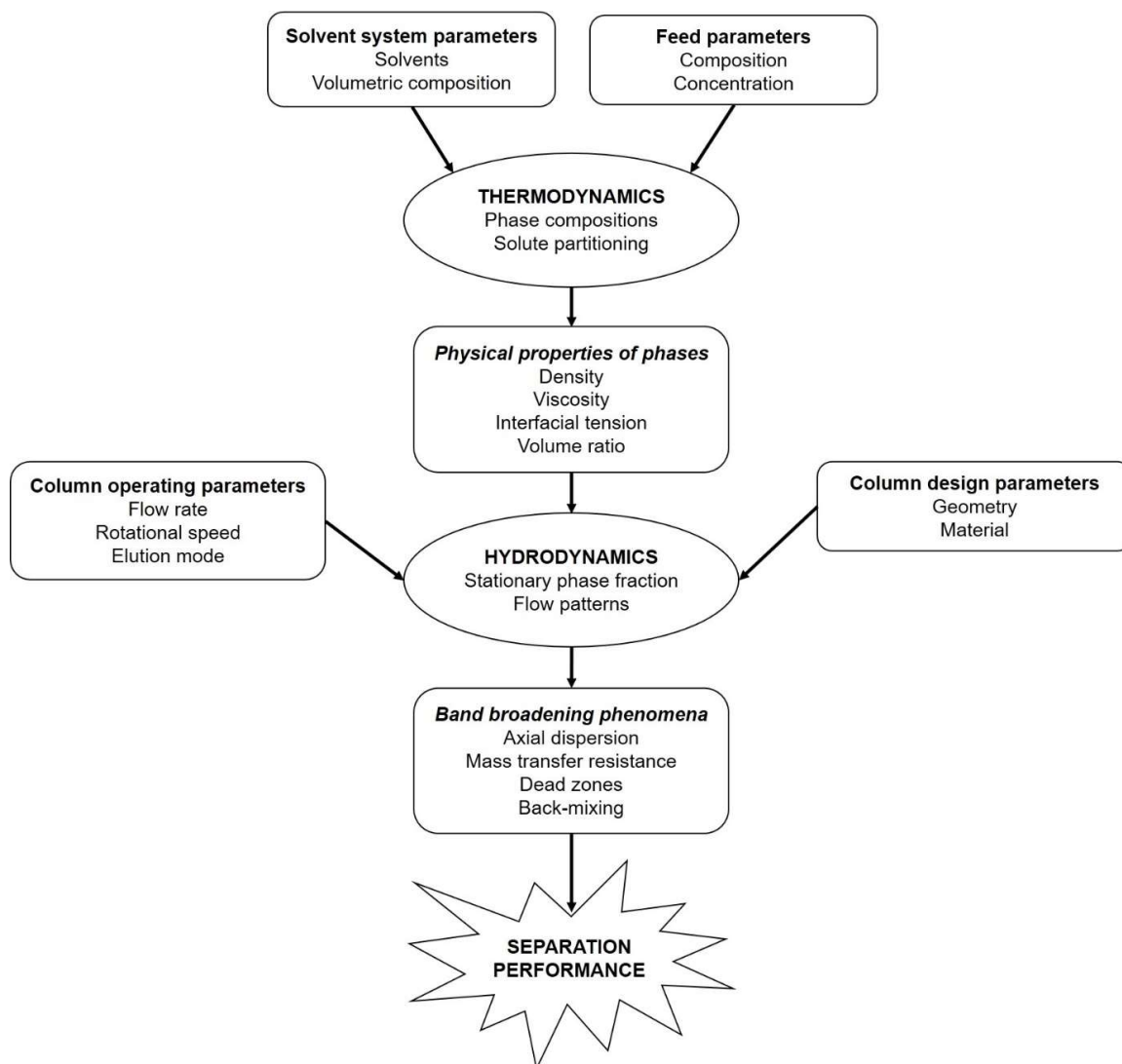
Figure 7. Interdependent effects of operating parameters, thermodynamic and hydrodynamic conditions, and physical phenomena on separation performance.

22

2.4.1 Thermodynamics

Following column preparation with the selected solvent system at the desired S_f, the mobile and stationary phases in the column are assumed to be at thermodynamic and hydrodynamic equilibria prior to feed introduction. From an LLC process standpoint, the original thermodynamic equilibrium is maintained when the compositions of the phases on a solute-free basis remain constant. High solute concentrations in the feed can give rise to solute-solute and solute-solvent interactions, leading to variations in phase composition and solute partition equilibria [49]. Above a certain solute concentration, partition equilibria and the resulting partition coefficients can no longer be considered independent of concentration nor constant, i.e., a departure from the linear range of the partition isotherm occurs. As changes in phase composition are accompanied by changes in solute partitioning, it follows that partition coefficient measurements can be used as an indirect indication of preservation of the thermodynamic equilibrium of the system.

In addition to feed introduction, changes in temperature can also affect the phase equilibria, their physical properties, and solute partition equilibria [11, 50-52]. Therefore, separation conditions should be kept as close to isothermal as possible, through temperature control of the mobile phase, feed solution, and the column unit. Temperature effects were not investigated within the scope of this thesis.

Changes in the phase compositions resulting from presence of the feed solutes or temperature changes can alter the physical properties of the two phases (e.g., density, viscosity, interfacial tension) as well as the phase volume ratio [49], especially when working with solutes that primarily partition into one phase. These changes can, in turn, affect the hydrodynamics and the outcome of the separation, as described in Section 2.4.2. When the physical properties of the feed solution (typically prepared in the mobile phase) substantially differ from that of the solute-free mobile phase, the injected feed behaves as a third phase that is not in thermodynamic equilibrium with the two phases of the solvent system. This unequilibrated state can lead to considerable or, when feed injection leads to miscibility of the mobile and stationary phases, even complete stationary phase loss [14].

LLC separations are therefore preferably performed in the linear partition isotherm range [53]. In addition to improved process stability gained at lower feed concentrations, this allows application of the linear chromatography assumption, greatly simplifying process modeling and performance prediction. Given the volumetric nature of solute partitioning in LLC, linear range operation is far less detrimental to process throughput than in liquid-solid chromatography separations at similar scale, in which only the stationary phase surface is available for solute adsorption. For comparison, the upper feed concentration limit of the linear partition isotherm can be up to approximately 100 mg ml^{-1} in LLC, whereas for silica-packed or reversed phase solid stationary phase columns the upper limit is typically only a few mg ml^{-1}

[54]. However, the precise limits are highly dependent on the solvent system and feed. Reports of experimental determination of the linear range appear only sporadically in the LLC literature [55-57].

In liquid-solid chromatography, non-linear adsorption isotherm data are often fit to standard mathematical models (e.g., Langmuir) for use in process modeling. In such adsorption isotherm models, the mobile and stationary phase compositions are considered independent of solute concentration, an assumption that cannot be applied in LLC. In liquid-liquid extraction, changes in phase compositions and solute partitioning induced by solute concentration can often be simultaneously described using a ternary diagram with the two solvents and the target solute as the three components. In LLC, the solvent system alone often consists of three or four solvents, and at the very minimum two feed solutes are of interest for the description of the process. Currently, a complete representation of the liquid-liquid equilibrium of all solvents and solutes would be highly complex and time-consuming task.

2.4.2 Hydrodynamics

Whereas the information in Section 2.4.1 is applicable to both CCC and CPC separations, the vastly different geometries and constructions of the two column types renders the following only applicable to CPC. In CPC, the hydrodynamic equilibrium state is defined by the flow patterns, namely mobile phase dispersion and coalescence, as well as back-mixing and dead zones in the stationary phase, and the resulting stationary phase retention [58]. Hydrodynamic equilibrium is reached within a cell when the mobile phase residence time and the necessary settling time (also called coalescence time; not equivalent to off-column settling time measurements) are equal [59]. The overall stationary phase fraction in the column remains constant, i.e., no stationary phase loss occurs. Three parameter categories affect the CPC hydrodynamics: the column parameters (cell geometry, cell material), the physical properties of the biphasic solvent system (density, viscosity, interfacial tension, phase volume ratio; including any changes caused by introduction of the feed), and the operating parameters (rotational speed, flow rate, elution mode) [60, 61].

For high separation performance, it is desired to have a strong degree of dispersion of the mobile phase in the stationary phase in the form of fine droplets at the cell inlet, creating a large interfacial area for mass transfer. Since mass transport supplies the main contribution to band broadening in CPC [61-63], changes in the interfacial area arising from changes in flow patterns and regimes can have a marked effect on separation performance. At the cell outlet, fast coalescence of the mobile phase should occur to prevent stationary phase loss through carryover of entrained droplets from one cell to the next. High stationary phase fractions (S_f >0.5) are generally preferred, as they often result in better resolution [52].

24

Undesirable flow patterns, on the other hand, can have a detrimental effect on separation performance. Stationary phase back-mixing caused by the Coriolis force [7] and the presence of dead zones in which little to no phase mixing takes place [52] can lead to increased band broadening and retention time shifts [63]. Additionally, off-column (periphery) volumes should be kept as low as possible to prevent additional band broadening as a result of axial dispersion in the mobile phase [61, 64].

Column parameters

The size and shape (geometry) of the CPC cells and channels as well as their material greatly contribute to the obtained hydrodynamic equilibrium. Ideally, the geometry of the cell inlet should promote mobile phase dispersion and that of the outlet mobile phase coalescence. Differences in wettability of the cell and channel walls, especially at the inlet, can also greatly affect flow patterns and dispersion [9, 52]. Several investigations comparing separation performance between different CPC column types and geometries have been performed [10, 59, 65]. Somewhat recently, computational fluid dynamics modeling has been implemented in cell design [9, 59]. The column geometry and construction of the CPC set-up determines the maximum allowable column pressure drop, which poses a limitation on the operable range of flow rates and rotational speeds for a certain solvent system. The characteristics of the column best-suited to a particular separation task will depend on the properties of the solvent system to be used and the difficulty of the separation to be performed.

Operating parameters

Both high rotational speeds and flow rates are generally beneficial for efficiency because they lead to high mobile phase dispersion and therefore a greater interfacial area for mass transfer. Neither can be increased indefinitely, however, due to an accompanying pressure drop increase across the column [66, 67]. In the case of increasing flow rate, the associated decrease in stationary phase retention must be considered as well. S_f decreases at higher flow rates due to the mobile phase entering the coalescence zone near the outlet with a high velocity, which can lead to stationary phase entrainment in the mobile phase as it flows to the next cell. The residence time also decreases with an increase in flow rate, and the stationary phase fraction must decrease accordingly to restore the balance between residence time and coalescence time [7]. Multiple studies have reported that there is no further increase in N_k or S_f above a certain rotational speed, [19, 59, 61, 68, 69]. Therefore, especially for solvent systems of medium stability, such as those of the ARIZONA and HEMWat families, it is recommended to determine a fixed rotational speed offering a compromise between column pressure drop, stationary phase retention, and efficiency. The flow rate is then varied as an independent parameter in the separation design [7].

When switching from one elution mode (Des or As) to the other, a change in flow pattern and stationary phase retention behavior occurs due to the switch of the roles of the mobile and stationary phases and the flow direction, leading to the establishment of a new hydrodynamic equilibrium state [52]. When switching between elution modes, such as during a trapping MDM separation, the flow rates should be selected to prevent any stationary phase loss (i.e., to maintain a constant ratio of the upper and lower phases in the column).

Physical properties

As touched upon in Section 2.4.1, the phase compositions determined by the liquid-liquid equilibria of the solvents (and feed solutes) influence the physical properties of the two phases, including density, viscosity, interfacial tension, as well as the volume ratio of the two phases. Since they affect the dispersion and coalescence behavior of the phases, these physical properties will in turn affect the hydrodynamics.

Solvent system stability, that is, the ability to obtain a high stationary phase fraction at high flow rates, has been found to be dependent on the ratio of the interfacial tension and the density difference between the phases, $\gamma/\Delta\rho$ [7, 70]. Moderate values of $\gamma/\Delta\rho$ are preferred for a compromise between high stationary phase retention and high column efficiency. The viscosity ratio between the phases was also demonstrated to be a useful estimate of system stability [7].

A disruption of the hydrodynamic equilibrium may occur following feed introduction at high concentrations or volumes when the physical properties of the feed solution differ greatly from those of the pure phases of the solvent system. For example, stationary phase loss may be observed when possible surfactant properties of the feed solutes lead to large alterations in interfacial tension, or when relative density differences between the feed and stationary phase may not allow for normal As or Des mode operation [14]. The occurrence and magnitude of these detrimental effects will depend on the specific characteristics of the feed solution and the selected solvent system and cannot be easily generalized or predicted.

2.5 Process modeling

As in conventional chromatography, there exists a wide range of modeling approaches for the description of LLC separation processes taking varying degrees of mechanistic detail into account and representing the column in different manners. A non-exhaustive list includes ideal models [32, 47, 71], non-equilibrium-dispersion/transport-dispersion [61-63] and equilibrium-dispersion [72] models, and non-equilibrium stage [73] and equilibrium stage models [18, 72, 74, 75]. All models in the LLC literature assume constant S_f and linear conditions, the reasons for which are elaborated in Section 2.4.1. The work in this thesis is primarily focused on the design and modeling of trapping MDM through implementation of an

26

ideal short-cut model (Section 2.5.1) with or without additional, more detailed simulations using the equilibrium stage model (Section 2.5.2).

2.5.1 Short-cut models (linear, ideal)

The ideal model, also known as the (plug flow) equilibrium model, neglects any hydrodynamic and kinetic effects on dispersion. The separation is influenced only by convection of the solutes with the mobile phase and the thermodynamics, described by solute partition isotherms. The linear, ideal representation of LLC processes forms the basis of the short-cut models and design equations collected in a review article written by the thesis author and included in Appendix C. Short-cut models are often sufficient for initial operating parameter selection in LLC, even for more complicated processes such as elution extrusion [32] and continuous binary separation separations with sequential centrifugal partition chromatography (sCPC) [71]. The ideal model-based triangle theory that has become indispensable in the design of multi-column simulated moving bed processes in liquid-solid chromatography is another powerful example [76-78].

The ideal chromatography assumption ignores any effects of axial dispersion, mass transfer resistance, and non-ideal flow patterns on solute band broadening. The column is considered to be infinitely efficient ($N_k \rightarrow \infty$), and all solute bands have infinitely steep concentration boundaries, i.e., they are identical to the ideal feed injection profile and travel unaltered through the column [79]. Local equilibrium between the mobile and stationary phases is permanently established [27]. These simplifications allow the derivation of LLC short-cut models based on the retention volume equation and time-dependent band front positions in the column (see Section 2.1, Equations (6)-(8)). The resulting model equations do not require a numerical solver, making short-cut models an easily-accessible design tool, even for those without process modeling expertise.

The trade-off to the simplicity of short-cut models is that the ideal chromatography assumption can lead to over-estimation of purities and yields achieved under real process conditions. Parameter safety margins can be applied compensate for band overlap resulting from dispersive effects. However, the magnitude of this margin necessary to ensure the required performance will be dependent on the particularities of the separation. More detailed models should be used when higher performance prediction accuracy is needed.

2.5.2 Equilibrium stage models (linear, non-ideal)

In the equilibrium stage model, originally developed by Martin and Synge [53], an approximation of the column is established by its representation as a finite number of identical equilibrium stages connected in series (the model assumptions are listed in Appendix D). Band

broadening effects due to axial dispersion and mass transfer resistance are described by a single parameter: the number of stages, N_k. Compared to the short-cut models, the equilibrium stage model provides a more accurate description of the process under non-ideal conditions and therefore better predicts separation performance, e.g., purity, yield, productivity. Despite using a single parameter to quantify all dispersive effects contributing to band broadening, differences in elution profiles of liquid-solid chromatography processes obtained using more detailed models are negligible when N_k>100 [27]. The use of the equilibrium stage model under the linear chromatography assumption has been frequently reported in the LLC literature [18, 72, 75, 80, 81].
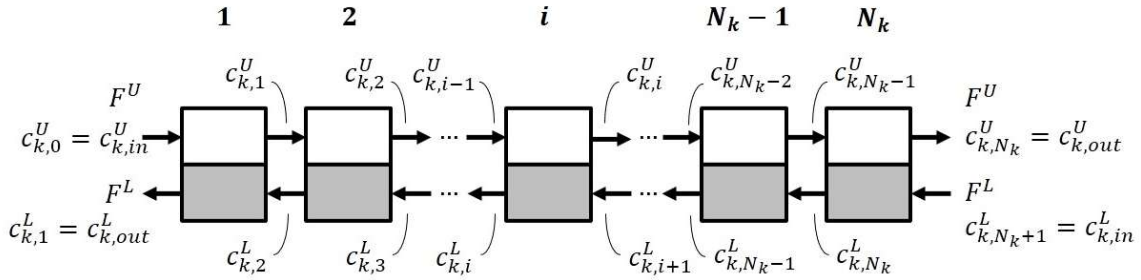
Figure 8. Equilibrium stage model representation of a liquid-liquid chromatography column. As and Des elution modes depicted simultaneously. White shading: upper phase. Gray shading: lower phase.

The mass balance around the ith equilibrium stage (see Figure 8), independent of elution mode, is given by Equation (11).

$$\frac{V^U}{N_k}\frac{dc_{k,i}^U}{dt} + \frac{V^L}{N_k}\frac{dc_{k,i}^L}{dt} = F^U\left(c_{k,i-1}^U - c_{k,i}^U\right) + F^L\left(c_{k,i+1}^L - c_{k,i}^L\right) \tag{11}$$

with $k = 1 \dots n$, where n is the total number of solutes to be modeled and $i = 1 \dots N_k$. For each solute k, a set of N_k ordinary differential equations must be solved at each time t, typically with a numerical solver. Before the start of a separation, the entire system is free of solutes. The batch injection initial and boundary conditions in the two elution modes are listed in Appendix D. Applying these conditions, Equation (11) can be rewritten for the As and Des modes as Equation (12) and Equation (13), respectively. As further described in Section 2.6, for a certain component, differing values of N_k are often encountered in the two elution modes as a result of differences in hydrodynamics and solute retention behavior. With appropriate selection of the initial and boundary conditions, other operating modes, such as trapping MDM, can also be modeled.

$$\frac{dc_{k,i}^U}{dt}\left(\frac{V^U}{N_k} + K_k^{As}\frac{V^L}{N_k}\right) = F^U\left(c_{k,i-1}^U - c_{k,i}^U\right) \tag{12}$$

$$\frac{dc_{k,i}^L}{dt}\left(\frac{V^U}{N_k}K_k^{Des} + \frac{V^L}{N_k}\right) = F^L\left(c_{k,i+1}^L - c_{k,i}^L\right) \tag{13}$$

28

2.6 Model-based design approach

Accurate prediction of the interdependent and cumulative effects of all LLC parameters on separation performance (see Section 2.4) is currently not possible. Recent CPC studies have used flow visualization experiments and dimensional analysis to describe mobile phase dispersion [82], mobile phase coalescence [58], and stationary phase retention [8], primarily with respect to phase physical properties and operating parameters. The resulting correlating functions represent a promising approach for predicting hydrodynamic conditions on a solute-free basis. However, further investigation is necessary to evaluate and improve the generality of these findings with respect to, e.g., different solvent systems and column geometries. The effects of feed introduction, which were not addressed, should also be explored.

Therefore, at present, a simplified design strategy for achieving the preparative separation goal of high throughput is needed. Only a handful of reports regarding throughput maximization are currently found in the LLC literature, studying the effects of feed volume [81, 83], concentration [14, 83], and flow rate [13]. However, all addressed batch injections only. A comprehensive, model-based design approach for throughput maximization was first presented in [20] and applied to continuous binary separations with sCPC. A similar approach, adapted to trapping MDM, is developed and implemented in this thesis. The design steps are summarized in the flow diagram in Figure 9 and described in the following.
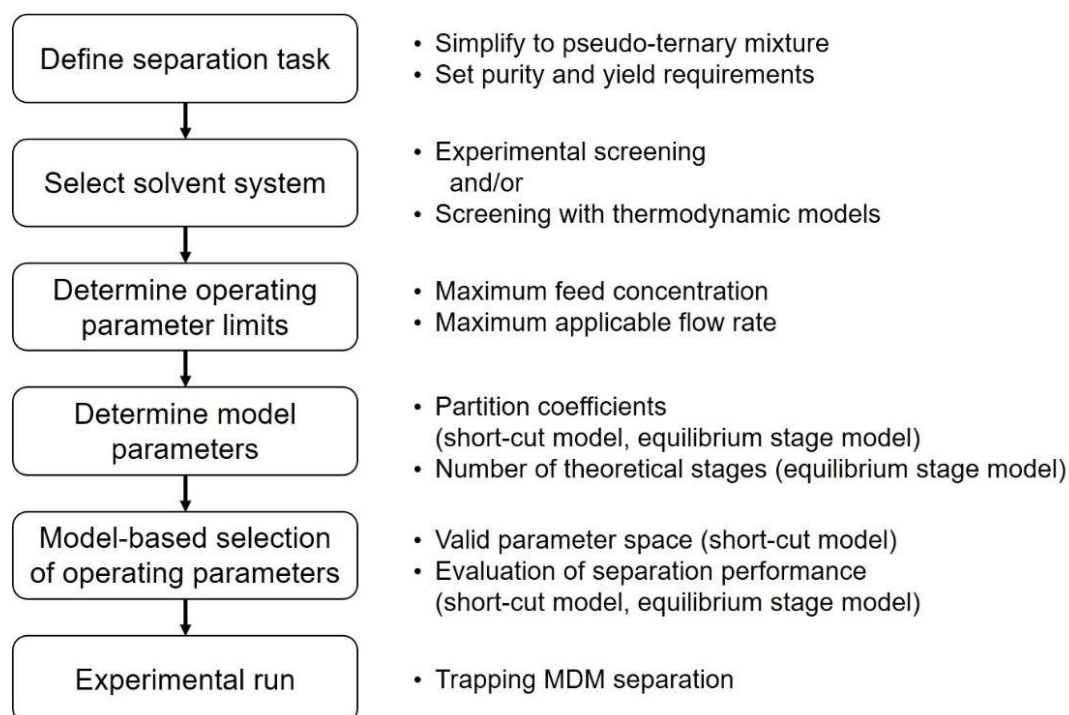

Figure 9. Model-based design approach for trapping multiple dual mode separations at maximized throughput.

To define the trapping MDM separation task, the intermediately-eluting target and main impurities must be identified. As mentioned in Section 2.3, a complex multi-component feed mixture can be reduced to a pseudo-ternary mixture for ease of modeling. The requirements of the separation, namely the purity and yield of the target, must also be established.

Next, a suitable solvent system must be selected that provides high solubility of the feed starting mixture, sufficient stationary phase retention, adequately high selectivity, and partition coefficients in the desired range. In trapping MDM, the partition coefficient of the intermediately-eluting target component should be close to 1 to have similar step durations and solvent consumption in both elution modes. Several solvent system selection methods have been developed based on structured experimental approaches and correlations [22, 84-86] as well as thermodynamic modeling [87-89]. However, the solvent system selection step did not play a prominent role in the investigations performed within the scope of this thesis.

Following solvent system selection, the operating parameter limits allowing for stable, predictable operation are then identified. Considering the thermodynamic and hydrodynamic effects discussed in Section 2.4 and assuming a fixed column set-up and geometry, isothermal operation, and prior selection of a suitable rotational speed, the maximum feed concentration and the corresponding maximum flow rate must be determined. As mentioned in Section 2.3.2, the As and Des feed solutions for a trapping MDM separation are prepared simultaneously by dissolving the model mixture solutes or natural product starting mixture in the two phases of the solvent system in a single vessel. Following a period of mixing and equilibration, the upper and lower phases are separated for use as the As and Des feed solutions, respectively. The maximum feed concentration, described as the total mass of the mixture solutes or natural product starting mixture per total volume of the two phases during feed solution preparation, is that which both lies in the linear range of the partition isotherm(s) and at which the physical properties of the upper and lower phase feed solutions do not exhibit substantial deviations from those of the phases on a solute-free basis.

The feed concentration at which a departure from the linear range of the partition isotherm occurs can be identified using the shake flask method. Known amounts of pure solute(s) or feed starting mixture are added to equal volumes of the upper and lower phases of the selected solvent system in a small vessel. Sufficient time and mixing energy for mass transfer and equilibrium partitioning of the solutes between the phases is supplied under isothermal conditions [49]. Aliquots are then taken from each phase and the solute concentrations in each determined using an analyte-appropriate method, such as high-performance liquid chromatography or gas chromatography-mass spectrometry. Typically, shake flask measurements are performed for a range of feed or solute concentrations at close measurement intervals. The linear range limit of the partition isotherm is then determined by plotting the results in a c_k^U vs. c_k^L diagram and performing a linear regression analysis. An

example plot is found in Figure 10. Each point corresponds to a different known (shake flask sample) feed concentration.
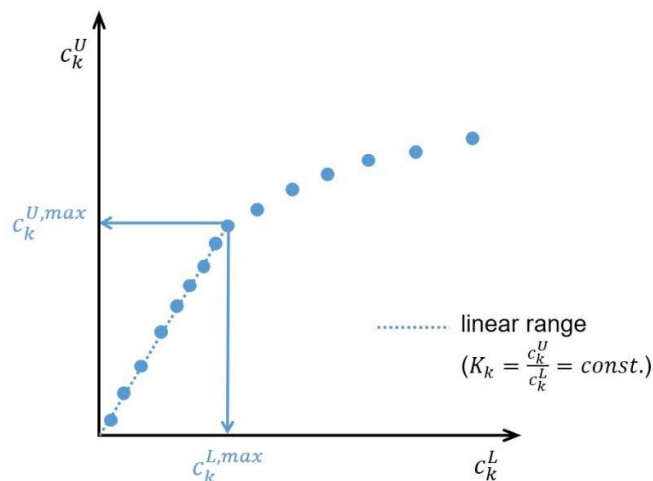
Figure 10. Example partition isotherm of solute k with demarcation of linear range.

The concentration-dependent influence of the feed solutes on the physical properties of the phases, such as density, viscosity, and interfacial tension, may be identified by measuring each property individually as in [20, 68]. In this thesis, the use of simple phase volume ratio [20] and settling time [24, 58, 90] measurements, using the same samples prepared for the shake flask measurements, is explored as an alternative. This approach has the advantage of not requiring any additional laboratory equipment, making it accessible to all LLC users.

Changes in the phase volume ratio of the two phases in the presence of the feed can indicate the occurrence of a similar change in the column, possibly affecting the established S_f and flow patterns. Settling time measurements, performed by vigorously mixing the sample and then observing the time needed for reestablishment of a unified phase interface, can be used to assess changes in mixing and coalescence without flow visualization experiments requiring special non-commercial equipment [91]. Assuming a fixed mixing intensity and vessel geometry, the settling time is dependent on the physical properties of the phases and the phase ratio [92]. Generally, the shorter the settling time, the higher the stationary phase retention obtained in the column during operation [24, 58, 90]. An increase in settling time can therefore indicate hydrodynamic conditions in the column leading to stationary phase loss, e.g., emulsion formation.

The maximum flow rate at fixed rotational speed at which the desired trapping MDM stationary phase fraction of 0.5 can be maintained is identified by performing stationary phase retention experiments. Using a solenoid valve to quickly alternate between pumping of the upper and lower phases before the start of rotation, the column is prepared with equal volumes of the two phases, equivalent to S_f=0.5 in both elution modes. Once the full rotational speed

is reached, the mobile phase flow rate is increased at appropriate intervals until stationary phase loss is observed. These experiments may be performed on a solute-free basis [20] (i.e., with the solute-free upper and lower phases only) or, as in this thesis, in the presence of the feed at the selected maximum concentration. In the latter variation, the identified maximum applicable flow rate is often lower than that obtained for the pure phases. This is the result of hydrodynamic changes brought about by the presence of the feed, e.g., changes in mixing and coalescence behavior.

With the operating parameter limits (maximum feed concentration, maximum flow rate) identified, the relevant model parameters are experimentally determined. For the linear, ideal short-cut model, the partition coefficients of the target and main impurities in the As and Des modes are required. For the equilibrium stage model, the number of theoretical stages of the three components in both elution modes must be determined as well. $K_{As,k}$, $K_{Des,k}$, and N_k can be measured from pulse injections performed at the selected flow rate. Under the Gaussian peak assumption, $K_{As,k}$ and $K_{Des,k}$ can be calculated from the retention time using Equation (6), and N_k can be derived using Equation (10).

It is possible that the partition coefficients obtained in the two elution modes may differ from those measured in the absence of hydrodynamic effects using the shake flask method. The pulse injection partition coefficients are measured under the dynamic conditions of the column and are therefore subjected to any retention time shifts caused by non-ideal flow patterns such as stationary phase back-mixing and dead zones (see Section 2.4.2). The use of pulse injection partition coefficients for CPC modeling is preferred, as they better describe the solute retention behavior during the chromatographic process. Similarly, differing hydrodynamic conditions in the two elution modes often result in the measurement of different $N_{As,k}$ and $N_{Des,k}$. For implementation of the equilibrium stage model, a constant value of N_k is required for simulation of the As and Des modes. The average of $N_{As,k}$ and $N_{Des,k}$ is then used for N_k. This is generally a valid assumption for the typical trapping MDM process conditions of S_f=0.5 and selection of the same mobile phase flow rate in both modes.

The remaining trapping MDM operating parameters to be selected are the step durations in the Loading and Separation stages, t_{As}^{load}, t_{Des}^{load}, t_{As}^{sep}, t_{Des}^{sep}, and the number of Separation stage cycles. The short-cut model can be used to identify valid combinations of these parameters that will result in a complete separation of the intermediately-eluting target under linear, ideal conditions. These parameter sets can then be screened for maximized throughput by evaluating the separation performance predicted by, in the case of this thesis, the short-cut model or the more detailed equilibrium stage model taking non-ideal band broadening into account (see Section 2.5). With the selected maximum feed concentration, maximum flow rate, step durations, and number of cycles at hand, the experimental trapping MDM separation at maximized throughput can be run.

32

3. Results

This section contains the four investigations published in the framework of this thesis and reprinted with permission from Elsevier. In Paper I (Section 3.1), the trapping MDM operating mode and associated short-cut model for operating parameter selection were presented and validated for the first time. Building off of Paper I, Paper II (Section 3.2) demonstrated the use of a model-based approach to achieve maximized trapping MDM throughput. The approach consisted of preliminary measurements for determination of the process limits (maximum feed concentration and mobile phase flow rate), as well as the use of the short-cut model coupled with detailed equilibrium stage model simulations for operating parameter selection (step durations and number of cycles). A model mixture was used for experimental validation. In Paper III (Section 3.3) a comparison study of the batch injection and trapping MDM operating modes was performed, also implementing the short-cut model coupled with equilibrium stage model simulations. Lastly, in Paper IV (Section 3.4), the model-based design approach, this time combining preliminary measurements and an extended version of the short-cut model, without the use of the equilibrium stage model, was successfully applied for the separation of a target compound (nootkatone) from a complex natural product mixture.

3.1 Paper I

Trapping multiple dual mode centrifugal partition chromatography for the separation of intermediately-eluting components: Operating parameter selection

Author contribution: The thesis author made the main contribution to the derivation and development of the trapping MDM short-cut model, as well as to the interpretation of the experimental data. She completed the majority of the writing and editing of the manuscript.

Summary: Paper I presented the trapping MDM operating mode for the first time along with the derivation of the associated short-cut model for the selection of the key operating parameters, namely the step durations and number of cycles. In an improvement over previous modeling attempts of similar processes [5, 47], the newly-derived short-cut model importantly considered the entire solute band widths within the column rather than a single-point position. The input parameters for the short-cut model are the flow rate, F, the phase volumes, V^U and V^L, and the partition coefficients, $K_{As,k}$ and $K_{Des,k}$, of the intermediately-eluting target B and impurities A and C. Additionally, the band positions of the trapped component B at the end of the Loading and Separation stage steps, x_B^{load} and x_B^{sep}, must be selected to fulfill the given set of restrictions. The step durations during Loading, $t_{As/Des}^{load}$, and Separation, $t_{As/Des}^{sep}$, are determined from the solute propagation velocity (Equation (7)) and band positions x_B^{load} and x_B^{sep}. The number of Separation cycles needed to fully elute impurity components A and C from the column before starting the Recovery stage are determined in a similar manner.

Two validation experiments using the short-cut model for the design of the separation of ternary feed mixtures (1:1:1) at low concentration were successfully performed. The model mixtures consisted of parabens differing only in their alkyl chain lengths with α as low as 1.5. In Experiment 1, ethylparaben, propylparaben, and butylparaben were used, with propylparaben as the trapped intermediately-eluting component B. The band front positions were x_B^{load}=0.3 and x_B^{sep}=0.7. In Experiment 2, methylparaben, ethylparaben, and propylparaben were used as the feed mixture, this time with ethylparaben as component B. The band front positions were x_B^{load}=0.1 and x_B^{sep}=0.5. Trapped component purities and yields were >99.9% and >96.5% in Experiment 1, respectively, and 99.3% and >97.0% in Experiment 2. In Experiment 1, 35% of the total column volume was loaded with the feed solution, a vast improvement compared to the 5% limit often recommended for LLC separations in batch injection mode [24]. These results demonstrate the beneficial use of trapping MDM for ternary separations with high feed loading volumes.

Trapping multiple dual mode centrifugal partition chromatography for the separation of intermediately-eluting components: Operating parameter selection☆

Johannes Goll, Raena Morley, Mirjana Minceva*

Biothermodynamics, TUM School of Life Sciences Weihenstephan, Technische Universität München, Gregor-Mendel-Str. 4, 85354 Freising, Germany

ARTICLE INFO

ABSTRACT

The preparative separation of intermediately-eluting components in liquid-liquid chromatography is commonly performed with isocratic batch injections, a technique which often leads to low yield and/or purity as a result of peak overlap. Two-column trapping multiple dual mode centrifugal partition chromatography, an alternative discontinuous method for the separation of a mixture into three product fractions (early-, intermediately-, and late-eluting components) at full recovery, is presented in this work. A mathematical shortcut method based on equilibrium theory assumptions is derived for the determination of the key operating parameters (i.e., step durations and number of steps). The feasibility of the technique and the accompanying short-cut method is demonstrated by proof-of-concept experiments for the separation of two paraben model mixtures.

© 2017 Elsevier B.V. All rights reserved.

1. Introduction

Liquid-liquid chromatography (LLC) has proven itself to be an effective technique for the separation of natural product compounds from complex mixtures [1]. The term LLC encompasses both countercurrent chromatography (CCC) with hydrodynamic units and centrifugal partition chromatography (CPC) with hydrostatic ones. LLC employs the two phases of a liquid-liquid biphasic system as the stationary and mobile phases. During a chromatographic run, the liquid stationary phase is held in place by means of the column geometry and the application of a centrifugal field; the mobile phase is then pumped through it. Separation is achieved as a result of the differing partition behavior of the mixture components between the two phases.

Working with a liquid stationary phase presents several advantages over conventional liquid chromatography techniques with a solid stationary phase, including high loading capacity and the absence of irreversible stationary phase adsorption. Additionally, the presence of a liquid stationary phase allows for high operational flexibility. Either one of the two phases of the selected biphasic system may be used as the stationary phase, and the roles of the phases may even be switched during operation. This key feature of LLC has led to the development of several unique operating modes not otherwise realizable with conventional chromatography techniques. Examples include batch processes such as elution-extrusion [2] and dual-mode [3], as well as continuous processes for binary separations [4,5]. It is often possible to run a variety of operating modes on a single LLC device, allowing the operator to select the mode best suited to the separation task at hand.

A common separation task in preparative chromatography is the isolation of an intermediately-eluting target component from a complex mixture. When the mixture has already undergone one or more preliminary separation steps of lower selectivity, the remaining impurity compounds often exhibit retention behavior similar to that of the target component (i.e., possess low separation factors). When working with isocratic batch injections, peak overlap resulting in decreased productivity and yield is often encountered, especially at the high column loadings desired for preparative separations. To improve target recovery, low purity cut fractions may be reinjected as part of an offline [6] or online [7–9] multi-dimensional (heart-cutting) separation strategy. However, these additional chromatographic runs add time and complexity to the process. Online selection and reinjection of cut fractions is difficult to automate and often involves complex equipment setups.

Continuous separation techniques in LLC, such as intermittent counter-current extraction (ICcE) [4,10–13] and sequential cen-

---

trifugal partition chromatography (sCPC) [14–17], exhibit high selectivity and can be used to process large volumes of feed. However, they yield only two product fractions. The product streams are collected sequentially at opposite ends of a two-column setup during continuous feed injection between the neighboring columns. To separate a feed mixture into three fractions with ICcE/sCPC, two consecutive process steps must be conducted, where the product stream from the first process step containing the intermediately-eluting target component serves as the feed mixture in the second process step.

An alternative for ternary separations is a form of dual mode operation in which the intermediately-eluting target component remains "trapped" inside the column while the impurities are alternately eluted from opposite column ends [18]. This discontinuous LLC method for the recovery of intermediately-eluting compounds was presented in [4] and [19]. In both studies, a two-column CCC set-up with feed introduction between the two columns was used. Multiple elution cycles were performed, each consisting of two steps of alternating mobile phase and flow direction. During these cycles, the neighboring impurity compounds eluted intermittently from the two ends of the device. Meanwhile, the majority of the intermediately-eluting target component remained "trapped" inside the unit. After "washing away" the impurities in this manner, the purified target component could be obtained. In [4], the target component was a bioactive terpenoid (triptolide) from a Chinese herbal medicine present at only 2% in the crude extract. Injection of the crude extract was performed continuously over several cycles. At the end of the process, triptolide was obtained at 98% purity with a yield of 75%. This operating mode was designated as a form of ICcE.

In [19], the target component was Coomassie Brilliant Blue G-250, a dye used for staining in the analysis and quantification of proteins. Multiple injections of the impure sample were made, always at the start of a new cycle. This study referred to the technique as trapping multiple dual mode (MDM). Solubility limits in one phase were considered during the separation design. A mathematical model developed in [20] based on the peak (band front) positions of the mixture components within the column was used to determine the step durations in the two elution modes. A highly pure product fraction was achieved but at a low yield of 37%. The mathematical model applied in [19] approximates solute position inside of the column as the band front position under ideal conditions. However, it does not take into account the wide solute bands encountered at high volume loadings. Therefore, after the elution mode switch, the distance traveled by the solute is calculated relative to the band front position of the previous step. This band "front", relative to the new flow direction, is now effectively the back end of the solute band. This will cause elution of the solute band to occur earlier than predicted, a factor which likely contributed to the separation's low yield.

In both [4,19], it was acknowledged that separation performance could be improved through adjustment of the operating parameters, such as step durations and flow rates. The high target component purities obtained in these two studies clearly demonstrate the effectiveness of this type of "trapping" operating mode for the isolation of intermediately-eluting components. However, an approach for accurate prediction of the process operating parameters to simultaneously satisfy high purity and yield requirements is lacking in the literature.

This work presents a modification of the operating modes described in [4,20] for the separation of intermediately-eluting components using a two-column hydrostatic CPC device. To the authors' knowledge, this is the first report of such a separation using CPC technology. In this method, the feed mixture is introduced during a single column loading cycle without simultaneous mobile phase flow, rather than continuously or repeatedly. For clarity, and to distinguish it from the previous studies using hydrodynamic (CCC) columns, the technique investigated in this work will be referred to as trapping multiple dual mode centrifugal partition chromatography (trapping MDM CPC). However, the presented technique and design methodology will be applicable to separations on both CPC and CCC instruments.

The objectives of this study were to demonstrate the feasibility of the trapping MDM CPC technique and to establish a method for determination of the key operating parameters (i.e., step durations, number of steps). A mathematical short-cut method was derived for determination of the operating parameters allowing for the complete separation of an intermediately-eluting component from a multicomponent mixture under ideal conditions. Proof-of-concept of the trapping MDM CPC technique and short-cut method was then demonstrated experimentally. To show the flexibility of the technique and short-cut method, two trapping MDM CPC experiments with different ternary feed mixtures were performed. The model feed mixtures contained parabens differing only in their alkyl chain lengths. The liquid-liquid biphasic system was ARIZONA N (n-heptane/ethyl acetate/methanol/water 1/1/1/1 v/v/v/v).

In a subsequent publication [21], the presented mathematical short-cut method is implemented as part of a simulation-based strategy for throughput maximization in trapping MDM CPC. This throughput maximization strategy involves selection of the maximum feed concentration, maximum flow rate, and step durations during column loading and separation.

2. Theory

The isolation of an intermediately-eluting target component from a complex mixture can be viewed as a pseudo-ternary separation. When performing the same separation using an isocratic batch injection, two product stream cuts would be required to obtain the target component fraction: one between the early-eluting components and the target component, followed by one between the target component and the remaining late-eluting components. In trapping MDM CPC, three distinct product streams analogous to these three cut fractions are obtained. The early- and late-eluting components elute from opposite ends of the unit while the intermediately-eluting target component remains trapped inside. The target component is then recovered at the end of the process.

Trapping MDM CPC is a cyclic, discontinuous, non-steady state process. One cycle consists of two steps in two different elution modes: descending (Des) mode and ascending (As) mode. In Des mode, the lower phase is used as the mobile phase. The roles of the phases and the mobile phase flow direction are reversed in As mode. The lower phase is the stationary phase while the upper phase is pumped through the columns as the mobile phase.

For the following explanation of the concept of trapping MDM CPC, the simplified case of a three-component feed mixture of compounds A, B, and C is considered. In this example, B is the intermediately-eluting target compound to be trapped within the columns and later recovered. Partition coefficients (K_k^{Des}, K_k^{As}) are defined for the process as the concentration of a component k in the stationary phase divided by its concentration in the mobile phase. Since the roles of the upper and lower phases are reversed from one mode to the other, two elution mode-specific definitions for the partition coefficients are given in Eqs. (1) and (2).

$$K_k^{Des} = \frac{c_k^S}{c_k^M} = \frac{c_k^U}{c_k^L} \tag{1}$$

$$K_k^{As} = \frac{c_k^S}{c_k^M} = \frac{c_k^L}{c_k^U} \tag{2}$$
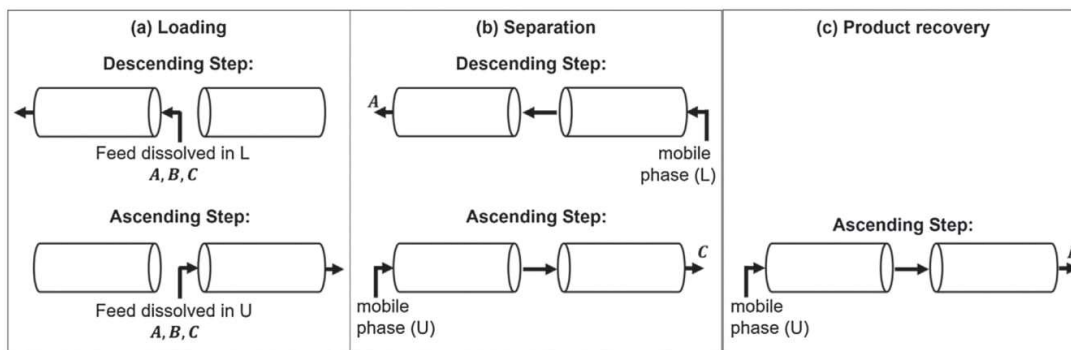
Fig. 1. Principle of trapping MDM CPC shown for the column loading (a), separation (b), and product recovery (c) stages for the separation of a ternary mixture of A, B, and C. (L: lower phase, U: upper phase).

where the superscripts S, M, U, and L stand for the stationary, mobile, upper, and lower phases, respectively. The partition coefficients of the three components in Des mode can be relatively defined as $K_A^{Des} < K_B^{Des} < K_C^{Des}$, which corresponds to $K_A^{As} > K_B^{As} > K_C^{As}$ in As mode as defined by Eqs. (1) and (2). A lower partition coefficient indicates lower affinity of the component to the stationary phase, leading to faster elution from the columns. Therefore, A will travel fastest through the columns in Des mode, while C will travel fastest in As mode.

The trapping MDM CPC technique proposed in this work consists of three process stages: column loading, separation, and product recovery (see Fig. 1).

The column loading stage (Fig. 1a) consists of a single cycle (one Des step and one As step), designated as Cycle 0, during which the feed is introduced between the two columns. There is no simultaneous pumping of mobile phase, and the feed solution flows in a single direction in each step. This means that in Des mode, the lower phase feed solution is pumped into the left-hand column, while in As mode, the upper phase feed solution is pumped into the right-hand column. A single column loading cycle without simultaneous mobile phase flow allows for minimal dilution of the feed upon introduction to the column. This approach is of interest when working with preconcentrated feed mixtures of similar molecules, where multiple or continuous injections could lead to concentrations outside of the stable operating range.

The separation stage (Fig. 1b) is started immediately following the column loading stage. The separation stage consists of multiple cycles of Des and As steps, with the first cycle designated as Cycle 1. In Des mode, A has the lowest partition coefficient and travels fastest toward the column outlet. Before B reaches the end of the column, a switch to As mode is made. In As mode, C moves fastest through the column. Again, the elution mode is reversed before B exits the column, starting a new cycle. In this manner, B remains trapped inside the two columns. Meanwhile, A and C separate from the B band and are alternately eluted from the left and right outlets of the two-column setup in Des and As mode, respectively. The separation stage is continued until A and C have fully eluted from the columns, leaving only B behind at high purity.

In the product recovery stage (Fig. 1c), the purified trapped component B is obtained. An extended step in a single elution mode (shown in Fig. 1c in As mode) is performed until the trapped component has completely eluted from the columns. Selection of the elution mode for the product recovery stage may be based on the mode in which the trapped component elutes fastest (i.e., has a lower partition coefficient), in which the mobile phase is easier to recover (i.e., evaporate), or the recovery of the target component is less cost-intensive. The trapped component could also be obtained

with an extrusion step as in the elution-extrusion technique. However, in extrusion, the trapped component may elute in a mixture of upper and lower phase, and the columns must be refilled and/or re-equilibrated before performing a second separation.

The proposed trapping MDM CPC technique is not restricted to mixtures of just three components. In a multicomponent mixture, component B would still correspond to the component to be trapped inside the columns. Component A, as described above, would represent the mixture components eluting before B in Des mode. Component C would then represent the fraction of components eluting earlier than component B in As mode.

Success of a trapping MDM CPC separation is dependent on appropriate selection of the operating parameters. In this work, a mathematical short-cut method is derived for determination of the Des and As step durations and number of separation stage steps (Section 4.1). The implementation of the short-cut method in trapping MDM CPC design is then explained in Section 4.2. Lastly, proof-of-concept of the trapping MDM CPC technique and the short-cut method is experimentally demonstrated for two different separations in Section 4.3.

3. Materials and methods

3.1. Materials

3.1.1. Chemicals

Ethyl paraben (EP), propyl paraben (PP), and butyl paraben (BP) used in the trapping MDM CPC and pulse injection experiments were obtained from Alfa Aesar GmbH & Co KG (Karlsruhe, Germany), methyl paraben (MP) from Molekula (Gillingham, UK). All parabens had a purity ≥99%.

The solvents n-heptane, ethyl acetate, and methanol for the preparation of the liquid biphasic system were of analytical grade and purchased from Merck KGaA (Darmstadt, Germany). For HPLC analysis, Milli-Q water (filtrated by a Milli-Q direct 8 water purification system) and methanol (gradient grade for liquid chromatography ≥ 99.9%) from Merck KGaA (Darmstadt, Germany) were used.

3.1.2. Equipment

An Armen TMB 250 unit (Armen Instrument, Saint Ave, France) was used for the pulse injection and trapping MDM CPC experiments. The unit is comprised of two adjacent 125 ml hydrostatic columns with twin-cells, which are mounted on two separate rotors and can be accelerated up to 3000 rpm (280 g). The two columns are connected via a small stainless steel tubing with a volume <1 ml. A 4-port valve in the middle of the tubing enables

feed introduction between the two columns in As and Des mode. In addition to the two feed pumps, two mobile phase pumps are used to deliver the corresponding mobile phase in each mode. The pumps can operate in a flow rate range between 1 and 50 ml min^{-1}. Monitoring of the effluent is done via two UV–vis detectors, one at each end of the two-column setup. One fraction collector (Model LS-5600, Armen Instrument, France) is placed after each UV–vis detector. A more detailed description can be found in [5,22].

3.2. Methods

3.2.1. Biphasic solvent system preparation

The biphasic solvent system ARIZONA N (*n*-heptane/ethyl acetate/methanol/water 1/1/1/1 v/v/v/v) was prepared by mixing equal volume amounts of *n*-heptane, ethyl acetate, methanol, and water. The system was stirred for 3 h at room temperature and allowed to equilibrate. The biphasic system was then transferred to a separatory funnel and the phases were conveyed into distinct reservoirs.

Sample solutions for the trapping MDM CPC experiments were prepared by two different methods. In Experiment 1, particular amounts of parabens (EP, PP, and BP) were dissolved in either upper or lower phase. In Experiment 2, parabens (MP, EP, and PP) were dissolved in equal volumes of upper and lower phase in a single container. The system was allowed to equilibrate before being separated into the two phases (feed solutions) with a separatory funnel. The sample solutions for the pulse injection experiments were prepared with all four parabens (MP, EP, PP, and BP) in the same manner as for trapping MDM CPC Experiment 1.

3.2.2. Pulse injection experiments for determination of partition coefficients

Pulse injection experiments with a mixture consisting of MP, EP, PP, and BP were performed in As and Des mode in order to determine the partition coefficients of the components. The columns were filled with equal volumes of the upper and lower phases ($V_U/V_L = 50/50$ vol.-%) without rotation by pumping upper and lower phase at short intervals of equal duration at a flow rate of 40 ml min^{-1}. The rotational speed was then set to 1700 rpm. Injections were manually performed using a 1 ml sample loop at 20 and 21 ml min^{-1}. The feed solutions used for the injections at 20 and 21 ml min^{-1} had single paraben concentrations of 5 and 1.25 mg ml^{-1}, respectively. The resulting chromatograms were analyzed using the moment method for partition coefficient determination. Experiments were performed at room temperature (22 ± 2 °C).

3.2.3. Trapping MDM CPC experiments

Prior to trapping MDM CPC experiments, the columns were prepared as described in Section 3.2.2 ($V_U/V_L = 50/50$ vol.-%) and the rotational speed was set to 1700 rpm. Experiments were performed at room temperature (22 ± 2 °C). The UV–vis detector signals were recorded during the separation and recovery stages at wavelengths of 280 nm and 254 nm. All cycles were begun in Des mode. Three process stages were executed during each trapping MDM CPC experiment:

3.2.3.1. Column loading.

During the column loading stage, the feed solution containing the ternary paraben mixture was successively introduced with the Des and As feed pumps without simultaneous pumping of the mobile phase for one cycle (Cycle 0). In the Des loading step, lower phase with dissolved parabens was pumped for a certain loading time t_{Des}^{load}; in the following As loading step, upper phase with parabens for the loading time t_{As}^{load}.

The entire Des and As eluent streams were collected from the two ends of the unit in graduated cylinders. Aliquots for HPLC analysis were taken from each collected eluent stream for determination of the average paraben concentrations in each step.

3.2.3.2. Separation.

After completion of the column loading stage, the feed pumps were stopped and the mobile phase pumps were used to deliver the mobile phase. In each separation cycle, lower and upper phase were pumped alternately in Des and As mode for the step durations t_{Des}^{sep} and t_{As}^{sep}, respectively. The separation stage was continued until the UV–vis detector signal indicated that the early- and late-eluting parabens had fully eluted. The eluent stream was collected during each step and aliquots taken for determination of the average paraben concentrations using HPLC.

3.2.3.3. Product recovery.

The product recovery stage consisted of a single extended As step. During the As step, upper phase was pumped with the corresponding As mobile phase pump until the UV–vis signal indicated that no more components were eluting. Fractions were collected from the product stream and analyzed via HPLC.

3.2.4. HPLC analysis

HPLC analysis was used to determine the concentrations of the eluting components in the upper and lower phase during trapping MDM CPC experiments. The collected samples were analyzed with a HPLC system from Gilson (Middleton, WI, USA). The HPLC setup consisted of a 322H2 binary gradient pump, GX Direct injection module, and 151 UV/VIS Detector. The analysis was controlled by Trilution LC software. A Nucleosil 100-5 C18 column was used (125 mm x 3 mm ID; 5 μm). Analysis of all samples was completed using a water:methanol gradient program with a mobile phase flow rate of 0.8 ml min^{-1} at 23 °C. The injection volume was 10 μl. The gradient program following injection was as follows: 40:60 from 0.0 min to 4.5 min; 38:62 at 5.0 min; 58:42 from 7.5 min to 10.0 min. The detection wavelength was set at 280 nm. Prior to analysis, samples collected in As and Des mode were diluted with upper and lower phase, respectively, when needed.

4. Results and discussion

The Results and Discussion section is divided into three parts. The first section (Section 4.1) focuses on the derivation of a mathematical short-cut method for selection of the operating parameters resulting in complete separation of a ternary mixture using trapping MDM CPC. Implementation of the short-cut method in the design of a trapping MDM CPC process is then discussed in the second section (Section 4.2). Finally, the trapping MDM CPC technique and accompanying short-cut method are validated by two proof-of-concept experiments (Section 4.3).

4.1. Mathematical short-cut method

Given the cyclic, multi-stage nature of the trapping MDM CPC process, the durations of the descending (Des) and ascending (As) steps in the column loading and separation stages ($t_{Des}^{load}, t_{As}^{load}, t_{Des}^{sep}, t_{As}^{sep}$) must be determined, as well as the number of separation stage steps in each elution mode ($n_{Des}^{sep}, n_{As}^{sep}$). In the following, a mathematical short-cut method for selection of the abovementioned operating parameters is derived for the complete separation of a ternary mixture using trapping MDM CPC. A related short-cut approach has been previously implemented for the design of continuous binary separations using the sCPC technique [5,14–17].
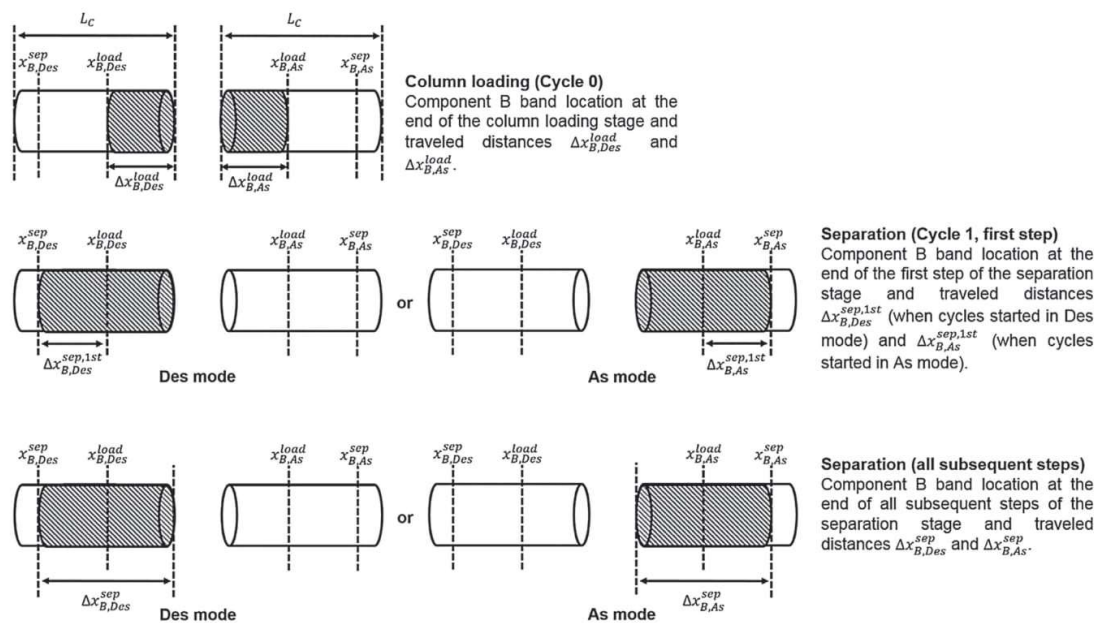
Fig. 2. Notation convention for trapping MDM CPC model equations. L_C = length of one column, $x_{B,Des}^{load}$ = band front position of component B after loading in Des mode, $x_{B,As}^{load}$ = band front position of component B after loading in As mode, $x_{B,Des}^{sep}$ = band front position of component B at the end of each Des separation step, $x_{B,As}^{sep}$ = band front position of component B at the end of each As separation step.

Table 1

Trapping MDM CPC process restrictions and corresponding parameter constraints for the complete separation of a ternary mixture of A, B, and C with B as the trapped component.

Restriction	Operating parameter constraints	
1. During the column loading stage, B remains inside the columns.	$0 \leq x_{B,Des}^{load} \leq L_c$	(3)
	$0 \leq x_{B,As}^{load} \leq L_c$	(4)
2. During the separation stage, B remains inside the columns.	$x_{B,Des}^{load} \leq x_{B,Des}^{sep} \leq L_c$	(5)
	$x_{B,As}^{load} \leq x_{B,As}^{sep} \leq L_c$	(6)
3. During the separation stage, B travels a net distance of zero during each cycle. (Exception: Cycle 1)	$\Delta x_{B,Des}^{sep} - \Delta x_{B,As}^{sep} = 0$	(7)
4. At the end of the separation stage (completion of n_{cyc}^{sep} cycles), both A and C have completely eluted from the columns.	see Eqs. (35) and (36)	

A significant difference between the short-cut method presented in this work and the mathematical model proposed in [20] is the consideration of the entire solute band width. By defining the positions of the two ends of the intermediately-eluting component B after loading, $x_{B,Des}^{load}$ and $x_{B,As}^{load}$, a more accurate prediction can be made of the solute band front locations relative to the column outlet in both elution modes. In [20], band position was represented by a single end of the solute band: the band front during loading. This "front" effectively becomes the back end of the solute band after the elution mode switch, which can lead to earlier elution of the solute than predicted by the model.

The proposed short-cut method is applicable to the complete separation and recovery (100% purity and yield) of intermediately-eluting component B from the simplified ternary system of A, B, and C described in Section 2 under ideal conditions (i.e., in the absence of band broadening effects). A and C elute from opposite ends of the two-column setup during the separation stage in Des and As mode, respectively, as defined by their partition coefficients ($K_A^{Des} < K_B^{Des} < K_C^{Des}$; $K_A^{Asc} > K_B^{Asc} > K_C^{Asc}$). Meanwhile, B remains trapped inside the two columns. The notation convention for the derivation of the short-cut method equations is graphically depicted in Fig. 2. $x_{B,Des}^{load}$ is the band front position of component B

after loading in Des mode, and $x_{B,As}^{load}$ is the position of the band front of component B after loading in As mode. In the separation stage, component B will travel the distance $\Delta x_{B,Des}^{sep}$ and $\Delta x_{B,As}^{sep}$ in Des and As mode, respectively, to reach $x_{B,Des}^{sep}$ as the band front position of component B at the end of each Des step and $x_{B,As}^{sep}$ as the band front position of component B at the end of each As step. The distance traveled in a single step is always positive and in the flow direction.

The restrictions for full recovery of the three components in pure form are listed in Table 1. L_c is the length of one column of the two-column CPC setup. The band front positions of the trapped component B ($x_{B,Des}^{load}$, $x_{B,As}^{load}$, $x_{B,Des}^{sep}$, and $x_{B,As}^{sep}$) must be selected to satisfy Restrictions 1 and 2 from Table 1. Here it should already be noted that it is not necessary to define a value for the column length, L_c, for implementation of the short-cut model. By defining x_B as a fraction of the column length, L_c can be cancelled out of the model equations. Given the process flow rates (F_U, F_L), volumes of the upper and lower phases in each column of the two-column setup (V_U, V_L), and the partition coefficients of the mixture components (K_k^{Des}, K_k^{As}), it is then possible to calculate the corresponding step durations and theoretical number of separation stage steps (n_{Des}^{sep}, n_{As}^{sep}). The general forms of the equations are presented

first, followed by those specific to each process stage. Guidelines for selection and/or determination of the short-cut method input parameters are given in Section 4.2.

The required step durations (t_{Des}, t_{As}) for a single component k depend on the distances to be traveled ($\Delta x_{k,Des}$, $\Delta x_{k,As}$) and the componens' velocities ($v_{k,Des}$, $v_{k,As}$). This relationship is expressed in Eqs. (8) and (9) for the Des and As elution modes, respectively.

$$t_{Des} = \frac{\Delta x_{k,Des}}{v_{k,Des}} \tag{8}$$

$$t_{As} = \frac{\Delta x_{k,As}}{v_{k,As}} \tag{9}$$

The velocity of component k can be derived from the retention volume equation (Eq. (10)).

$$V_{R,k} = V_M + K_k V_S \tag{10}$$

where the subscripts M and S represent the mobile and stationary phases, respectively. The retention volume, $V_{R,k}$, can alternatively be expressed as:

$$V_{R,k} = \frac{F_M L_C}{v_k} \tag{11}$$

Combining Eqs. (10) and (11), the component velocities specific to Des and As mode are given by Eqs. (12) and (13).

$$v_{k,Des} = \frac{F_L L_C}{V_L + K_k^{Des} V_U} \tag{12}$$

$$v_{k,As} = \frac{F_U L_C}{V_U + K_k^{As} V_L} \tag{13}$$

Substituting Eqs. (12) and (13) into Eqs. (8) and (9) yields the step durations as a function of the operating parameters (Eqs. (14) and (15)).

$$t_{Des} = \Delta x_{k,Des} \frac{\left(V_L + K_k^{Des} V_U\right)}{F_L L_C} \tag{14}$$

$$t_{As} = \Delta x_{k,As} \frac{\left(V_U + K_k^{As} V_L\right)}{F_U L_C} \tag{15}$$

Next, the general model equations (Eqs. (14) and (15)) are adapted to each of the three process stages and their corresponding restrictions.

4.1.1. Column loading

After fixing the B band front position after loading in each step ($x_{B,Des}^{load}$, $x_{B,As}^{load}$), the distances traveled by the component B band fronts during the loading step ($\Delta x_{B,Des}^{load}$, $\Delta x_{B,As}^{load}$) can be defined by Eqs. (16) and (17).

$$\Delta x_{B,Des}^{load} = x_{B,Des}^{load} - 0 \tag{16}$$

$$\Delta x_{B,As}^{load} = x_{B,As}^{load} - 0 \tag{17}$$

Substituting Eqs. (16) and (17) into Eqs. (14) and (15) yields Eqs. (18) and (19), respectively.

$$t_{Des}^{load} = x_{B,Des}^{load} \frac{\left(V_L + K_B^{Des} V_U\right)}{F_L L_C} \tag{18}$$

$$t_{As}^{load} = x_{B,As}^{load} \frac{\left(V_U + K_B^{As} V_L\right)}{F_U L_C} \tag{19}$$

4.1.2. Separation

Taking Restriction 3 from Table 1 into account, the distances traveled by the B band fronts during the Des and As steps of the separation stage can be expressed by Eq. (20). An exception exists for the distance traveled during the first step of the first cycle (Cycle 1), given by Eqs. (21) and (22) when cycles are begun in Des or As mode, respectively. The distance traveled during the second step of Cycle 1 is given by Eq. (20).

$$\Delta x_{B,Des}^{sep} = \Delta x_{B,As}^{sep} = \left(x_{B,Des}^{sep} - x_{B,Des}^{load}\right) + \left(x_{B,As}^{sep} - x_{B,As}^{load}\right) \tag{20}$$

$$\Delta x_{B,Des}^{sep,1st} = \left(x_{B,Des}^{sep} - x_{B,Des}^{load}\right) \tag{21}$$

$$\Delta x_{B,As}^{sep,1st} = \left(x_{B,As}^{sep} - x_{B,As}^{load}\right) \tag{22}$$

Substituting Eqs. (20)–(22) into Eqs. (14) and (15) yields Eqs. (23)–(26).

$$t_{Des}^{sep,1st} = \left(x_{B,Des}^{sep} - x_{B,Des}^{load}\right) \frac{V_L + K_B^{Des} V_U}{F_L L_C} \tag{23}$$

$$t_{As}^{sep,1st} = \left(x_{B,As}^{sep} - x_{B,As}^{load}\right) \frac{V_U + K_B^{As} V_L}{F_U L_C} \tag{24}$$

$$t_{Des}^{sep} = \left[\left(x_{B,Des}^{sep} - x_{B,Des}^{load}\right) + \left(x_{B,As}^{sep} - x_{B,As}^{load}\right)\right] \frac{V_L + K_B^{Des} V_U}{F_L L_C} \tag{25}$$

$$t_{As}^{sep} = \left[\left(x_{B,Des}^{sep} - x_{B,Des}^{load}\right) + \left(x_{B,As}^{sep} - x_{B,As}^{load}\right)\right] \frac{V_U + K_B^{As} V_L}{F_U L_C} \tag{26}$$

In reality, it is not necessary to keep the step durations during the separation stage the same from one cycle to the next. They could be longer in the first cycles, becoming shorter with each successive cycle to mitigate the additive effects of band broadening as the process progresses. It may also occur that the three solute bands (A, B, and C) already exhibit baseline separation inside of the unit before A and C have fully eluted. In this case, the product recovery stage could be started earlier, but cutting of the product stream would then be necessary to obtain intermediately-eluting component B separate from the remaining baseline-separated portions of the A and C bands. These process options would add to the complexity of the step duration selection procedure as well as the automation and control of the process and are not considered here. The concentration profiles of the three components inside the columns as a function of time would have to be known, requiring more complex modeling approaches (e.g., using the equilibrium cell model).

4.1.3. End of the separation stage/start of product recovery

The product recovery stage is begun after Restriction 4 in Table 1 is fulfilled. The number of separation stage steps to fully recover components A and C in Des and As mode (n_{Des}^{sep}, n_{As}^{sep}), respectively, can be determined as follows.

The net distances to be traveled by the back ends (last-eluting ends) of the A and C bands during the trapping MDM CPC process to elute the entire A band in Des mode and the entire C band in As mode are expressed by Eqs. (27) and (28). $x_{A,As}^{load}$ and $x_{C,Des}^{load}$ can be calculated using Eqs. (14) and (15), respectively.

$$\Delta x_{A,net}^{process} = x_{A,As}^{load} + L_C \tag{27}$$

$$\Delta x_{C,net}^{process} = x_{C,Des}^{load} + L_C \tag{28}$$

The net distances traveled by the A and C bands during each cycle of the separation stage are described by Eqs. (29)–(34). Eqs. (29) and (31) are applicable when cycles are begun in Des mode, while Eqs. (30) and (32) are applicable when cycles are begun in As
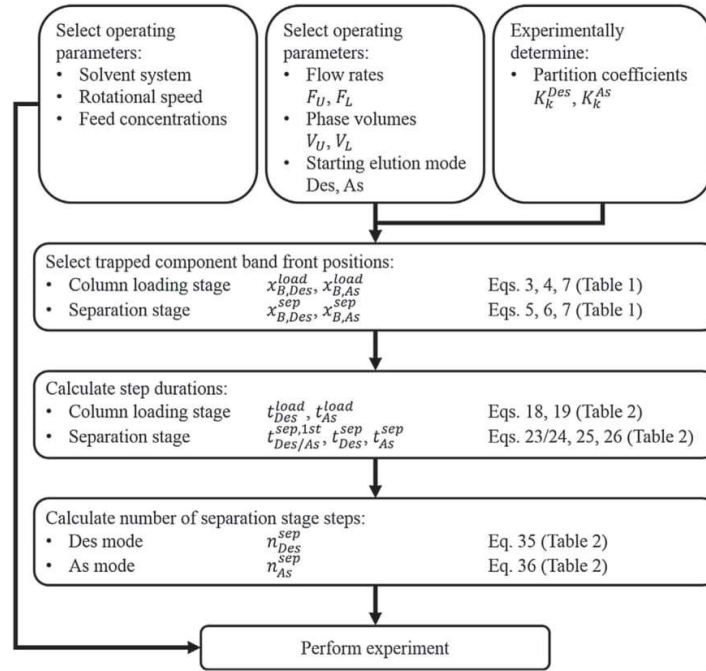
Fig. 3. Flow chart depicting the implementation of the short-cut method for the design of trapping MDM CPC processes.

mode. It should be noted that negative values may be obtained for Eqs. (29)–(32).

$$\Delta x_{A,net}^{sep,1st} = t_{Des}^{sep,1st} \frac{F_L L_C}{V_L + K_A^{Des} V_U} - t_{As}^{sep} \frac{F_U L_C}{V_U + K_A^{As} V_L} \tag{29}$$

or (Cycle 1)

$$\Delta x_{A,net}^{sep,1st} = t_{Des}^{sep} \frac{F_L L_C}{V_L + K_A^{Des} V_U} - t_{As}^{sep,1st} \frac{F_U L_C}{V_U + K_A^{As} V_L} \tag{30}$$

$$\Delta x_{C,net}^{sep,1st} = t_{Des}^{sep,1st} \frac{F_L L_C}{V_L + K_C^{Des} V_U} - t_{As}^{sep} \frac{F_U L_C}{V_U + K_C^{As} V_L} \tag{31}$$

or (Cycle 1)

$$\Delta x_{C,net}^{sep,1st} = t_{Des}^{sep} \frac{F_L L_C}{V_L + K_C^{Des} V_U} - t_{As}^{sep,1st} \frac{F_U L_C}{V_U + K_C^{As} V_L} \tag{32}$$

$$\Delta x_{A,net}^{sep} = t_{Des}^{sep} \frac{F_L L_C}{V_L + K_A^{Des} V_U} - t_{As}^{sep} \frac{F_U L_C}{V_U + K_A^{As} V_L} \quad \text{(subsequent cycles)} \tag{33}$$

$$\Delta x_{C,net}^{sep} = t_{As}^{sep} \frac{F_U L_C}{V_U + K_C^{As} V_L} - t_{Des}^{sep} \frac{F_L L_C}{V_L + K_C^{Des} V_U} \quad \text{(subsequent cycles)} \tag{34}$$

For complete elution of A and C to have occurred, n_{Des}^{sep} and n_{As}^{sep} must satisfy the relationships expressed in Eqs. (35) and (36), where n_{Des}^{sep} and n_{As}^{sep} are integers. A different value for n^{sep} may be obtained for each mode. Hence, the number of separation stage cycles to be performed corresponds to the greater value of n^{sep}.

$$n_{Des}^{sep} \geq \frac{\Delta x_{A,net}^{process} - \Delta x_{A,net}^{sep,1st}}{\Delta x_{A,net}^{sep}} + 1 \tag{35}$$

$$n_{As}^{sep} \geq \frac{\Delta x_{C,net}^{process} - \Delta x_{C,net}^{sep,1st}}{\Delta x_{C,net}^{sep}} + 1 \tag{36}$$

The implementation of the mathematical short-cut method in the design of a trapping MDM CPC process is described in Section 4.2.

4.2. Design of trapping MDM CPC separations

In this section, the design of trapping MDM CPC processes using the short-cut method derived in Section 4.1 is presented for the complete recovery of an intermediately-eluting component from a ternary mixture. The flow chart in Fig. 3 graphically depicts the design approach.

As summarized in Table 2, the short-cut method equations are used for determination of the following operating parameters: step durations in the loading (t_{Des}^{load}, t_{As}^{load}) and separation stages ($t_{Des/As}^{sep,1st}$, t_{Des}^{sep}, t_{As}^{sep}); and number of separation stage steps (n_{Des}^{sep}, n_{As}^{sep}). Before implementation of the short-cut method, the biphasic solvent system and following unit operating parameters must be selected: volumes of the lower and upper phases in each column of the two-column setup (V_L, V_U), rotational speed, mobile phase flow rates in the Des and As modes (F_L, F_U), feed concentrations, and initial elution mode for the process (Des or As). Furthermore, the partition coefficients (K_k^{Des}, K_k^{As}) of the feed components A, B, and C in the selected biphasic system must be determined. Recommendations for the selection of these parameters are briefly described in the following paragraph.

In trapping MDM CPC and related methods, it is advantageous to work with a biphasic solvent system in which the intermediately-eluting component has a partition coefficient close to unity [4,19], a phase volume ratio V_U/V_L of 50/50, and identical flow rates in both Des and As elution modes [14]. This results in similar column efficiency and elution speed of the trapped component in both modes, leading to the possibility to have similar step durations and, therefore, similar mobile phase consumption. In order to achieve high column efficiency, the mobile phase flow rate and rotational speed should be selected as high as possible within the limitations imposed by the maximum pressure drop and maintenance of the phase volume ratio. Feed concentrations should be selected with regard to changes of the physical properties of the biphasic system

Table 2

Summary of short-cut method equations derived in Section 4.1 for the design of trapping MDM CPC processes.

Process stage	Short-cut method equations	
Column loading	$t_{Des}^{load} = x_{B,Des}^{load} \dfrac{V_L + K_B^{Des} V_U}{F_L L_c}$	(18)
	$t_{As}^{load} = x_{B,As}^{load} \dfrac{V_U + K_B^{As} V_L}{F_U L_c}$	(19)
Separation	$t_{Des}^{sep,1st} = \left(x_{B,Des}^{sep} - x_{B,Des}^{load} \right) \dfrac{V_L + K_B^{Des} V_U}{F_L L_c}$	(23)
	$t_{As}^{sep,1st} = \left(x_{B,As}^{sep} - x_{B,As}^{load} \right) \dfrac{V_U + K_B^{As} V_L}{F_U L_c}$	(24)
	$t_{Des}^{sep} = \left[\left(x_{B,Des}^{sep} - x_{B,Des}^{load} \right) + \left(x_{B,As}^{sep} - x_{B,As}^{load} \right) \right] \dfrac{V_L + K_B^{Des} V_U}{F_L L_c}$	(25)
	$t_{As}^{sep} = \left[\left(x_{B,Des}^{sep} - x_{B,Des}^{load} \right) + \left(x_{B,As}^{sep} - x_{B,As}^{load} \right) \right] \dfrac{V_U + K_B^{As} V_L}{F_U L_c}$	(26)
	$n_{Des}^{sep} \geq \dfrac{\Delta x_{A,net}^{process} - \Delta x_{A,net}^{sep,1st}}{\Delta x_{A,net}^{sep}} + 1$	(35)
	$n_{As}^{sep} \geq \dfrac{\Delta x_{C,net}^{process} - \Delta x_{C,net}^{sep,1st}}{\Delta x_{C,net}^{sep}} + 1$	(36)

and partitioning behavior that can occur at high concentrations, which may have negative effects on the stability and predictability of the separation process. Lastly, the starting elution mode, Des or As, must be selected. This parameter determines which set of equations will be used in the short-cut method. Its potential effects on separation performance were not investigated in this work.

After selection of the abovementioned operating parameters and determination of the partition coefficients (depicted in the first row of Fig. 3), the short-cut method may be implemented. First, the trapped component band front positions in the column loading ($x_{B,Des}^{load}$, $x_{B,As}^{load}$) and separation stages ($x_{B,Des}^{sep}$, $x_{B,As}^{sep}$) must be selected to fulfill Restrictions 1 and 2 (Eqs. (3)–(6)) in Table 1. It is then possible to calculate the step durations during the column loading (t_{Des}^{load}, t_{As}^{load}; Eqs. (18) and (19)) and separation stages ($t_{Des/As}^{sep,1st}$, t_{Des}^{sep}, t_{As}^{sep}; Eqs. 23/24, 25, 26). After calculation of the step durations, the number of separation stage steps to be completed for full recovery of components A and C before the start of the product recovery stage (n_{Des}^{sep}, n_{As}^{sep}) can be determined using Eqs. (35) and (36). The short-cut method equations are summarized in Table 2. Several points for consideration during selection of the component B band front positions are discussed in the following paragraphs.

From an ideal standpoint, it would be desirable to operate the process with $x_{B,Des}^{sep} = x_{B,As}^{sep} = L_c$. In this scenario, the trapped component band would just reach the end of the column at the end of each separation stage step. This would correspond to the maximum possible step durations for a given column loading (fixed values of $x_{B,Des}^{load}$, $x_{B,As}^{load}$). It is beneficial to select step durations to be as long as possible to reduce wear on the valves and to allow reestablishment of the hydrodynamic equilibrium between the mobile and stationary phases within the columns after the elution mode switch [15]. When switching between Des and As mode is too frequent, the mobile and stationary phases will not have sufficient time to coalesce and reestablish hydrodynamic equilibrium within the cells, which can lead to stationary phase loss.

The short-cut method is valid for separations under ideal conditions, i.e., in the absence of band broadening effects such as mass transfer resistance and axial dispersion. In reality, the band broadening effects not taken into account by the ideal assumptions of the short-cut method would always cause the B band fronts to exceed the end of the columns when $x_{B,Des}^{sep} = x_{B,As}^{sep} = L_c$, leading to elution with the Des (A) and As (C) product streams. This would result in a decreased yield of the trapped target component B and decreased purity of A and C. Therefore, it is necessary to select a value of x_B^{sep} far enough from L_c to compensate for band broadening of the trapped component during the process. Taking the remarks of the previous paragraph into account, a compromise must be met in the selection of $x_{B,Des}^{sep}$ and $x_{B,As}^{sep}$ in order to achieve both a stable process and a successful separation.

Furthermore, it should be considered that high values of $x_{B,Des}^{load}$ and $x_{B,As}^{load}$ are desired for high column loading and high throughput. However, this leads to a reduction of the distances traveled during the separation stage ($\Delta x_{B,Des}^{sep}$, $\Delta x_{B,As}^{sep}$) as defined in Eqs. (20)–(22), which corresponds to shorter step durations. For longer step durations, the difference between x_B^{sep} and x_B^{load} in each elution mode should be sufficiently large. This necessitates either a lower column loading, resulting in lower throughput, or selection of x_B^{sep} closer to L_c, which can have a negative impact on purity and yield, as described in the previous paragraph. x_B^{sep} and x_B^{load} are therefore interconnected parameters, whose selection involves several compromises.

The ideal assumptions of the short-cut method may also lead to underestimation of the number of separation stage steps required for full recovery of the non-trapped components A and C under experimental conditions. Due to broadening of the last-eluting ends of the A and C bands, their complete elution from the columns will occur later than predicted. Therefore, the minimum values of n_{Des}^{sep} and n_{As}^{sep} satisfying Eqs. (35) and (36) should be considered as the theoretical numbers of separation stage steps corresponding to the minimum number of steps needed during the experiment. The detector signals should be monitored during a trapping MDM CPC separation run to determine if additional steps are needed to fully recover A and C.

Taking the abovementioned points into consideration, it is clear that the selection of the trapped component band front positions at the end of the steps of the column loading and separation stages represents a crucial part of the trapping MDM CPC design process. As previously discussed, the full separation and recovery of the intermediately-eluting target component B using the parameters determined by the short-cut method is only guaranteed under ideal conditions. Separation performance under real conditions may be evaluated experimentally or with simulations taking band broadening effects into account. In Section 4.3, experimental proof-of-concept of the presented short-cut method approach for the design of trapping MDM CPC processes for the separation of two different ternary mixtures is demonstrated. A subsequent publication [21] describes a simulation-based design approach for achieving maximum process throughput using the short-cut method along with the equilibrium cell model for selection of the best compromise between x_B^{load} and x_B^{sep}, as well as accurate determination of n_{Des}^{sep} and n_{As}^{sep}.

4.3. Trapping MDM CPC proof-of-concept experiments

Trapping MDM CPC experiments were designed with the presented short-cut method (Sections 4.1 and 4.2) and carried out for the separation of two different ternary model mixtures. Different

Table 3

Partition coefficients determined by pulse injection and shake flask methods; Experimental conditions, pulse injections: Upper/lower phase volume ratio = 50/50 vol.-%, F_U, F_L = 20 ml min^{-1} and 21 ml min^{-1}, Rotational speed = 1700 rpm, V_{Inj} = 1 ml, $c_{k,feed,20ml/min}$ = 5 mg ml^{-1}; $c_{k,feed,21ml/min}$ = 1.25 mg ml^{-1}. Experimental conditions, shake flask method: V_U = 2 ml, V_L = 2 ml, Concentration range: c_k = 0.01–2 mg ml^{-1}.

Component	K_k, pulse injection method				K_k, shake flask method [17]
	K_k^{AS}		K_k^{Des}		$K_k^{Des} = \frac{c_k^U}{c_k^L}$
	20 ml min^{-1}	21 ml min^{-1}	20 ml min^{-1}	21 ml min^{-1}	
MP	1.75	1.85	0.90	0.87	0.76 ± 0.00
EP	1.07	1.14	1.26	1.29	1.19 ± 0.01
PP	0.63	0.68	1.90	2.05	1.90 ± 0.04
BP	0.38	0.39	2.97	3.21	3.00 ± 0.11

Table 4

Trapping MDM CPC operating and design parameters, Experiments 1 and 2.

Parameter		Experiment	
	1	2	
Component A (elution in Des mode)		EP	MP
Component B (trapped component)		PP	EP
Component C (elution in As mode)		BP	PP
Measured column volume (single column), V_C/ml		123.5	
Active cell volume (single column)/ml		90.9	
Upper/lower phase volume ratio, V_U/V_L/vol.-%		50/50	
Rotational speed/rpm		1700	
Flow rate, F_U, F_L/ml min^{-1}		21	20
Feed concentration, $c_{k,Des/As}^{load}$/mg ml^{-1}		2.45	6.67
Trapped component band front position, end of loading stage	Des mode, $x_{B,Des}^{load}$/cm	0.3 L_c	0.1 L_c
	As mode, $x_{B,As}^{load}$/cm	0.3 L_c	0.1 L_c
Trapped component band front position, end of separation stage	Des mode, $x_{B,Des}^{sep}$/cm	0.7 L_c	0.5 L_c
	As mode, $x_{B,As}^{sep}$/cm	0.3 L_c	0.5 L_c
Loading stage step duration	Des mode, t_{Des}^{load}/min	2.68	0.70
	As mode, t_{As}^{load}/min	1.48	0.64
Separation stage step duration	Des mode, t_{Des}^{sep}/min	3.63	5.57
	Des mode (Cycle 1), $t_{Des}^{sep,1st}$/min	3.63	2.79
	As mode, t_{As}^{sep}/min	2.00	5.11
Separation stage steps, theoretical	Des mode, n_{Des}^{sep}/-	6	5
	As mode, n_{As}^{sep}/-	7	2
Separation stage steps, experiment	Des mode, n_{Des}^{sep}/-	11	5
	As mode, n_{As}^{sep}/-	10	4

values of x_B^{sep} and x_B^{load} were selected in the two experiments in order to demonstrate the general applicability and flexibility of the method. The separation objective was complete recovery of the intermediately-eluting component in pure form.

In Experiment 1, the feed mixture consisted of EP, PP, and BP with PP as the intermediately-eluting target component. In this experiment, $x_{B,As}^{sep}$ was set equal to $x_{B,As}^{load}$, that is, the trapped component band returned to its initial position (i.e., position at the end of the loading cycle) at the end of each separation cycle. This resulted in the same step durations in all separation cycles (including Cycle 1) as defined in Eqs. (23), (25), and (26). The band front positions of the trapped component during both steps of the column loading stage ($x_{B,Des}^{load}$, $x_{B,As}^{load}$) were selected to be 30% of one column length (0.3 L_c). In the separation stage, the band front position at the end of each Des step ($x_{B,Des}^{sep}$) was 0.7 L_c. At the end of each As step in the separation stage, the band front returned to its initial position after loading ($x_{B,As}^{sep} = x_{B,As}^{load} = 0.3\ L_c$). The feed concentration was 2.45 mg ml^{-1} (each paraben).

In Experiment 2, the feed mixture consisted of MP, EP, and PP with EP as the trapped component. Here, the band positions at the ends of both steps in the column loading and separation stages were equal ($x_{B,Des}^{sep} = x_{B,As}^{sep}$; $x_{B,Des}^{load} = x_{B,As}^{load}$). A higher feed concentration of 6.67 mg ml^{-1} (each paraben) was used at a lower column loading. The band front positions at the end of the column loading stage

($x_{B,Des}^{load}$, $x_{B,As}^{load}$) were selected to be 10% of one column length (0.1 L_c). The band front positions at the end of each step of the separation stage ($x_{B,Des}^{sep}$, $x_{B,As}^{sep}$) were 0.5 L_c.

The biphasic solvent system and remaining unit operating parameters (upper/lower phase volume ratio, rotational speed, and flow rate) were selected based on previous results. A screening study found that the four parabens exhibit partition coefficients in the preferred "sweet spot" range of 0.25–4 in the solvent system ARIZONA N (n-heptane/ethyl acetate/methanol/water 1/1/1/1 v/v/v/v) [17]. Another prior study with the ARIZONA solvent system family found that a rotational speed of 1700 rpm provides satisfactory column performance within the equipment's operating limits [5,16,17]. To obtain similar efficiencies and solvent consumption in both elution modes, the columns were initially filled with an upper/lower phase volume ratio of 50/50. Additionally, the same flow rate was used in both modes. At 1700 rpm, the maximum mobile phase flow rate to maintain the 50/50 phase volume ratio in both modes is 21 ml min^{-1} [16,17]. To achieve high column efficiency and fast separation, flow rates of 21 and 20 ml min^{-1} were selected for Experiments 1 and 2, respectively, for all stages of the process.

Partition coefficients of the four parabens were determined via pulse injection experiments at 20 and 21 ml min^{-1} in As and Des mode and summarized in Table 3. Shake flask measurements from

45
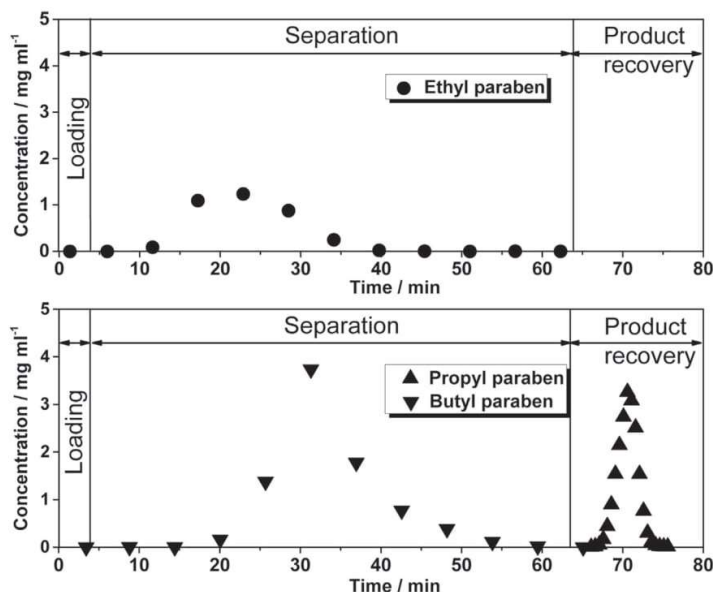
Fig. 4. Average product stream concentrations during each Des (top) and As (bottom) step during the column loading and separation stages and concentration profile obtained from fractions collected during the product recovery stage of trapping MDM CPC Experiment 1 (see Table 4 for operating parameters).
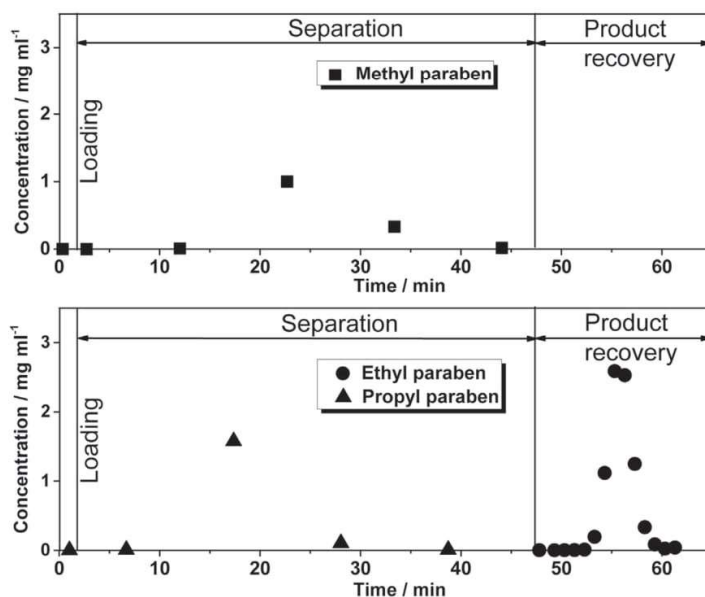
Fig. 5. Average product stream concentrations during each Des (top) and As (bottom) step during the column loading and separation stages and concentration profile obtained from fractions collected during the product recovery stage of trapping MDM CPC Experiment 2 (see Table 4 for operating parameters).

a previous publication from the group [17] are presented for comparison.

In comparison with the shake flask data, higher partition coefficients were generally obtained by pulse injections with the greatest deviations in As mode. It should be noted that the Des and As pulse injection values do not fulfill the relationship $K_k^{Des} = 1/K_k^{As}$, indicating differences in the column hydrodynamics between the two modes [23]. It is likely that back-mixing of the mobile phase is occurring [23,24], causing later elution than predicted by the shake flask partition coefficients and therefore the higher partition coefficient values measured by the pulse injection method. In the interest of obtaining a better description of the trapping MDM CPC process on the device used in this study, the pulse injection partition coefficients were used as input values in the short-cut

method design equations. However, in systems that do not exhibit back-mixing/short-circuiting phenomena, the simpler shake flask method would be the preferred measurement technique, since the resulting partition coefficients would be able to accurately describe retention behavior.

Following selection of the operating parameters and determination of the partition coefficients as detailed in the preceding paragraphs, the step durations during the column loading and separation stages and the theoretical number of separation stage steps were calculated from the equations in Table 2. In both experiments, each cycle was started in Des mode and the product recovery stage was performed as an extended As step. The operating parameters for Experiments 1 and 2 are summarized in Table 4.

The complete product streams in Des and As mode were collected during each cycle of the column loading and separation stages. Aliquots were taken and analyzed via HPLC to give the average concentration of the product stream in each step. During the product recovery stage, fractions from the As product stream were collected every 30 s (Experiment 1) or 60 s (Experiment 2). The average concentration of each component in the Des and As product streams in each cycle of the column loading and separation stages, as well as the concentration profiles during the product recovery stage, are found in Figs. 4 and 5 for Experiments 1 and 2, respectively. During the experiments, the separation and product recovery stages were continued until complete elution of the expected components as indicated by the UV–vis signals.

The HPLC results indicate that three pure product streams were obtained in both experiments. In Experiment 1, no solutes were detected during the column loading stage, while only EP and BP were identified in the Des and As streams of the separation stage, respectively (see Fig. 3). During the product recovery stage in As mode, only the trapped component PP was found. The theoretical number of separation stage steps as predicted by the short-cut method were seven (Des mode) and six (As mode). During the experiment, eleven and ten steps were performed in Des and As mode, respectively. As expected (see Section 4.2), more steps were needed to complete the separation stage during the experiment than calculated under the ideal assumptions of the short-cut method. Analysis of the fractions collected during the product recovery stage indicated a trapped component (PP) purity of >99.9% and a yield >96.5%. The fact that full PP recovery was not achieved is likely due to measurement uncertainties arising from the dilution of the collected fractions. Since PP was not present in the Des and As mode product streams during the column loading and separation stages, it can be concluded that 100% of the injected PP remained trapped in the columns during this time and was fully recovered during the product recovery stage.

A successful ternary separation was also achieved in Experiment 2. As in Experiment 1, only single components eluted during the Des and As steps of the column loading and separation stages (MP and PP, respectively). As a result of lower column loading and longer step durations during the separation stage in comparison with Experiment 1, the short-cut method predicted that only five Des and two As separation stage steps were needed for the complete elution of MP and PP. During Experiment 2, the UV–vis signal indicated that both MP and PP had fully eluted after five Des separation stage steps (corresponding to four As steps), at which point the extended As step for the product recovery stage was begun. In this case, the theoretical number of steps calculated with the short-cut method agreed with those determined experimentally. This could be attributed to the longer step durations and fewer cycles in Experiment 2 in comparison with Experiment 1. Every elution mode switch results in disruption of the hydrodynamic equilibrium between the upper and lower phases within the columns. When fewer cycles are needed, fewer of these disruptions occur. Additionally, longer step times allow more time for reestablish-

ment of hydrodynamic equilibrium before the next elution mode switch occurs. As a result of these two factors, operation closer to the ideal assumptions of the short-cut method is obtained, and with it a more accurate prediction of the real process. Analysis of the collected fractions from the product recovery stage indicated that only pure EP, the intermediately-eluting target component, was obtained with a purity of 99.3% and yield >97.0%. As in Experiment 1, incomplete EP recovery was likely due to measurement uncertainties, since EP was not detected in the MP and PP product streams.

The results of Experiments 1 and 2 confirm the feasibility of the trapping MDM CPC technique for the full recovery of an intermediately-eluting target component in pure form, as well as the applicability of the presented short-cut method for selection of the operating parameters. However, it is recognized that the maximum throughput of the trapping MDM CPC technique was likely not attained in the experiments comprising this work. Determination of the operating parameters for maximum throughput under a given set of purity requirements is addressed by the group in a subsequent publication [21].

5. Conclusion

In this study, two-column trapping MDM CPC was presented as a technique for the recovery of intermediately-eluting components from ternary mixtures in pure form. During this process, the intermediately-eluting component remains "trapped" in the columns while the other components are eluted from opposite ends of the two columns. A trapping MDM CPC separation consists of three process stages: column loading, separation, and product recovery.

A short-cut method for the design of trapping MDM CPC separations was derived. The underlying mathematical model was based on constraints on the distances traveled by the component bands during each stage under equilibrium theory assumptions. Given the flow rates, phase volumes within the columns, partition coefficients, and band front positions of the trapped component at the end of the Des and As steps in the column loading and separation stages, the step durations and number of separation stage steps can be easily calculated.

For the proof-of-concept, trapping MDM CPC experiments were carried out for the separation of two different ternary paraben mixtures. The operating parameters were selected using the proposed short-cut method. It was demonstrated that trapping MDM CPC offers great potential as an alternative to batch pulse injections. 35% of the total column volume was loaded with feed solution, and pure product fractions were obtained at high yield despite low separation factors of approximately 1.5. In both experiments, the intermediately-eluting components remained trapped in the columns during the column loading and separation stages and were collected in pure form in the product recovery stage as desired. As a priori predicted with the short-cut method, the early- and late-eluting components of the ternary mixture eluted in pure form at opposite ends of the two-column setup during the separation stage.

The further potential of this technique is demonstrated in a subsequent publication from the group [21] in which the mathematical short-cut method is implemented as part of a simulation-based strategy for throughput maximization in trapping MDM CPC. The simulations, based on the equilibrium cell model, take the effects of dispersion and mass transfer on separation performance into account. The simulation results are then validated experimentally. Additionally, a preliminary simulation-based comparison of the performance of trapping MDM CPC and stacked isocratic pulse injections is presented.

Acknowledgement

Appendix A. Supplementary data

Supplementary data associated with this article can be found, in the online version, at http://dx.doi.org/10.1016/j.chroma.2017.03.039.

References

[1] J.B. Friesen, J.B. McAlpine, S.-N. Chen, G.F. Pauli, Countercurrent separation of natural products: an update, J. Nat. Prod. 78 (2015) 1765–1796.

[2] A. Berthod, M.J. Ruiz-Angel, S. Carda-Broch, Elution-Extrusion countercurrent chromatography. Use of the liquid nature of the stationary phase to extend the hydrophobicity window, Anal. Chem. 75 (2003) 5886–5894.

[3] M. Agnely, D. Thiébaut, Dual-mode high-speed counter-current chromatography: retention: resolution and examples, J. Chromatogr. A 790 (1997) 17–30.

[4] P. Hewitson, S. Ignatova, H. Ye, L. Chen, I. Sutherland, Intermittent counter-current extraction as an alternative approach to purification of Chinese herbal medicine, J. Chromatogr. A 1216 (2009) 4187–4192.

[5] E. Hopman, J. Goll, M. Minceva, Sequential centrifugal partition chromatography: a new continuous chromatographic technology, Chem. Eng. Technol. 35 (2012) 72–82.

[6] Y. Cheng, M. Zhang, Q. Liang, G. Luo, Two-step preparation of ginsenoside-Re, Rb₁ Rc and Rb₂ from the root of *Panax ginseng* by high-performance counter-current chromatography, Sep. Purif. Technol. 77 (2011) 347–354.

[7] F. Yang, J. Quan, T.Y. Zhang, Y. Ito, Multidimensional counter-current chromatographic system and its application, J. Chromatogr. A 803 (1998) 298–301.

[8] J. Meng, Z. Yang, H. Zhou, S. Wu, Comprehensive multi-channel multi-dimensional counter-current chromatography for separation of tanshinones from *Salvia miltiorrhiza* Bunge, J. Chromatogr. A 1323 (2014) 73–81.

[9] M. Englert, L. Brown, W. Vetter, Heart-cut two-dimensional countercurrent chromatography with a single instrument, Anal. Chem. 87 (2015) 10172–10177.

[10] Y. Yang, H.A. Asia, Y. Ito, Mathematical model of computer-programmed intermittent dual countercurrent chromatography applied to hydrostatic and hydrodynamic equilibrium systems, J. Chromatogr. A (2009) 6310–6318.

[11] S. Ignatova, P. Hewitson, B. Mathews, I. Sutherland, Evaluation of dual flow counter-current chromatography and intermittent counter-current extraction, J. Chromatogr. A 1216 (2011) 6102–6106.

[12] P. Aihua, Y. Haoyu, H. Shichao, Z. Shijie, L. Shucai, C. Lijuan, Separation of honokiol and magnolol by intermittent counter-current extraction, J. Chromatogr. A 1217 (2010) 5935–5939.

[13] P. Hewitson, S. Ignatova, I. Sutherland, Intermittent counter-current extraction −Effect of the key operating parameters on selectivity and throughput, J. Chromatogr. A 1218 (2011) 6053–6060.

[14] E. Hopmann, M. Minceva, Separation of a binary mixture by sequential centrifugal partition chromatography, J. Chromatogr. A 1229 (2012) 140–147.

[15] J. Völkl, W. Arlt, M. Minceva, Theoretical study of sequential centrifugal partition chromatography, AIChE J. 59 (2013) 241–249.

[16] J. Goll, A. Frey, M. Minceva, Study of the separation limits of continuous solid support free liquid-liquid chromatography: separation of capsaicin and dihydrocapsaicin by centrifugal partition chromatography, J. Chromatogr. A 1284 (2013) 59–68.

[17] J. Goll, M. Minceva, Continuous fractionation of multicomponent mixtures with sequential centrifugal partition chromatography, AIChE J. 10.1002/aic. 15529.

[18] Y.W. Lee, Dual counter-current chromatography − its applications in natural products research, J. Chromatogr. A 538 (1991) 37–44.

[19] N. Mekaoui, J. Chamieh, V. Dugas, C. Demesmay, A. Berthod, Purification of Coomassie Brilliant Blue G-250 by multiple dual mode countercurrent chromatography, J. Chromatogr. A 1232 (2012) 134–141.

[20] N. Mekaoui, A. Berthod, Using the liquid nature of the stationary phase. VI. Theoretical study of multi-dual mode countercurrent chromatography, J. Chromatogr. A 1218 (2011) 6061–6071.

[21] R. Morley, M. Minceva, Trapping Multiple Dual Mode Centrifugal Partition Chromatography for the Separation of Intermediately-eluting Components: Throughput Maximization. Submitted Manuscript, 2016.

[22] J. Goll, G. Audo, M. Minceva, Comparison of twin-cell centrifugal partition chromatographic columns with different cell volume, J. Chromatogr. A 1406 (2015) 129–135.

[23] L. Marchal, A. Foucault, G. Patissier, J.M. Rosant, J. Legrand, Influence of flow patterns on chromatographic efficiency in centrifugal partition chromatography, J. Chromatogr. A 869 (2000) 339–352.

[24] S. Adelmann, T. Baldhoff, B. Koepcke, G. Schembecker, Selection of operating parameters on the basis of hydrodynamics in centrifugal partition chromatography for the purification of nybomycin derivatives, J. Chromatogr. A 1274 (2013) 54–64.

Supplementary material

Sample calculation of entrapment CPC operating parameters using the mathematical short-cut method

Experiment 2:

- Component A = MP   (elution in Des mode)
- Component B = EP   (trapped component)
- Component C = PP   (elution in As mode)

Set/determine values for:	
• Phase volumes, single column (V_U, V_L)	$V_U = V_L = 0.5V_C = 0.5 \cdot 123.5 \; ml = 61.75 \; ml$
• Flow rates (F_U, F_L)	$F_U = F_L = 20 \; ml \; min^{-1}$
• Partition coefficients $(K_k^{Des}, K_k^{As}; \; k = A, B, C)$	$K_A^{Des} = 0.90, K_B^{Des} = 1.26, K_C^{Des} = 1.90$ $(K_A^{Des} < K_B^{Des} < K_C^{Des})$ $K_A^{As} = 1.75, K_B^{As} = 1.07, K_C^{As} = 0.63$ $(K_A^{As} > K_B^{As} > K_C^{As})$
• Starting elution mode	Descending

Set values for:	
• Trapped component band front positions, column loading stage $(x_{B,Des}^{load}, x_{B,As}^{load})$	$x_{B,Des}^{load} = 0.1L_C \; cm, \; x_{B,As}^{load} = 0.1L_C \; cm$
• Trapped component band front positions, separation stage $(x_{B,Des}^{sep}, x_{B,As}^{sep})$	$x_{B,Des}^{sep} = 0.5L_C \; cm, x_{B,As}^{sep} = 0.5L_C \; cm$

Calculate step durations during the column loading stage for:		
• Descending mode (t_{Des}^{load})	Eq. 18	$t_{Des}^{load} = x_{B,Des}^{load} \dfrac{(V_L + K_B^{Des}V_U)}{F_L L_c}$ $= 0.1L_C \; cm \dfrac{61.75 \; ml + 1.26 \cdot 61.75 \; ml}{20 \; ml \; min^{-1} \cdot L_c \; cm}$ $= 0.70 \; min$
• Ascending mode (t_{As}^{load})	Eq. 19	$t_{As}^{load} = x_{B,As}^{load} \dfrac{V_U + K_B^{As}V_L}{F_U L_c}$ $= 0.1L_C \; cm \dfrac{61.75 \; ml + 1.07 \cdot 61.75 \; ml}{20 \; ml \; min^{-1} \cdot L_c \; cm}$ $= 0.64 \; min$

Calculate step durations during the separation stage for:	

- Descending mode step of the first cycle ($t_{Des}^{sep,1st}$)

$$t_{Des}^{sep,1st} = \left(x_{B,Des}^{sep} - x_{B,Des}^{load}\right)\frac{V_L + K_B^{Des}V_U}{F_L L_c}$$

Eq. 23

$$= (0.5 L_c\ cm$$
$$- 0.1 L_c\ cm)\frac{61.75\ ml + 1.26 \cdot 61.75\ ml}{20\ ml\ min^{-1} \cdot L_c\ cm}$$
$$= 2.79\ min$$

- All subsequent descending mode steps (t_{Des}^{sep})

$$t_{Des}^{sep} = \left[\left(x_{B,Des}^{sep} - x_{B,Des}^{load}\right) + \left(x_{B,As}^{sep} - x_{B,As}^{load}\right)\right]\frac{V_L + K_B^{Des}V_U}{F_L L_c}$$

Eq. 25

$$= [(0.5 L_c\ cm - 0.1 L_c\ cm)$$
$$+ (0.5 L_c\ cm$$
$$- 0.1 L_c\ cm)]\frac{61.75\ ml + 1.26 \cdot 61.75\ ml}{20\ ml\ min^{-1} \cdot L_c\ cm}$$
$$= 5.57\ min$$

- All ascending mode steps (t_{As}^{sep})

$$t_{As}^{sep} = \left[\left(x_{B,Des}^{sep} - x_{B,Des}^{load}\right) + \left(x_{B,As}^{sep} - x_{B,As}^{load}\right)\right]\frac{V_U + K_B^{As}V_L}{F_U L_c}$$

Eq. 26

$$= [(0.5 L_c\ cm - 0.1 L_c\ cm)$$
$$+ (0.5 L_c\ cm$$
$$- 0.1 L_c\ cm)]\frac{61.75\ ml + 1.07 \cdot 61.75\ ml}{20\ ml\ min^{-1} \cdot L_c\ cm}$$
$$= 5.11\ min$$

Calculate the theoretical number of separation stage steps for:
- Descending mode (n_{Des}^{sep})

$$t_{As}^{load} = \Delta x_{A,As}^{load}\frac{\left(V_U + K_A^{As}V_L\right)}{F_U L_c} \rightarrow \Delta x_{A,As}^{load}$$

Eq. 15

$$= t_{As}^{load}\frac{F_U L_c}{\left(V_U + K_A^{As}V_L\right)}$$
$$= 0.64\ min\ \frac{20\ ml\ min^{-1}L_c\ cm}{61.75\ ml + 1.75 \cdot 61.75\ ml}$$
$$= 0.08 L_c\ cm$$

Eq. 27 $\quad \Delta x_{A,net}^{process} = x_{A,As}^{load} + L_c = 0.08 L_c\ cm + L_c\ cm = 1.08 L_c\ cm$

$$\Delta x_{A,net}^{sep,1st} = t_{Des}^{sep,1st}\frac{F_L L_c}{V_L + K_A^{Des}V_U} - t_{As}^{sep}\frac{F_U L_c}{V_U + K_A^{As}V_L}$$

Eq. 29

$$= 2.79\ min\ \frac{20\ ml\ min^{-1}L_c\ cm}{61.75\ ml + 0.90 \cdot 61.75\ ml}$$
$$- 5.11\ min\ \frac{20\ ml\ min^{-1}L_c\ cm}{61.75\ ml + 1.75 \cdot 61.75\ ml}$$
$$= -0.13 L_c\ cm$$

Eq. 33

$$\Delta x_{A,net}^{sep} = t_{Des}^{sep} \frac{F_L L_C}{V_L + K_A^{Des} V_U} - t_{As}^{sep} \frac{F_U L_C}{V_U + K_A^{As} V_L}$$

$$= 5.57 \, min \frac{20 \, ml \, min^{-1} L_c \, cm}{61.75 \, ml + 0.90 \cdot 61.75 \, ml}$$

$$- 5.11 \, min \frac{20 \, ml \, min^{-1} L_c \, cm}{61.75 \, ml + 1.75 \cdot 61.75 \, ml}$$

$$= 0.35 L_C \, cm$$

Eq. 35

$$n_{Des}^{sep} \geq \frac{\Delta x_{A,net}^{process} - \Delta x_{A,net}^{sep,1st}}{\Delta x_{A,net}^{sep}} + 1$$

$$= \frac{1.08 L_c \, cm - (-0.13 L_c \, cm)}{0.35 L_c \, cm} + 1$$

$$= 4.46 \, steps \rightarrow 5 \, steps$$

- Ascending mode (n_{As}^{sep})

Eq. 14

$$t_{Des}^{load} = \Delta x_{C,Des}^{load} \frac{\left(V_L + K_C^{Des} V_U\right)}{F_L L_C} \rightarrow \Delta x_{C,Des}^{load}$$

$$= t_{Des}^{load} \frac{F_U L_C}{\left(V_U + K_C^{Des} V_L\right)}$$

$$= 0.70 \, min \frac{20 \, ml \, min^{-1} L_c \, cm}{61.75 \, ml + 1.90 \cdot 61.75 \, ml}$$

$$= 0.08 L_c \, cm$$

Eq. 28

$$\Delta x_{C,net}^{process} = x_{C,Des}^{load} + L_c = 0.08 L_c \, cm + L_c \, cm$$

$$= 1.08 L_c \, cm$$

Eq. 31

$$\Delta x_{C,net}^{sep,1st} = t_{Des}^{sep,1st} \frac{F_L L_C}{V_L + K_C^{Des} V_U} - t_{As}^{sep} \frac{F_U L_C}{V_U + K_C^{As} V_L} =$$

$$= 2.79 \, min \frac{20 \, ml \, min^{-1} L_c \, cm}{61.75 \, ml + 1.90 \cdot 61.75 \, ml}$$

$$- 5.11 \, min \frac{20 \, ml \, min^{-1} L_c \, cm}{61.75 \, ml + 0.63 \cdot 61.75 \, ml}$$

$$= 0.70 L_c \, cm$$

Eq. 34

$$\Delta x_{C,net}^{sep} = t_{As}^{sep} \frac{F_U L_C}{V_U + K_C^{As} V_L} - t_{Des}^{sep} \frac{F_L L_C}{V_L + K_C^{Des} V_U}$$

$$= 5.11 \, min \frac{20 \, ml \, min^{-1} L_c \, cm}{61.75 \, ml + 0.63 \cdot 61.75 \, ml}$$

$$- 5.57 \, min \frac{20 \, ml \, min^{-1} L_c \, cm}{61.75 \, ml + 1.90 \cdot 61.75 \, ml}$$

$$= 0.39 L_c \, cm$$

Eq. 36

$$n_{As}^{sep} \geq \frac{\Delta x_{C,net}^{process} - \Delta x_{C,net}^{sep,1st}}{\Delta x_{C,net}^{sep}} + 1$$

$$= \frac{1.08 L_c \, cm - 0.70 L_c \, cm}{0.39 L_c \, cm} + 1$$

$$= 1.95 \, steps \rightarrow 2 \, steps$$

3.2 Paper II

Trapping multiple dual mode centrifugal partition chromatography for the separation of intermediately-eluting components: Throughput maximization strategy

<u>Author contribution</u>: The thesis author held the primary role in this investigation, including conceptualization, methodology design, development of the gPROMS model, experiment execution, and results analysis. She both wrote and edited the manuscript.

<u>Summary</u>: In Paper II, the short-cut model validated in Paper I was integrated into a comprehensive model-based design approach for throughput maximization. The approach takes process limitations associated with the system thermodynamics and hydrodynamics into account as well as uses simulations to predict band broadening effects and performance.

As in Paper I, a model feed mixture of three parabens (1:1:1) was used with ethylparaben as the intermediately-eluting target. Stringent purity and yield requirements of ≥99% were set. Preliminary measurements found the limit of the linear range to be a feed concentration (i.e., all three parabens with respect to the combined volume of the two phases) of approximately 30 mg ml^{-1}. The stationary phase retention experiments were performed in the presence of the 30 mg ml^{-1} feed solution, identifying a maximum flow rate of 12 ml min^{-1} for maintenance of S_f=0.5. This flow rate was well below that obtained for the pure phases, which was attributed to the two-fold increase in settling time at a 30 mg ml^{-1} feed concentration. No significant change in the phase volume ratio was observed within this concentration range.

The short-cut model was used as a preliminary operating parameter selection tool and coupled with a time-saving iterative strategy for identification of the step durations resulting in the highest throughput predicted by equilibrium stage model simulations. Good agreement was found between the simulated and experimental results, and no stationary phase loss occurred. The loaded feed volume was approximately 52% of the total column volume, over 10-fold greater than the 5% column volume loading maximum often recommended for LLC batch injections [24]. The target ethylparaben was obtained at 99.5% purity and 98.4% yield.

A comparison of the simulated separation performance of the trapping MDM separation at maximized throughput and an equivalent stacked batch injection process was made. Trapping MDM achieved a 1.7-fold higher productivity and 40% lower solvent consumption. The results demonstrated trapping MDM to be a viable alternative to batch injections for the high-throughput isolation of intermediately-eluting compounds from ternary mixtures. However, a generalized description of the range of separation tasks for which the use of trapping MDM is advantageous remained to be determined. This topic formed the basis of Paper III.

Trapping multiple dual mode centrifugal partition chromatography for the separation of intermediately-eluting components: Throughput maximization strategy☆

Raena Morley, Mirjana Minceva *

Biothermodynamics, TUM School of Life Sciences Weihenstephan, Technical University of Munich, Maximus-von-Imhof-Forum 2, 85354 Freising, Germany

ARTICLE INFO

ABSTRACT

Trapping multiple dual mode centrifugal partition chromatography (trapping MDM CPC) is an alternative to isocratic pulse injections for the separation of intermediately-eluting components from complex mixtures using liquid-liquid chromatography. In this work, a throughput maximization strategy is developed and validated to investigate the full potential of trapping MDM CPC as a preparative technique. In the proposed approach, shake flask and stationary phase retention experiments are used to determine the maximum feed concentration and flow rate, respectively. A model-based parameter selection process combining a mathematical short-cut method and simulations based on the equilibrium cell model is used to obtain the column loading and step durations resulting in maximized process throughput. The proposed throughput maximization strategy is experimentally validated for the separation of a ternary model mixture of parabens. A preliminary comparison of trapping MDM CPC separation performance to that of stacked pulse injections is also made.

© 2017 Elsevier B.V. All rights reserved.

1. Introduction

Liquid-liquid chromatography (LLC) is a preparative separation technique employing the two phases of a liquid-liquid biphasic system as the mobile and stationary phases. Separation is achieved as a result of the differing partitioning behavior of the sample solutes between the two phases. The stationary phase is held in place during operation by means of the column geometry and application of a centrifugal field. LLC devices can be grouped into two main categories: hydrodynamic countercurrent chromatography (CCC) units and hydrostatic centrifugal partition chromatography (CPC) ones.

The presence of a liquid stationary phase in LLC presents several advantages over conventional liquid-solid chromatography techniques, such as no irreversible sample adsorption on the stationary phase, high loading capacity, and the possibility to tailor the stationary phase composition to the desired separation. Additionally, either phase of the biphasic system (upper or lower phase) may be employed as the stationary phase, and the roles of the two phases may even be switched during operation. As a result, a high degree of operational flexibility can be achieved in LLC, which has given rise to a variety of operating modes not realizable with conventional chromatography techniques [1]. One such operating mode, trapping multiple dual mode CPC (trapping MDM CPC), was presented in a previous publication from the group [2].

Trapping MDM CPC allows the preparative recovery of an intermediately-eluting component from a multicomponent mixture, offering an alternative to isocratic pulse injections. Pulse injections often result in overlapping peaks, and, therefore, reduced yield of the intermediately-eluting target component in pure form. In trapping MDM CPC, the feed mixture is loaded between the columns of a two-column set-up. The early- and late-eluting components are obtained at opposite ends of the column during multiple cycles, with each cycle consisting of two steps. These two steps correspond to the two elution modes in LLC: descending (Des) and ascending mode (As). In Des mode, the upper phase is the stationary phase and the lower phase is pumped through the column as the mobile phase. The roles of the phases are reversed in As mode (the upper phase becomes the mobile phase), as are the flow direction and elution order of the feed components. Meanwhile, the intermediately-eluting target component remains "trapped" within the columns. After the early- and late-eluting components have fully eluted, the trapped target compound is recovered in pure form.

The MDM technique was first introduced in [3] for the separation of a feed mixture into two product streams on a single column and has since been implemented for a wide range of (pseudo-)binary separation applications. The MDM technique was further developed for ternary separations using two-column CCC devices as described in [4,5]. In [4], the feed was injected continuously over several cycles, while in [5] injections were made repeatedly and always at the start of a new cycle. In the trapping MDM CPC technique presented in this work, column loading is performed at the start of the process and takes place during a single cycle. A short-cut method for selection of the trapping MDM CPC operating parameters (i.e., step durations) under the requirement of full recovery of the pure target was derived and experimentally validated in a previous publication from the group [2]. In order to explore the full potential of trapping MDM CPC as a preparative separation technique, the focus of this study is maximization of the process throughput. Although several recent publications have addressed throughput maximization in LLC [6–9], none of these have focused on the isolation of an intermediately-eluting component by "trapping" it on the column.

Throughput may be improved by increasing the loaded volume and/or the feed concentration. The loaded volume may be increased by performing repeated injections at certain intervals or by increasing the volume introduced during a single injection or loading step. In binary MDM separations without an intermediately-eluting "trapped" component, it has been shown that repeated loading of the feed may be used to increase the process throughput [3,10,11]. In trapping MDM CPC, repeated injections could be useful in cases where the trapped target component is present at low concentrations in the feed and the separation factors between the target and impurities are high. In this case, the majority if not all of the impurities would elute during a single cycle before the next feed introduction, avoiding the destabilizing effects of high solute concentrations on the column. However, the model mixture implemented in this work is meant to represent the situation often encountered at the end of a multistep downstream processing chain: a concentrated feed solution consisting of the target component and remaining impurities with low separation factors. In this case, repeated injections would lead to high solute concentrations within the column, especially near the site of injection.

The feed concentration is limited by the sample solubility as well as the effects of the presence of the solutes on both the thermodynamic equilibrium of the solvent system and the column hydrodynamics. High solute concentrations can result in changes of the partition coefficients and the volumes of the phases. In more extreme cases, a single or third phase (liquid or solid) may be formed. These effects, coupled with the accompanying changes in the phases' physical properties (e.g., density, viscosity, interfacial tension), affect the hydrodynamics within the column and can lead to stationary phase loss [8,12,13]. Prediction of the cumulative effects of the abovementioned changes would require full characterization of the system thermodynamics and hydrodynamics as a function of solute concentration. This task would require extensive experimental effort and/or the development of complex mathematical models. Therefore, in this work, a simplified approach for the selection of the column loading parameters was developed.

In addition to the column loading parameters, the flow rates and step durations during the trapping MDM CPC separation must also be selected. In the interest of processing the largest feed solute quantity in the shortest amount of time, flow rates should be as high as possible while still maintaining stable operating conditions (e.g., no stationary phase loss, not exceeding pressure drop limitations). The short-cut method derived in [2] can be used to facilitate selection of the step durations. Although a helpful starting point in trapping MDM CPC design, the short-cut method is fully valid only under ideal conditions (i.e., in the absence of band broaden-

ing effects). Separation performance under real conditions must be determined experimentally or predicted with the use of models taking band broadening effects into account.

Various models have been used for the description of LLC processes in the presence of band broadening, such as the equilibrium cell model of Martin and Synge [14–16], the countercurrent distribution model [17], the non-equilibrium (longitudinal mixing) cell model [18], and the plug flow with axial dispersion model [19,20]. In this work, simulations based on the equilibrium cell model were employed to evaluate separation performance with the parameters determined by the short-cut method.

The objective of this work is to provide a structured approach to selection of the operating parameters leading to maximized throughput in trapping MDM CPC. Completion of this objective comprised the following tasks:

- Experimental determination of the maximum applicable feed concentration and corresponding maximum applicable flow rate.
- Development of a model-based throughput maximization strategy incorporating the short-cut method for operating parameter selection introduced in [2] and simulations based on the equilibrium cell model.
- Experimental validation of the proposed model-based design approach.
- Comparison of trapping MDM CPC performance to that of isocratic pulse injections.

A model feed mixture consisting of three parabens (methyl paraben, ethyl paraben, and propyl paraben) was used to facilitate the theoretical development of the throughput maximization strategy. The parabens differ only in their alkyl chain lengths and represent a "difficult" separation (low separation factors). Ethyl paraben was the intermediately-eluting target component to be trapped and later recovered.

2. Theory

2.1. Principle of trapping MDM CPC

The principle of the trapping MDM CPC operating mode is described in detail in [2] and is revisited here for convenience.

The separation objective in trapping MDM CPC is the recovery of an intermediately-eluting target component from a complex mixture in pure form. This separation can be viewed as a pseudo-ternary separation represented by the components A, B, and C, with B as the intermediately-eluting target. The partition coefficients of the three components can be relatively defined as $K_A^{Des} < K_B^{Des} < K_C^{Des}$ in Des mode or $K_A^{Asc} > K_B^{Asc} > K_C^{Asc}$ in As mode. B will remain trapped inside the CPC unit while A and C elute from the two column ends in Des and As mode, respectively, allowing the recovery of pure B at the end of the process.

Due to the cyclic nature of the trapping MDM CPC process, a unit consisting of two hydrostatic CPC columns and four pumps (two for mobile phase and two for feed; one of each running in each mode) is used. Trapping MDM CPC consists of three process stages: column loading, separation, and product recovery. A schematic representation of the process (first appearing in [2] and re-printed here for clarity) is found in Fig. 1.

In the loading stage (Fig. 1a), the feed is introduced between the two columns during a single cycle, designated as Cycle 0. In Des mode, the lower phase feed solution is fed into the left-hand column, while in As mode, the upper phase feed solution is pumped into the right-hand column. There is no accompanying flow of pure mobile phase during feed introduction.
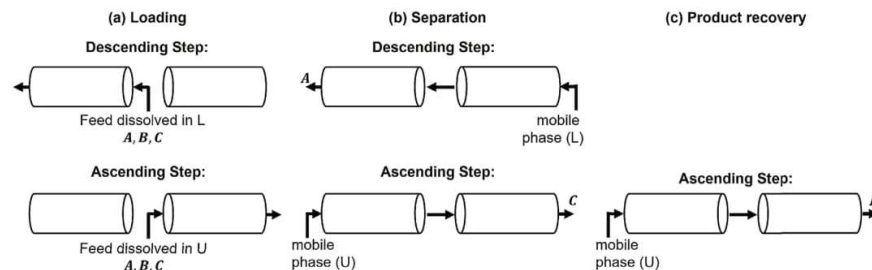
Fig. 1. Schematic representation of the three trapping MDM CPC process stages ((a) column loading, (b) separation, and (c) product recovery) for the separation of a ternary mixture of components A, B, and C. (L: lower phase, U: upper phase).
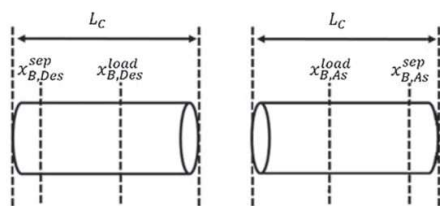

Fig. 2. Notation convention for the trapping MDM CPC short-cut method equations.

The separation stage (Fig. 1b) is begun immediately following completion of the column loading cycle. It consists of multiple cycles of Des and As steps, with the first cycle designated as Cycle 1. In Des mode, A travels fastest toward the outlet (left-hand side of the two-column set-up). Before B reaches the end of the column, a switch to As mode is made, reversing the flow direction and elution order. C now moves fastest through the column, and will elute from the right-hand side of the two-column set-up. Again, the elution mode is switched at some point before B begins to elute from column. B remains trapped inside the columns during the entire separation stage. The separation stage is complete when A and C have fully eluted, leaving only B behind at high purity.

The purified intermediately-eluting target component B is collected during the product recovery stage (Fig. 1c). This stage consists of one extended Des or As step. The recovery stage ends when B has fully eluted from the column.

2.2. Short-cut method for operating parameter selection

A mathematical short-cut method was derived in a previous publication from the group for determination of the durations of the Des and As steps in the column loading and separation stages (t_{Des}^{load}, t_{As}^{load}, t_{Des}^{sep}, t_{As}^{sep}) [2]. The short-cut method is applicable to the complete separation and recovery (100% purity and yield) of intermediately-eluting component B from the simplified ternary system of A, B, and C described in Section 2.1 under ideal conditions (i.e., in the absence of band broadening effects).

The following parameters are required as input for the short-cut method: volumes of upper and lower phases in a single column of the two-column set-up (V_U, V_L), flow rates in As and Des mode (F_U, F_L), length of a single column (L_c), and partition coefficients of the mixture components (K_k^{As}, K_k^{Des}). Additionally, the positions of the trapped component (B) band fronts at the end of the column loading ($x_{B,Des}^{load}$, $x_{B,As}^{load}$) and separation stage steps ($x_{B,Des}^{sep}$, $x_{B,As}^{sep}$) must be assigned. It is assumed that all operating parameters (F_U, F_L, V_U, V_L) as well as the partition coefficients for all compounds (K_k^{Des}, K_k^{As}) remain constant during all process stages. For the sake of clarity, the notation convention for the short-cut method equations is graphically depicted in Fig. 2.

Table 1
Trapping MDM CPC short-cut method equations for calculation of the process step durations.

Process stage	Step duration equation
Column loading	$t_{Des}^{load} = \dfrac{x_{B,Des}^{load} \cdot \left(V_L + K_B^{Des} V_U\right)}{F_L L_c}$
	$t_{As}^{load} = \dfrac{x_{B,As}^{load} \cdot \left(V_U + K_B^{As} V_L\right)}{F_U L_c}$
Separation	$t_{Des}^{sep,1st} = \left(x_{B,Des}^{sep} - x_{B,Des}^{load}\right) \cdot \dfrac{V_L + K_B^{Des} V_U}{F_L L_c}$
	$t_{As}^{sep,1st} = \left(x_{B,As}^{sep} - x_{B,As}^{load}\right) \cdot \dfrac{V_U + K_B^{As} V_L}{F_U L_c}$
	$t_{Des}^{sep} = \left[\left(x_{B,Des}^{sep} - x_{B,Des}^{load}\right) + \left(x_{B,As}^{sep} - x_{B,As}^{load}\right)\right] \cdot \dfrac{V_L + K_B^{Des} V_U}{F_L L_c}$
	$t_{As}^{sep} = \left[\left(x_{B,Des}^{sep} - x_{B,Des}^{load}\right) + \left(x_{B,As}^{sep} - x_{B,As}^{load}\right)\right] \cdot \dfrac{V_U + K_B^{As} V_L}{F_U L_c}$

The short-cut method equations for calculation of the step durations are summarized in Table 1. The full derivation of these equations, as presented in [2], can be found in the Supplementary data (Appendix A). By defining the band front positions as a fraction of the column length, the term L_c can be canceled out of the model equations.

The short-cut method presents a quick, simplified method for the initial selection of the step durations. However, selection of the trapped component band front positions x_B^{load} and x_B^{sep} is not necessarily straightforward. Maximization of the process throughput requires consideration of and compromise between the following factors:

- High column loading should be attained (improved by increasing x_B^{load}).
- Long step durations are desired during the separation stage to take full advantage of the virtual column-lengthening effect of the process as well as to reduce the frequency of switching between the Des and As modes and the total number of separation cycles (improved by decreasing x_B^{load} or increasing x_B^{sep}).
- Short step durations are desired during the separation stage to compensate for broadening of the trapped component band (improved by decreasing x_B^{sep} for a fixed x_B^{load}).

A more in-depth discussion of the interdependence of these factors is found in [2]. Separation performance under non-ideal conditions may be evaluated with simulations based on models accounting for band broadening effects. In Section 4.1.4, an approach combining the short-cut method with simulations based on the equilibrium cell model is described for determination of the best compromise between x_B^{load} and x_B^{sep}.
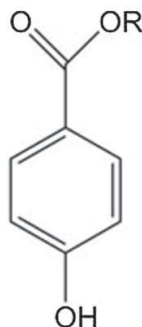
Fig. 3. Paraben molecular structure ($R_{MP} = -CH_3$, $R_{EP} = -CH_2-CH_3$, and $R_{PP} = -CH_2-CH_2-CH_3$).

2.3. Modeling and simulation of trapping MDM CPC

The trapping MDM CPC process was modeled with Martin and Synge's equilibrium cell model [21], also known as the stage or plate model. The analytical solution has been implemented for the modeling of MDM separations in [10,11,22]. In this work, instead of the analytical solution, a numerical solver is used for simultaneous solution of the model equations at each simulated time step to obtain temporal resolution of the concentration profiles of the mixture solutes inside the column (i.e., concentration in each equilibrium cell) as well as at the column outlets. The same approach has been successfully implemented for the prediction of separation performance in sequential centrifugal partition chromatography (sCPC) [15,16]. The equilibrium cell model assumptions and equations for the two-column CPC set-up used in this work are found in [23]. The boundary conditions necessary for modeling and simulation of the trapping MDM CPC process were defined for this work and are presented in Table 2.

3. Materials and methods

3.1. Materials

3.1.1. Chemicals

Methyl paraben (MP; 99%), ethyl paraben (EP; 99%), and propyl paraben (PP; 99+%) were purchased from Alfa Aesar GmbH & Co KG (Karlsruhe, Germany). The paraben molecular structure is found in Fig. 3.

The ARIZONA solvents n-heptane ($\geq$99.9%) and ethyl acetate ($\geq$99.5%) were purchased from Merck KGaA (Darmstadt, Germany), while methanol ($\geq$99.3%) was obtained from VWR Chemicals (France). De-ionized water was supplied by the in-house network. HPLC analysis was performed using Millipore 18-MOhm water and methanol (gradient grade for liquid chromatography, $\geq$99.9%) from Merck KGaA (Darmstadt, Germany).

3.1.2. Biphasic system preparation

All shake flask and CPC experiments were conducted using the biphasic solvent system ARIZONA N (n-heptane/ethyl acetate/methanol/water 1/1/1/1 v/v/v/v). This system was selected for the separation of the model components as a result of a previous screening study [9]. After combining the four solvents, the system was left to equilibrate for at least 2 h with stirring at room temperature (22 $\pm$ 2 °C). After equilibration, the upper and lower phases were split into two containers using a separatory funnel. Phases were degassed in an ultrasonic bath before use.

Table 2
Equilibrium cell model boundary conditions for the three trapping MDM CPC stages. Subscript F designates feed.

Process stage(s)	Des mode		As mode	
Column loading	Feed introduced between columns in Des direction	$F_{L,1} = F_{L,F} F_{L,2} = 0 c^L_{k,N_{c,1}=1} = c^L_{k,F}$	Feed introduced between columns in As direction	$F_{U,2} = F_{U,F} F_{L,1} = 0 c^U_{k,1,2} = c^U_{k,F}$
Separation and Product recovery	Mobile phase introduced at end of Column 2	$F_{L,1} = F_{L,2} = F_L$ $C^L_{k,N_{c,2},2} = 0$	Mobile phase introduced at end of Column 1	$F_{U,1} = F_{U,2} = F_U$ $C^U_{k,1,1} = 0$
	Mass balance at junction of Column 1 and Column 2	$F_{L,1} c^L_{k,N_{c,1},1} = F_{L,2} c^L_{k,1,2}$	Mass balance at junction of Column 1 and Column 2	$F_{U,1} c^U_{k,N_{c,1}} = F_{U,2} c^U_{k,1,2}$

3.1.3. CPC unit

CPC experiments (pulse injections, trapping MDM CPC) were performed on a TMB-250 unit from Armen Instrument (Saint-Avé, France). The unit consists of two 125 ml columns mounted on separate rotors in series, four HPLC gradient pumps, two UV-Vis detectors, and two fraction collectors. The maximum rotational speed of the columns is 3000 rpm and the maximum pressure drop is 100 bar. A detailed description of the unit is found in [24]. All experiments were performed at a rotational speed of 1700 rpm, as this speed was previously found to provide satisfactory stationary phase retention and separation efficiency for ARIZONA systems while remaining below the maximum pressure drop [24].

3.2. Experimental methods

3.2.1. Shake flask experiments

Shake flask experiments were performed using the paraben model mixture in the biphasic solvent system ARIZONA N with total global concentrations of the samples ranging from 0 to 80 mg ml^{-1}. MP, EP, and PP were always present in equal global concentrations. In this work, "total concentration" refers to the overall concentration of the three parabens in one phase (upper or lower phase). "Total global concentration" refers to the overall paraben concentration of the biphasic system viewed as a single volume.

All samples were prepared in 15 ml centrifuge tubes and had a measured volume of 10 ml (5 ml each, upper and lower phases). Samples with a total global concentration of 5 mg ml^{-1} or less were prepared by dilution of a stock solution (ARIZONA N lower phase, total concentration 10 mg ml^{-1}). All remaining samples were prepared by weighing the corresponding paraben amounts directly into the centrifuge tubes and then adding the two phases. Samples were left to equilibrate for 2 h at room temperature (22 ± 2 °C) with automatic mixing. The settling time (see Section 3.2.2) and phase volume ratio (see Section 3.2.3) of each sample were then recorded. Lastly, aliquots for HPLC analysis were taken from both phases of the samples and diluted with the same phase when necessary.

3.2.2. Settling time measurements

Settling time with respect to solute concentration was measured using the same samples prepared for the shake flask experiments (see Section 3.2.1). Samples were quickly inverted ten times by hand and then placed in a tube rack. The time needed for full reestablishment of the meniscus between the two phases was measured with a stopwatch. This procedure was repeated three times for each sample.

3.2.3. Phase volume ratio measurements

Phase volume ratios of the samples prepared for the shake flask experiments (see Section 3.2.1) were recorded. The lower phase and total sample volumes were read from the graduation of the centrifuge tubes. The upper phase volume was calculated as (total volume) – (lower phase volume). The phase volume ratio was calculated as (upper phase volume)/(lower phase volume).

3.2.4. Stationary phase retention experiments

Stationary phase retention as a function of flow rate is generally determined in the absence of feed solutes using the upper and lower phases of the solvent system of interest in pure form. However, in this study, it was desired to observe the effect of the loaded feed solution on stationary phase retention.

Feed solutions were prepared from an ARIZONA N biphasic system with a total global concentration of 30 mg ml^{-1} (10 mg ml^{-1} each paraben). The biphasic feed solution was formed by weighing the corresponding paraben amounts and then adding equal volume portions of pure upper and lower phase, previously prepared

as described in Section 3.1.2. The biphasic feed solution was equilibrated for at least 2 h under mixing at room temperature (22 ± 2 °C). The phases were then split into two feed reservoirs using a separatory funnel and degassed in an ultrasonic bath before use.

The CPC unit was prepared by filling the columns with the ARIZONA N biphasic system at a 50/50 upper/lower phase ratio without rotation in order to obtain an initial stationary phase retention, S_f, of 0.5 ($S_f = V_S/V_C$, where V_S and V_C are the stationary phase and total column volumes, respectively). Rotation was then set at 1700 rpm. After the set rotational speed was reached, the feed solution was introduced between the two columns. A feed solution volume of 62.5 ml, corresponding to the mobile phase volume in a single column, was introduced at the start of each experiment. Two series of experiments were performed at room temperature (22 ± 2 °C), one in Des mode and one in As mode. In Des mode, the lower phase feed solution was pumped into the left-hand column, and in As mode, the upper phase feed solution was pumped into the right-hand column, similar to the column loading stage of the trapping MDM CPC process (see Fig. 1a). Immediately following completion of feed loading, pumping of pure mobile phase (lower phase in Des mode; upper phase in As mode) was begun at the same flow rate as during feed introduction and continued until all three components had left the column, as indicated by the signal from the UV-Vis detector. The eluent stream was collected in graduated cylinders during both feed loading and pumping of pure mobile phase. Any loss of the stationary phase was recorded. If no stationary phase loss was observed, a new experiment (i.e., feed loading followed by mobile phase elution) was started at the next highest flow rate. Otherwise, the column was first newly prepared with the 50/50 upper/lower phase volume ratio ($S_f = 0.5$) before loading the feed. Experiments were performed at flow rates of 10, 12, 14, and 16 ml min^{-1}, with each series of experiments started at a flow rate of 10 ml min^{-1}.

3.2.5. Pulse injection experiments for determination of model parameters

Pulse injection experiments were performed at a mobile phase flow rate of 12 ml min^{-1} and rotational speed of 1700 rpm for determination of the equilibrium cell model parameters N_k (number of theoretical stages) and K_k^{Des}, K_k^{As} (partition coefficients). The CPC unit was initially filled with the ARIZONA N biphasic system with a 50/50 upper/lower phase volume ratio ($S_f = 0.5$) without rotation. The feed solutions (dissolved in lower phase in Des mode and upper phase in As mode) had concentrations of 2 mg ml^{-1} of each paraben. Injections were completed with a manual injection valve using a 1 ml sample loop. Two injections were made in each elution mode (Des and As).

3.2.6. Trapping MDM CPC experiment

The CPC unit was initially filled with the ARIZONA N biphasic system with a 50/50 upper/lower phase volume ratio ($S_f = 0.5$) without rotation. The rotational speed was then set at 1700 rpm. The experiment was performed at room temperature (22 ± 2 °C). Feed solutions containing the equilibrium phase concentrations at a total global concentration of 30 mg ml^{-1} were used. Preparation of the feed was as described for the stationary phase retention experiments in Section 3.2.4. The UV-Vis detector signal was recorded at wavelengths of 280 nm and 254 nm. The three process stages were executed as follows:

Column loading: The single loading stage cycle (Cycle 0) consisted of two steps: one in Des mode (5.56 min) followed by one in As mode (5.21 min). The lower and upper phase feed solutions were introduced between the two columns during the Des and As steps, respectively, at a flow rate of 12 ml min^{-1}. There was no accompanying flow of pure mobile phase. The Des and As eluent streams were continuously collected from the two ends of the unit in separate reservoirs. Aliquots for HPLC analysis were taken from each

collected eluent stream for determination of the average paraben concentrations.

Separation: After completion of the loading stage, the separation stage consisting of eight elution cycles (Cycles 1-8) was started. Each cycle began with a Des step followed by an As step. The flow rate in both elution modes was 12 ml min^{-1}. The Des and As step durations were 4.45 min and 4.17 min, respectively, with the exception of the shorter Des step in Cycle 1 (2.22 min). With the exception of Cycle 6, the Des and As eluent streams were collected during each cycle in separate reservoirs. During Cycle 6, fractions were collected every 30 s. Aliquots for HPLC analysis were taken from the collected eluent streams and fractions.

Product recovery: Following completion of Cycle 8 (ending with an As mode step), the recovery cycle (Cycle 9) was started with a Des step (duration of 4.45 min) followed by an extended As step. The flow rate in both elution modes was again 12 ml min^{-1}. The entire eluted volume was collected during the Des step. During the extended As step, product stream fractions were collected every 60 s. Aliquots for HPLC analysis were taken from the Des step stream and the As step fractions. Elution in As mode was continued until the UV-Vis detector signal indicated that all parabens had fully eluted from the column.

3.2.7. HPLC analysis

HPLC analysis was used to determine the concentrations of the three parabens (MP, EP, and PP) in the shake flask experiments as well as in the product stream samples and fractions collected during the trapping MDM CPC experiment.

The Gilson (Middleton, WI, USA) HPLC set-up consisted of a 322H2 binary gradient pump, GX Direct injection module, and 151 UV/VIS Detector. The analysis was controlled by Trilution LC software. A Nucleosil 100-5 C18 column was used (125 mm × 3 mm ID; 5 μm). Analysis of all samples was completed using a water:methanol gradient program with a mobile phase flow rate of 0.8 ml min^{-1} at 23 °C. The injection volume was 10 μl. The gradient program following injection was as follows: 40:60 from 0.0 min to 4.5 min; 38:62 at 5.0 min; 58:42 from 7.5 min to 10.0 min. The detection wavelength was set at 280 nm.

3.2.8. Simulations

Simulation of the trapping MDM CPC process was completed by numerical solution of the equilibrium cell model equations using gPROMS Model Builder v4.2 software from Process Systems Enterprise (London, UK).

4. Results and discussion

The objective of this work was to develop, apply, and validate a model-based design strategy for throughput maximization in trapping MDM CPC. This strategy is described in Section 4.1 and applied for the design of a trapping MDM CPC validation experiment (Section 4.2). A preliminary comparison of trapping MDM CPC performance to that of pulse injections by simulations is then made in Section 4.3.

4.1. Model-based design strategy for throughput maximization in trapping MDM CPC

Trapping MDM CPC is a batch process. Therefore, for maximum throughput, it is desired to load the highest possible amount of the feed components during the loading stage. The loaded amount can be increased by adjusting the feed volume and/or the feed concentration. As mentioned in Section 1, there exist limitations on the maximum applicable feed concentration and volume imposed by the performance requirements, column hydrodynamics, and partition equilibria.

The following subsections detail the design strategy for throughput maximization of trapping MDM CPC applied in this work. The first step is determination of the maximum feed concentration (Section 4.1.1). Next, the maximum applicable flow rate in the presence of this feed concentration is determined (Section 4.1.2). Pulse injections at the maximum flow rate are then performed to obtain the partition coefficients and number of equilibrium cells (theoretical stages) corresponding to the feed components (Section 4.1.3). The short-cut method can then be used to determine the possible sets of step durations resulting in complete separation under ideal conditions. Separation performance under non-ideal conditions is evaluated by simulations taking band broadening effects into account (Section 4.1.4). An iterative approach is used to arrive at the set of step durations resulting in the maximum throughput at which the performance requirements are still met.

4.1.1. Determination of the maximum feed concentration

To achieve maximum process throughput, the feed concentration should be as high as possible without exceeding the solubility limits and while still allowing for stable operation (i.e., no stationary phase loss). Stationary phase loss indicates disruption of the hydrodynamic equilibrium of the two phases within the column. This disruption can occur when the presence of the feed solutes in the biphasic system leads to changes in the physical properties of the phases (e.g., viscosity, density, interfacial tension). These changes can affect, in turn, the settling time and volume ratio of the two phases. Additionally, the partitioning behavior (partition coefficient) of the feed solutes is also a function of the solute concentration. The concentration dependency and interrelatedness of these various factors can make prediction of the process performance difficult. Therefore, for simplified process design, it is desired to find a limiting feed concentration below which stable, predictable operation is achieved.

Constant partition coefficients and phase volume ratios are generally observed within the linear range of the solutes' partition isotherms. For the model ternary mixture of MP, EP, and PP in ARIZONA N, the limiting concentration of this linear range was determined by performing shake flask experiments and phase volume ratio measurements at increasing total global paraben concentrations. Settling times of the samples were also measured. Samples were prepared using the ternary paraben mixture rather than the single parabens as the mixture better reflects the process conditions and takes possible interactions between the different paraben molecules into account.

In comparison to liquid-solid chromatography techniques, the linear range of the partition equilibria in LLC is extended to higher concentrations as a result of the accessibility of the entire liquid stationary phase volume to the feed solutes as opposed to only a solid surface. In this study, the limit of the linear range of the partition coefficients was defined as the maximum total global concentration at which the coefficient of determination (R^2) remains above 0.99 for all three components. This was found to occur at a total global concentration of 30 mg ml^{-1}, as seen in Fig. 4. The partition coefficients obtained from the slopes of the linear regression lines of the linear region were $K_{MP}^{Des} = 0.81$, $K_{EP}^{Des} = 1.27$, and $K_{PP}^{Des} = 2.23$. These values agree well with those reported for single parabens in ARIZONA N at low concentration ranges (0.01-2 mg ml^{-1}) in a previous study [9].

At the start of a trapping MDM CPC process, the column is filled with the pure, equilibrated phases of the biphasic system. Since trapping MDM CPC is a batch process and loading is performed during a single cycle, the highest feed solute concentrations will be obtained near the feed inlet (between the columns) during the loading stage. During loading, the mobile phase concentration near the inlet approaches that of the feed, with the corresponding stationary phase concentrations taking on the equilibrium values defined
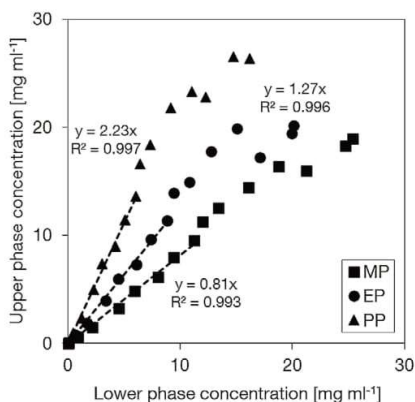
Fig. 4. Partition isotherms for a mixture of MP, EP, and PP in ARIZONA N for total global concentrations ranging from 0 to 80 mg ml^{-1} (equal concentrations of each paraben). Dashed lines: linear regression up to a total global concentration of 30 mg ml^{-1}.

by the partition coefficients. At all later points in the process, the solute concentrations inside the columns will decrease as a result of band broadening. Therefore, to achieve maximum throughput, the feed concentration should be selected at or near the total global concentration limit of the linear range of the partition isotherms determined by the shake flask experiments. Preparation of the corresponding upper phase and lower phase feed solutions containing the equilibrium concentrations is then simply a matter of equilibrating the biphasic system with the necessary paraben amounts and then separating the phases. The 30 mg ml^{-1} total global concentration limit of the linear range of the partition isotherms was selected for preparation of the feed solutions. The upper and lower phase concentrations at this total global concentration ($c_{MP}^U = 9.50$ mg ml^{-1}, $c_{MP}^L = 11.27$ mg ml^{-1}, $c_{EP}^U = 11.38$ mg ml^{-1}, $c_{EP}^L = 8.86$ mg ml^{-1}, $c_{PP}^U = 13.57$ mg ml^{-1}, $c_{PP}^L = 6.06$ mg ml^{-1}) can be read from Fig. 4.

Results of the settling time and phase volume ratio (V_U/V_L) measurements are found in Fig. 5a and b. The settling time increases above a total global concentration of 10 mg ml^{-1}, with an approximately two-fold increase observed between the blank and 30 mg ml^{-1} samples. Practically all variations in the phase volume ratio were within the range of measurement uncertainty. Therefore, it cannot be concluded that there is a significant change in the phase volume ratio within the measured paraben concentration range.

4.1.2. Determination of the maximum applicable flow rate

For fast separation and high column efficiency, it is desired to operate the trapping MDM CPC process at the highest flow rate allowing for maintenance of the initial upper to lower phase ratio. An initial 50/50 upper/lower phase volume ratio of the ARIZONA N system was used in this study, corresponding to a stationary phase retention (S_f) of 0.5 in both elution modes.

Stationary phase retention studies in the absence of feed solutes using ARIZONA N were previously performed on the same CPC unit in [9]. In this study, it was desired to determine the maximum applicable flow rates in the presence of the feed solutes at the maximum concentration determined from the linear range of the partition equilibrium (30 mg ml^{-1} total global concentration).

The decrease in stationary phase retention from the pre-set S_f of 0.5 with increasing flow rate is shown in Fig. 6 for the two elution modes. The reported S_f values correspond to the indicated elution mode ($S_{f,Des} = V_U/V_C$; $S_{f,As} = V_L/V_C$). The decrease in S_f with increas-

ing flow rate is most pronounced in As mode. This trend was also observed in the absence of feed solutes [9]. A slight loss of stationary phase in both modes is first observed at 12 ml min^{-1}. This is significantly lower than the values reported for the pure ARI-ZONA N system in the absence of the feed solutes (24 ml min^{-1} and 22 ml min^{-1} in Des and As mode, respectively). It is evident that introduction of the feed solution to the system has a destabilizing influence on the hydrodynamics of the system.

It is most probable that the increase in settling time observed with increasing concentration (see Fig. 5a) is responsible for the stationary phase loss occurring at 12 ml min^{-1}. The settling time at a total global concentration of 30 mg ml^{-1} is over twice as long as that of the blank sample. As the flow rate is increased, the residence time of the mobile phase within the cells of the column decreases. Due to the longer settling time, the two phases may not have time to fully coalesce within the cells, leading to droplets of stationary phase being carried over from one cell to the next with the mobile phase [25].

In the interest of performing the separation as fast as possible and with higher efficiency, a flow rate of 12 ml min^{-1} was selected for design of the maximum throughput trapping MDM CPC process in lieu of the lower 10 ml min^{-1} where no stationary phase loss was observed. For simplification of the process design, this flow rate was selected for use in all process stages (column loading, separation, and product recovery).

4.1.3. Determination of model parameters by pulse injections

Pulse injections at the selected maximum flow rate of 12 ml min^{-1} were used to determine the model parameters K_k^{Des}, K_k^{As} (partition coefficients), and N_k (number of theoretical stages) used in the short-cut method and equilibrium cell model simulations. The pulse injection partition coefficients slightly differ from those corresponding to the slope of the partition equilibria obtained from the shake flask experiments. Deviations from the static shake flask measurements are due to effects of the column hydrodynamics on the retention behavior, including back-mixing and short-circuiting phenomena [26]. The values obtained for N_k, K_k^{Des}, and K_k^{As} were averaged for the two pulse injections in each mode and are summarized in Table 3.

4.1.4. Simulation study for the selection of step durations

Following determination of the total global feed concentration (30 mg ml^{-1}) and the flow rate (12 ml min^{-1}) to be used for throughput maximization, it was necessary to determine the step durations for the three stages that would result in fulfillment of the separation performance requirements. For this study, requirements of $\geq$99% purity and yield were defined. However, it would be possible to apply the strategy described in this section for other separation performance requirements as well.

The following parameter simplifications were made:

- The flow rate remains constant in Des and As mode in all three process stages ($F_U = F_L$).
- The set position of the trapped component band (EP) at the end of the loading stage is the same in Des and As mode ($x_B^{load,Des} = x_B^{load,As} = x_B^{load}$).
- The set position of the trapped component band (EP) at the end of each separation stage step is the same in Des and As mode ($x_B^{sep,Des} = x_B^{sep,As} = x_B^{sep}$).

Since trapping MDM CPC is a batch process with a single loading stage, the highest column loading possible (x_B^{load}) is desired for the highest throughput. However, the extent of column loading stands in direct competition with the maximum possible duration of the separation stage steps (t_{Des}^{sep}, t_{As}^{sep}). It is beneficial to have step dura-
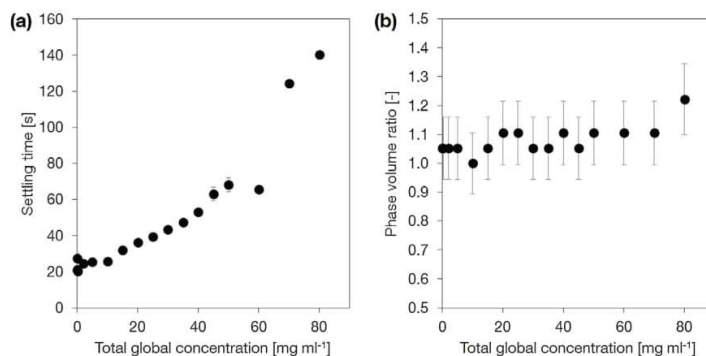
Fig. 5. (a) Influence of total global paraben concentration (MP, EP, and PP) in ARIZONA N on settling time. Error bars: standard deviation of the three measurements. (b) Influence of total global paraben concentration (MP, EP, and PP) in ARIZONA N on phase volume ratio (V_U/V_L). Single measurement per sample. Error bars: cumulative measurement uncertainty (± 0.25 ml).

Table 3
Partition coefficients and number of theoretical stages determined by pulse injections experiments at 12 ml min^{-1} (average values from two pulse injections in each mode). Comparison to partition coefficients obtained from shake flask measurements (slope of the linear range of the partition equilibria up to a total global concentration of 30 mg ml^{-1}). Additional experimental parameters: Feed concentration: 2 mg ml^{-1} each paraben; Injection volume: 1 ml; S_f: 0.5.

Elution mode	Component	Number of theoretical stages, N_k [−]	Partition coefficient, K_k [−]	
			Pulse injection	Shake flask
Des	MP	618	0.79	0.81
	EP	505	1.16	1.27
	PP	426	1.83	2.23
As	MP	474	1.72	1.23
	EP	559	1.03	0.79
	PP	691	0.59	0.45
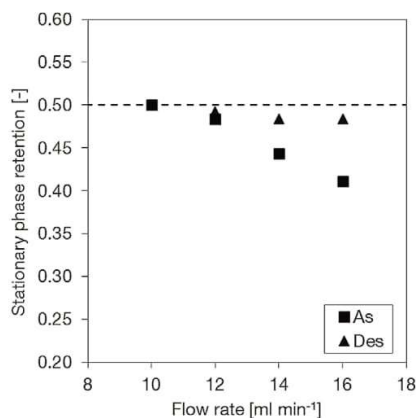
Fig. 6. Influence of flow rate on stationary phase retention in the presence of feed solution in As and Des mode. Solvent system: ARIZONA N (*n*-heptane/ethyl acetate/methanol/water 1/1/1/1 v/v/v/v). Feed solutions: Prepared from total global concentration of 30 mg ml^{-1} (MP, EP, and PP in equal amounts) in ARIZONA N. Feed volume: 62.5 ml. Rotational speed: 1700 rpm. Initial upper/lower phase volume ratio: 50/50.

tions as long as possible to reduce wear on the valves and allow reestablishment of the hydrodynamic equilibrium of the mobile and stationary phases within the column after switching from one elution mode to the other. When switching from Des to As mode is too frequent, the mobile and stationary phases will not have sufficient time to reestablish hydrodynamic equilibrium, which can lead to stationary phase loss. Therefore, a compromise must be met

between long step durations during the separation stage and high column loading.

To obtain the longest possible step durations during the separation stage for a set value of x_B^{load}, x_B^{sep} should be set equal to L_c. This would correspond to the EP band just reaching the end of the column at the end of each step. In reality, the band broadening effects not taken into account by the short-cut model would always cause the EP band fronts to exceed the end of the column at the end of each step. This would lead to decreased yield of the trapped target component EP and decreased purity of MP and PP due to elution of EP with the Des (MP) and As (PP) product streams. Therefore, it is necessary to select a value of x_B^{sep} less than L_c to compensate for band broadening of the trapped component, although this simultaneously shortens the separation stage step durations.

Taking these points into consideration, a time-saving strategy for the selection of the set of step durations resulting in maximum throughput was developed. This iterative strategy is graphically depicted in Fig. 7. It is first necessary to specify the performance requirements, the initial values for x_B^{load} and x_B^{sep}, and the minimum step durations allowing for stable operation (i.e., no stationary phase loss) (t_{Des}^{min}, t_{As}^{min}). After defining the necessary values, step durations are determined using the short-cut method equations in Table 1 as described in Section 2.2. If the minimum step duration requirement is not fulfilled, a decrease of x_B^{load} is made, x_B^{sep} is reassigned its initial value, and the short-cut method is again applied for step duration determination. When the minimum step duration requirement has been satisfied, a simulation is run and the separation performance evaluated. If the performance requirements are not met, a decrease of x_B^{sep} is made, and a new set of step durations is calculated. When t_{Des}^{min} and t_{As}^{min} are satisfied, a new simulation is run. When the desired separation performance is achieved, the maximum separation step durations at the maximum loading have
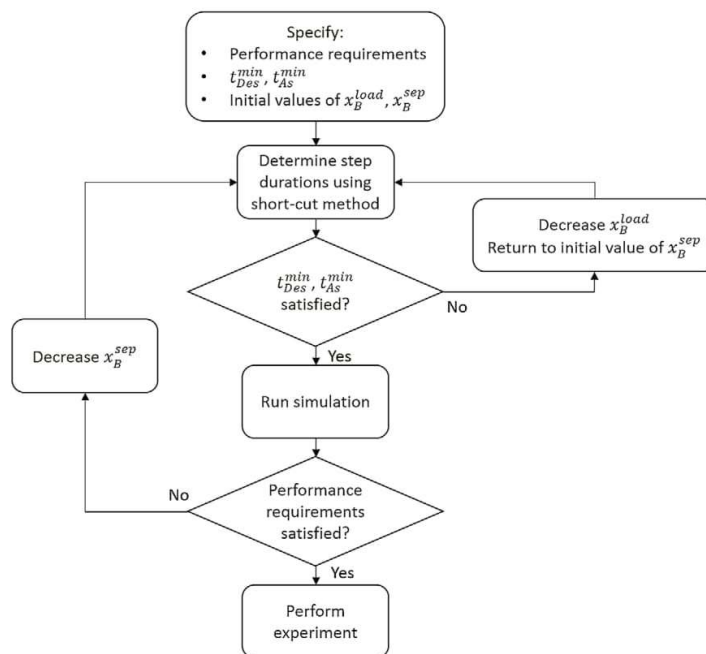
Fig. 7. Model-based strategy for the selection of the set of step durations resulting in maximum throughput in trapping MDM CPC.

Table 4
Model parameters used for trapping MDM CPC simulations with gPROMS.

| Parameter	Unit	Value
Flow rate (F_{Des}^{load}, F_{As}^{load}, F_{Des}^{sep}, F_{As}^{sep}, F^{rec})	ml min^{-1}	12
Total column volume (one column) (V_C)	ml	123.5
Total upper phase volume (one column) (V_U)	ml	61.75
Total lower phase volume (one column) (V_L)	ml	61.75
Feed concentrations MP ($c_{MP,Des}^{feed}$, $c_{MP,As}^{feed}$)	mg ml^{-1}	11.27; 9.50
Feed concentrations EP ($c_{EP,Des}^{feed}$, $c_{EP,As}^{feed}$)	mg ml^{-1}	8.86; 11.38
Feed concentrations PP ($c_{PP,Des}^{feed}$, $c_{PP,As}^{feed}$)	mg ml^{-1}	6.06; 13.57
Number of theoretical stages (one column)*(N_{MP}, N_{EP}, N_{PP},)	–	272; 259; 262
Partition coefficients, Des mode (K_{MP}^{Des}, K_{EP}^{Des}, K_{PP}^{Des})	–	0.79; 1.16; 1.83
Partition coefficients, As mode (K_{MP}^{As}, K_{EP}^{As}, K_{PP}^{As})	–	1.72; 1.03; 0.59

*N_k values for each component taken as the average of the two elution modes (As and Des).

been identified. With this approach, the number of necessary simulations is reduced, since conditions leading to unrealistic operating parameters (step durations below the defined minimum) are ruled out from the start.

The loading optimization strategy described in the preceding paragraph was applied to the separation of the intermediately-eluting target component EP from MP and PP. A minimum step duration of 2 min was selected based on previous experience. The purity and yield requirements for all three product streams (MP, EP, and PP) were set at $\geq$ 99%. The EP band positions in the loading and separation stages (x_B^{load}, x_B^{sep}) were assigned an initial value of 0.95 L_c. x_B^{load} and x_B^{sep} were decreased by increments of 0.05 L_c and 0.1 L_c, respectively. The model and operating parameters used for the simulations are listed in Table 4. The simulation results (purities and yields of the three parabens) are summarized in Table 5.

The performance requirements were first satisfied at x_B^{load} = 0.50 L_c and x_B^{sep} = 0.70 L_c. The simulated concentration profiles of the product streams in the (a) Des and (b) As operating modes for x_B^{load} = 0.50 L_c and x_B^{sep} = 0.70 L_c are presented in Fig. 8. The portions of the MP and PP bands eluted during the Des and As steps of the loading

and separation stages, respectively, are seen as multiple peaks. The concentration profile of EP eluted during the recovery stage in an extended As step is represented by the large single peak in Fig. 8b. As mode was selected for intermediately-eluting component recovery, since EP has a lower partition coefficient in As mode and will elute faster. Furthermore, the ARIZONA N upper phase, consisting primarily of n-heptane and ethyl acetate, is more volatile than the lower phase, which would make it easier to obtain EP in solid form by evaporation.

4.2. Trapping MDM CPC experiment and comparison to simulation

The separation performance under the operating parameters selected using the throughput maximization strategy described in Section 4.1 (total global feed concentration = 30 mg ml^{-1}; F = 12 ml min^{-1}; x_B^{load} = 0.50 L_c; x_B^{sep} = 0.70 L_c; step durations given in Table 6) was evaluated experimentally. A comparison of the experimental and simulated results is given in Fig. 9. The average concentration of the product streams collected during the loading

Table 5

(a) Product purity (mass-%) and (b) yield (mass-%) of (from top to bottom in each cell) MP (Des product), EP (trapped product), and PP (As product). Gray shaded parameter combinations did not fulfill the minimum step duration of 2 min.

(a) Purity [%]

x_B^{sep} [-]

x_B^{load} [-]	0.90L_c	0.80L_c	0.70L_c
0.75L_c			
0.70L_c	96.5 / > 99.9 / 95.6		
0.65L_c	95.9 / > 99.9 / 94.9		
0.60L_c	96.3 / > 99.9 / 95.6	98.4 / > 99.9 / 98.1	
0.55L_c	97.0 / > 99.9 / 96.4	98.2 / > 99.9 / 97.9	
0.50L_c	95.9 / > 99.9 / 95.3	97.9 / > 99.9 / 97.6	99.6 / > 99.9 / 99.6

(b) Yield [%]

x_B^{sep} [-]

x_B^{load} [-]	0.90L_c	0.80L_c	0.70L_c
0.75L_c			
0.70L_c	> 99.9 / 91.8 / > 99.9		
0.65L_c	> 99.9 / 89.8 / > 99.9		
0.60L_c	> 99.9 / 89.4 / > 99.9	> 99.9 / 96.4 / > 99.9	
0.55L_c	> 99.9 / 91.8 / > 99.9	> 99.9 / 95.5 / > 99.9	
0.50L_c	> 99.9 / 86.1 / > 99.9	> 99.9 / 94.0 / > 99.9	> 99.9 / 99.2 / > 99.9

and separation cycles are shown for the (a) Des (MP) and (b) As (PP) elution modes. Fig. 9c depicts the concentration profile of the trapped intermediately-eluting component (EP) obtained during the recovery stage with fraction collection every 60 s. During Cycle 6, fractions were collected from the Des and As streams every 30 s to obtain the elution profiles. The experimental elution profiles are plotted with those obtained by simulation in Fig. 10.

Generally, good agreement between the simulation and experimental results is found, especially for the average cycle concentrations of the As (PP) product stream (see Fig. 9b). The development of the average Des (MP) product stream concentration is similar in both the simulation and experiment (see Fig. 9a). However, MP elution begins one cycle later than predicted by the simulations. Due to this late start of elution, MP has not fully eluted by the start of the recovery stage. The portion of the MP band remaining in the column at the end of the separation stage is observed as a small peak after full elution of the trapped product EP (see Fig. 9c).

A comparison of the experimental and simulated purities and yields of the three product streams is found in Table 7. High purities and yields (>99.0%) were obtained for MP and PP. Due to the elution of the residual MP in the column after the end of the separation stage, the average EP purity of the entire product stream collected during the recovery stage was only 95.0%. However, pooling of the EP peak fractions collected between 4 and 22 min of elution (the limiting fractions where the EP concentration is still ≥1% of the peak maximum) would result in an increase of the experimental EP purity to 99.5%. Calculated product stream yields of the three parabens were lower than predicted, but still quite high (EP and PP above 98.4%; MP at 96.7%). The comparably lower yield of MP in the Des product stream can be attributed to the small amount eluted after EP in the recovery stage. The feed loading was 129.2 ml, or approximately 52% of the entire unit volume. This far exceeds the 5% loading often cited as typical for LLC separations [27].

The late start of MP elution may be attributed to the fact that the first Des step (Cycle 1) is significantly shorter than the remaining separation stage steps (2.22 min as compared to 4.45 min). The simulation model assumes instantaneous equilibrium after switching of the elution mode. However, in reality, the time needed for re-establishment of hydrodynamic equilibrium may impact the predicted movement of the mixture components within the column. Additionally, the mobile phase pumps need a few seconds to reach the set flow rate, which would also contribute to a later start of elution than predicted. This effect is observed in the single-cycle elution profiles in Fig. 10. Given its short duration, these delays make up a more significant part of the first Des step in comparison to the longer remaining separation steps. Due to the cyclic nature of the process, the delay of MP elution starting in the first cycle is propagated through all following cycles, resulting in the shift of the average product concentration profile. Better predictability of the process may be achieved by increasing the 2 min step duration minimum set for the throughput maximization approach. A future study of the effects of step duration on system stability for more accurate determination of the minimum step time would also be useful.

4.3. Comparison to stacked pulse injections

Simulations were used to compare trapping MDM CPC performance at maximized throughput to that of stacked pulse injections on the same CPC device. The comparison was made on the basis of equivalent throughput of the intermediately-eluting component EP. When possible, operating parameters for the stacked pulse injection simulations were the same as those selected for the trapping MDM CPC separation ($F = 12$ ml min^{-1}; $S_f = 0.5$). The purity and yield requirements for the separation were again ≥99.0% for all

Table 6
Step durations during the trapping MDM CPC experiment.

Stage	Cycle(s)	Des step duration, t_{Des} [min]	As step duration, t_{As} [min]
Column loading	0	5.56	5.21
Separation	1	2.22	4.17
	2–8	4.45	4.17
Product recovery	9	4.45	Manually stopped after 40 min

Table 7
Experimental and simulated trapping MDM CPC separation performance under maximum throughput conditions.

Product stream	Purity [mass-%]		Yield [mass-%]	
	Experiment	Simulation	Experiment	Simulation
MP (Des)	99.4	99.6	96.7	>99.9
EP (trapped component)	95.0	>99.9	98.4	99.2
PP (As)	99.2	99.6	98.7	>99.9
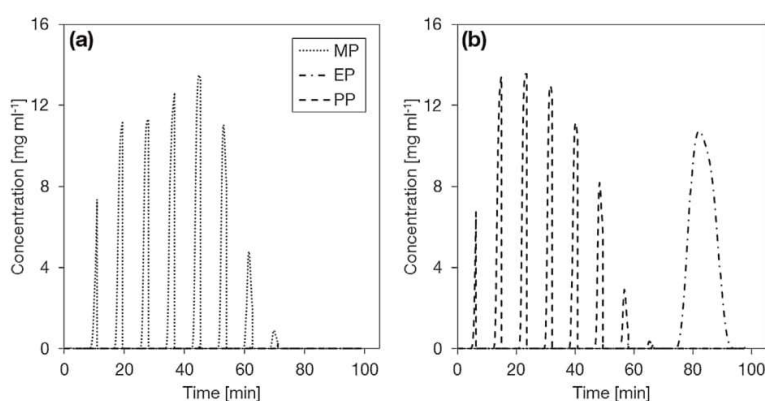
Fig. 8. Simulated concentration profiles in (a) Des and (b) As modes for the selected loading and separation positions of $x_B^{load} = 0.50 \, L_c$ and $x_B^{sep} = 0.70 \, L_c$. The simulation input parameters are listed in Table 4.

three components (MP, EP, and PP). Initial simulations showed that the purity and yield requirements could not be met in Des mode due to overlapping of the MP and EP peaks, even at very low injection volumes (<1 ml). Therefore, the stacked pulse injection process was evaluated in As mode only.

Since the pulse injections were to be simulated in As mode only, the upper phase equilibrium concentrations of the three parabens at the limit of the linear range of the partition isotherms (at a total global concentration of 30 mg ml^{-1}) were taken as their maximum possible feed concentrations (x_B^{load} = 9.50 mg ml^{-1}, c_{EP}^U = 11.38 mg ml^{-1}, c_{PP}^U = 13.57 mg ml^{-1}). This ensures that the linear range of the partition isotherms is not exceeded at any point in the process. To have a feed composition of equal concentrations of all components, the limiting concentration (c_{MP}^U = 9.50 mg ml^{-1}) was assigned to all three parabens.

Before evaluating stacked pulse injection performance, the maximum single injection volume (V_{inj}^{pulse}) satisfying the ≥99.0% purity and yield requirement was determined by simulations to be 14.6 ml. This is the largest injection volume at which baseline separation of the three components is still obtained. To inject an amount of EP equivalent to that in the simulated trapping MDM CPC separation, 9.4 stacked injections of 14.6 ml of feed are required. The simulated concentration profiles under these conditions are found in Fig. 11. The duration of the stacked pulse injection process was 194.4 min, nearly twice as long as the 104.0 min needed for completion of the experimental trapping MDM CPC separation. The process performance parameters of productivity, solvent consumption, and average EP concentration are summarized in Table 8 for the simu-

lated stacked pulse injection and trapping MDM CPC processes, as well as for the trapping MDM CPC experiment.

As seen in Table 8, in addition to the shorter process time, the experimental trapping MDM CPC separation demonstrates a 1.7-fold higher productivity, 40% lower solvent consumption, and a 2.8-fold increase in average concentration of the intermediately-eluting target component EP as compared to the simulated stacked pulse injection process. This indicates that the trapping MDM CPC process, when operated at maximum throughput, is a viable and, possibly, higher-performance alternative to conventional pulse injection processes in liquid-liquid chromatography. However, for a fully "fair" comparison, it would be necessary to first optimize each process individually. For example, it may be advantageous to operate at a S_f other than 0.5, a parameter that can play an important role in peak resolution (currently the subject of an ongoing work in the group).

5. Conclusion

A model-based design approach for throughput maximization in trapping MDM CPC was developed, applied, and experimentally validated for a model ternary mixture of MP, EP, and PP in ARIZONA N. Preliminary shake flask and stationary phase retention experiments were used to determine the maximum feed concentration (30 mg ml^{-1} total global concentration) and the corresponding maximum applicable flow rate (12 ml min^{-1}), respectively. A mathematical short-cut method developed in [2] was applied for the selection of step durations in the column loading and separation
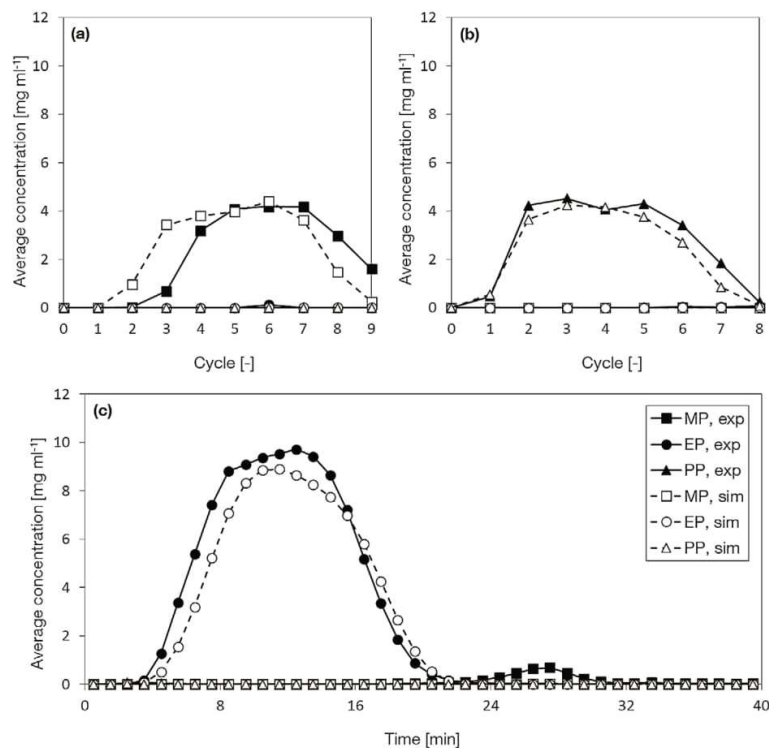
Fig. 9. Average (a) Des and (b) As eluent stream concentrations during the column loading and separation stage cycles. The concentration profiles obtained from fractions collected during the product recovery stage are shown in (c). Experimental conditions: V_c (both columns) = 247 ml; ω = 1700 rpm; F (mobile phase and feed) = 12 ml min^{-1}; S_f = 0.5 (both modes); solvent system = ARIZONA N; c^{feed} = equilibrium concentrations of MP, EP, and PP in the ARIZONA N upper and lower phases at a total global concentration of 30 mg ml^{-1}; x_B^{load} = 0.50 L_c; x_B^{sep} = 0.70 L_c; t_{Des}^{load} = 5.56 min; t_{As}^{load} = 5.21 min; $t_{Des}^{sep,1st}$ = 2.22 min; t_{Des}^{sep} = 4.45 min; t_{As}^{sep} = 4.17. Simulation input parameters: see Table 4.
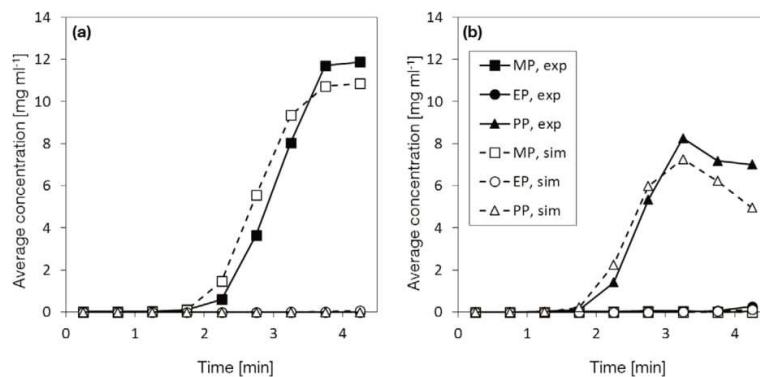
Fig. 10. Elution profiles obtained from fractions collected during the (a) Des and (b) As steps of Cycle 6 (separation stage). See experimental and simulation parameters listed in the caption of Fig. 9.

Table 8
Comparison of experimental and simulated trapping MDM CPC performance at maximum throughput with that of stacked pulse injections.

Operating mode	Process duration [min]	Productivity [g$_{EP}$ h^{-1}]	Solvent consumption [l g$_{EP}$$^{-1}$]	Average EP concentration [mg ml^{-1}]
Trapping MDM CPC (exp)	104.0	0.78	0.92	5.33
Trapping MDM CPC (sim)	103.6	0.84	0.86	6.06
Stacked batch injections, As mode (sim)	194.4	0.47	1.54	1.88

Fig. 11. Simulated chromatogram of the stacked pulse injection process with equivalent EP throughput in As mode. Simulation input parameters: V_{inj}^{pulse} = 14.6 ml; c_{MP}^{feed} = c_{EP}^{feed} c_{PP}^{feed} = 9.50 mg ml^{-1}; number of injections = 9.4; see Table 4 for remaining parameter values.

stages of the trapping MDM CPC process. With the help of simulations based on the equilibrium cell model, the set of step durations resulting in maximum throughput under the purity and yield requirements of $\geq$99.0% was determined. The model-based design approach was then experimentally validated, obtaining generally good agreement with the predictive simulations. High purities and yields of all three components were obtained at a column loading of over 50% of the total column volume.

Simulations were used to make a preliminary comparison between trapping MDM CPC and stacked pulse injection performance. It was found that the trapping MDM CPC process demonstrates a 1.7-fold higher productivity, 40% lower solvent consumption, and a 2.8-fold increase in the average concentration of the intermediately-eluting target component EP under comparable operating conditions. Trapping MDM CPC can be considered a viable alternative to pulse injections for the recovery of intermediately-eluting components from mixtures of compounds possessing similar retention behavior. With the help of the model-based design approach for throughput maximization developed in this work, maximum trapping MDM CPC throughput can be achieved with reduced experimental effort. The application of the throughput maximization strategy to real mixtures of natural product compounds will be the topic of a future publication.

Acknowledgement

Appendix A. Supplementary data

Supplementary data associated with this article can be found, in the online version, at http://dx.doi.org/10.1016/j.chroma.2017.04.033.

References

[1] J.B. Friesen, J.B. McAlpine, S.-N. Chen, G.F. Pauli, Countercurrent Separation of Natural Products: An Update, J. Nat. Prod. 78 (2015) 1765–1796.

[2] J. Goll, R. Morley, M. Minceva, Trapping multiple dual mode centrifugal partition chromatography for the separation of intermediately-eluting components: operating parameter selection, J. Chromatogr. A 1496 (2017) 68–79.

[3] E. Delannay, A. Toribio, L. Boudesocque, J.-M. Nuzillard, M. Zeches-Hanrot, E. Dardennes, G. Le Dour, J. Sapi, J.-H. Renault, Multiple dual-mode centrifugal partition chromatography, a semi-continuous development mode for routine laboratory-scale purifications, J. Chromatogr. A 1127 (2006) 45–51.

[4] P. Hewitson, S. Ignatova, H. Ye, L. Chen, I. Sutherland, Intermittent counter-current extraction as an alternative approach to purification of Chinese herbal medicine, J. Chromatogr. A 1216 (2009) 4187–4192.

[5] N. Mekaoui, J. Chamieh, V. Duga, C. Demesmay, A. Berthod, Purification of Coomassie Brilliant Blue G-250 by multiple dual mode countercurrent chromatography, J. Chromatogr. A 1232 (2012) 134–141.

[6] A.E. Kostanyan, On influence of sample loading conditions on peak shape and separation efficiency in preparative isocratic counter-current chromatography, J. Chromatogr. A 1254 (2012) 71–77.

[7] E. Bouju, A. Berthod, K. Faure, Scale-up in centrifugal partition chromatography: the "free-space between peaks" method, J. Chromatogr. A 1409 (2015) 70–78.

[8] A. Peng, P. Hewitson, H. Ye, L. Zu, I. Garrard, I. Sutherland, L. Chen, S. Ignatova, Sample injection strategy to increase throughput in counter-current chromatography: Case study of Honokiol purification, J. Chromatogr. A 1476 (2016) 19–24.

[9] J. Goll, M. Minceva, Continuous fractionation of multicomponent mixtureswith sequential centrifugal partition chromatography, AIChE J. 10.1002/aic.15529.

[10] A.E. Kostanyan, Multiple dual mode counter-current chromatography with periodic sample injection: steady-state and non-steady-state operation, J. Chromatogr. A 1373 (2014) 81–89.

[11] A.E. Kostanyan, A.A. Erastov, Steady state preparative multiple dual mode counter-current chromatography: productivity and selectivity. Theory and experimental verification, J. Chromatogr. A 1406 (2015) 118–128.

[12] A. Berthod, B. Billardello, S. Geoffroy, Polyphenols in countercurrent chromatography. An example of large scale separation, Analusis 27 (1999) 750–757.

[13] L. Marchal, O. Intes, A. Foucault, J. Legrand, J.-M. Nuzillard, J.-H. Renault, Rational improvement of centrifugal partition chromatographic settings for the production of 5-n-alkylresorcinols from wheat bran lipid extract. I. Flooding conditions—optimizing the injection step, J. Chromatogr. A 1005 (2003) 51–62.

[14] A.E. Kostanian, Modelling counter-current chromatography: a chemical engineering perspective, J. Chromatogr. A 973 (2002) 39–46.

[15] E. Hopmann, M. Minceva, Separation of a binary mixture by sequential centrifugal partition chromatography, J. Chromatogr. A 1229 (2012) 140–147.

[16] J. Goll, A. Frey, M. Minceva, Study of the separation limits of continuous solid support free liquid-liquid chromatography: separation of capsaicin and dihydrocapsaicin by centrifugal partition chromatography, J. Chromatogr. A 1284 (2013) 59–68.

[17] I.A. Sutherland, J. de Folter, P. Wood, Modelling CCC using an eluting countercurrent distribution model, J. Liq. Chromatogr. Relat. Technol. 26 (9-10) (2003) 1449–1474.

[18] A.E. Kostanyan, V.V. Belova, A.I. Kholkin, Modelling counter-current and dual counter-current chromatography using longitudinal mixing cell and eluting counter-current distribution models, J. Chromatogr. A 1151 (2007) 142–147.

[19] M.J. van Buel, A.M. van der Wielen, K.Ch.A.M. Luyben, Effluent concentration profiles in centrifugal partition chromatography, AIChE J. 43 (1997) 693–702.

[20] L. Marchal, J. Legrand, A. Foucault, Mass transport and flow regimes in centrifugal partition chromatography, AIChE J. 48 (2002) 1692–1704.

[21] A.J. Martin, R.L. Synge, A new form of chromatogram employing two liquid phases: a theory of chromatography 2. Application to the micro-determination of the higher monoamino-acids in proteins, Biochem. J. 35 (1941) 1358.

[22] A.E. Kostanyan, A.A. Erastov, O.N. Shishilov, Multiple dual mode counter-current chromatography with variable duration of alternating phase elution steps, J. Chromatogr. A 1347 (2014) 87–95.

[23] J. Völkl, W. Arlt, M. Minceva, Theoretical Study of Sequential Partition Chromatography, AIChE J. 9 (2013) 241.

[24] E. Hopmann, J. Goll, M. Minceva, Sequential centrifugal partition chromatography: a new continuous chromatographic technology, Chem. Eng. Technol. 35 (2012) 72–82.

[25] C. Schwienheer, J. Merz, G. Schembecker, Investigation, comparison and design of chambers used in centrifugal partition chromatography on the basis of flow pattern and separation experiments, J. Chromatogr. A 1390 (2015) 39–49.

[26] S. Adelmann, G. Schembecker, Influence of physical properties and operating parameters on hydrodynamics in Centrifugal Partition Chromatography, J. Chromatogr. A 1218 (2011) 5401–5413.

[27] Y. Ito, Golden rules and pitfalls in selecting optimum conditions for high-speed counter-current chromatography, J. Chromatogr. A 1065 (2005) 145–168.

Supplementary material

A. Derivation of the trapping MDM CPC short-cut method equations

The derivation of the trapping MDM CPC short-cut method equations for determination of the step durations in the column loading (t_{Des}^{load}, t_{As}^{load}) and separation stages (t_{Des}^{sep}, t_{As}^{sep}) first presented in [2] is reprinted here for convenience.

The restrictions for full recovery of the three components A, B, and C (with B as the intermediately-eluting target component) in pure form are listed in Table A1.

Table A1: Trapping MDM CPC process restrictions and corresponding parameter constraints for the complete separation of a ternary mixture of A, B, and C with B as the entrapped component.

Restriction	Operating parameter constraints
1. During the column loading stage, B remains inside the columns.	$0 \leq x_{B,Des}^{load} \leq L_c$ $0 \leq x_{B,As}^{load} \leq L_c$
2. During the separation stage, B remains inside the columns.	$x_{B,Des}^{load} \leq x_{B,Des}^{sep} \leq L_c$ $x_{B,As}^{load} \leq x_{B,As}^{sep} \leq L_c$
3. During the separation stage, B travels a net distance of zero during each cycle. (Exception: Cycle 1)	$\Delta x_{B,Des}^{sep} - \Delta x_{B,As}^{sep} = 0$

The required step durations (t_{Des}, t_{As}) for a single component k depend on the distance to be traveled ($\Delta x_{k,Des}$, $\Delta x_{k,As}$) and the components' velocities ($v_{k,Des}$, $v_{k,As}$). This relationship is expressed in Eqs. A1 and A2 for the Des and As elution modes, respectively.

$$t_{Des} = \frac{\Delta x_{k,Des}}{v_{k,Des}} \tag{A1}$$

$$t_{As} = \frac{\Delta x_{k,As}}{v_{k,As}} \tag{A2}$$

The velocity of component k can be derived from the retention volume equation (Eq. A3)

$$V_{R,k} = V_M + K_k V_S \tag{A3}$$

where the subscripts M and S represent the mobile and stationary phases, respectively. The retention volume, $V_{R,k}$, can alternatively be expressed as:

1

68

$$V_{R,k} = \frac{F_M L_C}{v_k} \tag{A4}$$

Combining Eqs. A3 and A4, the component velocities specific to Des and As mode are given by Eqs. A5 and A6.

$$v_{k,Des} = \frac{F_L L_C}{V_L + K_k^{Des} V_U} \tag{A5}$$

$$v_{k,As} = \frac{F_U L_C}{V_U + K_k^{As} V_L} \tag{A6}$$

Substituting Eqs. A5 and A6 into Eqs. A1 and A2 yields the step durations as a function of the operating parameters (Eqs. A7 and A8).

$$t_{Des} = \Delta x_{k,Des} \cdot \frac{\left(V_L + K_k^{Des} V_U\right)}{F_L L_c} \tag{A7}$$

$$t_{As} = \Delta x_{k,As} \cdot \frac{\left(V_U + K_k^{As} V_L\right)}{F_U L_c} \tag{A8}$$

Next, the general forms of the model equations (Eqs. A7 and A8) are adapted to each of the three process stages and their corresponding restrictions.

Column loading: After fixing the B band front position after loading in each step ($x_{B,Des}^{load}$, $x_{B,As}^{load}$), the distances traveled by the component B band fronts during the loading step ($\Delta x_{B,Des}^{load}$, $\Delta x_{B,As}^{load}$) can be defined by Eqs. A9 and A10.

$$\Delta x_{B,Des}^{load} = x_{B,Des}^{load} - 0 \tag{A9}$$

$$\Delta x_{B,As}^{load} = x_{B,As}^{load} - 0 \tag{A10}$$

Substituting Eqs. A9 and A10 into Eqs. A7 and A8 yields Eqs. A11 and A12, respectively.

$$t_{Des}^{load} = x_{B,Des}^{load} \cdot \frac{\left(V_L + K_B^{Des} V_U\right)}{F_L L_c} \tag{A11}$$

$$t_{As}^{load} = x_{B,As}^{load} \cdot \frac{\left(V_U + K_B^{As} V_L\right)}{F_U L_c} \tag{A12}$$

Separation: Taking Restriction 3 from Table A1 into account, the distances traveled by the B band fronts during the Des and As steps of the separation stage can be expressed by Eq. A13. An exception exists for the distance traveled during the first step of the first cycle (Cycle 1),

2

69

given by Eqs. A14 and A15 when cycles are begun in Des or As mode, respectively. The distance traveled during the second step of Cycle 1 is given by Eq. A13.

$$\Delta x_{B,Des}^{sep} = \Delta x_{B,As}^{sep} = \left(x_{B,Des}^{sep} - x_{B,Des}^{load}\right) + \left(x_{B,As}^{sep} - x_{B,As}^{load}\right) \tag{A13}$$

$$\Delta x_{B,Des}^{sep,1st} = \left(x_{B,Des}^{sep} - x_{B,Des}^{load}\right) \tag{A14}$$

$$\Delta x_{B,As}^{sep,1st} = \left(x_{B,As}^{sep} - x_{B,As}^{load}\right) \tag{A15}$$

Substituting Eqs. A13, A14, and A15 into Eqs. A7 and A8 yields Eqs. A16-A19.

$$t_{Des}^{sep,1st} = \left(x_{B,Des}^{sep} - x_{B,Des}^{load}\right) \cdot \frac{V_L + K_B^{Des} V_U}{F_L L_c} \tag{A16}$$

$$t_{As}^{sep,1st} = \left(x_{B,As}^{sep} - x_{B,As}^{load}\right) \cdot \frac{V_U + K_B^{As} V_L}{F_U L_c} \tag{A17}$$

$$t_{Des}^{sep} = \left[\left(x_{B,Des}^{sep} - x_{B,Des}^{load}\right) + \left(x_{B,As}^{sep} - x_{B,As}^{load}\right)\right] \cdot \frac{V_L + K_B^{Des} V_U}{F_L L_c} \tag{A18}$$

$$t_{As}^{sep} = \left[\left(x_{B,Des}^{sep} - x_{B,Des}^{load}\right) + \left(x_{B,As}^{sep} - x_{B,As}^{load}\right)\right] \cdot \frac{V_U + K_B^{As} V_L}{F_U L_c} \tag{A19}$$

3

3.3 Paper III

Operating mode selection for the separation of intermediately-eluting components with countercurrent and centrifugal partition chromatography

R. Morley, M. Minceva, Journal of Chromatography A, 1594 (2019) 140-148.

<u>Author contribution</u>: The study performed in this paper was led by the thesis author, from conceptualization, to coding and model development in MATLAB, as well as execution of the simulations and analysis of the results. She wrote the manuscript and completed the necessary edits.

<u>Summary</u>: The objective of Paper III was to explore the question opened at the end of Paper II: Which ternary separation operating mode, trapping MDM or batch injections, is best-suited for which separation tasks? The 64 separation tasks evaluated in this study were defined by three parameters representing a difficulty range from preliminary feed fractionation to final product polishing: separation factors from easy (α=2.0) to very difficult (α=1.1) and purity and yield requirements between 75% and 99%. For a fair comparison of performance, all simulations were based on the same CPC column, and productivities were maximized with respect to the corresponding independent parameters of the two operating modes. These were the flow rate, F, and the injection volume, V_{inj}, for batch injections and the short-cut model band positions, x_B^{load} and x_B^{sep}, for trapping MDM.

Simulations based on the equilibrium stage model were run using realistic column parameters and empirical correlations $S_f = f(F)$ and $N_k = f(F, K_k)$. Several improvements were made to the model used in Paper II. For trapping MDM simulations, the number of cycles was determined on-the-fly by running a test Recovery stage at the end of each cycle until a productivity maximum was obtained. The requirement of complete elution of impurities A and C from the column before the start of the Recovery stage was also lifted. Chromatogram evaluation was automated using an algorithm [93] to determine the product collection interval for maximum yield at a set purity requirement.

The results showed that, unlike batch injections, trapping MDM could fulfill nearly all studied separation tasks except for the two most difficult (α=1.1, Yld_{req}=99%, Pur_{req}=95% and 99%). The advantage of trapping MDM was most pronounced for α=1.3, at which only low purity and yield requirements could be met with batch injections. At α=1.5 or higher, batch injections generally outperformed trapping MDM. This study is the only known example of a detailed operating mode comparison in the LLC literature and provides helpful heuristics for operating mode selection for ternary separations.

Operating mode selection for the separation of intermediately-eluting components with countercurrent and centrifugal partition chromatography☆

Raena Morley, Mirjana Minceva *

Biothermodynamics, TUM School of Life Sciences Weihenstephan, Technical University of Munich, Maximus-von-Imhof-Forum 2, 85354 Freising, Germany

ABSTRACT

Two operating modes that can be used for the separation of intermediately-eluting target components from complex mixtures using solid support-free liquid-liquid chromatography (LLC) include batch injections and trapping multiple dual mode (trapping MDM). Batch injections offer the advantage of simpler equipment and process design, while the trapping MDM process, although more complex, can provide improved resolution at low separation factors. In this study, a thorough comparison of batch injection and trapping MDM performance with respect to productivity is made using simulations for a wide range of separation tasks (target component/impurity separation factors; minimum purity and yield requirements). For each separation task, the maximum productivities obtained by the two operating modes were separately determined with respect to their independent parameters. The results indicate that trapping MDM can be used to extend the application of LLC down to separation factors as low as 1.1, with its use being most advantageous for separation factors of approximately 1.3. However, the simpler batch injection process remains preferable for separation factors around or greater than 1.5.

© 2019 Elsevier B.V. All rights reserved.

1. Introduction

Solid support-free liquid-liquid chromatography (LLC), also known as centrifugal partition chromatography (CPC) or countercurrent chromatography (CCC), has established itself as a highly effective technique for the preparative separation of target components from complex starting matrices. Separation is achieved in LLC as the result of differing partitioning behavior of sample solutes between the two phases of a liquid-liquid biphasic system, i.e., the stationary and mobile phases. The use of a liquid stationary phase offers the advantages of high sample loading capacity, an extended linear partition range, and the absence of sample loss through irreversible adsorption. Additionally, either phase of the selected biphasic system can be used as the mobile or stationary phase, and the roles of the two phases may be switched during operation. This grants LLC a high degree of flexibility and has led to the development of several unique operating modes that cannot be performed using conventional chromatography techniques with solid stationary phases [1].

LLC has found its niche in the separation of target components from natural product extracts, such as bioactive molecules, flavors, fragrances, and pigments [2]. Numerous LLC separations have also been reported for proteins and peptides, nanoparticles, metal ions, and rare earth elements [3]. Regardless of the application, a commonly encountered task is the separation of an intermediately-eluting target component from earlier- and later-eluting impurities possessing similar partitioning behavior, i.e., low separation factors. Two LLC operating modes suited to such separations include isocratic batch injections and trapping multiple dual mode (trapping MDM).

When working with batch injections, peak overlap often occurs under the high column loading conditions desired for high productivity, resulting in the need for heart-cutting of the target fraction. This subsequently leads to low target component yields when purity requirements are high. Batch injection yields can be improved through an increase in peak resolution achieved by reinjection of the heart-cut fraction [4–7], recycling of the entire effluent [8,9], or with 2-D orthogonal separations employing two solvent systems of differing selectivity [10–12]. However, use of these techniques can considerably add to the separation run time and complicate the design of the process.

Trapping MDM, an operating mode unique to LLC, is specifically tailored to the preparative ternary separation of intermediately-eluting target components and offers an alternative to batch

---

injections. Trapping MDM makes use of the ability to switch the roles of the mobile and stationary phases during LLC operation, creating a virtual "lengthening" of the column and allowing for increased resolution at low separation factors. Despite these advantages, compared to batch injections, trapping MDM requires a more complex equipment set-up as well as the selection of several additional operating parameters.

The multiple dual mode (MDM) process for binary separations was first introduced in [13] and theoretically treated in [14]. This theoretical study concluded that MDM could be used to obtain higher peak resolution than with batch injections, and that the MDM operating mode was especially advantageous for the separation of components with low partition coefficient values. A variant of the MDM process, trapping MDM enables the isolation of an intermediately-eluting target component and was first explored in [15] (referred to as intermittent countercurrent extraction (ICcE)) and [16]. A structured model-based design approach for selection of the trapping MDM operating parameters was previously developed by the group [17] and applied as part of a throughput maximization strategy with purity and yield requirements of $\geq$ 99% [18].

Although trapping MDM has been demonstrated to outperform batch injections with respect to throughput in both [15] and [18], these assessments were made for single applications only. A thorough evaluation and comparison of the separation performance of these two operating modes for a wide range of separation tasks involving intermediately-eluting target components has yet to be completed. The results of such an investigation would assist LLC users in quickly selecting the most appropriate operating mode for their application and render this underutilized yet effective preparative chromatography technique more accessible to industry.

The objective of this simulation study was therefore to establish simple design heuristics to answer the question, "Which operating mode, batch injections or trapping MDM, is best-suited to my separation task?" A separation task was defined by the following parameters: the partition coefficient of the intermediately-eluting target component, the separation factors between the target component and its nearest-neighbor impurities, and the minimum purity and yield requirements set on the product fraction. To achieve a fair comparison between the performance of the batch injection and trapping MDM operating modes, the maximum productivity obtained by each mode was separately determined with respect to the corresponding independent parameters.

2. LLC operating modes for ternary separations

This section describes the batch injection and trapping MDM operating modes with focus on the process parameters most relevant to this study. As for all preparative chromatography separations, the design goal for both operating modes was to obtain high productivity by isolating as much product at the set purity and yield requirements as possible, as quickly and with the least amount of mobile phase possible.

The term "ternary separation" will be used throughout this work to denote the separation of an intermediately-eluting target component B, possessing an intermediate partition coefficient value, from neighboring impurities A and C. The partition coefficient of a component k, K_k, is defined as the ratio of the concentration of k in the stationary (SP) and mobile (MP) phases at thermodynamic equilibrium (Eq. (1)).

$$K_k = \frac{c_k^{SP}}{c_k^{MP}} \tag{1}$$

In the descending (Des) elution mode, in which the lower phase of the biphasic solvent system is used as the mobile phase while the upper phase is kept stationary, the following relationship between the partition coefficients is defined: $K_A^{Des} < K_B^{Des} < K_C^{Des}$. Component A will elute first, followed by B and then C. It follows from Eq. (1) that the inverse is true for the ascending (As) elution mode. The upper phase is used as the mobile phase, the lower phase is the stationary phase, and the elution order is reversed: $K_A^{As} > K_B^{As} > K_C^{As}$.

2.1. Batch injections

The simplest LLC operating mode, batch injections consist of feed introduction via injection loop or pump at the start of the chromatographic run followed by isocratic elution with the mobile phase. A schematic diagram of the process on the two-column set-up also used for trapping MDM separations is found in Fig. 1a.

The amount of stationary phase retained on the column at a certain rotational speed and flow rate is quantified by the stationary phase fraction, S_f, defined as the ratio between the stationary phase volume, V^{SP}, and the total volume of the column, V_C (Eq. (2)).

$$S_f = \frac{V^{SP}}{V_C} \tag{2}$$

To obtain a high productivity, it is desired to load as much feed on the column during the injection as possible, quantified by the feed concentration, $c_{k,feed}$, and the injection volume, V_{inj}.

High feed concentrations can result in physical properties of the sample, e.g., density, viscosity, and interfacial tension, that vary significantly from those of the mobile and stationary phases. This may lead to stationary phase loss that negatively affects the performance and robustness of the separation. Therefore, the feed concentration should be kept below a certain maximum at which stable operation is achievable.

When process instabilities due to the feed concentration can be neglected, the maximum V_{inj} under a specific set of product requirements, i.e., purity and yield, will depend on the column efficiency specific for each component k, N_k, and the differences in the retention volumes, $V_{R,k}$, of the target component B and impurities A and C. The differences in retention volumes, i.e., how "far apart" two components are located in the chromatogram, can also be described by the separation factor, $\alpha_{k,l} = K_k/K_l$, with $K_k \geq K_l$ and $\alpha_{k,l} \geq 1$. For a fixed column geometry, biphasic solvent system serving as the mobile and stationary phases, and feed mixture, the efficiency will be dependent on the column hydrodynamics, governed by the column rotational speed, ω, and the mobile phase flow rate, F. Meanwhile, the difference in retention volumes is subject to the partition coefficients, K_k, and stationary phase fraction, S_f, the latter of which also depends on ω and F. A more detailed discussion follows.

Retention volume, $V_{R,k}$, depends on S_f and the partition component, K_k, as given in Eq. (3).

$$V_{R,k} = V_C \left[(1 - S_f) + K_k S_f\right] \tag{3}$$

For partition coefficients less than 1, a decrease in S_f will result in higher retention volumes, while the opposite is observed for components with partition coefficients greater than 1. Therefore, the preferred value of S_f for a certain separation with respect to the difference in retention volumes depends on the partition coefficients of the feed components. During process development, it is therefore advisable to fix ω at a value providing sufficient retention of the stationary phase while varying only F.

The differences in retention volumes that can be predicted with Eq. (3) are alone not sufficient for determination of the maximum V_{inj} for a sample, as column efficiency is not taken into account. A high column efficiency, N_k, also referred to as the number of theoretical plates, stages, or cells, indicates less dispersed, narrower peaks and, as a result, less detrimental peak overlap at high loadings. An increase in F and/or ω generally results in higher efficiencies due to an increase in the interfacial area available for

a. Batch injection mode

Feed injection; isocratic elution in a single elution mode

b. Trapping multiple dual mode (trapping MDM)

(1) Loading
Feed introduced during a single cycle

(2) Separation
Multiple cycles of As and Des steps
A elutes in Des mode, C in As mode
B remains trapped in columns

(3) Recovery
Collection of target B in a single step
(As or Des; shown for As mode)
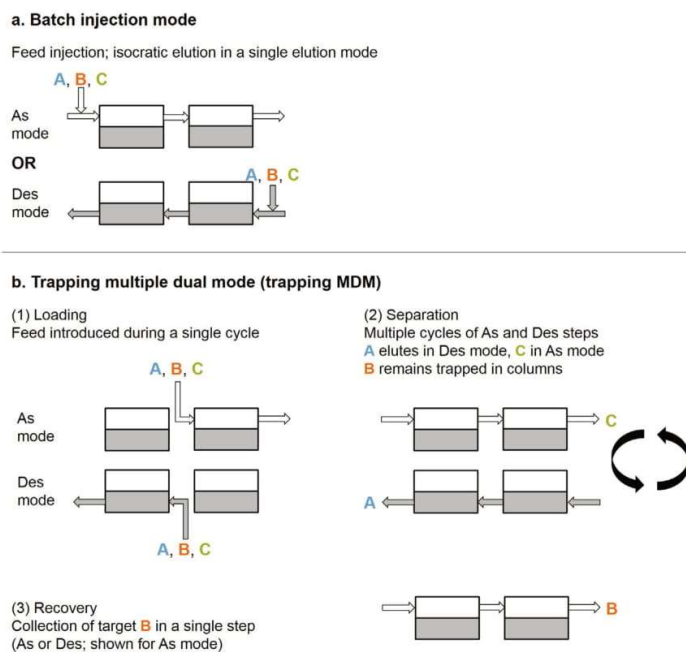
Fig. 1. Schematic depiction of the a) batch injection and b) trapping MDM operating modes. White shading: upper phase; gray shading: lower phase.

mass transfer resulting from an enhancement of flow turbulence [19]. However, LLC separations cannot be perpetually improved by increasing ω and F, as pressure drop limitations, and, in the case of F, the reduction of S_f, place restrictions on both of these parameters. Commercial CPC rotors possessing larger duct boring have been recently developed to address the pressure drop issue. It has often been reported that no further increase in neither efficiency nor S_f is seen above a certain rotational speed [20–24]. Therefore, for the design of a LLC separation it is again advisable to fix ω at a constant value obtaining satisfactory efficiency while varying F. In addition to the operating parameters ω and F, the column efficiency for a certain component also depends its partition coefficient. Components with higher partition coefficients exhibit higher degrees of peak dispersion, i.e., lower values of N_k, as they are retained longer on the column.

To summarize, in the design of LLC separations, it is useful to have expressions for the stationary phase fraction as a function of the flow rate, $S_f = f(F)$, and for efficiency as a function of both the flow rate and the partition coefficient, $N_k = f(F, K_k)$, at a fixed rotational speed. The advantages of increased efficiency associated with increased flow rate may be offset by the accompanying changes in retention time differences brought about by a reduction of S_f. This then directly influences the maximum V_{inj} for a set feed concentration, making it necessary to consider these interdependencies in the design of LLC processes. As S_f can be directly correlated with the flow rate at a set rotational speed, it is then advisable to select F and V_{inj} as the batch injection independent parameters.

2.2. Trapping MDM

The operating parameter relationships described in Sec. 2.1 for the batch injection operating mode also apply to trapping MDM. As the trapping MDM process is more complex, several additional parameters must be considered as well. The process and these parameters are described below.

Trapping MDM is a discontinuous, cyclic process consisting of three stages: (1) loading, (2) separation, and (3) recovery. The process is thoroughly described in [17] and depicted in Fig. 1b. During the loading stage, the feed is introduced by an injection pump between the two columns connected in series without accompanying flow of pure mobile phase. Loading consists of one cycle of Des and As steps. During the Des step, the feed mixture is dissolved in the lower phase, while during the As step it is dissolved in the upper phase. Dissolving and injecting a sample in both phases can allow for higher feed solubility and therefore injection of a greater amount of the target component, especially when working with complex mixtures of components with widely varying polarities.

Immediately following the loading stage, the separation stage is begun. The separation stage consists of multiple cycles of Des and As steps during which the neighboring impurities may be alternately eluted from opposite ends of the column. A is collected in Des mode and C in As mode. The Des and As step durations are selected to allow the target component to remain "trapped" on the column during the separation stage. After sufficient resolution of the target component is achieved, the recovery stage is begun. The target component B and remaining impurities are eluted in a single extended step in Des or As mode, and the product fraction is collected.

In contrast to the design of batch injection separations, flow rate must not be treated as an independent variable in the design of trapping MDM processes. It is recommended to perform trapping MDM separations at a fixed stationary phase fraction of 0.5 in both elution modes. In this case, the column is filled with equal volumes of upper and lower phase for the duration of the process. Similar mobile phase flow rates can then be selected for the Des and As mode steps, providing similar step durations throughout the entire process when the "trapped" intermediately-eluting target component has a partition coefficient around 1. At a pre-determined, fixed rotational speed, the maximum flow rate allowing for maintenance

of S_f of 0.5 should be selected for a short process duration and high column efficiency, as discussed in Sec. 2.1.

Several additional operating parameters unique to the trapping MDM process must also be selected: the step durations during the loading and separation stages, t_{Des}^{load}, t_{As}^{load}, t_{Des}^{sep}, t_{As}^{sep}, and the number of separation stage cycles, n_{cyc}. As the loading and separation stage step durations are intrinsically coupled and the number of possible combinations nearly limitless, a short-cut method was developed by the group to facilitate their selection [17]. Under the constraints defined in [17], use of the short-cut method will return loading and separation step durations and the number of cycles resulting in complete isolation, i.e., "100%" purity and yield, of an intermediately-eluting target component in the absence of band-broadening effects. Separation performance under real conditions must then be evaluated experimentally or with models accounting for non-idealities.

Possible step duration combinations and their associated numbers of cycles are calculated using the short-cut method by setting values for the trapped component B band front positions as a fraction of the dimensionless column "length" at the end of the loading stage, $x_{B,Des}^{load}$, $x_{B,As}^{load}$, and at the end of each step of each separation cycle, $x_{B,Des}^{sep}$, $x_{B,As}^{sep}$, that satisfy the given set of restrictions. The only additional parameters needed for use of the short-cut method are the volumes of the upper and lower phases in the column, the partition coefficient of component B, and the mobile phase flow rate. In the interest of achieving high productivity, $x_{B,Des}^{load}$ and $x_{B,As}^{load}$, analogous to V_{inj} for batch injections, should be high, yet low enough to allow for selection of $x_{B,Des}^{sep}$ and $x_{B,As}^{sep}$ values that will allow the product requirements to be met at a low number of cycles. As F and S_f are kept constant in the design of trapping MDM processes, the independent parameters are then the short-cut method parameters $x_{B,Des}^{load}$, $x_{B,As}^{load}$ and $x_{B,Des}^{sep}$, $x_{B,As}^{sep}$.

3. Modeling and simulations

This section describes the general framework of the batch injection and trapping MDM models, the model input parameters, and the approach and equations utilized in evaluating the separation performance.

3.1. Column model

Models for both operating modes, batch injections and trapping MDM, were based on the equilibrium cell model of Martin and Synge [25]. The column is represented as a number of perfectly mixed chambers connected in series, in which equilibrium partitioning between the two phases is instantaneously achieved by all solutes. The theoretical cell number, N_k, is the only parameter describing all band broadening effects arising from axial dispersion and mass transfer resistance and can differ for each solute. The equilibrium cell model has been successfully employed in previous works from several groups for the simulation of various LLC processes [26–29]. All simulated separations were considered to take place under linear chromatography conditions, i.e., constant partition coefficient values. An arbitrary feed solute concentration, $c_{k,feed}$, of $10\,\mathrm{mg\,ml^{-1}}$ was selected for all simulations. Part A of the Supplementary material details the cell model equations and assumptions used in this work.

The cell model equations were solved numerically with MATLAB R2015b software using the ode45 solver, returning a spatial and temporal resolution of the solute concentration profiles within the column and at the outlet(s). The numerical solution of the equilibrium cell model equations was found to match the analytical solution derived for non-impulse loadings in [30] and later presented in a more convenient form in [31]. However, as the large

Parameter		Unit	Value(s)
Partition coefficient, target component	K_B	[−]	1.0
Separation factor	α	[−]	1.1, 1.3, 1.7, 2.0
Minimum purity requirement	Pur_{req}	[%]	75, 85, 95, 99
Minimum yield requirement	Yld_{req}	[%]	75, 85, 95, 99

factorial terms of the analytical solution pose computational difficulties starting at values of N around 100 [32], its use throughout the entirety of the study was not possible.

3.2. Model parameters

This section describes the input parameters necessary for completion of the batch injection and trapping MDM simulations, beginning with the separation task parameters (Sec. 3.2.1). Further descriptions of parameters derived from experimental correlations (S_f and N_k) and the independent parameters for the productivity maximization are given in Secs. 3.2.2 and 3.2.3, respectively.

3.2.1. Separation task parameters

64 separation tasks were evaluated in this study. Each separation task was defined by the following parameters:

- Partition coefficient of the intermediately-eluting target component B, K_B
- Separation factor between B and impurities A and C, α, with $\alpha = \alpha_{B,A} = \alpha_{C,B}$
- Minimum required purity of product fraction, Pur_{req}
- Minimum required yield of product fraction, Yld_{req}

The value ranges of these parameters are listed in Table 1. A single value of the partition coefficient of the target component B was selected as 1.0, as this is the main criterion for solvent system selection in LLC [33,34]. It follows that there is no need to define different partition coefficients of B for the Des and As modes, since in this case $K_{B,Des} = K_{B,As} = 1.0$. Furthermore, the target component B will have similar retention volumes in both elution modes when S_f is kept constant at 0.5 and the flow rate is the same. This is advantageous for the design of trapping MDM processes, as similar step durations can then be selected for the two elution modes.

For a certain separation task, the partition coefficients of the impurities A and C were defined relative to that of B by the separation factor. The selected range of separation factors represented separations varying from "very difficult" ($\alpha = 1.1$) to "easy" ($\alpha = 2.0$). These separation factors result in partition coefficients of impurities A and C residing in the preferred LLC "sweet spot" range of 0.4 to 2.5, which provides a compromise between resolution and run time [34].

Values lying in the range from 75% through 99% were selected for the minimum purity and yield requirements of the collected target component B fraction, representing a wide range of preparative separations for which LLC may be used. This may be as a preliminary separation step in which yield rather than purity is the priority or as a final polishing step in which the product purity is of utmost importance. Applications falling between these two extremes will exist as well. Depending on the final product's value, application, and associated regulations, the minimum purity and yield requirements can vary widely.

3.2.2. Parameter correlations based on experimental data

In order to have realistic values typical of commonly used LLC solvent systems for the stationary phase fraction, S_f, and theoretical cell numbers, N_k, correlations for these parameters were

Table 2
Parameter correlations based on experimental data.

Parameter		Unit	Batch injection mode	Trapping MDM mode
Theoretical cell number	N_k	[–]	f(F,K_k)	f(F,K_k); $F = 17$ ml min^{-1}
Stationary phase fraction	S_f	[–]	f(F)	0.5

Table 3
Independent parameters for productivity maximization.

Parameter		Unit	Batch injection mode	Trapping MDM mode
Flow rate	F	[ml min^{-1}]	$4 \leq F \leq 30$ $\Delta F = 2$	17
Injected volume	V_{inj}	[ml]	$5 \leq V_{inj} \leq 100$ $\Delta V_{inj} = 5$	–
Band position, loading	x_B^{load}	[–]	–	$0.05 \leq x_B^{load} \leq 1.00$ $\Delta x_B^{load} = 0.05$
Band position, separation	x_B^{sep}	[–]	–	$x_B^{sep} \geq (x_B^{load} + 0.05)$ $\Delta x_B^{sep} = 0.05$

Table 4
Trapping MDM process restrictions and corresponding short-cut method constraints on the band front positions of intermediately-eluting target component B at reduced purity and yield requirements.

Restriction	Parameter constraint
1. During the loading stage, B does not elute from the columns.	$0 < x_B^{load} \leq 1$
2. During the separation stage, the B band front positions exceed those of corresponding loading stage step	$x_B^{sep} > x_B^{load}$
3. During the separation stage, B travels a net distance of zero during each cycle. (Exception: Cycle 1)	$\Delta x_{B,Des}^{sep} - \Delta x_{B,As}^{sep} = 0$ with $\Delta x_{B,Des}^{sep} = \Delta x_{B,As}^{sep} = \left(x_{B,Des}^{sep} - x_{B,Des}^{load} \right) + \left(x_{B,As}^{sep} - x_{B,As}^{load} \right)$

derived from experimental data presented in [35]. Stationary phase fraction measurements and pulse injections were performed in Des mode using the Arizona N solvent system (*n*-heptane/ethyl acetate/methanol/water 1/1/1/1 v/v/v/v) and a model mixture of four different parabens. All experiments were performed at a rotational speed of 1700 rpm, as it was previously found that this speed allows for satisfactory stationary phase retention and column efficiency within the operating limits of the equipment, i.e., flow rate and the associated pressure drop, and that further increase of the rotational speed has a negligible effect on the column efficiency [22]. A total column volume of 182.1 ml, equal to that of the experimental set-up, was used for all simulations. The fitted experimental data and resulting correlations $S_f = f(F)$ and $N_k = f(F, K_k)$ are provided in Part B of the Supplementary material.

The batch injection simulations were performed in one "elution mode" only, namely Des mode. With B having a partition coefficient of 1.0 and the separation factors for A and C relative to B always being equal, the same elution profiles would be obtained in both modes under the assumption that the correlations $S_f = f(F)$ and $N_k = f(F, K_k)$ do not differ in the two modes.

For all trapping MDM simulations, the stationary phase fraction was fixed at 0.5 for the reasons described in Sec. 2.2. The maximum flow rate for maintenance of this stationary phase fraction was taken from the abovementioned experimental data and set as 17 ml min^{-1} for all process stages. The same S_f and N_k correlations were used for simulation of both the Des and As elution modes, with the N_k values being the average of those obtained from the correlations for the different partition coefficients of the Des and As modes. It is well-known that S_f and N_k can vary differently depending on the elution mode due to differences in viscosity and phase mixing. However, the magnitude of this difference will be highly dependent on the biphasic system used. For the objective of this generalized simulation study, which was to provide a separation task-based guideline for operating mode selection, the assumption of identical S_f and N_k correlations for the Des and As modes was deemed acceptable. For the design of a specific real-world application, it would of course be beneficial for the model accuracy to take these differences into account. Values and correlations for S_f and N_k for the two operating modes are summarized in Table 2.

3.2.3. Independent parameters

The independent parameters selected for this study differed for the two operating modes and are listed in Table 3. For the batch injection simulations, mobile phase flow rate, F, and injected sample volume, V_{inj}, were selected. The flow rate range from 4 to 30 ml min^{-1} corresponded to that of the experimental CPC set-up under

pressure drop limitations at a rotational speed of 1700 rpm (see Sec. 3.2.2). The range of injection volumes from 5 to 100 ml was selected so as to permit the emergence of a productivity maximum in the V_{inj}, F parameter space for all investigated separation tasks.

For the trapping MDM simulations, the independent parameters were the trapped component B band front positions during the loading, $x_{B,Des}^{load}$, $x_{B,As}^{load}$, and separation stages, $x_{B,Des}^{sep}$, $x_{B,As}^{sep}$, used in conjunction with the short-cut method [17] to determine the corresponding step durations. Since the current study involved the evaluation of separation performance at reduced purity and yield requirements, modification of the original constraints set on the selection of the component B band front positions in [17] for "100%" purity and yield of the target component was necessary. The modified constraints are listed in Table 4 and permit the use of separation stage step durations during which elution of the target component B can occur. This was considered to be possibly advantageous for obtaining a high productivity at reduced yield requirements. Additionally, the restriction "At the end of the separation stage, both A and C have completely eluted from the columns" found in [17] is no longer included, since at reduced purity and yield requirements, higher productivities can be achieved by allowing peak overlap during the collection of the target component in the recovery stage.

To reduce the number of possible step duration combinations, the component B band front positions were always the same for the Des and As steps, i.e., $x_B^{load} = x_{B,Des}^{load} = x_{B,As}^{load}$ and $x_B^{sep} = x_{B,Des}^{sep} = x_{B,As}^{sep}$. Given the "symmetry" of the separation, that is, a target component B partition coefficient of 1.0 and identical separation factors between B and impurities A and C, this would likely be a reasonable relationship between the Des and As step durations. Two additional trapping MDM process restrictions were made to simplify the productivity maximization: the first step of each cycle is a Des step and the second step an As step; the recovery stage is always in As mode.

3.3. Evaluation of separation performance

This section describes the analysis of the simulated batch injection and trapping MDM recovery stage chromatograms for the determination of the mass recovery of the target component B, as well as the equations used for determination of the purity and yield of the collected product fraction and the productivity of the process.

3.3.1. Chromatogram analysis

The simulated chromatograms in both operating modes often contained overlapping peaks. It was therefore necessary to determine the collection interval for the product fraction that would allow for maximum recovery of the intermediately-eluting target component B while satisfying the minimum purity and yield requirements set by the separation task, Pur_{req} and Yld_{req}. This was done using the iterative algorithm described in [36] with expansion of the initial collection interval in two directions. The algorithm identifies the minimum and maximum start and end times, respectively, of the product fraction collection interval, $t_{B,coll}^{start}$ and $t_{B,coll}^{end}$.
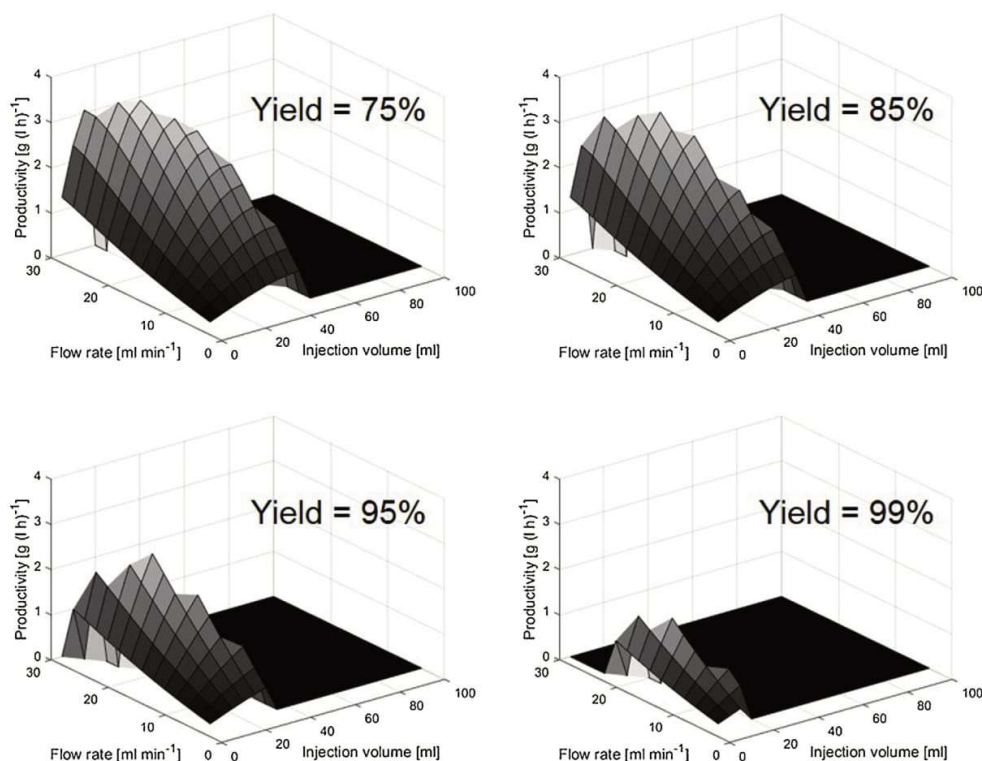
Fig. 2. Batch injection simulations, maximum productivity vs. F and V_{inj}. Separation factor = 1.7; minimum purity requirement = 99%; varying yield requirement.

The threshold concentration for all peak start and end times was 0.001 mg ml^{-1} and the reported time interval, Δt, was 0.01 min.

The mass recoveries of the three components, m_k, were calculated by numerical integration of the concentration elution profiles using the trapezoidal rule over the interval defined by $t_{B,coll}^{start}$ and $t_{B,coll}^{end}$. The m_k can then be used to calculate the corresponding purity and yield of the product fraction, as well as the productivity of the overall process, as described below.

3.3.2. Purity

The purity of the product fraction with respect to the target component B was calculated as given in Eq. (4).

$$Pur = \frac{m_B}{\sum_{k=A,B,C} m_k} \times 100\% \tag{4}$$

3.3.3. Yield

The yield of target component B with respect to the amount loaded at the start of the run, $m_{B,inj}$, was defined by Eq. (5).

$$Yld = \frac{m_B}{m_{B,inj}} \times 100\% \tag{5}$$

$m_{B,inj}$ was calculated according to Eq. (6)

$$m_{B,inj} = V_{inj} c_{B,feed} \tag{6}$$

where $V_{inj} = F(t_{Des}^{load} + t_{As}^{load})$ for trapping MDM.

3.3.4. Productivity

Productivity, Pr, was defined for this study by Eq. (7) as the amount of target component B collected in the product fraction per volume mobile phase per time

$$Pr = \frac{m_B}{V_{MP,process} t_{process}} \tag{7}$$

where $V_{MP,process}$ is the total amount of mobile phase eluted during the separation neglecting the column loading time and $t_{process}$ is the total process time, beginning with the start of loading ($t = 0$ min) and ending with the time point at which the concentration of the last eluting component drops below the peak threshold concentration. In trapping MDM mode, only the recovery stage chromatograms were evaluated. $V_{MP,process}$ was calculated with Eq. (8).

$$V_{MP,process} = F\left(t_{process} - t_{inj}\right) \tag{8}$$

For batch injection mode, $t_{inj} = V_{inj}/F$, while $t_{inj} = t_{Des}^{load} + t_{As}^{load}$ for trapping MDM. As this definition of productivity indirectly takes solvent consumption into account, solvent consumption trends were not investigated separately.

The number of trapping MDM separation stage cycles, n_{cyc}, resulting in the maximum productivity for each separation task and combination of x_B^{load} and x_B^{sep} was determined by sequentially increasing the number of cycles and running a hypothetical "test" recovery stage after each. The "test" recovery stage chromatograms were evaluated as described above and the productivities calculated. Once the number of cycles resulting in a productivity maximum was identified, the simulation run was ended.
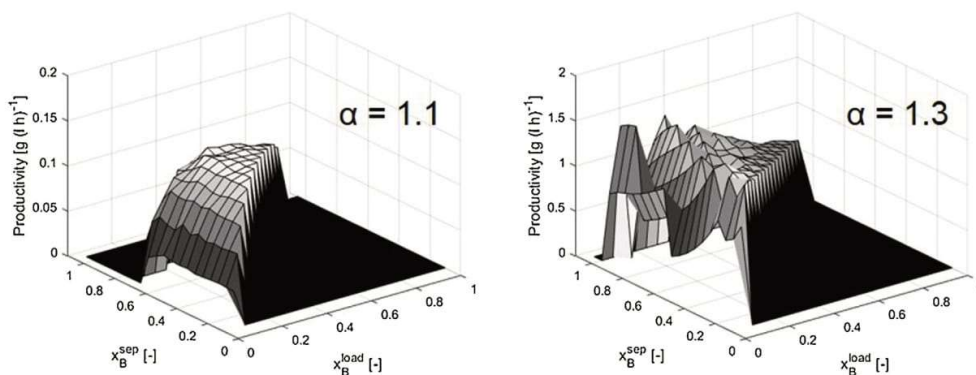
Fig. 3. Trapping MDM simulations, maximum productivity vs. x_B^{load} and x_B^{sep}. Minimum purity requirement = 85%; minimum yield requirement = 85%.

4. Results and discussion

For each operating mode and each of the 64 separation task parameter combinations described in Sec. 3.2.1, a series of simulations covering all independent parameter combinations was run and the resulting productivities determined. For each separation task, it was then possible to identify the maximum productivity that can be achieved by each operating mode and the corresponding values of the independent parameters. Tables containing the maximum productivities and associated independent parameter values for all separation tasks are found in Part C of the Supplementary material.

This section describes the trends observed for the batch injection and trapping MDM operating modes in the investigated independent parameter spaces. A final overall comparison of the two operating modes is then made to conclude the range of separation tasks for which each mode is best-suited.

As would be expected, both the flow rate and the injection volume at which maximum productivity is achieved for batch injections increase with increasing separation factor and decreasing purity and yield requirements, since in both cases reduced peak resolution is required. However, it is observed that it is often not advantageous to work at the highest allowable flow rate, despite the gain in efficiency. This is especially true at higher purity and yield requirements. The accompanying decrease in S_f with increasing F can lead to a decrease in resolution as described in Sec. 2.1. A moderate flow rate will allow for a compromise between a fast separation and high resolution. The separation task of $\alpha = 1.7$, $Pur_{req} = 99\%$ can be taken as an example (see Fig. 2). With increasing minimum yield requirements of 75%, 85%, 95%, and 99%, the flow rates at maximum productivity were 24, 22, 20, and 16 ml min^{-1}, respectively, with corresponding injection volumes of 25, 25, 20, and 15 ml. Since the injected volume influences peak width and consequently resolution, lower injection volumes are required at higher purity and yield requirements.

The highest injected volume at maximum productivity for the range of separation tasks studied was 45 ml, corresponding to approximately 25% of the total column volume. This was for the "easiest" separation task of $\alpha = 2.0$ and $Pur_{req} = Yld_{req} = 75\%$. Injection volumes at maximum productivity for separation tasks with $\alpha = 1.5$ and $\alpha = 1.7$ were in the range from 10 to 35 ml, corresponding to approximately 5 to 20% of the total column volume. The maximum productivity trends indicate that further improvement of performance could in some cases be achieved at higher flow rates beyond the upper limit of the set parameter range, especially for "easier" separations at high separation factors and decreased Pur_{req}

and Yld_{req}. However, this would be dependent on mitigation of the maximum allowed pressure drop for the equipment, a limitation inherent to the column geometry and construction.

For the trapping MDM simulations, productivity as a function of the target component band front positions, x_B^{load}, x_B^{sep}, resulted in irregular surface plots. Focusing on separation tasks for which $\alpha = 1.1$ and 1.3, it is seen that a single, well-defined productivity maximum does not exist (see exemplary plots in Fig. 3). For $\alpha = 1.1$, an initial sharp increase in productivity with increasing x_B^{load} is observed, followed by a plateau-like surface for which multiple combinations of x_B^{load} and x_B^{sep} can result in similar productivity values. For $\alpha = 1.3$, a jagged productivity surface is seen with deep "valleys" at lower loadings resulting from the discrete nature of the cyclic process. Each productivity "valley" represents the x_B^{load}, x_B^{sep} combination at which an extra separation stage cycle becomes necessary to satisfy the product requirements set by the separation task. This feature is more apparent for $\alpha = 1.3$, since far fewer cycles are performed compared to $\alpha = 1.1$, resulting in each cycle having a greater overall contribution to the productivity.

Fig. 4 presents a graphical summary of the maximum productivities for all separation tasks, arranged by separation factor. For the investigated range of V_{inj}, F, none of the separation tasks with a separation factor of 1.1 could be achieved with batch injections. For $\alpha = 1.3$, only separation at tasks at lower purity and yield requirements could be met, i.e., maximum $Yld_{req} = 95\%$ for $Pur_{req} = 75\%$; maximum $Yld_{req} = 85\%$ for $Pur_{req} = 85\%$. Batch injections become a viable option beginning with a separation factor of 1.5, at which only the most difficult separation task, i.e., $Pur_{req} = Yld_{req} = 99\%$, cannot be achieved.

With trapping MDM, fulfillment of nearly all separation tasks was theoretically possible, with the exception of the most difficult, i.e., $\alpha = 1.1$, $Yld_{req} = 99\%$ at purity requirements of $Pur_{req} = 95\%$, 99%. However, at this separation factor the process becomes likely impractical at purity and yield requirements above 95%, as the number of required separation stage cycles quickly jumps to over 100. This results in extremely low productivities, which would render the process uneconomical unless the target component was of extremely high value.

For separation tasks with $\alpha = 1.3$, the advantage of trapping MDM clearly manifests itself. Separation is achieved at all purity and yield requirements with less than 10 separation cycles, with the exception of $Pur_{req} = Yld_{req} = 99\%$ with 16 cycles. The number of cycles increases with increasing purity and yield requirements. Typical loadings at maximum productivity correspond to loading band front positions, x_B^{load}, between 0.10 and 0.30 (approximately 18–55% of the total column volume), often exceeding the maxi-
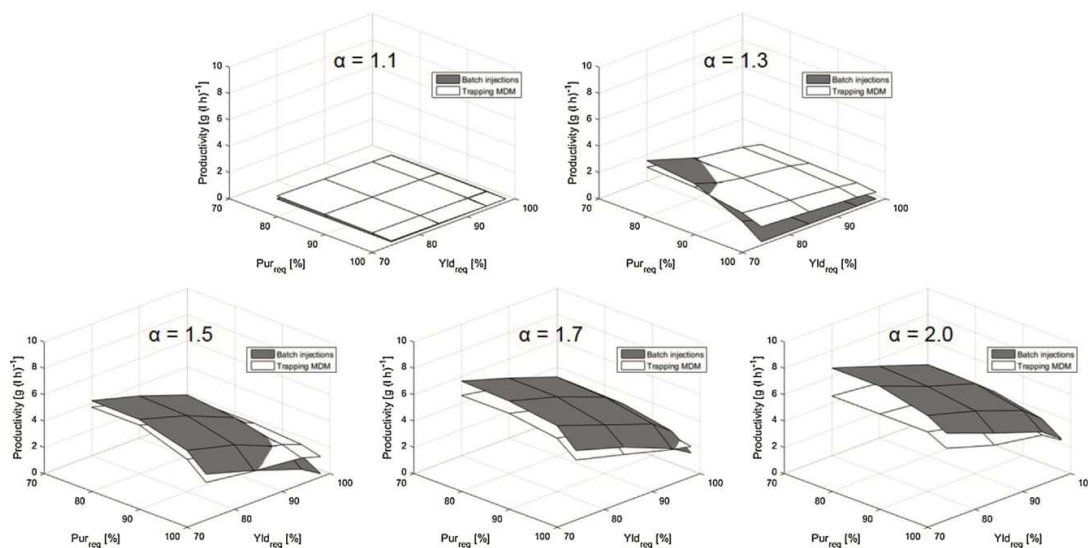
Fig. 4. Maximum batch injection and trapping MDM productivities for all separation tasks, grouped by separation factor.

mum column loading of approximately 25% achieved with batch injections.

Starting with a separation factor of 1.3, maximum trapping MDM productivity is achieved with only one separation stage cycle when purity and yield requirements are low. At separation factors of 1.5 and greater, nearly all separation tasks can be achieved with a single separation stage cycle. In these cases, there is no advantage in the use of trapping MDM over batch injections with respect to productivity.

5. Conclusions

From this investigation of 64 separation tasks covering a wide range of product requirements and separation factors relevant for the preparative LLC separation of an intermediately-eluting target component, it can be concluded that the use of trapping MDM mode is generally advantageous for separation factors around 1.3 or lower, with separations possible but at very low productivities when $\alpha = 1.1$. At separation factors of 1.5 or higher, the simpler batch injection process is generally preferred, except at very high purity and yield requirements. These findings agree with the "rule of thumb" given in [33] stating that the separation factor should be greater than 1.5 in the design of batch injection separations with LLC.

It should be noted that this study was based on a model system comprising a typical LLC solvent system, model solutes, and a particular CPC unit. Although the observed trends may slightly vary depending upon the system, solutes, and unit used, it is likely that the final conclusions will be similar. Additionally, the model ternary mixture of components A, B, and C used in this study can be applied to complex multicomponent mixtures containing more than three components. For these "pseudo-ternary" separations, B remains the intermediately-eluting target component, while components A and C represent the nearest neighbor impurities located directly before and after the target component in the chromatogram. The condition $\alpha_{B,A} = \alpha_{C,B}$, selected as a simplification, is seldom encountered in the laboratory. Nevertheless, the operating mode comparison approach presented in this study and the underlying short-cut and process models are compatible with any combination of target and

impurity partition coefficients, i.e., separation factors, and could be applied to specific real-world applications as well.

The findings of this investigation serve as a useful starting point in the decision of which operating mode to choose in the separation of intermediately-eluting target components from (pseudo-)ternary mixtures using LLC. An extension of this comparative investigation to the performance of continuous ternary separations using a sequential centrifugal partition chromatography (sCPC) [37] cascade is currently being conducted.

Appendix A. Supplementary data

Supplementary material related to this article can be found, in the online version, at doi:https://doi.org/10.1016/j.chroma.2019.02.020.

References

[1] A. Berthod, Fundamentals of countercurrent chromatography, in: A. Berthod (Ed.), Countercurrent Chromatography. The Support-Free Liquid Stationary Phase, Volume 38, Comprehensive Analytical Chemistry, 2002, pp. 1–20.
[2] G.F. Pauli, S.M. Pro, J.B. Friesen, Countercurrent separation of natural products, J. Nat. Prod. 71 (2008) 1489–1508.
[3] A. Berthod, M.J. Ruiz-Ángel, S. Carda-Broch, Countercurrent chromatography: people and applications, J. Chromatogr. A 1216 (2009) 4206–4217.
[4] Q.-Z. Du, C.-Q. Ke, Y. Ito, Recycling high-speed countercurrent chromatography for separation of taxol and cephalomannine, J. Liq. Chromatogr. Relat. Technol. 21 (1&2) (1998) 157–162.
[5] F. Yang, J. Quan, T.Y. Zhang, Y. Ito, Multidimensional counter-current chromatographic system and its application, J. Chromatogr. A 803 (1998) 298–301.
[6] Q. Liu, H. Zeng, S. Jiang, L. Zhang, F. Yang, X. Chen, H. Yang, Separation of polyphenols from leaves of *Malus hupehensis* (Pamp.) Rehder by off-line two-dimensional high speed counter-current chromatography combined with recycling elution mode, Food Chem. 186 (2015) 139–145.
[7] J.-M. He, S.-Y. Zhang, Q. Mu, Online-storage recycling counter-current chromatography for preparative isolation of naphthaquinones from *Arnebia euchroma* (Royle) Johnst, J. Chromatogr. A 1464 (2016) 79–85.

[8] Q.B. Han, J.Z. Song, C.F. Qiao, L. Wong, H.X. Xu, Preparative separation of gambogic acid and its C-2 epimer using recycling high-speed counter-current chromatography, J. Chromatogr. A 1127 (2006) 298–301.

[9] J. Xie, J. Deng, F. Tan, J. Su, Separation and purification of echinacoside from *Penstemon barbatus* (Can.) Roth by recycling high-speed counter-current chromatography, J. Chromatogr. A 878 (2010) 2665–2668.

[10] G. Tian, T. Zhang, Y. Zhang, Y. Ito, Separation of tanshinones from *Salvia miltiorrhiza* Bunge by multidimensional counter-current chromatography, J. Chromatogr. A 945 (2002) 281–285.

[11] Y. Wei, Y. Ito, Preparative isolation of imperatorin, oxypeucedanin and isoimperatorin from traditional Chinese herb "bai zhi" *Angelica dahurica* (Fisch. ex Hoffm) Benth. et Hook using multidimensional high-speed counter-current chromatography, J. Chromatogr. A 1115 (2006) 112–117.

[12] M. Englert, L. Brown, W. Vetter, Heart-cut two-dimensional countercurrent chromatography with a single instrument, Anal. Chem. 87 (2015) 10172–10177.

[13] E. Delannay, A. Toribio, L. Boudesocque, J.-M. Nuzillard, M. Zeches-Hanrot, E. Dardennes, G. Le Dour, J. Sapi, J.-H. Renault, Multiple dual-mode centrifugal partition chromatography, a semi-continuous development mode for routine laboratory-scale purifications, J. Chromatogr. A 1127 (2006) 45–51.

[14] N. Mekaoui, A. Berthod, Using the liquid nature of the stationary phase. VI. Theoretical study of multi-dual mode countercurrent chromatography, J. Chromatogr. A 1218 (2011) 6061–6071.

[15] P. Hewitson, S. Ignatova, H. Ye, L. Chen, I. Sutherland, Intermittent counter-current extraction as an alternative approach to purification of Chinese herbal medicine, J. Chromatogr. A 1216 (2009) 4187–4192.

[16] N. Mekaoui, J. Chamieh, V. Dugas, C. Demesmay, A. Berthod, Purification of Coomassie Brilliant Blue G-250 by multiple dual mode countercurrent chromatography, J. Chromatogr. A 1232 (2012) 134–141.

[17] J. Goll, R. Morley, M. Minceva, Trapping multiple dual mode centrifugal partition chromatography for the separation of intermediately-eluting components: operating parameter selection, J. Chromatogr. A 1496 (2017) 68–79.

[18] R. Morley, M. Minceva, Trapping multiple dual mode centrifugal partition chromatography for the separation of intermediately-eluting components: throughput maximization strategy, J. Chromatogr. A 1501 (2017) 26–38.

[19] L. Marchal, A. Foucault, G. Patissier, J.M. Rosant, J. Legrand, Influence of flow patterns on chromatographic efficiency in centrifugal partition chromatography, J. Chromatogr. A 869 (2000) 339–352.

[20] L. Marchal, J. Legrand, Mass transport and flow regimes in centrifugal partition chromatography, AIChE J. 48 (8) (2002) 1692–1704.

[21] T.A. Maryutina, S.N. Ignatova, B.Ya. Spivakov, I.A. Sutherland, The efficiency of substance separation in countercurrent liquid chromatography, J. Anal. Chem. 58 (2003) 762–767.

[22] E. Hopmann, J. Goll, M. Minceva, Sequential centrifugal partition chromatography: a new continuous chromatographic technology, Chem. Eng. Technol. 35 (1) (2012) 72–82.

[23] C. Schwienheer, J. Merz, G. Schembecker, Investigation, comparison and design of chambers used in centrifugal partition chromatography on the basis of flow pattern and separation experiments, J. Chromatogr. A 1390 (2015) 39–49.

[24] N. Fumat, A. Berthod, K. Faure, Effect of operating parameters on a centrifugal partition chromatography separation, J. Chromatogr. A 1474 (2016) 47–58.

[25] A.J. Martin, R.L. Synge, A new form of chromatogram employing two liquid phases: a theory of chromatography 2. Application to the micro-determination of the higher monoamino-acids in proteins, Biochem. J. 35 (1941) 1358.

[26] A.E. Kostanian, Modelling counter-current chromatography: a chemical engineering perspective, J. Chromatogr. A 973 (2002) 39–46.

[27] A.E. Kostanyan, A.A. Erastov, O.N. Shishilov, Multiple dual mode counter-current chromatography with variable duration of alternating phase elution steps, J. Chromatogr. A 1347 (2014) 87–95.

[28] E. Hopmann, M. Minceva, Separation of a binary mixture by sequential centrifugal partition chromatography, J. Chromatogr. A 1229 (2012) 140–147.

[29] P. Hewitson, I. Sutherland, A.E. Kostanyan, A.A. Voshkin, S. Ignatova, Intermittent counter-current extraction—equilibrium cell model, scaling and an improved bobbin design, J. Chromatogr. A 1303 (2013) 18–27.

[30] A.E. Kostanyan, On influence of sample loading conditions on peak shape and separation efficiency in preparative isocratic counter-current chromatography, J. Chromatogr. A 1254 (2012) 71–77.

[31] A.E. Kostanyan, Modeling of preparative closed-loop recycling liquid-liquid chromatography with specified duration of sample loading, J. Chromatogr. A 1471 (2016) 94–101.

[32] A.E. Kostanyan, O.N. Shishilov, An easy-to-use calculating machine to simulate steady state and non-steady-state preparative separations by multiple dual mode counter-current chromatography with semi-continuous loading of feed mixtures, J. Chromatogr. A 1552 (2018) 92–98.

[33] Y. Ito, Golden rules and pitfalls in selecting optimum conditions for high-speed counter-current chromatography, J. Chromatogr. A 1065 (2005) 145–168.

[34] J.B. Friesen, G.F. Pauli, G.U.E.S.S.—a generally useful estimate of solvent systems for CCC, J. Liq. Chromatogr. Relat. Technol. 28 (2005) 2777–2806.

[35] S. Röhrer, M. Minceva, Separation method transfer in liquid-liquid chromatography, presentation at the 10th International Conference on Countercurrent Chromatography, 1–3 Aug, 2018, Braunschweig, Germany.

[36] Y. Shan, A. Seidel-Morgenstern, Analysis of the isolation of a target component using multicomponent isocratic preparative elution chromatography, J. Chromatogr. A 1041 (2004) 53–62.

[37] J. Völkl, W. Arlt, M. Minceva, Theoretical study of sequential centrifugal partition chromatography, AIChE J. 59 (2013) 241–249.

Supplementary material

A. Equilibrium cell model

Cell model assumptions

- Off-column volumes are negligible
- The volumes of the upper and lower phases are equal in all cells (constant stationary phase fraction S_f)
- Solute partition coefficients for each elution mode are constant and independent of the concentration (linear chromatography assumption)
- Ascending (As) mode partition coefficients are the inverse of their descending (Des) mode values, and vice versa ($K_k^{As} = 1/K_k^{Des}$)
- In trapping multiple dual mode, the number of cells N_k is the same in the As and descending Des elution modes; N_k is equal to the average number of cells for component k in the As and Des modes

Generic cell model mass balance equation

Representation of a LLC column as a series of equilibrium cells N_k, depicted simultaneously for ascending (As) and descending (Des) elution modes
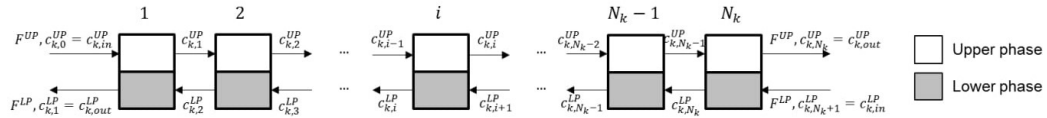
$$\frac{V^{UP}}{N_k}\frac{dc_{k,i}^{UP}}{dt} + \frac{V^{LP}}{N_k}\frac{dc_{k,i}^{LP}}{dt} = F^{UP}\left(c_{k,i-1}^{UP} - c_{k,i}^{UP}\right) + F^{LP}\left(c_{k,i+1}^{LP} - c_{k,i}^{LP}\right)$$

$V^{UP/LP}$ total volume of upper (UP) or lower (LP) phase in column
N_k number of theoretical cells associated with component k ($k = A, B, C$)
$F^{UP/LP}$ flow rate in ascending (As) or descending (LP) mode
$c_{k,i}^{UP/LP}$ concentration of component k in UP/LP in cell i

In Des mode: $F^{UP} = 0$
In As mode: $F^{LP} = 0$

1

Initial and boundary conditions, batch injections

Simplified cell model representation; As and Des modes depicted simultaneously; single LLC column
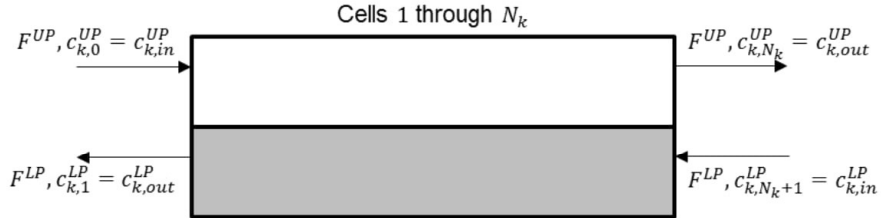
Initial conditions
$c_{k,i}^{UP} = c_{k,i}^{LP} = 0$ at $t = 0$

Boundary conditions

Process stage	As mode	Des mode
All $(t > 0)$	$F^{LP} = 0$ $c_{k,in}^{LP} = 0$	$F^{UP} = 0$ $c_{k,in}^{UP} = 0$
Sample injection $(t > 0$ to $t = \frac{V_{inj}}{F})$	$F^{UP} = F$ $c_{k,in}^{UP} = c_{k,feed}^{UP}$	$F^{LP} = F$ $c_{k,in}^{LP} = c_{k,feed}^{LP}$
Elution $(t > \frac{V_{inj}}{F})$	$F^{UP} = F$ $c_{k,in}^{UP} = 0$	$F^{LP} = F$ $c_{k,in}^{LP} = 0$

2

Initial and boundary conditions, trapping multiple dual mode

Simplified cell model representation; As and Des modes depicted simultaneously; two LLC columns of equal volume connected in series; total volume of two trapping MDM columns equivalent to total volume of single batch injection column
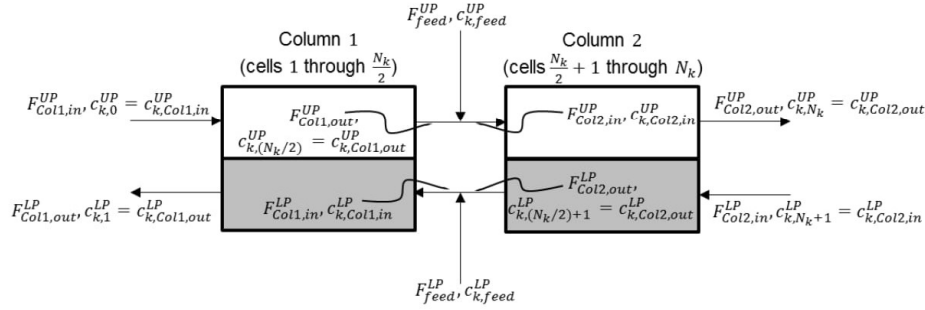
Mass and flow balance at feed node

As mode: $\qquad F_{Col1,out}^{UP} + F_{feed}^{UP} = F_{Col2,in}^{UP}$

$\qquad\qquad\quad F_{Col1,out}^{UP} c_{k,Col1,out}^{UP} + F_{feed}^{UP} c_{k,feed}^{UP} = F_{Col2,in}^{UP} c_{k,Col2,in}^{UP}$

Des mode: $\qquad F_{Col2,out}^{LP} + F_{feed}^{LP} = F_{Col1,in}^{LP}$

$\qquad\qquad\quad F_{Col2,out}^{LP} c_{k,Col2,out}^{LP} + F_{feed}^{LP} c_{k,feed}^{LP} = F_{Col1,in}^{LP} c_{k,in,Col1}^{LP}$

Initial conditions

$c_{k,i}^{UP} = c_{k,i}^{LP} = 0$ at $t = 0$

Boundary conditions

Process stage	As mode	Des mode
All	$F_{in}^{LP} = 0;\ F_{feed}^{LP} = 0$ $c_{k,Col2,in}^{LP} = 0;\ c_{k,feed}^{LP} = 0$	$F_{in}^{UP} = 0;\ F_{feed}^{UP} = 0$ $c_{k,Col1,in}^{UP} = 0;\ c_{k,feed}^{UP} = 0$
(1) Loading	$F_{Col1,in}^{UP} = 0;\ F_{feed}^{UP} = F$ $c_{k,Col1,in}^{UP} = 0;\ c_{k,feed}^{UP} = c_{k,feed}$	$F_{Col2,in}^{LP} = 0;\ F_{feed}^{LP} = F$ $c_{k,Col2,in}^{LP} = 0;\ c_{k,feed}^{LP} = c_{k,feed}$
(2) Separation & (3) Recovery	$F_{Col1,in}^{UP} = F;\ F_{feed}^{UP} = 0$ $c_{k,Col1,in}^{UP} = 0;\ c_{k,feed}^{UP} = 0$	$F_{Col2,in}^{LP} = F;\ F_{feed}^{LP} = 0$ $c_{k,Col2,in}^{LP} = 0;\ c_{k,feed}^{LP} = 0$

3

B. Correlations for S_f and N_k derived from experimental data

Experiment parameters

Solvent system	Arizona N (*n*-heptane/ethyl acetate/methanol/water 1/1/1/1 v/v/v/v)
Solutes	methyl paraben, ethyl paraben, propyl paraben, butyl paraben
Feed concentration	2 mg ml^{-1}
Injection volume	1 ml
CPC column	SCPC-250 (Armen Instrument); 182.1 ml total volume
Rotational speed	1700 rpm
Elution mode	Descending

Stationary phase fraction vs. flow rate ($S_f = f(F)$)
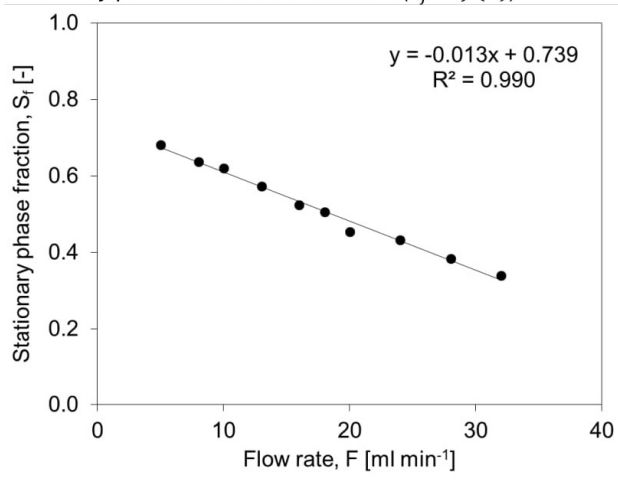
Theoretical cell number vs. flow rate ($N_k = f(F)$)

Component	Slope	y-Intercept	R^2
MP	23.29	168.68	0.94
EP	19.21	187.11	0.98
PP	10.94	200.77	0.95
BP	7.36	219.25	0.75
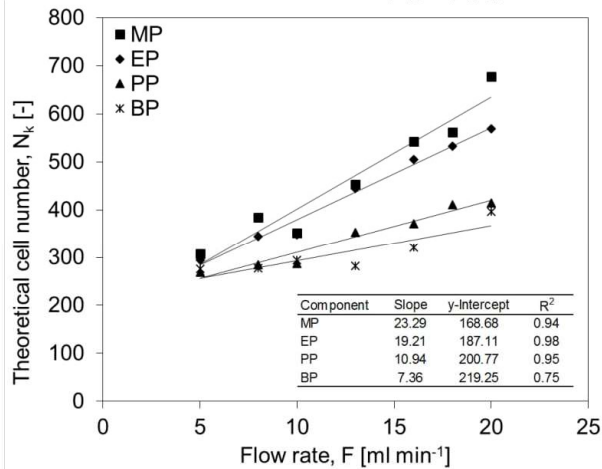
Slope and y-intercept of $N_k = f(F)$ plots vs. solute partition coefficient

Component	K_k, avg [-]
MP	0.89
EP	1.44
PP	2.44
BP	4.14

$y = 14.59x + 161.46$
$R^2 = 0.95$

$y = -4.90x + 26.10$
$R^2 = 0.91$

5
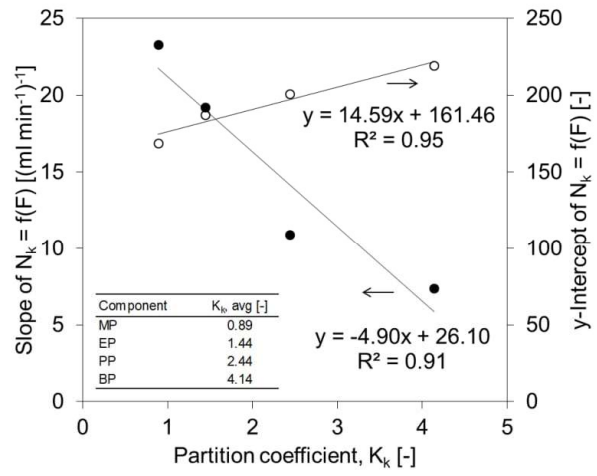
C. Summary of maximum productivity and corresponding independent parameters values for each separation task

Batch injection mode

	Parameter	Unit	$\alpha = 1.1$ Yld$_{req}$ 75%	$\alpha = 1.1$ Yld$_{req}$ 85%	$\alpha = 1.1$ Yld$_{req}$ 95%	$\alpha = 1.1$ Yld$_{req}$ 99%	$\alpha = 1.3$ Yld$_{req}$ 75%	$\alpha = 1.3$ Yld$_{req}$ 85%	$\alpha = 1.3$ Yld$_{req}$ 95%	$\alpha = 1.3$ Yld$_{req}$ 99%	$\alpha = 1.5$ Yld$_{req}$ 75%	$\alpha = 1.5$ Yld$_{req}$ 85%	$\alpha = 1.5$ Yld$_{req}$ 95%	$\alpha = 1.5$ Yld$_{req}$ 99%
Pur$_{req}$ 75%	Maximum productivity	[g l^{-1} h^{-1}]	n/a	n/a	n/a	n/a	2.90	2.52	1.01	n/a	5.54	5.48	4.48	3.23
	Flow rate	[ml min^{-1}]	n/a	n/a	n/a	n/a	20	20	12	n/a	26	28	20	20
	Injection volume	[ml]	n/a	n/a	n/a	n/a	20	15	10	n/a	30	25	30	20
Pur$_{req}$ 85%	Maximum productivity	[g l^{-1} h^{-1}]	n/a	n/a	n/a	n/a	1.74	1.29	n/a	n/a	4.54	4.41	3.55	2.15
	Flow rate	[ml min^{-1}]	n/a	n/a	n/a	n/a	16	16	n/a	n/a	26	24	22	18
	Injection volume	[ml]	n/a	n/a	n/a	n/a	15	10	n/a	n/a	25	25	20	15
Pur$_{req}$ 95%	Maximum productivity	[g l^{-1} h^{-1}]	n/a	n/a	n/a	n/a	n/a	n/a	n/a	n/a	3.26	2.90	2.08	0.87
	Flow rate	[ml min^{-1}]	n/a	n/a	n/a	n/a	n/a	n/a	n/a	n/a	24	20	18	12
	Injection volume	[ml]	n/a	n/a	n/a	n/a	n/a	n/a	n/a	n/a	20	20	15	10
Pur$_{req}$ 99%	Maximum productivity	[g l^{-1} h^{-1}]	n/a	n/a	n/a	n/a	n/a	n/a	n/a	n/a	2.01	1.64	0.84	n/a
	Flow rate	[ml min^{-1}]	n/a	n/a	n/a	n/a	n/a	n/a	n/a	n/a	20	16	12	n/a
	Injection volume	[ml]	n/a	n/a	n/a	n/a	n/a	n/a	n/a	n/a	15	15	10	n/a

Batch injection mode (cont'd)

	Parameter	Unit	α = 1.7				α = 2.0			
			Yld_{req} 75%	Yld_{req} 85%	Yld_{req} 95%	Yld_{req} 99%	Yld_{req} 75%	Yld_{req} 85%	Yld_{req} 95%	Yld_{req} 99%
Pur_{req} 75%	Maximum productivity	[g l^{-1} h^{-1}]	5.54	5.48	4.48	3.23	8.02	8.02	7.15	6.34
	Flow rate	[ml min^{-1}]	26	28	20	20	30	30	30	30
	Injection volume	[ml]	30	25	30	20	45	45	35	30
Pur_{req} 85%	Maximum productivity	[g l^{-1} h^{-1}]	4.54	4.41	3.55	2.15	6.80	6.63	6.12	4.99
	Flow rate	[ml min^{-1}]	26	24	22	18	30	30	30	26
	Injection volume	[ml]	25	25	20	15	40	35	30	30
Pur_{req} 95%	Maximum productivity	[g l^{-1} h^{-1}]	3.26	2.90	2.08	0.87	5.55	5.48	4.78	3.71
	Flow rate	[ml min^{-1}]	24	20	18	12	30	30	26	24
	Injection volume	[ml]	20	20	15	10	35	30	30	25
Pur_{req} 99%	Maximum productivity	[g l^{-1} h^{-1}]	2.01	1.64	0.84	n/a	4.46	4.32	3.60	2.64
	Flow rate	[ml min^{-1}]	20	16	12	n/a	28	26	24	22
	Injection volume	[ml]	15	15	10	n/a	30	30	25	20

Trapping MDM mode

	Parameter	Unit	$\alpha = 1.1$				$\alpha = 1.3$				$\alpha = 1.5$			
			Yld_{req} 75%	Yld_{req} 85%	Yld_{req} 95%	Yld_{req} 99%	Yld_{req} 75%	Yld_{req} 85%	Yld_{req} 95%	Yld_{req} 99%	Yld_{req} 75%	Yld_{req} 85%	Yld_{req} 95%	Yld_{req} 99%
Pur_{req} 75%	Maximum productivity	[g l^{-1} h^{-1}]	0.22	0.19	0.14	0.07	2.40	2.24	1.66	1.14	5.05	5.05	3.81	2.60
	x^{load}	[-]	0.25	0.30	0.35	0.25	0.10	0.15	0.25	0.25	0.10	0.10	0.10	0.10
	x^{sep}	[-]	0.70	0.60	0.40	0.30	0.50	0.90	0.80	0.70	0.15	0.15	0.30	0.50
	Separation stage cycles	[-]	7	13	103	126	1	1	2	3	1	1	1	1
Pur_{req} 85%	Maximum productivity	[g l^{-1} h^{-1}]	0.15	0.13	0.10	0.04	1.68	1.58	1.26	0.92	4.07	3.85	3.03	2.09
	x^{load}	[-]	0.30	0.30	0.40	0.15	0.10	0.10	0.25	0.20	0.10	0.10	0.10	0.25
	x^{sep}	[-]	0.60	0.60	0.45	0.20	0.70	0.85	0.65	0.65	0.20	0.25	0.20	0.65
	Separation stage cycles	[-]	14	16	134	134	1	1	3	3	1	1	2	2
Pur_{req} 95%	Maximum productivity	[g l^{-1} h^{-1}]	0.09	0.08	0.06	n/a	1.19	1.13	0.89	0.66	2.73	2.59	2.20	1.73
	x^{load}	[-]	0.40	0.45	0.35	n/a	0.25	0.20	0.20	0.25	0.10	0.20	0.15	0.25
	x^{sep}	[-]	0.55	0.55	0.40	n/a	0.90	0.80	0.65	0.50	0.15	0.95	0.90	0.75
	Separation stage cycles	[-]	42	75	164	n/a	2	2	3	7	3	1	1	2
Pur_{req} 99%	Maximum productivity	[g l^{-1} h^{-1}]	0.06	0.05	0.03	n/a	0.86	0.80	0.67	0.50	1.95	1.94	1.67	1.30
	x^{load}	[-]	0.50	0.45	0.25	n/a	0.20	0.25	0.30	0.30	0.15	0.15	0.25	0.20
	x^{sep}	[-]	0.55	0.50	0.30	n/a	0.90	0.80	0.70	0.45	0.90	0.95	0.75	0.75
	Separation stage cycles	[-]	180	190	193	n/a	2	3	5	15	1	1	2	2

Trapping MDM mode (cont'd)

	Parameter	Unit	α = 1.7				α = 2.0			
			Yld_{req} 75%	Yld_{req} 85%	Yld_{req} 95%	Yld_{req} 99%	Yld_{req} 75%	Yld_{req} 85%	Yld_{req} 95%	Yld_{req} 99%
Pur_{req} 75%	Maximum productivity	[g l^{-1} h^{-1}]	5.94	5.94	5.41	4.30	5.89	5.89	5.89	5.19
	x^{load}	[-]	0.15	0.15	0.15	0.10	0.20	0.20	0.20	0.15
	x^{sep}	[-]	0.20	0.20	0.25	0.20	0.25	0.25	0.25	0.20
	Separation stage cycles	[-]	1	1	1	1	1	1	1	1
Pur_{req} 85%	Maximum productivity	[g l^{-1} h^{-1}]	5.30	5.03	4.74	3.36	5.53	5.53	5.10	4.07
	x^{load}	[-]	0.15	0.15	0.10	0.10	0.20	0.20	0.15	0.15
	x^{sep}	[-]	0.20	0.25	0.15	0.30	0.25	0.25	0.20	0.30
	Separation stage cycles	[-]	1	1	1	1	1	1	1	1
Pur_{req} 95%	Maximum productivity	[g l^{-1} h^{-1}]	4.20	3.90	3.25	2.37	4.78	4.78	3.97	3.47
	x^{load}	[-]	0.10	0.10	0.10	0.15	0.15	0.15	0.15	0.10
	x^{sep}	[-]	0.15	0.20	0.30	0.70	0.20	0.20	0.30	0.20
	Separation stage cycles	[-]	1	1	1	1	1	1	1	1
Pur_{req} 99%	Maximum productivity	[g l^{-1} h^{-1}]	3.02	2.90	2.35	2.06	4.11	3.94	3.36	2.56
	x^{load}	[-]	0.10	0.10	0.10	0.30	0.15	0.15	0.10	0.40
	x^{sep}	[-]	0.25	0.30	0.45	0.75	0.20	0.25	0.20	0.80
	Separation stage cycles	[-]	1	1	1	2	1	1	1	2

3.4 Paper IV

Trapping multiple dual mode liquid-liquid chromatography: Preparative separation of nootkatone from a natural product extract

Author contribution: The thesis author had the leading role in completion of this paper, from conceptualization to experiment execution and data analysis. She completed the manuscript and performed the necessary edits.

Summary: Paper IV concerned the implementation of the trapping MDM model-based design strategy for the high-throughput separation of nootkatone from a real natural product mixture of over 90 compounds. The starting mixture was obtained from an industrial orange juice processing side stream in which the target, nootkatone (NK), was present at 17%, and only three of the remaining compounds were found at greater than 2%: valencene (13%), eudesmenol (ED, 9%), and intermedeol (IM, 6%).

In this demonstrative study, NK was found to co-elute with ED, leading to the two components to be treated as a single pseudo-component for the process design: NK+ED. The remaining major impurity considered was IM, with a separation factor of approximately 1.2 with respect to NK+ED. According to the findings of Paper III, this separation factor rendered the use of trapping MDM advantageous.

The maximum feed concentration and flow rate were determined in the same manner as in Paper II. The linear range limit of the partition isotherm of NK as well as increases in settling time and phase volume ratio all coincided at approximately 100 mg ml^{-1}. A maximum flow rate of 14 ml min^{-1} was measured in the presence of the feed solution. Safety margins were applied to these parameters for the remaining design steps and final separation, which were performed with a feed concentration of 75 mg ml^{-1} and 12 ml min^{-1} flow rate.

For selection of the step durations and number of cycles, the short-cut model was extended for calculation of the process throughput. The trapped component B band position during the Separation stage, x_B^{sep}, was fixed at 0.8 while varying x_B^{load}. An x_B^{load} of 0.42 was identified for the maximized-throughput experiment, corresponding to a feed loading of 46% of the total column volume. No stationary phase loss occurred during the experiment. The Recovery stage NK+ED yield was 85%, with a purity of 97% with respect to IM only and 78% with respect to all impurities. These purities far exceeded those obtained with the low volume pulse injections. The results of this study demonstrate the effectiveness of trapping MDM and the model-based design approach for separations of complex mixtures, even when using only the mathematically simple short-cut model.

Trapping multiple dual mode liquid-liquid chromatography: Preparative separation of nootkatone from a natural product extract

Raena Morley, Mirjana Minceva*

Biothermodynamics, TUM School of Life Sciences Weihenstephan, Technical University of Munich, Maximus-von-Imhof-Forum 2, 85354 Freising, Germany

ARTICLE INFO

ABSTRACT

Trapping multiple dual mode (trapping MDM) is a preparative liquid-liquid chromatography (LLC) technique well-suited to difficult separations of intermediately-eluting components from similarly structured impurities. In this demonstrative study, a design approach for high process throughput is applied for the trapping MDM separation of a target component, nootkatone (NK), initially comprising 16.7% of an industrial side stream mixture with over 90 impurities. This design approach, previously developed and validated using ternary mixtures of model solutes, is applied to a complex real mixture for the first time. The approach consists of five steps: (1) determination of the maximum starting mixture concentration for feed preparation; (2) determination of the maximum flow rate for maintenance of the pre-set stationary phase fraction; (3) determination of the partition coefficients of the target and main impurities; (4) selection of step durations and number of cycles using an established short-cut method; (5) execution of the trapping MDM separation. The target, NK, was obtained along with a co-eluting component at 78.7% purity and 84.6% yield, demonstrating the effectiveness of trapping MDM for the separation of intermediately-eluting natural product target components from complex starting mixtures.

© 2020 Elsevier B.V. All rights reserved.

1. Introduction

The preparative separation of natural products from complex starting mixtures with chromatography often poses the challenge of isolating an intermediately-eluting target component from similarly-structured impurities possessing very low separation factors. Extensive peak overlap is frequently observed when batch injections are used, negatively affecting the yield and/or purity of the collected target component fraction. Peak overlap becomes especially critical at the high volume and high concentration feed loadings preferred for preparative separations at high throughput. Trapping multiple dual mode (trapping MDM) [1–3], a solid support-free liquid-liquid chromatography (LLC) technique, can be used as an effective alternative to batch injections for such ternary separations.

LLC comprises a wide array of techniques including Martin and Synge columns, countercurrent distribution (CCD), droplet countercurrent chromatography (DCCC), pulsed Kostanyan columns, as well as the more common and better-known countercurrent chromatography (CCC) and centrifugal partition chromatography (CPC) [4]. These diverse techniques are united by their use of the two phases of liquid-liquid biphasic system as the mobile and stationary phases. The stationary phase is retained during operation without the use of a solid support. In CCC and CPC, stationary phase retention is achieved through the application of a centrifugal force. Compared with conventional chromatography techniques utilizing solid stationary phases, the use of a liquid stationary phase in LLC offers several advantages, such as high sample loading, the absence of adverse adsorption effects, and a high degree of operational flexibility [5]. LLC has emerged as a technique well-suited to the preparative separation of target components from natural product starting mixtures [6,7]. As a result of the ability to switch the roles of the mobile and stationary phases and, with this switch, to reverse the flow direction and elution order of the sample solutes, a wide variety of operating modes can be performed in LLC that have no direct counterpart in conventional chromatography [8], such as the aforementioned trapping MDM technique.

In this work, the trapping MDM separation of an intermediately-eluting target component from a real complex mixture and the application of the corresponding design approach for operating parameter selection under high throughput conditions are reported for the first time. The target component to be "trapped" in this exemplary study was nootkatone (NK), a sesquiterpene found primarily in grapefruit as well as in other citrus fruits and natural sources. The starting mixture was a NK-enriched extract obtained from an industrial orange juice processing side stream. In addition to being used as an

* Corresponding author.
E-mail address: mirjana.minceva@tum.de (M. Minceva).

aroma compound in the food, beverage, and cosmetic industries, studies have shown nootkatone to possess a range of bioactive properties, such as pest-repellant and anti-obesity effects [14]. In the last decade, commercial-scale nootkatone production has been implemented using microbial fermentation [15,16], rendering naturally-sourced nootkatone less favorable for the large-scale production of this compound. Nevertheless, this study serves as a useful demonstration of the trapping MDM technique for difficult separations of natural product target components with intermediately-eluting behavior.

The utilized trapping MDM design approach has been previously developed and validated with model mixtures of three components only [1,2]. The five-step design approach consisted of preliminary measurements and experiments for the determination of the maximum starting mixture concentration for feed preparation (Step 1), the maximum flow rate (Step 2), and the partition coefficients of the components of interest (Step 3). A short-cut method for selection of step durations and number of cycles (Step 4) was then implemented, followed by execution of the high throughput trapping MDM separation run (Step 5).

2. Theory

2.1. Trapping MDM process description

Trapping multiple dual mode (trapping MDM) is a discontinuous LLC operating mode for the separation of intermediately-eluting components, i.e., target components with an intermediate partition coefficient with respect to the other starting mixture components, from impurities possessing low separation factors. In a previous study, it was found that the use of trapping MDM is especially advantageous in comparison with batch injections for the isolation of intermediately-eluting targets at high purity and yield from impurities with separation factors of approximately 1.3 or lower [3]. The trapping MDM process and an associated short-cut method for selection of the key operating parameters (step durations and number of cycles) were first presented in [1]. A throughput maximization strategy implementing this short-cut method was developed and validated using a model mixture in [2]. Separation techniques similar to trapping MDM have been previously reported as variants of the intermittent countercurrent extraction (ICcE) [9] and multiple dual mode (MDM) processes [10].

The trapping MDM technique is based on the ability to switch the roles of the two phases during a separation, resulting in two possible elution modes: ascending mode (As) and descending mode (Des). In As mode, the less dense upper phase (U) is used as the mobile phase while the denser lower phase (L) is kept stationary. In Des mode, the upper phase is the stationary phase, while the lower phase is pumped through it as the mobile phase. Switching the elution mode necessitates a reversal of the flow direction while at the same time reversing the elution order of the mixture components. The fastest eluting components become the slowest, and vice versa, as seen from the relationship between the As and Des partition coefficients of a component i given in Eq. (1). The partition coefficient is defined as the ratio of the equilibrium concentrations of a component in the stationary and mobile phases.

$$K_{i,Des} = \frac{c_{i,U}}{c_{i,L}} = \frac{1}{K_{i,As}} \tag{1}$$

The trapping MDM process is most simply described for a ternary mixture of three components (A, B, C) with relative partition coefficient values $K_{A,Des} < K_{B,Des} < K_{C,Des}$ and $K_{A,As} > K_{B,As} > K_{C,As}$. B is the intermediately-eluting component that will remain "trapped" on the two-column LLC unit during the separation. A trapping MDM separation consists of three process stages, depicted in Fig. 1: Loading, Separation, and Recovery. In

Stage 1: Loading
Feed introduced during a single cycle
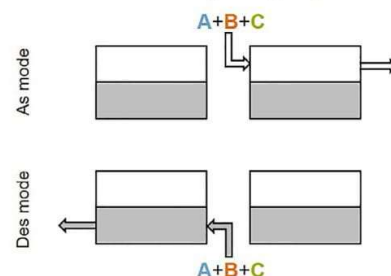
Stage 2: Separation
Multiple cycles of As and Des steps
Net movement of A in Des direction, C in As direction
B trapped in columns
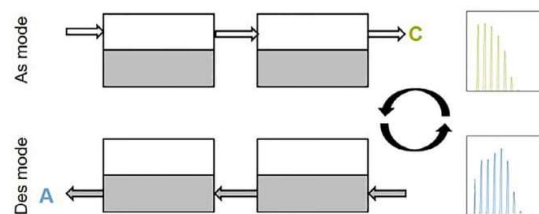
Stage 3: Recovery
Collection of target B in a single step (As or Des)
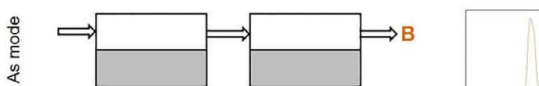
Fig. 1. Trapping MDM separation of three components (A, B, C) with B as the intermediately-eluting target. Relative partition coefficients: $K_{A,Des} < K_{B,Des} < K_{C,Des}$ and $K_{A,As} > K_{B,As} > K_{C,As}$. White shading: upper phase. Gray shading: lower phase.

the first stage (Loading), the feed solutions dissolved in the upper and lower phases are introduced at the inlets between the two columns during the corresponding elution mode step (lower phase feed solution in Des mode; upper phase feed solution in As mode). There is no accompanying flow of pure mobile phase. The second stage (Separation) consists of multiple cycles, each consisting of two steps (one in each elution mode), during which only pure mobile phase (lower phase in Des mode; upper phase in As mode) is introduced from the corresponding end of the two-column unit. The step durations of the two elution modes are chosen to prevent component B from eluting at either outlet. With each cycle, A and C, on the other hand, travel a net distance toward opposite ends of the unit. During Separation, A and C may be partially or completely eluted from the unit. When satisfactory separation of B from A and C has been achieved, the third stage (Recovery) is begun. To collect B in purified form, an extended elution step in a single mode is performed (As or Des). A more detailed description of the trapping MDM process can be found in [8].

2.2. Trapping MDM short-cut method

The success of a trapping MDM separation is dependent on appropriate selection of the step durations during the Loading and Separation stages, as well as the number of Separation stage cy-

cles to be performed. The step durations and number of cycles are interdependent and cannot be selected individually. To avoid step duration selection by trial and error, a rational parameter selection short-cut method was developed and validated in [1] and applied in two subsequent studies [2,3]. The short-cut method is based on solute band front propagation velocities under linear and ideal chromatography assumptions, i.e., constant partition coefficients and no dispersive effects. These propagation velocities are defined for the As and Des elution modes in Eqs. (2) and (3), respectively,

$$v_{i,As} = \frac{F_U}{V_{R,i,As}} \tag{2}$$

$$v_{i,Des} = \frac{F_L}{V_{R,i,Des}} \tag{3}$$

where F_U and F_L are the upper and lower phase (As and Des mode) flow rates and $V_{R, i, As}$ and $V_{R, i, Des}$ are the elution mode-specific retention volumes defined in Eqs. (4) and (5). V_U and V_L are the volumes of the upper and lower phases in the CPC unit.

$$V_{R,i,As} = V_U + K_{i,As}V_L \tag{4}$$

$$V_{R,i,Des} = V_L + K_{i,Des}V_U \tag{5}$$

The short-cut method equations for selection of the step durations (Eqs. (6)–(11)) and number of cycles (Eqs. (12)–(15)) are listed in Table 1. The retention volumes ($V_{R,i}$) used for calculation of the propagation velocities (v_i) must be based on the volumes of the upper and lower phases (V_U, V_L) in a single column of the two-column trapping MDM unit. F_U and F_L are the As and Des mode flow rates of feed introduction in the Loading stage and of the mobile phase in the Separation and Recovery stages. The elution mode of the first step in each cycle and the of Recovery stage must be specified. Additionally, the dimensionless position of the trapped solute band front at the end of each Des and As step in the Loading ($x_{B,Des}^{load}$, $x_{B,As}^{load}$) and Separation stages ($x_{B,Des}^{sep}$, $x_{B,As}^{sep}$) must be selected.

For all band position combinations satisfying the restrictions named in [1], the short-cut method equations return the step durations during the Loading (t_{Des}^{load}, t_{As}^{load}) and Separation stages (t_{Des}^{sep}, t_{As}^{sep}; $t_{Des}^{sep,1st}$ or $t_{As}^{sep,1st}$, depending on the elution mode of the first step in each cycle) and the number of cycles (with respect to components A and C; n_A^{sep}, n_C^{sep}) that will result in complete separation and recovery of B from A and C under ideal conditions. The reader is directed to [1] for more details regarding the derivation and implementation of the short-cut method equations. A strategy for identifying the band position combination providing the highest process throughput is described in Section 4.2.4.

Despite being defined for a ternary mixture of components A, B, and C, the trapping MDM process and short-cut method are easily adapted to a complex multi-component starting mixture by representing it as a simplified pseudo-ternary mixture. B represents the intermediately-eluting target component(s) while A and C are the nearest-neighbor impurities, i.e., possessing the lowest separation factors with respect to B, to be considered in the process design. All remaining impurities with partition coefficients lower than A in Des mode and lower than C in As mode will leave the column before A and C, respectively. Their separation from B is therefore intrinsically accounted for with that of A and C.

3. Materials and methods

3.1. Materials

3.1.1. Starting mixture
The starting mixture, a nootkatone-enriched extract from an industrial orange juice processing side stream, was obtained from Erich Ziegler GmbH.

3.1.2. Solvent system
The biphasic solvent system used throughout this study was n-hexane/ethyl acetate/methanol/water 9/1/9/1 v/v/v/v, a relatively non-polar solvent system commonly known as "HEMWat -7″ [11].

Table 1
Trapping MDM short-cut method equations.

Parameter	Equation	
Step durations, Stage 1: Loading		
Des	$t_{Des}^{load} = \dfrac{x_{B,Des}^{load}}{v_{B,Des}}$	(6)
As	$t_{As}^{load} = \dfrac{x_{B,As}^{load}}{v_{B,As}}$	(7)
Step durations, Stage 2: Separation		
Des, 1st cycle (first mode Des)	$t_{Des}^{sep,1st} = \dfrac{(x_{B,Des}^{sep} - x_{B,Des}^{load})}{v_{B,Des}}$	(8)
As, 1st cycle (first mode As)	$t_{As}^{sep,1st} = \dfrac{(x_{B,As}^{sep} - x_{B,As}^{load})}{v_{B,As}}$	(9)
Des	$t_{Des}^{sep} = \dfrac{[(x_{B,Des}^{sep} - x_{B,Des}^{load}) + (x_{B,As}^{sep} - x_{B,As}^{load})]}{v_{B,Des}}$	(10)
As	$t_{As}^{sep} = \dfrac{[(x_{B,Des}^{sep} - x_{B,Des}^{load}) + (x_{B,As}^{sep} - x_{B,As}^{load})]}{v_{B,As}}$	(11)
Number of cycles, Stage 2: Separation		
Component A (first mode Des)	$n_A^{sep} = \dfrac{(t_{As}^{load} + t_{As}^{sep})v_{A,As} - t_{Des}^{sep,1st}v_{A,Des} + 1}{t_{Des}^{sep}v_{A,Des} - t_{As}^{sep}v_{A,As}} + 1$	(12)
Component A (first mode As)	$n_A^{sep} = \dfrac{(t_{As}^{load} + t_{As}^{sep})v_{A,As} - t_{Des}^{sep,1st}v_{A,Des} + 1}{t_{Des}^{sep}v_{A,Des} - t_{As}^{sep}v_{A,As}} + 1$	(13)
Component C (first mode Des)	$n_C^{sep} = \dfrac{(t_{Des}^{load} + t_{Des}^{sep})v_{C,Des} - t_{As}^{sep}v_{C,As} + 1}{t_{As}^{sep}v_{C,As} - t_{Des}^{sep}v_{C,Des}} + 1$	(14)
Component C (first mode As)	$n_C^{sep} = \dfrac{(t_{Des}^{load} + t_{Des}^{sep})v_{C,Des} - t_{As}^{sep,1st}v_{C,As} + 1}{t_{As}^{sep}v_{C,As} - t_{Des}^{sep}v_{C,Des}} + 1$	(15)

The HEMWat (n-hexane/ethyl acetate/methanol/water) solvent system family is often used for natural product separations with LLC [12] and consists of 16 volumetric compositions covering a wide polarity range numbered from −7 to +8. HEMWat -7 was selected following a screening of several compositions with preliminary measurements of partition coefficients, starting mixture solubility, and settling time. In comparison with the other screened systems, HEMWat -7 provided the highest solubility and lowest settling time when combined with the starting mixture, indicating the possibility of high feed loading and stability within the column. Additionally, it provided a partition coefficient of the target component nootkatone (NK) close to 1, lying within the recommended "sweet spot" partition coefficient range of 0.4 to 2.5. This range affords a compromise between peak resolution, band broadening, and separation run time [11]. A target partition coefficient near unity is especially desirable in trapping MDM, as similar step durations can then be selected in both elution modes [9,10].

The following solvents were used for preparation of the HEMWat -7 solvent system: n-hexane (>95%, DHC Solvent Chemie, Muelheim, Germany), ethyl acetate (>99.8%, CSC Jaeklechemie, Nuremberg, Germany), methanol (>99.85%, CSC Jaeklechemie, Nuremberg, Germany), and de-ionized water (in-house network).

The HEMWat -7 solvent system used throughout this study was prepared by mixing n-hexane, ethyl acetate, methanol, and water in the volume proportion 9/1/9/1. The solvents were left to mix for at least 2 h at room temperature (22±2 °C) on a magnetic stir plate. A separatory funnel was then used to split the upper and lower phases between two reservoirs. Phases were degassed in an ultrasonic bath before use in the CPC. The necessary solvent system volume was newly prepared before each experiment or set of measurements.

3.1.3. Analytical solvents

The mobile phase used for HPLC analysis consisted of acetonitrile (>99.95%, VWR Chemicals, Ismaning, Germany) and Millipore 18-MOhm water. When necessary, samples were diluted with the corresponding phase (HEMWat -7 upper or lower phase).

The starting mixture was diluted with n-hexane (>98.0%, Merck KGaA, Darmstadt, Germany) preceding analysis with GC-MS. All other samples were diluted with the corresponding HEMWat -7 phase (upper or lower) when necessary.

3.2. Analytics

3.2.1. HPLC analysis

Quantitative analysis of nootkatone only was performed with HPLC using a NUCLEODUR 100-5 C18 ec column (125 mm length, 4 mm ID; Machery-Nagel, Dueren, Germany) fitted with a guard column. The HPLC set-up (Gilson, Middleton, WI, USA) consisted of a 322H2 binary gradient pump, a GX Direct injection module, and a 151 UV–Vis Detector. Sample analysis was automated with Trilution LC software.

The analysis method for all samples was performed at ambient temperature (22±2 °C) and consisted of a water:acetonitrile (A:B) gradient program with a mobile phase flow rate of 0.8 ml min^{-1} and 10 μl injection volume. The detection wavelength was set at 280 nm. The gradient program was as follows: 50%:50% for 5 min; ramp to 0%:100% in 12 min; ramp down to 50%:50% in 4 min; 50%:50% for 4 min. A calibration curve was produced with a 90% pure nootkatone sample obtained from Erich Ziegler GmbH.

3.2.2. GC-MS analysis

Qualitative GC-MS analysis was performed on a Zebron ZB-5 ms Guardian Capillary column (30 m with 5 m Guardian length, 0.25 mm ID, 0.25 μm film thickness; Phenomenex, Aschaffenburg, Germany). The set-up consisted of a 6890 N Network GC System,

5973Network Mass Selective Detector, and 7683 Series Injector. Instrument control and analysis were automated using Enhanced ChemStation software (G1701DA Version D.00.00.38). The carrier gas was helium.

The oven temperature program (total duration 50.17 min) was started at 50 °C, increased to 105 °C at a rate of 5 °C min^{-1}, then increased to 220 °C at a rate of 6 °C min^{-1}, after which the temperature was held for 20 min. The mass spectrometer was operated in EI mode with a scan range of 50 to 350 amu, 4.72 scans s^{-1}, and an electron energy of 70 eV. The temperatures of the injector inlet, MS source, and MS quad were set at 220 °C, 230 °C, and 150 °C, respectively. Injections (1.0 μl volume) were performed in split mode with a split ratio of 10 in constant pressure mode (91 kPa). Compounds were identified using the Enhanced ChemStation software by comparison with the NIST98 library.

3.3. CPC experiments

The following subsections describe the two-column CPC set-up and feed solution preparation method used in Steps 2, 3, and 5 of the trapping MDM design approach.

3.3.1. CPC unit

CPC experiments were performed on a TMB-250 unit manufactured by Armen Instrument (Saint-Avé, France). The unit consisted of two CPC columns mounted on separate rotors and connected in series with a total measured volume of 182.1 ml. The set-up additionally included four HPLC gradient pumps (two for mobile phase introduction and two for the feed solutions), two UV-Vis detectors, and two automated fraction collectors. The mobile phase (upper phase in As mode; lower phase in Des mode) is introduced from one of the ends of the unit, while feed is introduced between the two columns in either the As or Des flow direction. Feed introduction by pump can be performed independently or with simultaneous mobile phase flow. The column can be operated at a pressure drop of up to 100 bar and a maximum rotational speed of 3000 rpm. More details regarding the TMB-250 unit are found in [13]. Mobile phase and feed solution reservoirs were kept in a water bath set at 20 °C.

The column was prepared in the same manner prior to the start of all CPC experiments. The two-column unit was first filled with a 1:1 ratio of HEMWat -7 upper and lower phases, equivalent to a stationary phase fraction (S_f) of 0.5 in both elution modes. Column filling was completed without rotation and at a flow rate of 30 ml min^{-1}. Rotation at a set speed of 1700 rpm was then started. After reaching the set rotational speed, feed introduction (stationary phase fraction measurements in Step 2; trapping MDM separation in Step 5) or mobile phase flow before sample injection (pulse injections in Step 3) could be started.

3.3.2. Feed solution preparation

For the stationary phase fraction measurements for maximum flow rate determination (Step 2), pulse injections for partition coefficient determination (Step 3), and trapping MDM experiment (Step 5) described below, feed solutions were prepared by adding the starting mixture to equal volumes of HEMWat -7 upper and lower phases in a single vessel corresponding to the required starting mixture concentration (with respect to the total volume of the upper and lower phases) and feed solution volumes. The system was then left to mix on a magnetic stir plate at room temperature (22±2 °C) for 2 h before being transferred to a separatory funnel. The upper and lower phase feed solutions (used as feed in the As and Des elution modes, respectively) were then split into separate reservoirs and degassed in an ultrasonic bath before use.

3.4. Trapping MDM design approach

For clarity and consistency with the structure of Section 4, the procedures associated with each of the design approach steps are detailed in the following subsections.

3.4.1. Step 1: Determination of maximum starting mixture concentration for feed solution preparation

Sample preparation: Samples were prepared in duplicate by dissolving the starting mixture over a concentration range (starting mixture concentration with respect to the total volume of the upper and lower phases) from 0 (blank sample) to 300 mg ml^{-1} in 5 ml upper phase and 5 ml lower phase (10 ml total volume) of the biphasic solvent system HEMWat -7 in 15 ml centrifuge tubes. Samples were then subjected to automated mixing for 2 h at room temperature (22±2 °C). For each sample, settling time, phase volume ratio, and partition equilibrium measurements were performed as described below.

Settling time measurements: Each sample was quickly inverted 10 times, then immediately placed in a tube rack. The elapsed time between placement in the rack and the reestablishment of a stable interface between the two phases was recorded. The settling time was measured for each sample in triplicate.

Phase volume ratio measurements: The volumes of the upper and lower phases were read from the graduation marks on the centrifuge tubes (0.5 ml, with a tolerance of ± 0.1 ml). The phase volume ratio was subsequently calculated as (upper phase volume)/(lower phase volume).

Partition equilibrium measurements: Aliquots were taken from the upper and lower phases and analyzed with HPLC to determine the nootkatone concentration in each.

3.4.2. Step 2: Determination of maximum flow rate

Stationary phase fraction, S_f, is defined by Eq. (16)

$$S_f = \frac{V_S}{V_C} \tag{16}$$

where V_S is the volume of the stationary phase retained on the column and V_C is the total column volume. S_f is typically measured with pure phases only, i.e., in the absence of the feed solution.

As in [2], in this study, S_f with respect to flow rate was measured in the presence of the upper and lower phase feed solutions (used for As and Des mode measurements, respectively). The feed solutions were prepared using the maximum starting mixture concentration of 100 mg ml^{-1} determined in Step 1.

Following preparation of the CPC unit as described in Section 3.3.1, 45 ml of feed solution, approximately equivalent to the mobile phase volume of one column of the two-column unit, was introduced at the feed inlet between the columns over the corresponding feed pump (As or Des). The feed solution entered the unit in the flow direction corresponding to the elution mode; at the end of feed loading, only one of the two columns contained the feed solution. Elution with the corresponding mobile phase (upper phase in As mode; lower phase in Des mode) was then begun and the effluent collected in a 250 ml graduated cylinder. After elution of 180 ml of mobile phase (approximately equivalent to two single column volumes), pumping was stopped and the amount of stationary phase loss, if any, recorded. The resulting S_f was then calculated. This procedure was performed for flow rates of 12, 14, 16, 20, and 28 ml min^{-1} in both elution modes, with new preparation of the column each time.

3.4.3. Step 3: Determination of partition coefficients

Pulse injections were performed on the CPC unit in both elution modes for determination of the partition coefficients ($K_{i,Des}$, $K_{i,As}$)

of the target component and major impurities: NK, VC, IM, and ED (see Section 4.1.).

Before injection, the CPC unit was prepared with $S_f = 0.5$ as described in Section 3.3.1. Feed solution injections (75 mg ml^{-1} starting matrix concentration) were made over a 5 ml manual sample loop 1 min after the start of mobile phase flow (12 ml min^{-1}). The effluent was monitored with UV–Vis detection (240 and 254 nm). Online UV–Vis monitoring did not play a role in component identification but served as a indication of completion of NK elution during the Recovery stage. Fractions were collected every 20 s beginning after elution of the non-retained solute retention volume. Aliquots taken from the fractions were analyzed with GC-MS without dilution for chromatogram reconstruction of the components of interest. Partition coefficients were calculated for the As and Des elution modes from the reconstructed chromatograms using the corresponding LLC retention volume equation Eq. (4) or ((5)).

3.4.4. Step 4: Selection of step durations and number of cycles

The short-cut method for parameter selection described in Section 2.2. was used in conjunction with process throughput calculations (introduced in Section 4.2.4.) to determine the step durations and number of cycles for the trapping MDM separation performed in Step 5. The input parameters and a detailed description are found in Section 4.2.4.

3.4.5. Step 5: Trapping MDM separation

Before the start of the trapping MDM separation, the two-column CPC unit ($S_f = 0.5$) and feed solutions (75 mg ml^{-1} starting matrix concentration) were prepared as described in Secs. 3.3.1 and 3.3.2., respectively. The feed and mobile phase flow rate was 12 ml min^{-1} throughout the process. The step durations are listed in Table 4.

Loading: The Des and As feed solutions were introduced for step durations t_{Des}^{load} and t_{As}^{load}, corresponding to a total loaded volume of 84.1 ml (33.2 ml in Des mode; 50.9 ml in As mode). In both elution modes, the entire effluent was collected in a 50 ml graduated cylinder and aliquots taken for GC–MS analysis (10x dilution).

Separation: 10 Separation stage cycles were completed; each starting in Des mode. All cycles had step durations t_{Des}^{sep} and t_{As}^{sep}, with the exception of the Des step of the first cycle with $t_{Des}^{sep,1st}$. This shorter step duration compensates for the position of the component B band fronts directly following the end of the Loading stage. During each step, the entire mobile phase effluent was collected in a 50 ml graduated cylinder and aliquots taken for GC–MS analysis (10x dilution).

Recovery: Following the end of the As mode step of the 10th Separation stage cycle, elution with pure As mode mobile phase was continued for 22 min. 60 s fractions were collected with the As mode fraction collector during the entire Recovery stage. Aliquots were taken from all fractions and analyzed by GC–MS (10x dilution).

4. Results and discussion

The objective of this study was to apply the previously developed trapping MDM design approach for the high throughput separation of intermediately-eluting components [2] to a complex natural product starting mixture. To obtain high throughput in preparative chromatography separations, the largest amount of feed solution (high concentration, high injection volume) should be processed in the least amount of time possible (high flow rate, short process duration). The five-step design strategy as presented in this work is graphically depicted in Fig. 2.

Following preliminary analysis and evaluation of the starting mixture (Section 4.1.), the maximum starting mixture concentration for preparation of the feed solutions (c_{feed}^{max}) is determined
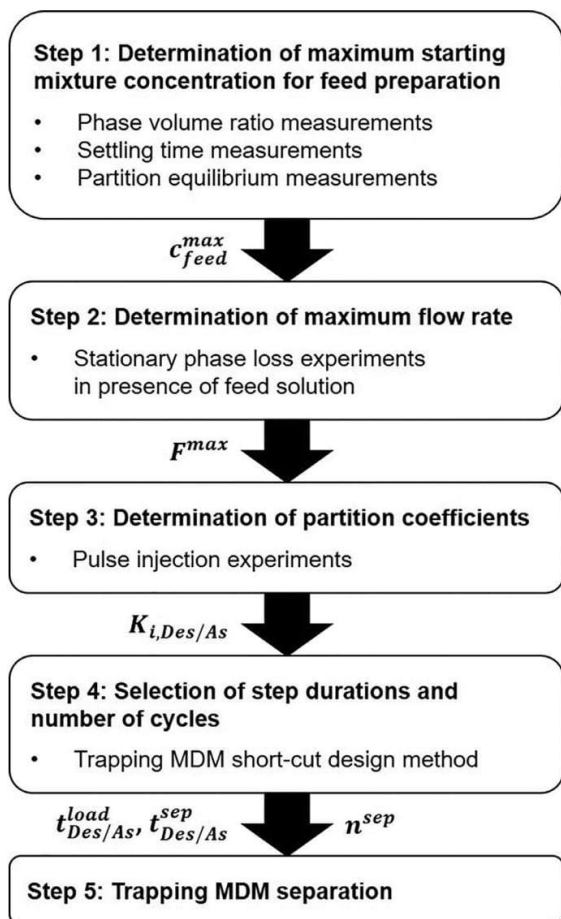
Fig. 2. Trapping MDM design approach.

with the help of phase volume ratio, settling time, and partition equilibrium measurements in Step 1 (Section 4.2.1.). In Step 2 (Section 4.2.2.), the maximum applicable flow rate (F^{max}) in the presence of c_{feed}^{max} is ascertained through stationary phase loss experiments. Pulse injection experiments are then performed in Step 3 (Section 4.2.3.) to obtain the partition coefficients of the components of interest ($K_{i,Des}$, $K_{i,As}$) under the column-specific hydrodynamic conditions resulting from operation at c_{feed}^{max} and F^{max}. The short-cut method is then applied with the parameters F^{max}, $K_{i,Des}$, and $K_{i,As}$ in Step 4 (Section 4.2.4.) for the selection of the trapping MDM Loading and Separation stage step durations (t^{load}, t^{sep}) and number of cycles (n^{sep}). The combination of short-cut method band front positions (x_B^{load}, x_B^{sep}) leading to the highest throughput under the set process restrictions is identified. The selected operating parameters are then implemented for the execution of the trapping MDM separation at high throughput conditions in Step 5 (Section 4.2.5.).

4.1. Preliminary analysis of the starting mixture

The starting mixture was qualitatively analyzed with GC-MS to determine the key impurities to be considered in the design of the separation with the short-cut method. The normalized total ion count (TIC) chromatogram is found in Fig. 3. The starting mixture was found to contain at least 90 different compounds, many of them sesquiterpene alcohols and oxides. In addition to nootkatone (NK, 16.7 area%), only 3 of these compounds were present at greater than 2 area%: valencene (VC, 13.0%), eudesm-7(11)-en-4α-ol (ED, 9.0%), and intermedeol (IM, 6.0%). All remaining components were regarded as minor impurities and were not taken into consideration in the design approach steps concerning component-specific data, i.e., partition coefficients (Steps 3 and 4). The peaks corresponding to these compounds are indicated in Fig. 3 and their molecular structures provided in Fig. 4.

Preliminary shake flask measurements using the HEMWat -7 solvent system and GC-MS area% analysis indicated similar Des partition coefficients of K_{ED}, K_{IM}, and K_{NK} ranging from 0.74 to 0.87. As a non-oxygenated hydrocarbon, VC strongly partitions into the less polar upper phase, resulting in a much higher K_{VC} of approximately 20. Therefore, VC elutes quickly in As mode and can be easily separated from NK, while the separation of NK from ED and IM is expected to be much more difficult.
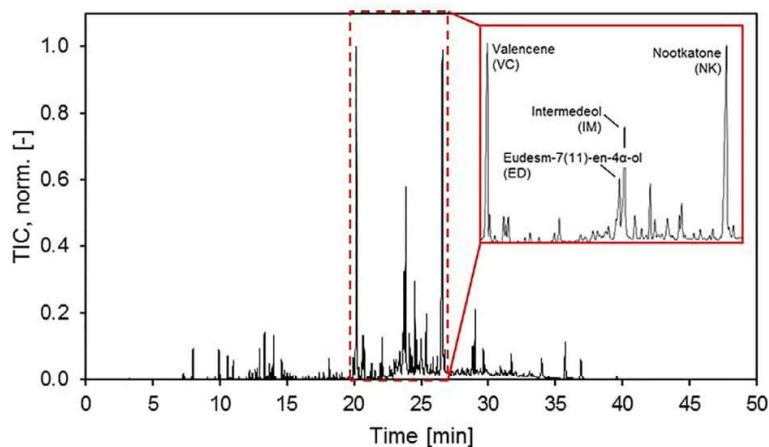

Fig. 3. GC-MS analysis of starting mixture.
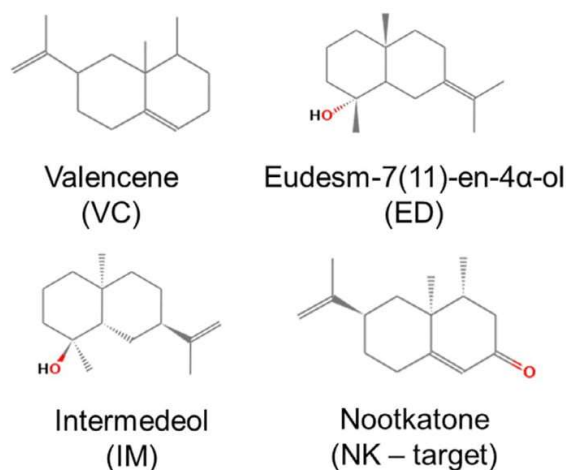
Fig. 4. Target component and starting mixture major impurities.

4.2. Trapping MDM design approach

4.2.1. Step 1: Determination of the maximum starting mixture concentration for feed solution preparation

Step 1 of the design approach focuses on determination of the maximum starting mixture concentration that can be used for preparation of the feed solutions without significant deviation from the properties of the pure mobile and stationary phases, e.g., phase volume ratio, density, viscosity, interfacial tension. Changes in these properties can lead to undesirable hydrodynamic conditions resulting in stationary phase loss, negatively affecting the performance and repeatability of a separation [17–19].

Solute partition equilibria also play an important role in the selection of the maximum starting mixture concentration. Partition equilibria increasingly deviate from linear with increasing solute (starting mixture) concentration as a result of intermolecular interactions between the solute molecules. Outside of the linear range of the partition equilibrium, the partition coefficient can no longer be considered independent of concentration (constant) and short-cut methods based on linear, ideal chromatography assumptions, such as the one used in this study, become more likely to fail.

In packed-bed chromatography, concentration-dependent partition equilibria can be described by adsorption isotherms determined experimentally using, e.g., frontal analysis measurements. Such techniques are however not suitable for partition equilibria determination in LLC, as changes in solute partitioning due to increased starting mixture concentration are often coupled to changes in phase properties and composition, which can in turn affect the column hydrodynamics and the achievable stationary phase fraction [20]. As these secondary effects depend strongly on the solvent system, feed solution, and LLC unit, they cannot yet be reliably predicted. It is therefore preferred to perform LLC separations at feed solution concentrations within the linear range of the partition coefficients of the components of interest and at which significant deviations from the properties of the pure phases are not observed.

The identification of this working concentration range is rarely reported in the LLC literature, and it is acknowledged that the time and effort required may not be justifiable for a one-off separation. However, it is highly useful for the design and establishment of high throughput, robust processes for routine separations in laboratory and industrial settings.

To quickly identify the maximum applicable starting mixture concentration for feed solution preparation without the need for physical property measurements, phase volume ratio and settling time were determined over a wide starting mixture concentration range. An increase in settling time can be indicative of an increase in the residence time needed for phase coalescence in the cells of the CPC column [21], while a change in the phase volume ratio may signify the occurrence of local changes in the stationary phase fraction. Both effects can lead to hydrodynamic instabilities resulting in stationary phase loss that is detrimental to both separation performance and repeatability. The partition equilibrium of the target component, NK, was measured over the same starting mixture concentration range as for the settling time and phase volume ratio measurements. This approach has been previously used in [2,20] with model feed mixtures of three components.

The phase volume ratio measurements show that an increase in the upper phase volume occurs with an increase in the concentration of the starting mixture in the HEMWat -7 solvent system (see Fig. 5). This deviation from the blank sample (pure phases only) begins to become prominent above concentrations of approximately 100 mg ml^{-1}.

A slight initial decrease in the settling time is observed at low concentrations (up to approximately 50 mg ml^{-1}), followed by a
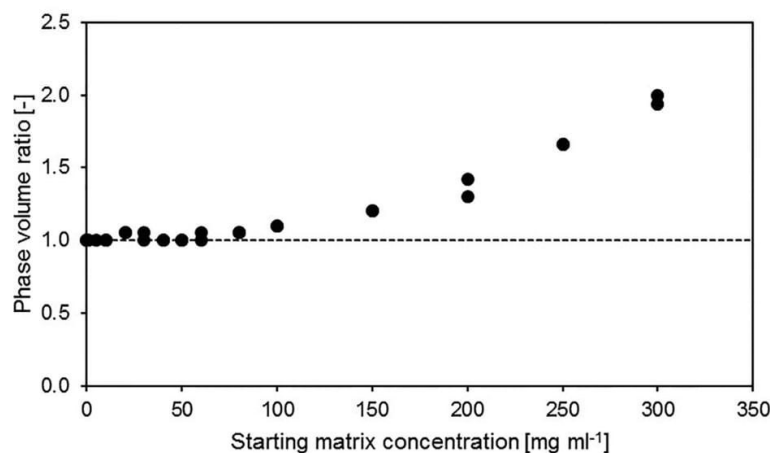

Fig. 5. Phase volume ratio vs. starting mixture concentration. Dashed line: blank sample.
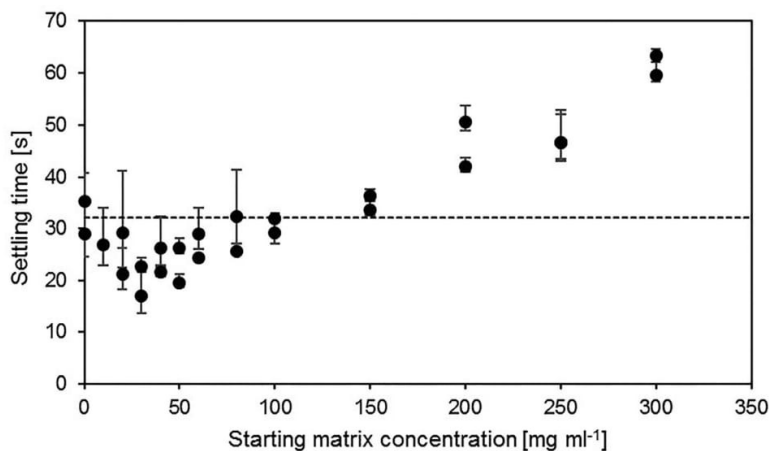
Fig. 6. Settling time vs. starting mixture concentration. Error bars: standard deviation. Dashed line: blank sample.
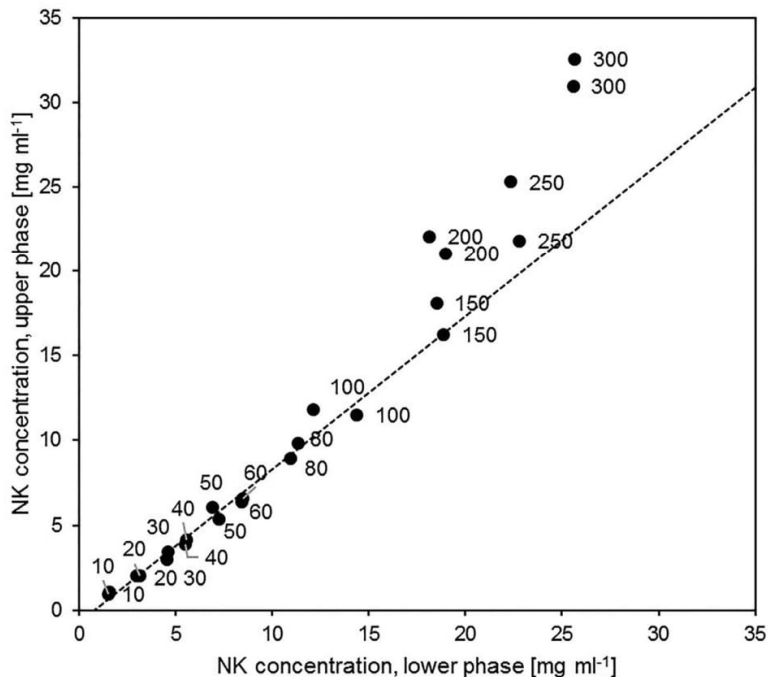

Fig. 7. Nootkatone (NK) partition equilibria. Labels: starting mixture concentration for feed solution preparation in mg ml^{-1}. Dashed line: linear regression, starting mixture concentration 10-100 mg ml^{-1}.

continuous increase in settling time as the starting mixture concentration is further increased above 100 mg ml^{-1} (see Fig. 6).

Fig. 7 depicts the results of the nootkatone partition equilibrium measurements. The partition equilibrium can be considered linear up to a starting mixture concentration of approximately 100 mg ml^{-1}. At higher concentrations, nootkatone increasingly partitions into the upper phase, producing a deviation from linear behavior. This departure from linearity at 100 mg ml^{-1} coincides with the increase in phase volume ratio as well as the steady increase in settling time. Therefore, 100 mg ml^{-1} was selected as the maximum starting mixture concentration, i.e., the concentration at

which the partition coefficient can be considered constant (maximum of the linear range of the partition isotherm) and the phase volume ratio and settling time do not substantially differ from the pure phases.

4.2.2. Step 2: Determination of the maximum flow rate

Following determination of the maximum starting mixture concentration for feed solution preparation in Step 1, stationary phase loss experiments were performed on the CPC unit in the presence of these feed solutions. These experiments are complementary to the preliminary measurements for the maximum feed con-
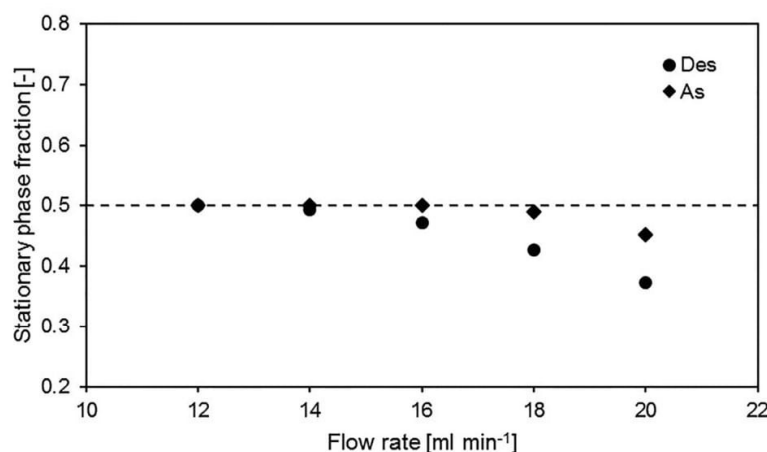
Fig. 8. Stationary phase fraction vs. flow rate, measured in the presence of feed solutions prepared with a 100 mg ml^{-1} starting mixture concentration. Dashed line: pre-set $S_f = 0.5$.

centration performed under static conditions, as they account for the effects of feed solution introduction in the presence of the system-specific column hydrodynamics. For example, the feed solution may have a higher density or viscosity than the pure phases in the column, leading to a partial displacement of the mobile and/or stationary phase. Feed introduction may also lead to interfacial mixing effects that destabilize coalescence regions in the cells, or the feed solution may be perceived as a third, immiscible phase until sufficiently diluted by the mobile phase. All of these phenomena can disrupt the process stability and lead to stationary phase loss [18,22].

In trapping MDM, the column is initially prepared with the selected solvent system at an upper phase:lower phase volume ratio of 1:1, corresponding to $S_f = 0.5$ in both elution modes (Des and As). This allows for the selection of similar Des and As flow rates and step durations, resulting in similar column efficiency and solvent consumption in both modes as well [1]. For a fast separation and high column efficiency, the feed and mobile phase flow rates should be selected as high as possible while maintaining the initial S_f of 0.5 in both modes, i.e., in the absence of stationary phase loss (bleeding).

The results of the stationary phase loss experiments are shown in Fig. 8. Each measurement was conducted at a set initial S_f of 0.5. In Des mode, a decrease in S_f is already observed starting at a flow rate of 14 ml min^{-1}. In As mode, the deviation from $S_f = 0.5$ first begins at a higher flow rate of 18 ml min^{-1}. Therefore, a maximum flow rate of 14 ml min^{-1} was designated for both elution modes in order to simplify the process design and allow the selection of similar Des and As step durations.

4.2.3. Step 3: Determination of partition coefficients

Pulse injections were performed in Step 3 to determine the partition coefficients of the target component NK and the main impurities identified in Section 4.1. (VC, ED, IM). Accurate partition coefficient values are needed for successful implementation of the short-cut method in Step 4. As defined in Eq. (1), the partition coefficient is the ratio between the equilibrium concentrations of a component i in the stationary and mobile phases. However, it has been previously observed that partition coefficients measured under the static conditions of shake flask measurements can slightly differ from those derived from the retention volumes obtained by pulse injections experiments [2]. LLC retention volumes can devi-

Table 2
Partition coefficients and separation factors with respect to NK obtained from pulse injection experiments.

Component	Mode	K_i [-]	α [-]
NK	Des	0.74	-
	As	1.66	-
ED	Des	0.74	1.00
	As	1.66	1.00
IM	Des	0.88	1.19
	As	1.41	1.18

ate from those predicted by shake flask partition coefficients due to hydrodynamic patterns such as back-mixing and short-circuiting as well as the mass transfer kinetics of the solute components [23]. As these effects are difficult to accurately characterize and highly dependent on the column, solvent system, and operating parameters, working with partition coefficients derived from retention volumes measured under the operating conditions of the planned separation is advisable.

In Steps 1 and 2, a maximum starting mixture concentration of 100 mg ml^{-1} and a maximum flow rate of 14 ml min^{-1} were determined, respectively. After applying a margin of safety to these two parameter limits to help ensure stable, robust operation, it was decided to proceed with a starting mixture concentration for feed preparation of 75 ml min^{-1} and flow rate of 12 ml min^{-1} in both elution modes for the remaining steps of the design approach and the final trapping MDM separation. The pulse injections were therefore performed under these conditions.

The reconstructed pulse injection chromatograms are found in Fig. 9. The chromatograms confirm the trends of the preliminary shake flask measurements performed with the starting mixture (Section 4.1). VC is observed eluting very quickly in As mode, while IM elutes close to the co-eluting NK and ED. All remaining components of the starting mixture, present at <2%, were regarded as minor impurities and not considered in the chromatogram reconstruction.

The pulse injection partition coefficients and separation factors of NK, IM, and ED are found in Table 2. As can be deduced from the chromatograms, NK and ED possess a separation factor
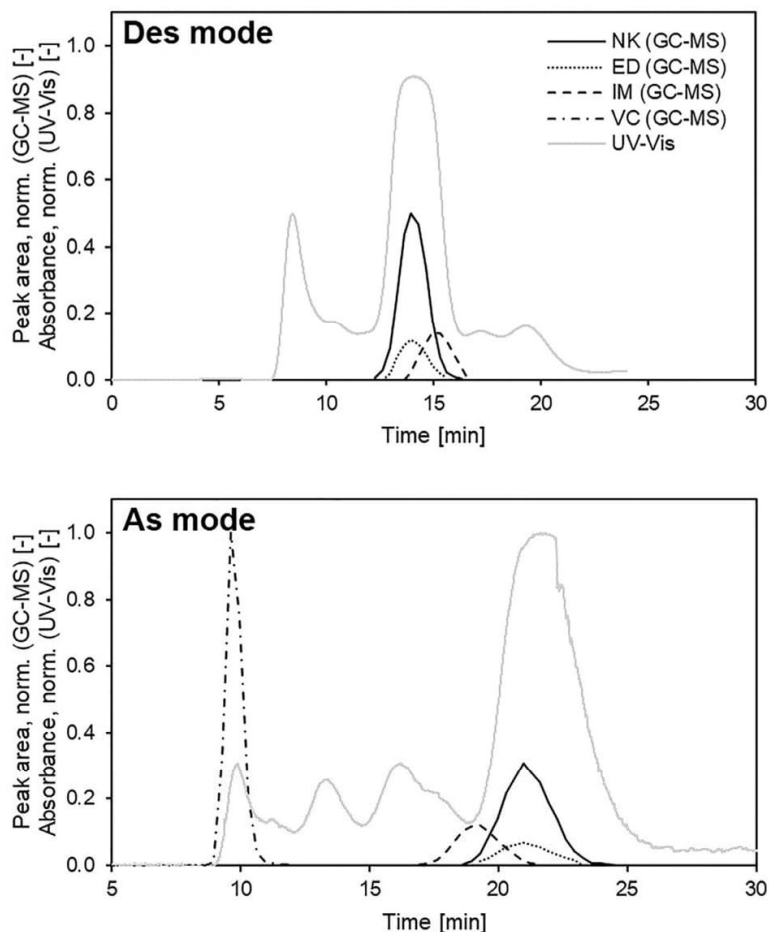
Fig. 9. Pulse injection experiments. Top: Des mode. Bottom: As mode. Parameters: V_{inj} = 5 ml, c_{feed} = 75 mg ml^{-1}, F = 12 ml min^{-1}, 1700 rpm, S_f = 0.5. Black lines: GC–MS area of collected fractions. Gray lines: UV–Vis trace.

of unity, leading to their co-elution. Therefore, it is not possible to separate NK and ED with the selected solvent system. For this primarily demonstrative study of a complex mixture separation with trapping MDM, they will be considered together as a pseudo-component (NK+ED) represented by a single partition coefficient in each elution mode for the remainder of the separation design.

IM elutes faster than NK+ED in As mode and, accordingly, more slowly in Des mode. A separation factor of approximately 1.2 is obtained for NK+ED and IM in both elution modes, making a separation with trapping MDM advantageous in comparison with batch mode, according to the findings of a previous study [3]. VC, eluting long before NK+ED and IM in As mode, will no longer be considered in the design of the trapping MDM separation. A separation designed for the isolation of IM from NK+ED using the short-cut method will automatically include all components with $K_{i,As} \leq K_{IM,As}$, including VC.

4.2.4. Step 4: Selection of step durations and number of cycles

In Step 4, the step durations in the Loading and Separation stages as well as the number of Separation stage cycles to be completed were chosen based on the short-cut method (see detailed description in Section 2.2.) and process throughput calcu-

lations. As a result of the partition coefficients obtained in Step 3 (Section 4.2.3.), only the target pseudo-component NK+ED and impurity IM were considered in the short-cut method design equations, designated as short-cut method components B (target) and C (impurity eluting fastest in As mode), respectively. The short-cut method component A (impurity eluting fastest in Des mode) was not explicitly defined.

Despite the inclusion of only B and C in the implementation of the short-cut method equations, the separation remains a pseudo-ternary one. In designing the separation of NK+ED from IM, the separation of all additional impurities eluting before NK in Des mode and possessing separation factors similar to or higher than that of NK+ED and IM is intrinsically considered. As can be seen in Eqs. (6)–(11), only the component B propagation velocity is required for the calculation of viable step durations. The impurities A and C and their propagation velocities appear only in the calculation of the number of cycles to be performed (Eqs. (12)–(15)). When designing a separation with all three short-cut method components (A, B, and C), only the highest calculated number of cycles (n_A^{sep} or n_C^{sep}) is selected, often corresponding to the most "difficult" separation, i.e., lowest separation factor, with respect to B. In this case, only n_C^{sep} will be considered.

As explained in Section 2.2, all trapped component band position combinations satisfying the restrictions named in [1] will result in step durations and a number of cycles resulting in complete recovery and separation of B from A and C under ideal conditions. However, the separation performance associated with these different combinations will vary. In this study, it was desired to perform a high throughput trapping MDM separation. Therefore, different combinations of the trapped component band positions were screened based on the process throughput.

Process throughput was defined in this study as the volume of feed processed per unit time under the linear and ideal chromatography assumptions of the short-cut method. The total volume of the As and Des feed solutions introduced during the Loading stage, V_{feed}^{load}, is given by Eq. (17).

$$V_{feed}^{load} = F_U t_{As}^{load} + F_L t_{Des}^{load} \qquad (17)$$

The total process duration, t^{pro}, includes all Loading and Separation stage cycles as well as the Recovery stage. The Recovery stage is considered complete when the back end of the band of the last eluting component, relative to the elution mode, has reached the outlet.

To calculate the duration of the Recovery stage, the dimensionless distance between the back end of the last-eluting component and the column outlet at the completion of the last Separation stage cycle must first be determined. In the case studied in this work, the trapped target component B (NK+ED) was the last-eluting component in the As mode Recovery stage, since design component A was not explicitly included. The trapped component experiences no net displacement toward either end of the two-column unit during the Separation stage cycles. Therefore, the dimensionless distance to be traveled by component B, Δx_B^{rec}, can be calculated with Eq. (18).

$$\Delta x_B^{rec} = x_{B,Des}^{load} + x_{B,As}^{load} + \left(1 - x_{B,As}^{sep}\right) \qquad (18)$$

The Recovery stage duration is given by Eq. (19).

$$t^{rec} = \frac{\Delta x_B^{rec}}{v_{B,As}} \qquad (19)$$

The total process duration specific to the trapping MDM separation described in this work, t^{pro}, is calculated with Eq. (20).

$$t^{pro} = t_{As}^{load} + t_{Des}^{load} + t_{Des}^{sep,1st} + \left(n_C^{sep} - 1\right)t_{Des}^{sep} + n_C^{sep}t_{As}^{sep} + t^{rec} \qquad (20)$$

The process throughput can then be determined using Eq. (21).

$$Th = \frac{V_{feed}^{load}}{t^{pro}} \qquad (21)$$

For simplification, band positions in the Loading and Separation stages were defined as equivalent, i.e., $x_{B,Des}^{load} = x_{B,As}^{load} = x_B^{load}$ and $x_{B,Des}^{sep} = x_{B,As}^{sep} = x_B^{sep}$. x_B^{sep} was fixed at 0.8 to compensate for band broadening caused by dispersive effects not accounted for in the short-cut method while still allowing for high loadings. x_B^{load} was varied from 0.02 to 0.78 with a step interval of 0.02. The short-cut method equations specific to the trapping MDM variation used in this study (Eqs. (6)–(8), (10), (11), (14)) were used to calculate the step durations and number of cycles for each band position combination (see Tables 2 and 3 for input parameters). To preserve valve life and avoid high cycle numbers, all band position combinations not resulting in fulfillment of the restrictions $t_{Des}^{sep} \geq 2.00$ min and $n_C^{sep} \leq 10$ cycles were eliminated. The corresponding process throughput for each remaining combination was then calculated using Eqs. (17)–(21).

The band position combination resulting in the highest throughput was $x_B^{load} = 0.42$, $x_B^{sep} = 0.80$, corresponding to a throughput of 0.72 ml feed min^{-1} and a total loaded feed volume of 84.1 ml (approximately 47% of the total column volume). The

Table 3
Trapping MDM short-cut method input parameters.

Parameter	Symbol	Unit	Value
Flow rate (feed and mobile phase)	F	ml min^{-1}	12
First elution mode each cycle	-	-	Des
Recovery stage elution mode	-	-	As
Lower phase volume (one column)	V_L	ml	45.5
Upper phase volume (one column)	V_U	ml	45.5

Table 4
Selected band positions and corresponding trapping MDM process parameters obtained with the short-cut method.

Parameter	Symbol	Unit	Value
Stage 1: Loading			
Band position	x_B^{load}	-	0.42
Step durations	t_{Des}^{load}	min	2.77
	t_{As}^{load}	min	4.24
Stage 2: Separation			
Band position	x_B^{sep}	-	0.80
Step durations	$t_{Des}^{sep,1st}$	min	2.51
	t_{Des}^{sep}	min	5.01
	t_{As}^{sep}	min	7.67
Number of cycles	n_C^{sep}	-	8 (+2)

step durations and number of cycles obtained with the short-cut method are summarized in Table 4. For the experimental separation, 2 additional cycles were added to the 8 calculated with the short-cut method in order to compensate for broadening of the component C band under real, non-ideal conditions.

4.2.5. Step 5: Trapping MDM separation

Having obtained all necessary operating parameters (c_{feed}, F, t_{Des}^{load}, t_{As}^{load}, $t_{Des}^{sep,1st}$, t_{Des}^{sep}, t_{As}^{sep}, n_C^{sep}) with completion of design Steps 1 through 4, the trapping MDM separation at high throughput was performed. The results are presented in Fig. 10. For the Loading and Separation stages, the plotted points correspond to the entire mobile phase effluent collected during each step. The plotted points for the Recovery stage in As mode represent fractions collected every 60 s. Aliquots were taken from the collected volumes and fractions and subjected to GC–MS to qualitatively determine the sample content of the target pseudo-component (NK+ED, solid circles) and the main impurity (IM, empty circles) based on area% analysis. All reported purities and yields are based on these results. NK+ED and IM were designated as components B and C in the short-cut method, respectively. Elution of the remaining impurities is indicated by the online UV-Vis trace plotted in gray. However, not all compounds were UV-Vis active.

It can be seen in Fig. 10 that, as expected, neither NK+ED (B) nor IM (C) eluted from the column in Des mode. IM nearly completely left the column in As mode during the Separation stage (89.9% yield). During the Recovery stage, the intermediately-eluting target NK+ED was obtained, accompanied by a small amount of IM. A plot of the Recovery stage fractions and several fraction pooling scenarios are found in Fig. 11. Pooling of Recovery fractions 1–16 resulted in a cumulative NK+ED purity of 96.9% with respect to IM only (GC–MS area%), corresponding to an overall NK+ED purity of 78.7% with respect to all (minor) impurities of the >90 component starting mixture. The Recovery stage NK+ED yield for pooled fractions 1–16 was 84.6%. To the detriment of the yield, selective pooling could increase the overall NK+ED purity with respect to all impurities to, for example, to 90.0% when pooling fractions 1–8 (71% yield) or 95.3% for fractions 1–4 (35.3% yield). A maximum
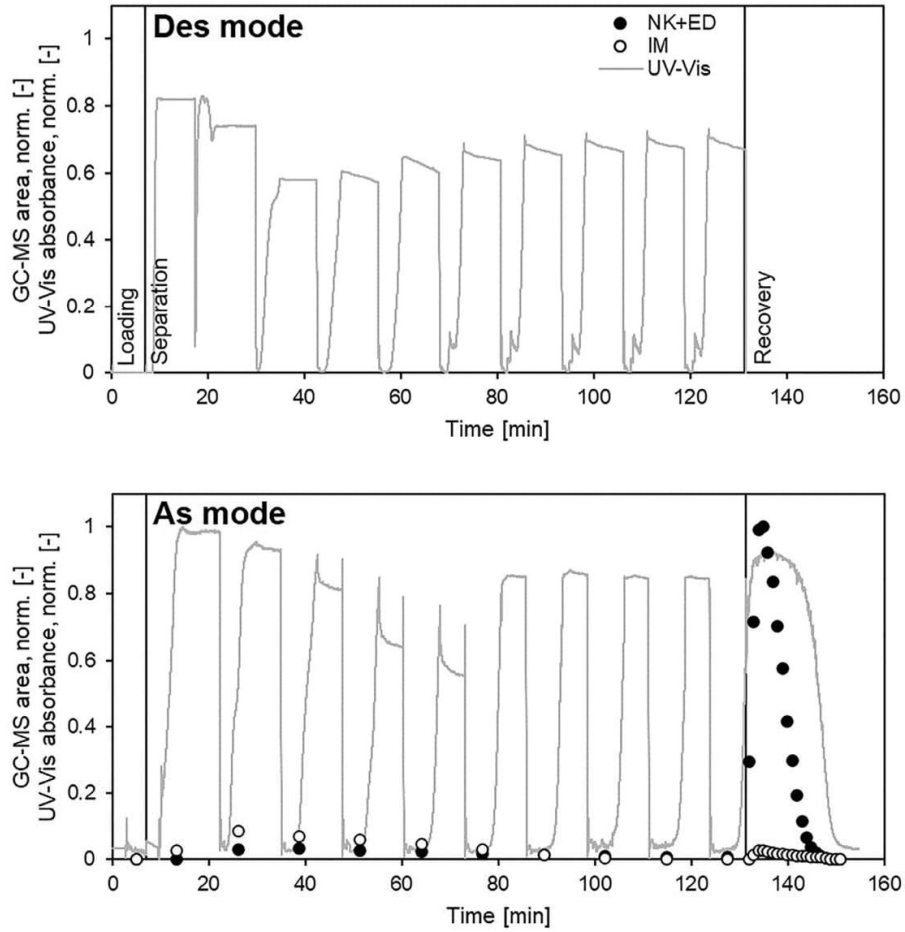
Fig. 10. Trapping MDM experiment. Top: Des mode. Bottom: As mode. Parameters: $c_{feed} = 75$ mg ml^{-1}, $F = 12$ ml min^{-1}, 1700 rpm, $S_f = 0.5$, first mode Des, Recovery mode As, step durations and cycle number in Table 4. Circles: GC–MS area, full cycle effluent volume (Loading and Separation) and fractions (Recovery). Gray lines: UV-Vis trace.
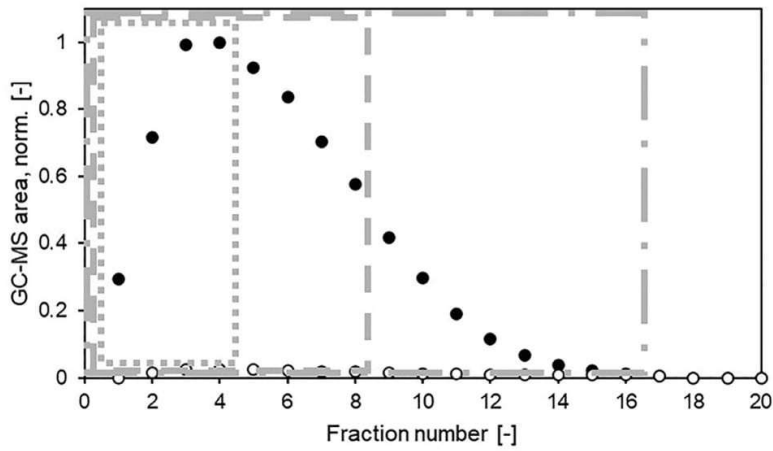

Fig. 11. Recovery stage fractions, trapping MDM experiment in Fig. 10. Fraction pooling scenarios: 1–4 (dot), 1–8 (dash), 1–16 (dash dot).
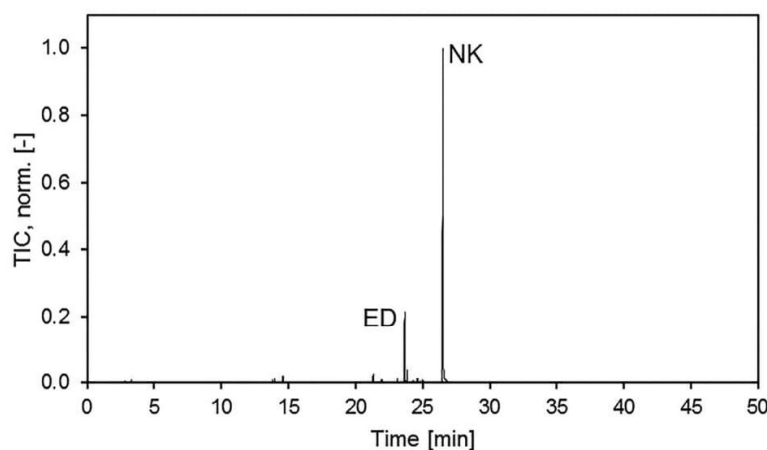
Fig. 12. GC-MS analysis of Recovery stage fraction 4 with 81.8% NK, 13.1% ED (GC–MS area%).

overall NK purity of 81.8% (not including ED), or 94.9% NK+ED, was obtained in Recovery fraction 4. However, this would correspond to a NK yield (not including ED) of only 12.3%. The GC-MS chromatogram of this fraction is found in Fig. 12.

The loss of NK+ED in As mode during the Separation stage indicates a deviation from the ideal condition assumption associated with the short-cut method. The loss likely could have been mitigated by setting a lower band position at the end of the separation stage steps, x^{sep}, when calculating and selecting the step durations. Target purity could have been improved by, e.g., performing more cycles to allow for further separation of the numerous minor impurities. However, this would likely come at the cost of a lower target yield. A more detailed understanding of the effects on retention behavior brought about by hydrodynamic non-idealities caused by feed introduction and possible solute-solute interactions could also allow for improved purity and recovery of the target. However, such an evaluation was outside the scope of this study.

An impression of the NK purity and yield obtainable with batch injections can be gleaned from the results of the pulse injections performed in Step 3 (Section 4.2.3). The highest single-fraction NK purity (not including ED) was 65.8% and achieved in As mode, corresponding to 15.5% yield. Pooling of all fractions containing NK resulted in an overall purity of only 38.3%. At injection volumes higher than the 5 ml used in the pulse injections and comparable to that used in the trapping MDM separation (84.1 ml total feed volume), even lower purities and yields would be obtained. However, for a full, "fair" comparison of the two operating modes, the operating parameters in each case would have to be optimized for a specified purity and yield of the target.

These results demonstrate the effectiveness of the trapping MDM technique, design approach, and short-cut method for application to complex natural product starting mixtures. Further improvement of the separation investigated in this study could be achieved by fine-tuning of the operating parameters, e.g., with the help of detailed simulations taking dispersive band-broadening effects into account [2,3]. However, depending on the final application of the natural product target, reduced purities may also be acceptable. For example, high purities become less critical when the remaining (trace) impurities have no negative effect on the bioactive efficacy or desired organoleptic properties of the target. Should the technique and design approach be used for commercial or industrial application, of course more accurate quantitation of the product purity would be necessary to ensure compound efficacy and consumer safety.

5. Conclusion

For the first time, this study demonstrated the successful application of a design approach and associated short-cut parameter selection method for the high throughput trapping MDM separation of an intermediately-eluting target from a complex natural product starting mixture. Following preliminary measurements and experiments for determination of the maximum applicable starting mixture concentration for feed preparation (Step 1), maximum flow rate (Step 2), and the partition coefficients of the components of interest (Step 3), the short-cut method was used for selection of step durations and the number of cycles (Step 4). The target pseudo-component NK+ED was obtained in the Recovery stage of the trapping MDM separation (Step 5) at a maximum overall purity of up to 94.9%.

It has been shown that trapping MDM has the potential for further application in the valorization of food industry waste and side streams, such as the starting mixture used in this study. Given the extensive number of and broad polarity range covered by the available LLC solvent systems, the trapping MDM technique and corresponding design approach for high throughput can be utilized for a wide variety of difficult separations of intermediately-eluting natural product target compounds.

Declaration of Competing Interest

None.

CRediT authorship contribution statement

Raena Morley: Methodology, Investigation, Writing - original draft, Visualization. **Mirjana Minceva:** Conceptualization, Writing - review & editing.

this study as well as for their support in analytical method development (HPLC, GC-MS).

References

[1] J. Goll, R. Morley, M. Minceva, Trapping multiple dual mode centrifugal partition chromatography for the separation of intermediately-eluting components: operating parameter selection, J. Chromatogr. A 1496 (2017) 68–79.

[2] R. Morley, M. Minceva, Trapping multiple dual mode centrifugal partition chromatography for the separation of intermediately-eluting components: through-put maximization strategy, J. Chromatogr. A 1501 (2017) 26–38.

[3] R. Morley, M. Minceva, Operating mode selection for the separation of intermediately-eluting components with countercurrent and centrifugal partition chromatography, J. Chromatogr. A 1594 (2019) 140–148.

[4] J.B. Friesen, J.B. McAlpine, S.N. Chen, G.F. Pauli, Countercurrent separation of natural products: an update, J. Nat. Prod 78 (2015) 1765–1796.

[5] A. Berthod, Countercurrent chromatography and the journal of liquid chromatography: a love story, J. Liq. Chromatogr. R T 30 (2007) 1447–1463.

[6] G.F. Pauli, S.M. Pro, J.B. Friesen, Countercurrent separation of natural products, J. Nat. Prod. 71 (2008) 1489–1508.

[7] J.B. Friesen, J.B. McAlpine, S.N. Chen, G.F. Pauli, Countercurrent separation of natural products: an update, J. Nat. Prod. 78 (2015) 1765–1796.

[8] R. Morley, M. Minceva, Operating mode and parameter selection in liquid-liquid chromatography, J. Chromatogr. A 1617 (2020) 460479.

[9] P. Hewitson, S. Ignatova, H.Y. Ye, L.J. Chen, I. Sutherland, Intermittent counter-current extraction as an alternative approach to purification of Chinese herbal medicine, J. Chromatogr. A 1216 (2009) 4187–4192.

[10] N. Mekaoui, J. Chamieh, V. Dugas, C. Demesmay, A. Berthod, Purification of Coomassie brilliant blue G-250 by multiple dual mode countercurrent chromatography, J. Chromatogr. A 1232 (2012) 134–141.

[11] J.B. Friesen, G.F. Pauli, GUESS - A generally useful estimate of solvent systems in CCC, J. Liq. Chromatogr. R T 28 (2005) 2777–2806.

[12] K. Skalicka-Wozniak, I. Garrard, A comprehensive classification of solvent systems used for natural product purifications in countercurrent and centrifugal partition chromatography, Nat. Prod. Rep. 32 (2015) 1556–1561.

[13] E. Hopmann, J. Goll, M. Minceva, Sequential Centrifugal partition chromatography: a new continuous chromatographic technology, Chem. Eng. Technol. 35 (2012) 72–82.

[14] T. Murase, K. Misawa, S. Haramizu, Y. Minegishi, T. Hase, Nootkatone, a characteristic constituent of grapefruit, stimulates energy metabolism and prevents diet-induced obesity by activating AMPK, Am. J. Physiol.-Endoc. M 299 (2010) E266–E275.

[15] S. Jenkins, Allylix enters commercial-scale production of nootkatone, https://www.chemengonline.com/allylix-enters-commercial-scale-production-of-nootkatone/, (2011).

[16] Our nootkatone. A fresh alternative., https://www.evolva.com/nootkatone-flavor/, (2016).

[17] A. Berthod, B. Billardello, S. Geoffroy, Polyphenols in countercurrent chromatography. An example of large scale separation, Analusis 27 (1999) 750–757.

[18] L. Marchal, O. Intes, A. Foucault, J. Legrand, J.M. Nuzillard, J.H. Renault, Rational improvement of centrifugal partition chromatographic settings for the production of 5-n-alkylresorcinols from wheat bran lipid extract - I. Flooding conditions-optimizing the injection step, J. Chromatogr. A 1005 (2003) 51–62.

[19] A.H. Peng, P. Hewitson, H.Y. Ye, L.S. Zu, I. Garrard, I. Sutherland, L.J. Chen, S. Ignatova, Sample injection injection strategy to increase throughput in counter-current chromatography: case study of Honokiol purification, J. Chromatogr. A 1476 (2016) 19–24.

[20] J. Goll, M. Minceva, Continuous fractionation of multicomponent mixtures with sequential centrifugal partition chromatography, Aiche. J. 63 (2017) 1659–1673.

[21] A.F. Fromme, D.Klump C., G. Schembecker, Correlating the phase settling behavior of aqueous-organic solvent systems in a centrifugal partition chromatograph, J. Chromatogr. A 1620 (2020) 461005 In Press, Corrected Proof.

[22] Y. Ito, Golden rules and pitfalls in selecting optimum conditions for high-speed counter-current chromatography, J. Chromatogr. A 1065 (2005) 145–168.

[23] S. Adelmann, G. Schembecker, Influence of physical properties and operating parameters on hydrodynamics in centrifugal partition chromatography, J. Chromatogr. A 1218 (2011) 5401–5413.

4. Overall discussion

As stated in the Introduction, this thesis aims to fulfill two objectives: (1) to develop and validate a model-based design approach for trapping MDM operating parameter selection and (2) to demonstrate the effectiveness and flexibility of this approach through its implementation in varying contexts. Section 4.1 discusses the preliminary measurements for determination of the process limits (feed concentration and flow rate) with respect to the thermodynamics and hydrodynamics of the two-phase solvent system making up the mobile and stationary phases. Section 4.2 reviews the application of model-based approaches of varying detail to selection of the trapping MDM step durations and cycle numbers. In Section 4.3, the use of the model-based approach for operating mode comparison is addressed.

4.1 Determination of process limits

As LLC is a preparative separation technique, it is desired to process large amounts of feed in a short amount of time to obtain a high throughput. However, the high feed concentrations, feed volumes, and flow rates associated with high-throughput conditions can adversely affect process stability (e.g., observed as stationary phase loss) and predictability (e.g., expected solute retention times and band broadening). As discussed in Section 2.4, the complex interplay of changes in the thermodynamic and hydrodynamic conditions in the column brought about by the introduction of high feed loadings cannot be fully predicted yet. Preliminary experiments to determine the operating parameter limits are therefore necessary.

A simple method for determination of the operating parameter limits (maximum feed concentration and associated maximum mobile phase flow rates) available to all LLC users was investigated in Papers II and IV. The maximum feed concentrations were identified through phase volume ratio and settling time measurements, as well as linear range determination of the partition isotherms of the components of interest using the shake flask method. For method simplicity, direct measurements of the physical properties of the phases, such as density, viscosity, and interfacial tension, were not made. Stationary phase retention experiments were then carried out in presence of the maximum concentration feed solutions to determine the highest mobile phase flow rate at which the desired trapping MDM stationary phase fraction of 0.5 could be maintained in both elution modes. The loaded feed volume in the stationary phase retention experiments, equivalent to 50% of the mobile phase volume in the column, corresponded to the upper volume loading range typically encountered in trapping MDM. By monitoring stationary phase loss with respect to flow rate, an indirect assessment of the hydrodynamic stability of the two-phase system in the presence of the feed solution was obtained, bypassing the need for, e.g., flow visualization techniques requiring specialized, non-commercial equipment [7, 94].

The two feed mixtures and selected solvent systems evaluated in Papers II and IV exhibited different behavior with respect to the linear range, settling time, and phase volume ratio as a function of feed concentration. The settling time of the model paraben mixture (Paper II) already started increasing above a feed concentration (defined with respect to the total mass of all solutes dissolved in the total volume of the sample, i.e., the upper and lower phases) of 10 mg ml^{-1}, whereas the complex nootkatone starting mixture (Paper IV) first exhibited a settling time increase at a concentration approximately 10-fold higher. For the nootkatone starting mixture, a maximum feed concentration of 100 mg ml^{-1} was selected, corresponding to the onset of increases in settling time and phase volume ratio, as well as with the linear range limit of the partition coefficient of the target nootkatone. A safety margin was applied to this value for the experimental run, in which a feed concentration of 75 mg ml^{-1} was used. For the paraben mixture, the linear range limit (30 mg ml^{-1}) was selected as the concentration maximum in the interest of higher throughput, despite the earlier increase in settling time.

In the stationary phase retention experiments performed in presence of the feed solutions, considerably lower maximum flow rates were identified for both the paraben and nootkatone mixtures (up to approximately 50% and 30% lower, respectively) compared to previous measurements with solute-free mobile and stationary phases. The lower maximum flow rates for maintenance of $S_f = 0.5$ identified by the stationary phase retention experiments agree with the recommendation to decrease the mobile phase flow rate when working with high-concentration feed solutions to reduce stationary phase loss found in [13, 15, 52]. It is claimed that lower flow rates allow additional time for the high-concentration feed solution to be diluted by the mobile phase following introduction to the column. As the properties of the diluted feed solution approach those of the solute-free mobile phase, its disruptive effects on stationary phase retention become less pronounced [13, 15, 52]. The longer residence time in the cells obtained with a lower flow rate may also compensate for prolonged coalescence time of the mobile phase in the presence of the feed, preventing stationary phase carry-over from one cell to the next that can be observed as stationary phase loss at the outlet.

The successful experimental trapping MDM separations achieved in Papers II and IV in the absence of stationary phase loss demonstrate the effectiveness of the simple operating parameter limit determination method described above. In the case of the nootkatone mixture, it is observed that the hydrodynamics of the column can be strongly negatively affected even when substantial increases in settling time and phase volume ratio are not observed. Therefore, in selecting the maximum feed concentration, it may suffice to only perform shake flask measurements to determine the linear range limit. The subsequent determination of the maximum flow rate (i.e., stationary phase retention measurements performed in presence of the high-concentration feed solutions) account for hydrodynamic changes brought about by

alterations of the physical properties of the phases, without the need for direct (e.g., density, viscosity, interfacial tension) or indirect evaluation (e.g., settling time) of physical property changes. This hypothesis should be applied to other feed mixtures and solvent system types to evaluate and verify its generality of application.

A key advantage of the simple operating parameter limit determination method is that no additional equipment is required other than an analytical method for concentration measurement of the aliquots taken in the shake flask experiments. With this experiment-based method, however, the identified operating parameter limits are only applicable for a certain feed mixture, solvent system, column, and rotational speed. Ideally, it would be possible to predict these limits using general correlations or models and with few or no experimental measurements. Before such options are available, there remains much research to be done to better understand and predict the combined effects of feed and solvent system properties, column parameters, and operating parameters on process stability. Several relevant CPC studies reported in the literature are discussed below.

Recent investigations into the effects of physical properties and operating parameters on stationary phase retention using flow visualization have indicated that correlations based on the dimensionless Capillary number, which quantifies the mobile phase dispersion process at the cell inlet expressed as the ratio of the product of the mobile phase viscosity and its velocity at the cell inlet and the interfacial tension ($Ca = (\eta_m v_m)/\gamma$), can be used to predict stationary phase retention [8, 58]. This approach requires measurements of viscosity and interfacial tension and calculation of the mobile phase velocity from the volumetric flow rate and the cell inlet geometry. The presented correlation was found to predict trends in S_f for the studied ARIZONA systems in both As and Des modes and under different operating conditions. Trends for other aqueous-organic systems as well as ARIZONA systems modified with additives could also be described. Although a useful approach for preliminary evaluation of different solvent systems, S_f could not be predicted to a high degree of accuracy, making the correlation unsuitable for rigorous process design in its current form. The applicability of the correlation to other CPC devices and geometries, as well as to other classes of solvent systems (e.g., aqueous two-phase systems) remains to be evaluated. With the development of a generalized, accurate correlation, it could also be possible to predict the effects of feed solution introduction by comparing predicted S_f values of the solvent system and the feed. It should be noted, however, that the development of the correlation was based on experiments performed with equilibrated mobile and stationary phases, and the effects of the sudden introduction of a feed solution not in equilibrium with the two-phase system in the column were not explored.

The destabilizing effects of high-concentration feed solutions, namely complete loss of the stationary phase (flooding), have been studied using flow visualization in [14]. To avoid

flooding conditions, the authors recommended the construction of a pseudo-ternary phase diagram describing the miscibility of the mobile phase, stationary phase, and feed solution. This phase diagram is then used to determine the maximum feed concentration at which two distinct phases exist, i.e., remain immiscible. This approach differs from the criteria used to determine the maximum feed concentration in this thesis. All feed concentrations studied in Papers II and IV were within the immiscible two-phase composition region. Although the study in [14] provided valuable insights into the effects of high feed loading on hydrodynamic stability, only one natural product feed mixture was studied, and the influence of the operating parameters was not considered. Despite successfully avoiding the extreme case of flooding, the preliminary experiments (e.g., pseudo-ternary diagram construction) were not able to predict the conditions at which stationary phase loss was completely prevented [14, 15].

In addition to the development of correlations or models for accurate prediction of S_f under high-concentration feed loadings, studies of the trade-off between feed concentration and applicable mobile phase flow rate for maintenance of the desired stationary phase fraction would also be of interest. As the feed concentration is lowered, the composition and physical properties approach those of the mobile phase, leading to improved hydrodynamic stability and rendering operation at higher flow rates possible. Although this decreases the feed amount processed per run, working at a higher flow rate can have a positive effect on the throughput by both decreasing the separation time and increasing the column efficiency, i.e., by increasing mass transfer through increase of the interfacial area between the mobile and stationary phases. Given the current state of research and understanding of the complex thermodynamic and hydrodynamic effects affecting CPC separation performance, the approach for operating parameter limit determination demonstrated in this thesis (i.e., identification of maximum feed concentration through evaluation of the linear range limit using the shake flask method, selection of the maximum mobile phase flow rate with stationary phase retention experiments performed in presence of the high-concentration feed solutions) can be recommended as a simple, effective, and accurate method.

4.2 Model-based operating parameter selection

After choosing the feed concentration and flow rate, there remain five interdependent parameters to be selected in the design of a trapping MDM separation: the step durations in the Loading, t_{Des}^{load}, t_{As}^{load}, and Separation stages t_{Des}^{sep}, t_{As}^{sep}, as well as the number of Separation stage cycles. The trapping MDM short-cut model was twice demonstrated in Paper I to allow selection of a set of step durations and cycles resulting in complete separation of the intermediately-eluting target component. However, although the short-cut model allows access to the operating parameter space (combinations of step durations and number of cycles)

resulting in a complete separation under ideal chromatography assumptions, its original form derived in Paper I does not provide any information regarding the selection of the optimal set of parameters fulfilling the separation objective (e.g., throughput maximization).

Several approaches for selection of the best set of operating parameters were explored in this thesis. In Papers II and III, the short-cut model was used for identification of valid operating parameter sets under linear, ideal conditions, followed by process simulations based on the equilibrium stage model to evaluate the separation performance (i.e., throughput and productivity, respectively). In Paper IV, evaluation of the process throughput for different operating parameter sets was performed using an extended form of the short-cut model, without detailed equilibrium stage model simulations.

In the throughput maximization study using a paraben ternary model mixture in Paper II, an iterative approach was used for screening of the parameter sets defined by the short-cut model, with the use of process simulations taking non-ideal band broadening into account for evaluation of the separation performance. The time-saving iterative approach was begun with parameter sets defined by the short-cut model at the highest values of x_B^{load} and x_B^{sep}. The band positions were incrementally decreased in a rational manner until the purity and yield restrictions of 99% were satisfied according to the simulated separation performance. This allowed determination of the maximum process throughput with a minimal number of simulations, and a successful experimental validation was completed. The slight discrepancy between the predicted and experimental elution profiles was likely due to hydrodynamic changes brought about by the high-concentration feed, which was selected at the identified maximum of the linear range without the application of a safety margin. However, as the study did not screen the entire parameter space and only focused on a single separation task, a more thorough investigation of trapping MDM separation performance was conducted in Paper III.

A comparison study of batch injection and trapping MDM performance was made in Paper III. Productivity calculations based on the results of equilibrium stage model simulations were used to thoroughly screen the trapping MDM operating parameter space defined by the short-cut model (i.e., all x_B^{load}, x_B^{sep} pairs) for 64 different separation tasks. An analogous procedure was performed for the batch injection operating mode. This time, the equilibrium stage model was used to simulate a variation of the trapping MDM process that allowed for shorter run times. The number of Separation stage cycles was determined on-the-fly rather than defined with the input variables. When the test Recovery stage chromatogram performed after each cycle indicated a productivity maximum under fulfillment of the purity and yield requirements, the simulation was ended. It was not necessary to fully elute impurity components A and C from the column before the start of Recovery. The obtained plots of productivity vs. the trapped component band positions in the Loading, x_B^{load}, and Separation

stages, x_B^{sep}, gave insight into typical trapping MDM performance trends. These results could be used to inform future studies using numerical optimization procedures.

A simplified approach for operating parameter selection was explored in Paper IV. As simulation tools for process design are often unavailable to the LLC operator, the effectiveness of using the short-cut model alone for high-throughput process design was investigated. The short-cut model from Paper I was extended to allow for throughput evaluation for screening of valid operating parameter sets under linear, ideal conditions. This approach was applied to the separation of nootkatone (NK) from a complex natural product starting mixture. The results of the successful experimental separation run demonstrated the applicability of this simplified design approach using only the short-cut model to even complex mixtures. Higher purities could have perhaps been obtained, however, by accounting for the numerous trace impurities and increasing the number of cycles. Nevertheless, the short-cut model was again proven to be a simple and accessible, yet powerful, design tool.

Papers II, III, and IV all used the short-cut model to determine the valid operating parameter space followed by separation performance evaluation using modeling approaches of varying detail. The results of these investigations demonstrate the flexibility of the model-based design approach, allowing it to be tailored to the available software and simulation expertise of the operator, as well as the final design goal, e.g., a single separation run of a complex natural product sample or a detailed optimization for the isolation of a product from a well-defined starting mixture.

4.3 Operating mode comparison

Paper III demonstrated the use of the model-based design approach for the thorough comparison of trapping MDM performance with that of batch injections, the standard ternary separation operating mode. A fair comparison between the two operating modes was made by optimizing each for maximum productivity with respect to the independent operating parameter variables. These variables were the flow rate and injection volume in batch injection mode and the trapped component band positions at the end of the Loading and Separation steps in trapping MDM.

The results of Paper III positioned trapping MDM as especially advantageous when α=1.3 and moderate to high purities and yields are required (approximately >80%). The results highlight the separation tasks for which the improvement in separation performance may be worth the additional hardware and design complexity associated with trapping MDM. Additionally, trapping MDM expands the applicability of LLC from the recommended α=1.5 with batch injections [24] to separation factors as low as α=1.1. However, the high cycle numbers encountered at very low separation factors, leading to long run times and high solvent

consumption, indicate that trapping MDM is a viable option in these cases only when the product has an economic value high enough to offset the production cost.

Batch injections were found to be advantageous over trapping MDM at α=1.5 and higher, coinciding with one of the experimentally established heuristics of LLC separation design [24]. These results demonstrate that the same conclusions and helpful design guidelines can be obtained from simulation studies such as those performed in Paper III in place of time- and material-consuming experiments and the need to collect years of practical experience through trial-and-error lab work. This operating mode comparison strategy based on the model-based design approach could in the future be applied to any separation task and any LLC operating modes, pending that an appropriate process model and necessary experimental data, e.g., $S_f = f(F)$, are available. To the best knowledge of the author, Paper III contains the only LLC study of this type to date.

5. Conclusions

The investigations constituting this thesis and published in Papers I through IV explored the development and implementation of the model-based design approach for trapping MDM separations of intermediately-eluting target components. In Paper I, the trapping MDM operating mode was presented for the first time along with an ideal chromatography short-cut model and proof-of-concept experimental validation using two ternary model mixtures. The short-cut model was used for rational selection of five interdependent trapping MDM operating parameters: As and Des step durations during the Loading and Separation stages, and the number of cycles.

In Paper II, a trapping MDM throughput maximization strategy using the LLC model-based design approach was developed and validated, again using a model ternary mixture. The maximum feed concentration was selected based on settling time and phase volume ratio measurements, as well as shake flask measurements to determine the linear ranges of the partition isotherms. Stationary phase retention experiments were then used to select the maximum flow rate at which the set stationary phase fraction of 0.5 could be maintained in the presence of the high-concentration feed. The short-cut model was used to identify combinations of Loading and Separation step durations resulting in complete separation under ideal conditions (i.e., in the absence of dispersive effects). The set of step durations resulting in the highest throughput was selected using an iterative evaluation procedure based on equilibrium stage model simulations and taking non-idealities into account. The successful experimental run exhibited good agreement with the simulations.

The comparison study in Paper III identified the range of separation tasks (i.e., separation factors, purity and yield requirements) for which trapping MDM outperformed standard batch injections with respect to productivity. Again, the short-cut model was used in conjunction with equilibrium stage model simulations. Trapping MDM was found to be especially advantageous for difficult separations with α of approximately 1.3 or lower, extending the application of LLC beyond the minimum separation factor of 1.5 recommended for batch injections. The results provide LLC users with clear guidelines for selection of the best-suited operating mode for their ternary separation, eliminating the need for time-consuming experimental studies of performance comparison.

Paper IV applied the model-based design strategy for throughput maximization to a complex natural product mixture. A successful trapping MDM separation was achieved using only the mathematically simple short-cut model, which was extended for evaluation of the process throughput. Despite the lower performance prediction accuracy of the short-cut model compared to modeling approaches taking non-ideal band broadening effects into account, its effectiveness was nevertheless demonstrated. Such a design tool is especially useful for the fast design of one-off separations or when a more detailed model is not available.

With the results of the two throughput maximization studies in Papers II and IV, it was shown that selection of the feed concentration maximum within the linear range of the partition isotherm and determination of the corresponding maximum applicable flow rate are sufficient for identification of the LLC process limits. Despite its straightforward nature and lack of detailed description of the physical properties of the two-phase solvent system altered by the presence of the feed, this method nevertheless addresses the highly variable and unpredictable interplay of the feed solution, solvent system, column and operating parameters, and their cumulative effects on the system thermodynamics and hydrodynamics.

In conclusion, with the model-based design approach and the operating mode selection guidelines presented in this thesis, the threshold to the implementation of trapping MDM and other LLC operating modes in research and industry has been drastically lowered. It is hoped that this will contribute to a wider acceptance of LLC, allowing the technique to fulfill its potential as a flexible and adaptable downstream processing option for natural products as well as other diverse groups of target molecules.

6. Outlook

The investigations conducted in the scope of this thesis invite the further study and exploration of trapping MDM and ternary separations with LLC, as well as improvements in process modeling and control, and future areas of application. The development of a comprehensive process model considering the coupled effects of thermodynamics and hydrodynamics on process performance is an especially interesting challenge.

Although a wide range of trapping MDM separation tasks were evaluated in the comparison study in Paper III, several simplifications were made which could be lifted in subsequent investigations. Separation tasks in which K_B is not equal to unity, the separation factors between B and impurities A and C are different, and the three components are present at unequal concentrations in the feed could be evaluated, as these conditions better represent those encountered when working with real mixtures. The operating parameter simplifications used in Papers I through IV could also be removed. For example, the use of different short-cut model band positions x_B^{load} and x_B^{sep} in the As and Des elution modes could be assessed, as could the possible advantages of working with an S_f other than 0.5.

An interesting trapping MDM process variation to explore would be the use of variable step durations. Elution mode switches in the Separation stage could be made as late as possible and step durations would become shorter with subsequent cycles as the degree of band broadening of the target component increases. These variable step durations could be predicted with simulations or, with the integration of online detection with process control, the elution mode switches could be triggered during operation whenever the detection of the target at the outlet reached a certain threshold value.

A further step in improving the throughput of ternary separations would be to move from a discontinuous process, such as batch injections or trapping MDM, to a continuous one. Continuous ternary separations could in theory be achieved with a cascade of two continuous binary separations, for example, through the connection of two sCPC units in series with a feed concentration unit between them (e.g., organic solvent nanofiltration [95, 96]). This would however first require a thorough investigation of the operating parameter space of the single-stage sCPC process, as joining two stages together in a cascade results in a high level of process complexity and multiple interdependent operating parameters that must be selected.

Following establishment of a continuous ternary cascade separation, it would be of interest to compare its performance with that of the discontinuous batch and trapping MDM operating modes, in a similar manner to the study in Paper III. Apart from the evaluation of ternary separation processes, additional comparison studies could be performed between batch injections and other alternative LLC operating modes, such as elution extrusion for the improved resolution of highly retained components or continuous binary separations with

sCPC. The results of such studies are useful when deciding which operating mode to apply for a certain separation task, as well as in the decision to invest in a more complex process and its corresponding equipment. Comparison studies of LLC performance to conventional downstream separation techniques (e.g., liquid-solid chromatography, liquid-liquid extraction) would also be beneficial for the adoption of the technology in industrial settings.

The ideal (short-cut) and equilibrium stage models implemented in the model-based design approach presented in this thesis have been demonstrated to be suitable for the design and performance prediction of CPC separations under high-throughput conditions. However, it was necessary to experimentally determine the limiting feed concentration and flow rate for which the model assumptions could be considered valid. These assumptions included operation in the linear range of the partition isotherm (i.e., constant partition coefficients), a constant stationary phase fraction, and, in the case of the equilibrium stage model, constant and equivalent band broadening effects (i.e., number of theoretical stages) in both elution modes for each component. From a process throughput standpoint, it may be desirable to use feed concentrations beyond the limit of the linear range, but this can introduce the added complexity of changes in mobile and stationary phase compositions and physical properties, phase volume ratio, and the hydrodynamics (e.g., mixing and coalescence behavior) that determine column efficiency and stationary phase retention. In conventional liquid-solid chromatography, such effects generally do not occur under conditions of non-linear partitioning. A mathematical description of the non-linear isotherm (e.g., Langmuir model) can be simply introduced into an existing model.

To predict the complex interplay of solvent system and solute partition equilibria and column hydrodynamics in LLC fully and accurately will require a complex, comprehensive modeling approach. It will be necessary to describe the liquid-liquid equilibria of the multi-component system of feed and solvent system, in the simplest case consisting of three to four solvents and two or more solutes, either through time-consuming laboratory measurements or thermodynamic modeling. The phase volume ratio and relevant physical properties corresponding to the mobile and stationary phase compositions defined by the liquid-liquid equilibria must also be measured or predicted, and their effects on the flow patterns and stationary phase retention described with, e.g., fluid dynamic models. Only then can an accurate prediction of solute elution profiles and separation performance be made.

Visualization studies have played a key role in the understanding of the effects of operating parameters and solvent system properties on hydrodynamic patterns and stationary phase retention in CPC columns on a solute-free basis [59, 94]. CPC studies involving computational fluid dynamics are rare [9], but they show promise in the design of optimal column geometries as well as solvent system and operating parameter selection. There is likely much knowledge to be borrowed and adapted from the established field of multiphase

modeling in liquid-liquid extraction [97, 98] and chemical reactors [99]. The establishment of a comprehensive CPC modeling paradigm will require multi-disciplinary expertise from the fields of thermodynamics of liquid-liquid equilibria, fluid dynamics, and the practical and mechanical aspects of CPC.

The industrial adoption of LLC, and especially more complex LLC process options such as trapping MDM, will eventually also require a high degree of process control and automation currently underdeveloped in the field. Ideally, the user should be able to set the operating parameters in the process control software, start the separation, and at the end obtain the purified product without the need for manual intervention. This would require maintenance of, e.g., the process temperature and the stationary phase fraction through online detection and feedback control. Such stationary phase fraction monitoring has been demonstrated using online permittivity measurements [100]. Automated fraction evaluation and collection can be enabled through online detection with hyphenated analytical techniques [101]. Predictive control would also allow to compensate for slight variations with respect to composition and physical properties from one run to the next, an especially important aspect in the processing of variable feedstocks obtained from natural sources. It would also be convenient for LLC users to have access to process modeling software allowing immediate implementation of both short-cut and detailed models without the need for expertise in simulation. Several open-source and commercially available software options exist for conventional chromatography, such as ChromWorks (Ypso-Facto), ChromX (GoSilico), CADET (Forschungszentrum Jülich), Aspen Chromatography, and gPROMS, but not yet for LLC.

With the nootkatone separation in Paper IV, it has again been demonstrated that LLC can play a role in the valorization of industrial waste streams through the targeted separation of natural product compounds. The notion of a circular bioeconomy with more efficient use of nutrients and resources is gaining popularity as environmental consciousness grows, demand for naturally-sourced compounds increases, and stricter regulations make waste stream processing more expensive. Waste and side stream valorization extends beyond biomass processing and is also becoming important in the recovery of rare-earth elements from industrial wastewater as well as from end-of-life products [102]. LLC has already been demonstrated to be a promising technique for rare earth separations [103-106]. Of course, the solvents used for the separation of high value-added compounds and their possible negative environmental and economic impact must be considered [107]. Environmentally friendly solvent options such as ionic liquids, deep eutectic solvents, and naturally-sourced alcohols and terpenes can be used in the place of toxic conventional solvents [108]. In all cases, solvent regeneration and reuse should be considered in industrial LLC process design.

The model-based design approach for high-throughput ternary separations with trapping MDM presented in this thesis serves as a practical starting point for the

implementation of the technique for difficult separations of intermediately-eluting components. Nevertheless, further research remains to investigate trapping MDM process variations, compare the technology with existing downstream processing techniques, obtain a deeper understanding of LLC process phenomena, improve the accuracy of modeling under non-linear partitioning conditions, and develop robust process automation, all of which will allow LLC a wider range of acceptance and application in the future.

Symbols

$\alpha_{k,l}$	selectivity/separation factor between components k and l
$c_k^{M/S}$	concentration of component k in the mobile/stationary phase
$c_k^{U/L}$	concentration of component k in the upper/lower phase
$c_{k,i}^{U/L}$	concentration of component k in the lower phase in the ith equilibrium stage
$c_k^{U/L,feed}$	concentration of component k in the upper/lower phase feed
$c_{k,in/out}^{U/L}$	concentration of component k in the upper/lower phase feed at the inlet/outlet
Ca	Capillary number
$\Delta\rho$	density difference
η_m	mobile phase viscosity
$F^{U/L}$	flow rate of the mobile upper/lower phase
γ	interfacial tension
K_k	partition coefficient of component k
$K_{As/Des,k}$	partition coefficient of component k in ascending/descending mode
N_k	number of theoretical stages associated with component k
Pur_{req}	purity requirement
S_f	stationary phase retention/fraction
σ_k	Gaussian peak variance of component k
t	elapsed time since start of separation
t_{end}	end of elution time
t_{inj}	injection time
$t_{As/Des}^{load/sep}$	step duration in ascending/descending mode during loading/separation stage
$t_{R,k}$	retention time of component k
V_C	column volume
V_{inj}	injection volume
$V^{M/S}$	volume of mobile/stationary phase in column
$V^{U/L}$	volume of upper/lower phase in column
$V_{R,k}$	retention volume of component k
v_k	propagation velocity of component k
v_m	velocity of mobile phase at cell inlet
x_k	band front position of component k
$x_k^{load/sep}$	band front position of component k at the end of the Loading/Separation stage
Yld_{req}	yield requirement

Abbreviations

ARIZONA	solvent system family, *n*-heptane/ethyl acetate/methanol/water
As	ascending elution mode
CCC	countercurrent chromatography
CPC	centrifugal partition chromatography
Des	descending elution mode
ED	eudesmenol
HEMWat	solvent system family, *n*-hexane/ethyl acetate/methanol/water
IM	intermedeol
LLC	solid support-free liquid-liquid chromatography
NK	nootkatone
NK+ED	pseudo-component, nootkatone+eudesmenol
sCPC	sequential centrifugal partition chromatography
trapping MDM	trapping multiple dual mode

List of figures

Appendix A. Derivation of retention volume equation

Under linear, ideal chromatography conditions, and assuming a column that is initially solute-free ($c_k^M = c_k^S = 0$), the retention volume, $V_{R,k}$, is derived as follows (adapted from description in [54] for liquid-solid chromatography).

mobile phase $\quad\square\ c_k^M = 0 \quad \boxtimes\ c_k^M = c_k^{feed}$

stationary phase $\quad\blacksquare\ c_k^S = 0 \quad \boxtimes\ c_k^S = K_k c_k^M$
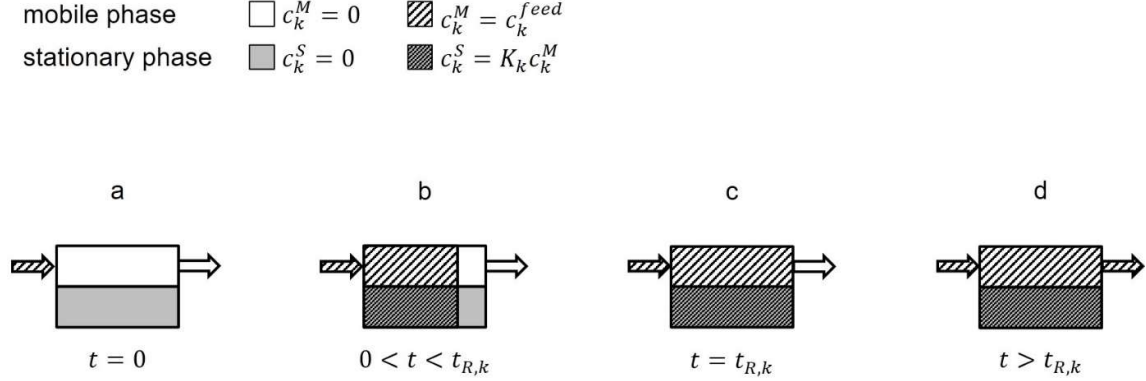
Figure A1. Feed loading of a liquid-liquid chromatography column under linear, ideal conditions.

Starting at time $t = 0$, a feed solution containing a single solute k dissolved in the mobile phase with concentration $c_k^M = c_k^{feed}$ is fed to the column at a constant flow rate F (Figure A1a). The feed is continually introduced at the inlet (Figure A1b), with the mobile phase volume behind the solute k concentration front having a concentration $c_k^M = c_k^{feed}$. As instantaneous partition equilibrium of solute k takes place between the two phases, the corresponding stationary phase volume has a concentration determined by the partition coefficient, $c_k^S = K_k c_k^M$ (see Equation (3)). At the point in time when the solute k band front just reaches the column outlet, equivalent to the retention time $t_{R,k}$ (Figure A1c), the entire mobile phase volume in the column has the concentration c_k^{feed}. At all $t > t_{R,k}$, the mobile phase concentration at the outlet is also equivalent to that of the feed (Figure A1d). At time $t_{R,k}$, the amount of solute that has been fed to the column is equal to the amount of solute currently contained in the column. A mass balance around the column at $t = t_{R,k}$ yields Equation A1.

$$F t_{R,k} c_k^{feed} = c_k^M V^M + c_k^S V^S \tag{A1}$$

By substituting $c_k^{feed} = c_k^M$ and dividing by c_k^M, the retention volume equation is obtained (Equation A2).

$$V_{R,k} = F t_{R,k} = V^M + K_k V^S \tag{A2}$$

128

Appendix B. Two-column TMB-250 centrifugal partition chromatography set-up

Table B1. Specifications of two-column TMB-250 CPC set-up (Armen Instrument).

| Parameter	Value
Total volume	247 ml; 182 ml
Disks per rotor	10
Cells per disk	93
Cell geometry	twin-cells
Maximum flow rate	50 ml min^{-1}
Maximum rotational speed	3000 rpm
Maximum pressure drop	100 bar
UV-Vis detector	DAD600 2WL 200–600nm (ECOM)
Fraction collector	LS 5600 (Armen Instrument)
Thermostatic water bath	Ecoline Staredition E 140 (Lauda)
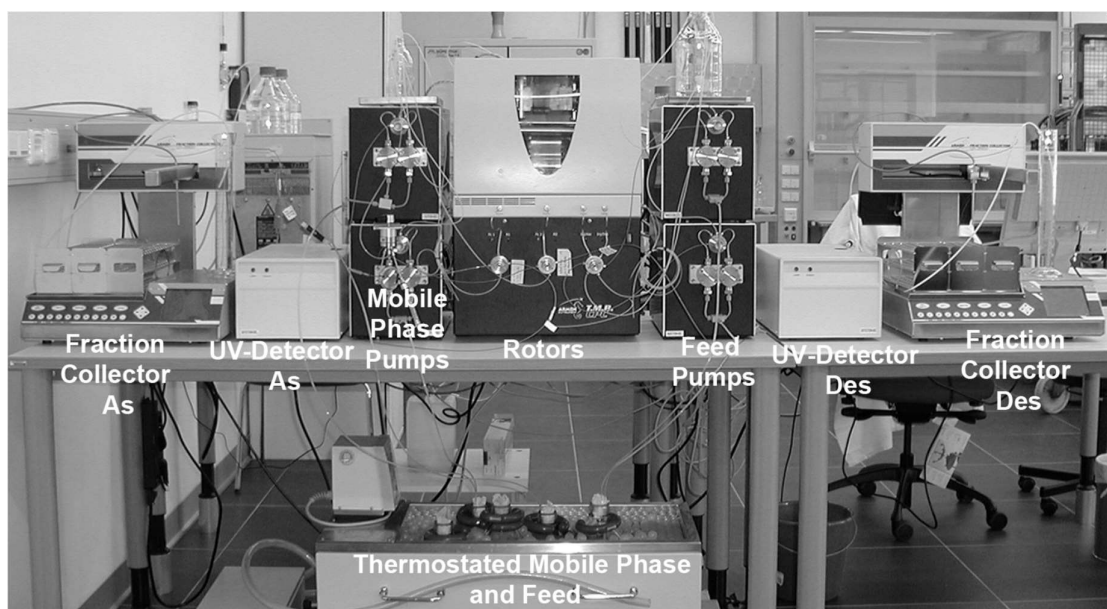
Figure B1. Two-column TMB-250 CPC set-up (Armen Instrument).
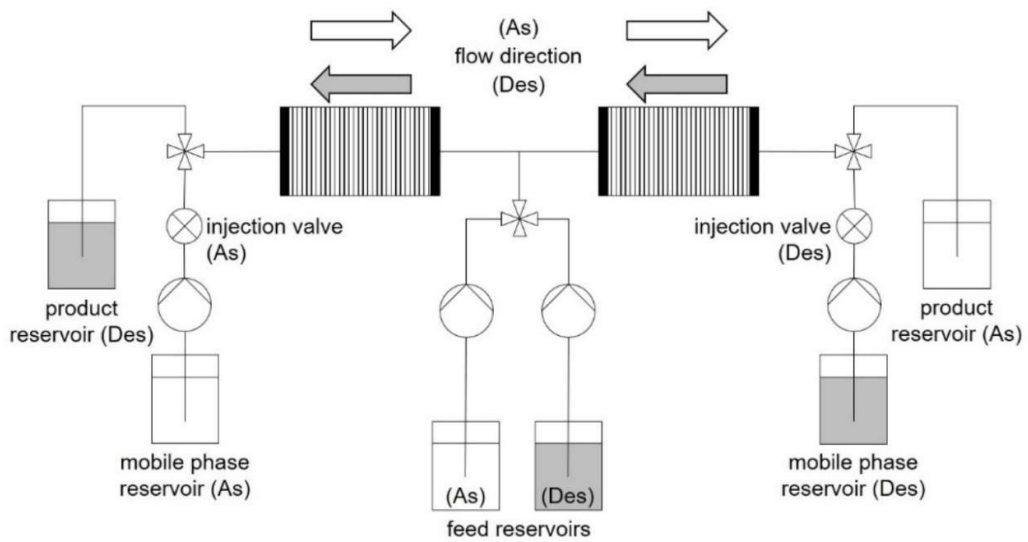
Figure B2. Schematic diagram of two-column TMB-250 CPC set-up (Armen Instrument).

White shading: upper phase. Gray shading: Lower phase

Appendix C. Review article, liquid-liquid chromatography short-cut models

Review article

Operating mode and parameter selection in liquid–liquid chromatography

Raena Morley, Mirjana Minceva*

Biothermodynamics, TUM School of Life Sciences Weihenstephan, Technical University of Munich, Maximus-von-Imhof-Forum 2, 85354 Freising, Germany

A B S T R A C T

The presence of a liquid stationary phase in liquid–liquid chromatography (LLC) allows for high versatility of operation as well as adaptability to different sample types and separation tasks. LLC, also known as countercurrent chromatography (CCC) or centrifugal partition chromatography (CPC), offers the user a variety of operating modes, many of which have no direct equivalent in conventional preparative liquid–solid chromatography. These operating modes have the potential to greatly improve LLC separation performance compared to the standard "classical" isocratic batch injection mode, and they often require minimal to no addition of equipment to the standard set-up. However, reports of the use of alternative LLC operating modes make up only a fraction of the literature. This is likely due, at least in part, to the lack of clear guidelines and methods for operating mode and parameter selection, leaving alternative process options to be avoided and underutilized. This review seeks to remedy this by providing a thorough overview of the available LLC operating modes, identifying the key characteristics, advantages and disadvantages, and areas of application of each. Additionally, the equations and short-cut models aiding in operating mode and parameter selection are presented and critiqued, and their notation is unified for clarity. By rendering LLC and its alternative operating modes more accessible to current and prospective users, it is hoped to help expand the application of this technology and support the achievement of its full potential.

© 2019 Elsevier B.V. All rights reserved.

1. Introduction

Solid support-free liquid–liquid chromatography (LLC) is a versatile and highly adaptable preparative separation technique combining the selectivity of liquid–solid chromatography with the sample loading capacity of liquid–liquid extraction. The "column" in LLC can have a coiled tube structure (hydrodynamic countercurrent chromatography, CCC), or it may consist of a large number of small chambers connected in series by ducts (hydrostatic centrifugal partition chromatography, CPC). The LLC column is mounted on a rotor and subjected to a centrifugal field by rotation, allowing the stationary phase to be kept immobile while the mobile phase is pumped through it. The mobile and stationary phases are the two pre-equilibrated phases of a biphasic solvent system, often consisting of 3 or 4 solvents. Either phase of the solvent system may be used as the stationary phase, and the roles of the phases can be switched during a separation run. This unique characteristic of LLC has led to the development of numerous operating modes beyond standard isocratic batch injections, many of which cannot be real-ized using conventional chromatography techniques with solid stationary phases.

The variety of available operating modes makes LLC highly adaptable to different sample types and separation tasks. The technique can be applied, for example, to the separation of mixtures possessing narrow or wide polarity ranges, be used for targeted separation or sample screening, and be implemented as a batch or continuous process. Nevertheless, the selection of the best-suited operating mode and its accompanying operating parameters for a certain separation task can pose a time-consuming challenge when using an experimental trial-and-error approach. The equations and short-cut models available in the LLC literature offer a time-saving alternative approach. However, as numerous research groups have contributed to this valuable information over a span of multiple decades, its accessibility and comprehension are impaired by dispersion throughout the literature, diverse derivation paths, and inconsistent notation. Therefore, this review aims to present a comprehensive and critical overview of the LLC operating modes and their corresponding design equations and short-cut models, thus facilitating operating mode comparison, selection, and preliminary process design.

---

* Corresponding author.
  E-mail address: mirjana.minceva@tum.de (M. Minceva).

The scope of this review is limited to LLC operating modes employing a truly immobile stationary phase. Therefore, cocurrent and dual flow methods with simultaneous pumping of both phases are not considered. Techniques involving solvent system modification such as pH-zone refining and elution strength gradients are not included, nor are orthogonal separations involving multiple solvent systems and hyphenated techniques. Process modeling approaches requiring numerical solvers are not discussed, as the focus is on lowering the threshold to quick preliminary process design without the need for additional computational tools or expertise.

2. LLC fundamentals

In this section, the general concepts, equations, and definitions used throughout this work are presented for the reader unfamiliar with LLC. The information in this section is relevant for all LLC separations and forms the basis for the discussion of the different operating modes in Section 3. Section 2.1 describes the particularities of working with a liquid stationary phase, while Sections 2.2–2.6 introduce the important general LLC parameters and equations. For additional information and a more detailed explanation of the fundamentals of CCC and CPC operation, several review articles are recommended: [1–4].

2.1. Particularities of a liquid stationary phase

The presence of a liquid stationary phase presents several advantages over conventional chromatography techniques with solid stationary phases. High loadings can generally be achieved in LLC, since the sample molecules have access to the entire volume of the liquid stationary phase, as opposed to only the surface of a solid stationary phase. Since LLC separations are often performed at ambient temperature and the sample molecules are not subjected to any physical sorption processes, the original physicochemical properties of the sample constituents, such as bioactivity, are most often preserved. By emptying the column, complete recovery of the injected sample is always possible, even for components partitioning exclusively in the stationary phase, and precludes the risk of contamination from one separation run to the next. Moreover, the operator can freely select the composition of the biphasic solvent system, tailoring it to the sample and separation task. The solvent system used as the mobile and stationary phases can be easily exchanged from run to run, allowing widely different sample types to be separated on the same LLC set-up.

For these reasons, LLC has found its niche in the separation of natural products obtained from, e.g., plants, marine organisms, and microbial fermentation media [4]. These samples may be injected as pre-purified fractions or crude extracts and are often complex mixtures of molecules varying in size, structure, hydrophobicity, and polarity [5]. Although most publications report LLC separations at the lab-scale, relatively simple scale-up and the possibility of continuous operation has made the technique an interesting option for industrial-scale downstream processing applications [6–9].

Selection of a suitable biphasic solvent system is the first step in the design of a LLC separation. The solvent system should provide satisfactory sample solubility as well as sufficient retention of the stationary phase in the column during separation. Additionally, the solutes of interest, i.e., the target(s) and main impurity or impurities, should exhibit adequate partitioning behavior between the phases. Solvent system screening and selection can be facilitated by the use of solvent system families [10–13] and thermodynamic models [14–17]. Although organic-aqueous solvent systems are most often encountered in the LLC literature, aqueous two phase systems and water-free systems have been successfully

used as well [13]. Working within realistic time and material restrictions, it is unlikely that the optimal solvent system for a certain separation will be found. Strategic selection of the operating mode and operating parameters can often be used to compensate for shortcomings in the characteristics of the solvent system.

Despite its many advantages, working with a liquid stationary phase can pose several challenges as well. The success and reproducibility of a LLC separation often depends on the ability to maintain a constant stationary phase volume in the column during operation. Whereas the surface area of the solid stationary phase available to the sample solutes is generally independent of the operating conditions in liquid–solid chromatography, the retained stationary phase volume in LLC will vary with the operating parameters (mobile phase flow rate, F; rotational speed, ω; temperature; choice of mobile and stationary phases), the physicochemical properties of the solvent system (density, viscosity, interfacial tension), and the geometry and characteristics of the LLC column (column volume; CCC: tubing bore, coil winding and number; CPC: chamber and duct size and shape).

To maintain a constant stationary phase volume during a LLC separation, hydrodynamic and thermodynamic equilibria must be preserved. The compositions and resulting properties of the two phases of the biphasic solvent system used as the mobile and stationary phases are subject to the thermodynamics of liquid–liquid equilibria, meaning that a change in composition occurring in one phase due to a change in temperature or the introduction of the sample induces a change in the other. Changes in composition may be accompanied by changes in the volume ratio between the phases as well as in their physicochemical properties, which can affect the hydrodynamic equilibrium. Stationary phase loss and/or changes in the partitioning behavior of the sample solutes may consequently occur [18–20], negatively affecting the separation and impairing the effectiveness of predictive models. These undesired effects can be avoided through appropriate selection of F and ω, temperature control of the LLC unit, and by performing sample injection at volumes and concentrations not affecting the phase equilibria.

2.2. Stationary phase fraction

During a LLC separation, the total column volume, V_C, is completely occupied by the mobile, V_M, and stationary, V_S, phases as expressed by Eq. (1).

$$V_C = V_M + V_S \tag{1}$$

As the mobile and stationary phases are the two phases of a biphasic solvent system, the column volume can alternatively be expressed by Eq. (2)

$$V_C = V_U + V_L \tag{2}$$

where the subscripts U and L denote the upper (less dense) and lower (denser) phases. Throughout this review, V_M, V_S, V_U, and V_L are used to indicate the phase volumes present in the column at the start of the separation run, i.e., immediately following column preparation as described below.

The stationary phase volume is described in relation to the total column volume by the stationary phase retention volume ratio, S_f (Eq. (3)).

$$S_f = \frac{V_S}{V_C} \tag{3}$$

S_f can be considered analogous to the complement of the void fraction in liquid–solid chromatography, $1 - \epsilon$. As S_f is governed by complex hydrodynamic and thermodynamic phenomena and is highly dependent on the solvent system and LLC column geometry, its purely theoretical prediction for a certain set of operating parameters is quite challenging. In general, S_f is higher when the less

dense upper phase is the mobile phase, decreases with increasing F, and increases with increasing ω. S_f above 0.50 is recommended to achieve satisfactory separation, although lower S_f can in some cases also be used [1]. The effect of S_f on a separation is dependent on the partition coefficients of the solutes of interest. Preliminary experiments are recommended to obtain S_f as a function of F, as well as to determine the working ranges of F and ω providing sufficient S_f within the pressure drop limitations of the set-up.

Before sample introduction, the LLC column must be prepared with the pre-equilibrated mobile and stationary phases to be used for the separation. There are two methods of column preparation: by mobile phase equilibration or with a pre-set phase ratio. In equilibration, the most commonly used method, the column is first completely filled with the stationary phase and rotation started at the speed to be used throughout the separation run. Pumping of the mobile phase is then begun at the flow rate to be applied during the separation. A portion of the stationary phase is displaced and elutes from the column outlet until hydrodynamic equilibrium is reached. The volume of stationary phase remaining in the column is the maximum that can be retained for the column and solvent system under the current set of operating conditions. This column preparation method can also be used in preliminary experiments to determine S_f with respect to F by incrementally increasing F and observing the accompanying displacement of stationary phase.

The column is prepared with a pre-set phase ratio when the desired volume of retained stationary phase is equivalent to or less than that which would be obtained through the equilibration method. This can, for example, be advantageous for the flow reversal modes treated in Section 3.3, when S_f of 0.5 is preferred regardless of which phase of the solvent system is used as the stationary phase, corresponding to a pre-set phase ratio of 50/50. A pre-set phase ratio can be obtained in two ways. In the first, applicable for use in both CCC and CPC columns, equilibration is performed at the flow rate resulting in the desired stationary phase retention. To preserve the pre-set phase ratio, the maximum flow rate that can be used during the separation run is equivalent to that used for the equilibration. When working with CPC columns, a second option is available. To fill the non-rotating column, the mobile and stationary phases are alternately pumped at quick succession, with the ratio of their pumping durations corresponding to the desired phase ratio. Once the column has been completely filled, rotation is started. Pumping of the mobile phase can be begun after the set rotational speed has been reached. The maximum applicable flow rate during the separation is equivalent to that which would result in the pre-set phase ratio when using the mobile phase equilibration method. Following column preparation, the mobile and stationary phases exist at thermodynamic and hydrodynamic equilibrium, regardless of the method used.

2.3. Solute partitioning

Separation in LLC occurs as a result of the differing partitioning behavior of the sample solutes, quantified for a component i by the dimensionless partition coefficient, K_i, defined as the ratio of its equilibrium concentrations in the stationary, $c_{S,i}$, and mobile phases, $c_{M,i}$, of a particular solvent system (Eq. (4)).

$$K_i = \frac{c_{S,i}}{c_{M,i}} \tag{4}$$

K_i describes the affinity of a component to the stationary phase. A higher value of K_i indicates a higher retention volume and a longer retention time. K_i can be determined for a particular solvent system by shake flask experiments or pulse injections (see Section 3.1.1). The separation factor, α, can be used to quantify the difficulty of a separation and is defined as the ratio of the partition

coefficients of two solutes of interest (Eq. (5))

$$\alpha_{2,1} = \frac{K_2}{K_1} \tag{5}$$

where $K_2 \geq K_1$ and therefore $\alpha \geq 1$.

In the linear range of the partition isotherm (analogous to the linear range of the adsorption isotherm in liquid–solid chromatography), K_i is considered constant. In general, the upper concentration limits of the linear partition region in LLC are higher than those typically found for adsorption on solid stationary phases. The limit of the linear region of the partition coefficient isotherm for the solutes of interest can be determined by performing preliminary shake flask experiments over a range of concentrations. The feed concentration, $c_{feed,i}$, should then be selected below this limit to allow the partition coefficient to be considered constant throughout the separation run. In doing so, linear chromatography conditions can be assumed, which considerably simplify modeling of the process. Additionally, the overall feed concentration as well as the sample volume should be selected so as to not disturb the hydrodynamic or thermodynamic equilibrium existing following column preparation, both of which can negatively affect the process as previously described in Section 2.1.

2.4. Elution modes

Either of the two phases of the selected biphasic solvent system may be assigned the role of the stationary phase, resulting in two elution modes: "tail-to-head" or "ascending" (As) mode when the lower phase is stationary and the upper phase is mobile; "head-to-tail" or "descending" (Des) mode when the upper phase is stationary and the lower phase is mobile. Since the upper phase is generally the less polar of the two phases in many commonly-used organic-aqueous solvent systems, As/tail-to-head mode can be considered analogous to normal-phase liquid–solid chromatography, while Des/head-to-tail mode can be considered comparable to reverse-phase operation with polar mobile phases. However, it should be noted that this analogy does not necessarily hold for organic-aqueous solvent systems containing organic solvents with a density greater than that of water, e.g., chloroform. In these cases, a non-polar, organic-rich lower phase may be obtained. The terms tail-to-head/head-to-tail are most often used in association with CCC separations, with the "head" and "tail" of the column being the ends to which the upper and lower phases move, respectively, in the absence of a centrifugal field. As/Des are most often encountered in the description of CPC processes and refer to the direction of the mobile phase flow in the chambers. The As/Des notation is used throughout this review to designate the elution mode. The definition of the partition coefficient Eq. (4) can be expressed for the Des and As elution modes as Eqs. (6) and (7), respectively.

$$K_{Des,i} = \frac{c_{U,i}}{c_{L,i}} \tag{6}$$

$$K_{As,i} = \frac{c_{L,i}}{c_{U,i}} \tag{7}$$

To maintain retention of the stationary phase in the presence of the centrifugal field, a change in elution mode necessitates a change in the mobile phase flow direction. Changing the elution mode without a change in mobile phase flow direction (or vice versa) results in displacement of the stationary phase from the column, often called extrusion in LLC. Additionally, as it can be seen from the inverse relation between $K_{Des,i}$ and $K_{As,i}$ (Eq. (8)), changing the elution mode also changes the elution order of the feed solutes, i.e., the most retained become the least retained, and vice versa. The separation factor, α, however, remains unaffected by a change in elution mode. When the elution mode is not specified

by the subscript in equations, K_i represents the partition coefficient value corresponding to the elution mode being implemented.

$$K_{Des,i} = \frac{1}{K_{As,i}} \tag{8}$$

The ability to switch the elution mode during a LLC separation run and, when desired, to extrude one of the phases by switching the mobile phase flow direction or the pumped phase, forms the basis of the majority of the operating modes described in this review.

2.5. Column efficiency

The solute-specific column efficiency, N_i, also referred to as the number of theoretical plates or stages, describes the degree of band broadening arising during the separation process as a result of axial dispersion and mass transfer resistance. Hundreds of theoretical plates are typically encountered in LLC, while N_i values in the thousands are common in liquid–solid chromatography. Satisfactory separations are nevertheless possible in LLC as a result of the extremely high ratio of stationary phase available for solute interaction to mobile phase compared to that found in liquid–solid chromatography [21]. Higher values of N_i are preferred and indicate narrower, less dispersed peaks resulting from high rates of mass transfer. Mass transfer is enhanced by increasing the contact area between the mobile and stationary phases. For a particular LLC column and solvent system, F and ω determine S_f and flow regime and, consequently, the phase contact area and the resulting mass transfer rate. Column efficiency trends reported in the literature with respect to F and ω are varied. More detailed information regarding the hydrodynamics affecting LLC column efficiency can be found in, for example, [22–30]. In the scope of this review, N_i is necessary for determination of the resolution, R_S, which indicates the degree of separation achieved between two component peaks.

N_i can be experimentally determined for a certain column, solvent system, and set of operating parameters by evaluating the chromatograms obtained from pulse injections performed at low sample concentrations and volumes (see Section 3.1.1). Assuming linear partition isotherms and sample volume underload, Gaussian peak forms can be expected. N_i is then related to the retention time, $t_{R,i}$, equivalent to the location of the peak maximum, and the variance, σ_i, by the well-known Eq. (9)

$$N_i = \left(\frac{t_{R,i}}{\sigma_i}\right)^2 \tag{9}$$

where σ_i has units of time. The peak width is commonly defined as that measured at the baseline by drawing tangent lines through the inflection points. In this case, the measured width, $w_{b,i}$, is equivalent to $4\sigma_i$ and also has units of time. Eq. (9) then becomes Eq. (10) [31].

$$N_i = 16\left(\frac{t_{R,i}}{w_{b,i}}\right)^2 \tag{10}$$

Accordingly, the peak start and end times, t_i^{start} and t_i^{end}, can be expressed by Eqs. (11) and (12), respectively.

$$t_i^{start} = t_{R,i} - 2\sigma_i \tag{11}$$

$$t_i^{end} = t_{R,i} + 2\sigma_i \tag{12}$$

In LLC, retention volumes, $V_{R,i}$, are often used in place of retention times, $t_{R,i}$. Assuming a constant flow rate with accurate metering, eluted volume and elapsed process time are related by the mobile phase flow rate, F, as shown in Eq. (13) for the specific case of $t_{R,i}$ and $V_{R,i}$.

$$t_{R,i} = \frac{V_{R,i}}{F} \tag{13}$$

Eqs. (9)–(12) can thus be alternatively expressed in terms of eluted volume. Eluted volume and elapsed process time are used interchangeably throughout this review.

2.6. Performance indicators

A variety of performance indicators can be used to evaluate a preparative chromatographic separation, such as resolution, solvent consumption, and productivity. The resolution between two peaks, R_s, can be applied for quick prediction of the improvement of a separation through the use of a different operating mode or a change of operating parameters. The resolution equations found in this review are valid for Gaussian peaks and solutes exhibiting the same column efficiency, N_i. However, the resolution equations can vary between operating modes, and in some cases the standard concept of resolution, which is better-suited to the evaluation of analytical separations, is not applicable at all. The elution profiles obtained in preparative separations are often non-Gaussian in form as the result of sample volume overloading for high throughput. For these reasons, other performance indicators applicable for all operating modes and types of elution profiles are preferable.

The objective of preparative chromatography separations is to obtain the highest amount of the target component(s) at the specified purity and yield with respect to the process economics (time, equipment, and/or material costs). Therefore, solvent consumption, SC, production rate, $\dot{m}$, and productivity, Pr, are extensively used in the evaluation, comparison, and optimization of preparative chromatography separations [32]. Although these performance indicators are seldom reported in the LLC literature, they would be a welcome alternative to the frequently encountered yet vaguely defined parameter "throughput" (amount of sample treated per unit time, often without regard for the amount of product meeting the purity and yield requirements finally obtained). Additionally, their adoption by the LLC community would facilitate comparison between different operating modes on a practical (economic) basis, as well as provide an objective function for operating parameter optimization using numerical methods.

The target solute-specific solvent consumption, SC_i, can be defined by Eq. (14)

$$SC_i = \frac{V_{proc}^{tot}}{m_i} \tag{14}$$

where V_{proc}^{tot} is the total volume of solvents used during the separation run (column preparation and separation; both the stationary and mobile phases) and m_i is the mass of the target solute obtained at the required purity. m_i can be determined experimentally by collecting fractions, performing offline composition analysis, and pooling those that meet the product specifications when combined. Alternatively, when complete chromatograms are available for the solutes of interest, the cut fraction meeting the product specifications can be determined by integration of the peak areas. The corresponding collected product mass can then be calculated.

In preparative liquid–solid chromatography, productivity is often defined as the production rate per unit mass of stationary phase packing or per column cross-sectional area. The former takes into consideration the costs incurred by the packing material, while the latter accounts for those associated with the column size. The target solute-specific production rate, $\dot{m}_i$, expresses the amount of target component i meeting the required purity obtained per unit time (see Eq. (15)), with t_{proc}^{tot} as the total process run time.

$$\dot{m}_i = \frac{m_i}{t_{proc}^{tot}} \tag{15}$$

With modifications, analogous definitions for productivity can be established for LLC. In comparison to liquid–solid chromatog-

raphy, the cost of the liquid stationary phase in LLC is generally relatively low compared to that of the required volume of the mobile phase. Therefore, V_{proc}^{tot} is used in the definition of the solvent volume-specific productivity, $Pr_{VP,i}$ (Eq. (16)), instead of a term related to the stationary phase alone.

$$Pr_{VP,i} = \frac{\dot{m}_i}{V_{proc}^{tot}} \tag{16}$$

Alternatively, productivity can be expressed with respect to the column size (volume) in place of a cross-sectional area (which cannot be defined for CPC columns) by the column volume-specific productivity, $Pr_{VC,i}$ (Eq. (17)).

$$Pr_{VC,i} = \frac{\dot{m}_i}{V_C} \tag{17}$$

In improving a preparative separation, it is desired to decrease SC and increase $\dot{m}_i$ and Pr. From Eqs. (15)–(17), it can be seen that this can be achieved by increasing m_i and decreasing V_{proc}^{tot} and t_{proc}^{tot}. A higher m_i can be obtained by increasing the feed concentration and/or the injection volume, but, as previously described, neither can be increased indefinitely. High solute concentrations can lead to operation outside of the linear range of the partition isotherm. Yet more critical for process stability, unwanted disruptions of the thermodynamic and hydrodynamic equilibria of the two phases in the column may occur as well, leading to possible changes in the compositions of the mobile and stationary phases, their phase ratio within the column, and stationary phase loss. Such detrimental effects are less common in liquid–solid chromatography, as the compositions of the solid stationary phase and the mobile phase are generally independent of the solute concentration. High injection volumes result in wider peaks, increasing the chances of peak overlap and consequently negatively affecting product purity and yield.

Theoretically, a reduction of V_{proc}^{tot} could be achieved by decreasing either the mobile phase flow rate, F, or the run duration, t_{proc}^{tot}. Contradictorily, a decrease in t_{proc}^{tot} can in turn be achieved by increasing F. As mentioned before, changes in F can have a positive or negative effect on the separation, depending on the accompanying changes in S_f and N_i and their implications for the separation at hand. Both V_{proc}^{tot} and t_{proc}^{tot} can be potentially reduced by changing the elution mode in order to elute all sample components from the column faster. The use of alternative operating modes in LLC offers the opportunity to further improve resolution, solvent consumption, and productivity beyond that which can be achieved with standard isocratic batch injections.

3. LLC operating modes

Given the wide variety of LLC operating modes available, it may be difficult to choose the one best-suited for the sample type and separation task at hand. Ito's "golden rules" [1] and Friesen and Pauli's binary choices [33] both present a structured approach to basic operating parameter selection, but they stop short when it comes to the selection of an operating mode other than standard isocratic batch injections. The following subsections address the advantages, disadvantages, and applicable separation scenarios attributed to the various LLC operating modes. The design equations and short-cut models available in the literature are also be presented.

As LLC samples are often complex natural product extracts sometimes consisting of dozens or hundreds of different components, a certain degree of simplification is necessary for the preliminary design of a separation. Unless the separation task is to evaluate a sample's overall polarity range, generally only two or three (groups of) solutes of interest need to be considered. Therefore, the majority of design equations and short-cut models presented in this review can be applied to complex multi-component mixtures by simplifying them to pseudo-binary or pseudo-ternary mixtures. The term "solutes of interest" will be used throughout this review to refer to the target solute(s) and main impurity or impurities that are taken into account during separation design.

Implementation of the short-cut models presented in this review assume that a suitable solvent system has been found and that the following are known from preliminary experiments (not all listed parameter values are needed in all equations):

- Total column volume, V_C
- Partition coefficients of solutes of interest, K_i
- Stationary phase retention volume ratio, S_f, obtained by column preparation with mobile phase equilibration (and therefore phase volumes V_M, V_S, V_U, and V_L), for the flow rate, F, and rotational speed, ω, ranges of interest
- Column efficiencies, N_i, for the ranges of S_f, F, and ω of interest

Additionally, the following simplifying assumptions are made:

- Linear chromatography conditions: all sample components exhibit linear partition isotherms, i.e., their partition coefficients are constant and independent of concentration and the presence of other solutes.
- Constant operating conditions: unless their change is characteristic of the operating mode itself, all operating parameters, e.g., F, S_f, ω, remain constant during operation.
- Ideal chromatography conditions (applicable to those equations not containing a term for the column efficiency, N_i): band broadening effects arising from mass transfer resistance and axial dispersion are not considered, i.e., all solute bands exhibit rectangular elution profiles. Peak shift resulting from non-ideal flow patterns such as back-mixing and short-cutting is not taken into account, nor are extra-column volumes.

An important comment should be made regarding all short-cut models solely employing the retention time, $t_{R,i}$, or retention volume, $V_{R,i}$, of a certain solute in the determination of, e.g., step durations or the switch from one process stage to the next. Basing such parameters on $t_{R,i}$ or $V_{R,i}$ alone does not take into account the entire solute band width, as both retention time and volume correspond to the midpoint of the width of a Gaussian peak. For higher precision when the band width is not already considered by the model, the peak end or start time, t_i^{end} or t_i^{start} as defined by Eqs. (11) and (12), can be used instead.

The operating modes described in this review are discussed in order of increasing complexity from a process design standpoint. Those employing a single elution mode are addressed first in Section 3.1. Section 3.2 focuses on the extrusion modes, which incorporate the complete displacement of one phase by the other. The batch operating modes consisting of one or more elution mode switches are covered in Section 3.3, and the continuous operating modes based on the same concept are presented in Section 3.4.

3.1. Classical mode and variations

This section begins with classical mode, the simplest LLC operating mode (Section 3.1.1). Its variations, stacked injections (Section 3.1.2) and closed-loop recycling (Section 3.1.3), follow. All operating modes addressed in this section are performed using a single elution mode and have analogous implementations in liquid–solid chromatography.

3.1.1. Isocratic batch injections (classical mode)

Isocratic batch injection mode, also referred to as classical mode in the literature, is the simplest and most often reported LLC operating mode. It can be performed on all LLC set-ups and consists of sample injection from one end of the column followed by isocratic

Classical mode

Single feed injection; isocratic elution in a single elution mode

As mode;
UP mobile

A+B

B then A

OR

Des mode;
LP mobile

A then B

A+B
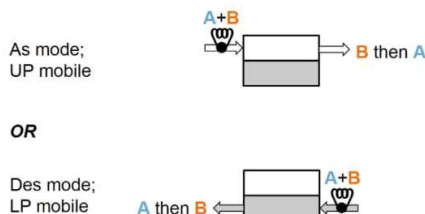
Fig. 1. Classical mode, depicted for As and Des elution modes. $K_{As,\ A} > K_{As,\ B}$ and $K_{Des,\ A} < K_{Des,\ B}$. White shading: upper phase. Gray shading: lower phase.

elution with the mobile phase in a single elution mode (see Fig. 1). The classical mode retention volume, $V_{R,i}^{CM}$, can be calculated using Eq. (18) [34].

$$V_{R,i}^{CM} = V_M + K_i V_S \qquad (18)$$

For successful separations in classical mode, it is often recommended that sample components exhibit partition coefficients in the range of $0.5 < K_i < 1$ [1] or in the wider "sweet spot" range of $0.25 < K_i < 4$, with a preferred target component partition coefficient close to 1 [10]. These ranges represent a compromise between short run time and sufficient peak resolution and serve as a main criterion in solvent system selection. It is additionally recommended that a minimum separation factor, α, of 1.5 be met for the solutes of interest [1].

As mentioned in Sections 2.3 and 2.5, preliminary pulse injection experiments can be used to determine retention behavior ($t_{R,i}$ and/or $V_{R,i}$) as well as N_i and K_i. Such experiments are performed using small injection volumes and solute concentrations to ensure volume underload conditions and operation in the linear range. When these pulse injections are performed in classical mode, K_i can be determined from chromatograms by simple rearrangement of the retention volume equation (Eq. (18)), resulting in Eq. (19).

$$K_i = \frac{V_{R,i}^{CM} - V_M}{V_S} \qquad (19)$$

Pulse injection experiments in classical mode may also be used to screen the sample polarity range, i.e., K_i range, to determine solvent system suitability and/or as an initial characterization step. However, classical mode becomes impractical when solutes possessing high K_i are present in the sample, resulting in long run times.

The classical mode resolution, R_S^{CM}, is given by Eq. (20)

$$R_S^{CM} = \frac{\sqrt{N}}{4} \frac{K_2 - K_1}{\frac{V_M}{V_S} + \frac{K_2 + K_1}{2}} \qquad (20)$$

where $K_2 \geq K_1$ and a single value of N is assumed for the two components [35]. Baseline separation of two peaks, each with a width of $4\sigma_i$, is achieved at $R_S = 1.5$.

When a resolution greater than 1.5 is obtained in preliminary experiments, the injected sample volume can be increased to obtain a higher recovered target mass, m_i, using, for example, the approach described in [36]. To further increase productivity by introducing more sample to the column, stacked injections (Section 3.1.2) may be used. In the case that the desired resolution cannot be achieved with classical mode, closed-loop recycling may be implemented (Section 3.1.3).

3.1.2. Stacked injections

When sample solubility in the mobile phase and/or the target component concentration is low, or when limited to small injection volumes in order to obtain baseline resolution [37], one approach for increasing the total injected sample amount is by performing stacked injections. In this technique, also referred to as repeated, consecutive, or successive injections in the literature, sample injections are made at regular intervals without new preparation of the column. The completion of 5 or less stacked injections is generally reported in the literature [38–42], although separations consisting of 12 [43] and 20 injections [44] have also been successfully performed.

A critical operating parameter for stacked injections is the selection of the time interval between injections. Ideally, this interval should be as short as possible while preventing overlap of the target and impurity peaks from one injection to the next [45]. A simple way to determine the time interval between injections is to perform a preliminary classical mode injection and determine the elapsed time between the start and end of elution of all solute peaks [46]. The time interval between stacked injections, t_{int}^{SI}, is defined by Eq. (21)

$$t_{int}^{SI} = t_n^{end} - t_1^{start} \qquad (21)$$

where t_i^{start} and t_i^{end} are the start and end of elution of the peak of component i, and $i = 1, \ldots, n$, with 1 and n as the first- and last-eluting peaks of the sample mixture. When partition coefficients and the column efficiency are known, t_n^{end} and t_1^{start} can be predicted using Eqs. (11) and (12) in Section 2.5. In the common case that the target component has an intermediate elution speed, separation duration and mobile phase consumption may be further reduced by allowing overlap of the late-eluting impurities from one injection and the early-eluting impurities from the next injection.

The use of stacked injections is best-suited to samples possessing a narrow range of partition coefficients, resulting in short time intervals between injections. When working with complex samples covering a wide range of partition coefficients, the time interval between injections may become quite long due to late-eluting components.

3.1.3. Closed-loop recycling

When satisfactory resolution cannot be achieved with a single chromatographic run in classical mode, the portion of the mobile phase eluent containing the unresolved peaks of the solutes of interest may be directly recycled back to the column inlet. Multiple passes through the column result in a virtual lengthening of the column, subjecting the components to a higher number of theoretical stages and allowing for an increase in resolution. This method offers an alternative to physical lengthening of the column or the connection of multiple columns in series, both of which can require increased equipment costs and lead to increased column pressure drop [47]. The closed-loop recycling operating mode is depicted in Fig. 2.

Closed-loop recycling, with direct re-introduction of the effluent to the column inlet, was first reported on a LLC column in [48]. The technique requires connection of the outlet of the column or of the post-column detector to the column inlet. The change from normal elution to recycling mode (from (1) Classical mode elution to (2) Recycling in Fig. 2) is made using a switching valve. The switch to recycling mode may occur immediately following sample injection or at a later point in time. Starting the recycling mode immediately before elution of the target solute(s) has been recommended to prevent the carryover of any hydrodynamic disturbances resulting from the injection to the next cycle and to allow earlier-eluting impurities to leave the column, preventing their possible overlap with peaks of subsequent cycles [49]. The switching valve is returned to its original position after satisfactory resolution has been achieved in order to allow collection of the target(s) (switch from (2) Recycling to (3) Product collection in Fig. 2). Multiple switches between closed-loop recycling and classical mode elution can be

Closed-loop recycling mode

(1) Classical mode elution

As mode;
UP mobile

(2) Recycling
Effluent reintroduced at inlet

As mode;
UP mobile

(3) Product collection
Recycling stopped; solutes allowed to elute

As mode;
UP mobile
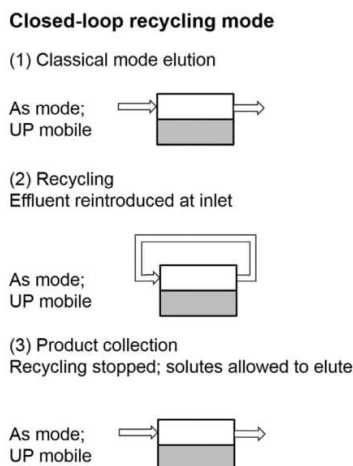
Fig. 2. Closed-loop recycling mode, depicted for As elution mode. White shading: upper phase. Gray shading: lower phase.

made throughout a run, allowing purified peak fractions to be collected while unresolved solutes are subjected to additional cycles [50]. Although all reports of recycling LLC have been performed on CCC columns, implementation of the technique would also be possible on CPC columns, as it is only dependent on modification of the peripheral equipment.

The closed-loop recycling operating mode has been studied in-depth in a series of primarily theoretical studies [50–56]. A key operating parameter in closed-loop recycling LLC is the number of cycles to be performed before solute peak collection. Two competing types of resolution must be considered: resolution between peaks of a single cycle and the resolution between peaks of neighboring cycles, namely the slowest-eluting peak of the preceding cycle and the fastest-eluting of the current cycle. Equations for these two types of resolution were derived for impulse injections and a zero extra-column volume recycling line in [50]. For two peaks of the same cycle, the resolution at cycle k is given by Eq. (22)

$$R_S^{CLR}(k) = \sqrt{kN} \frac{a_1 - a_2}{2(a_1 + a_2)} \qquad (22)$$

where the subscripts 1 and 2 denote two solutes satisfying $K_2 \geq K_1$, and $a_i = \frac{1}{1 - S_f + S_f K_i} = \frac{V_C}{V_{R,i}^{CM}}$, with $V_{R,i}^{CM}$ determined using Eq. (18). This equation is essentially identical to that derived from experimental observations and reported in [57]. The resolution between peaks of consecutive cycles possessing the lowest and highest partition coefficients, denoted by subscripts 1 and n, respectively, can be calculated using Eq. (23)

$$R_{S,cyc}^{CLR}(k) = \sqrt{N} \frac{a_n k - a_1 (k-1)}{2 \left(a_n \sqrt{k} + a_1 \sqrt{k-1} \right)} \qquad (23)$$

where the fastest-moving peak is located in cycle k while the slowest-moving peak is still undergoing the previous cycle $k-1$. Since $R_S^{CLR}(k)$ increases with increasing k while $R_{S,cyc}^{CLR}(k)$ decreases, Eqs. (22) and (23) can be used together to select an intermediate number of cycles in which satisfactory resolution of the target component(s) is achieved before the start of overlap of peaks from neighboring cycles.

The introduction of the recycling line to the LLC set-up may introduce a significant extra-column volume to the system. It was concluded in [50] that an extra-column volume equivalent to less than 1% of V_C has a negligible influence on the resolution.

However, in practice, the effect of the addition of the recycling line depends on the additional dispersion introduced to the system. This dispersion is dependent on the line dimension as well as the periphery, i.e., connectors and recycling pump. A further theoretical and experimental study concluded that in closed-loop recycling it can actually be beneficial to have a longer recycling line [53]. Although this contradicts the general recommendation in chromatography that the extra-column volume should be kept to a minimum in order to reduce the negative effects of additional dispersion on the separation [58], the same conclusion was previously reached for liquid–solid chromatography in [59,60]. Up to a certain recycling line volume, the separation may be improved due to a reduction in the decrease in resolution between the slowest- and fastest-moving peaks of neighboring cycles, $R_{S,cyc}^{CLR}(k)$. This allows more cycles to be run, increasing the resolution between peaks of the same cycle, $R_S^{CLR}(k)$, before detrimental peak overlap occurs. Above a certain recycling extra-column volume, negative effects on the separation are again observed, due to worsening resolution between peaks of the same cycle as a result of increased band broadening effects.

Due to the detrimental effect of peak overlap from neighboring cycles, closed-loop recycling is best-suited for mixtures of a few solutes of interest in a narrow partition coefficient range, i.e., with low separation factors. It has been recommended to select a solvent system in which the target components have relatively low partition coefficients, as they undergo less band broadening per cycle, allowing more cycles to be performed before overlap of peaks from neighboring cycles occurs [48]. Compared to other operating modes resulting in a virtual column lengthening, such as the flow reversal modes described in Section 3.3, closed-loop recycling LLC can potentially require less solvent consumption, since the mobile phase is recirculated through the column while the system is in recycling mode [50]. For liquid–solid chromatography, it was concluded that recycling always increases target recovery, but in many cases reduces the overall productivity compared to the single-pass classical mode process [61]. Therefore, closed-loop recycling may be preferred for separation tasks in which the target yield is of primary importance.

Closed-loop recycling is often reported as a second separation step following an initial fractionation of a crude sample by, e.g., classical mode, when improved resolution of the target is required [62–65]. The operating mode has also been implemented on custom LLC set-ups allowing for the cut and storage of fractions to be recycled during the same run [66] as well as flexible operation of multiple columns in classical or closed-loop recycling mode in parallel or in series [47]. Both custom set-ups allow for the separation of solutes with low separation factors from complex multi-component mixtures. An additional variation to the closed-loop recycling method includes multiple injections timed to allow for the concentration of a single target component present in low amounts in the sample mixture [54,55,67]. However, only one experimental demonstration of this technique, performed on a related controlled-cycle pulsed liquid–liquid chromatography (CPLC) column, has been reported [55].

3.2. Extrusion modes

In LLC, complete displacement of one phase by the other occurs when, with respect to the elution mode definitions (Section 2.4), either the mobile phase is pumped in the "wrong" direction, or the "wrong" phase is used as the mobile phase. This corresponds to the mobile upper phase being pumped in the Des mode direction or the mobile lower phase being pumped in the As mode direction. This extrusion effect can be used to shorten the run duration as well as preserve high-concentration, well-resolved peak profiles within the column belonging to highly-retained components.

Elution extrusion mode

(1) Classical mode elution

As mode;
UP mobile

(2) Sweep elution
Following start of pumping of stationary phase; mobile phase continues to elute from outlet
Normal isocratic elution experienced by solutes until overtaken by stationary phase front

As mode;
LP mobile

(3) Extrusion
Begins when solute overtaken by stationary phase front
Solute "extruded" from column with stationary phase; partitioning between phases no longer occurs

As mode;
LP mobile

Fig. 3. Elution extrusion mode, depicted for As elution mode and extrusion with lower phase. White shading: upper phase. Gray shading: lower phase.

There exist two extrusion operating modes: elution extrusion (Section 3.2.1) and back extrusion (Section 3.2.2).

3.2.1. Elution extrusion

The elution extrusion technique was first theoretically treated in a series of publications [68–70]. The last, [70], provides the most accurate description of the elution extrusion process, breaking it down into three stages based on the process conditions currently being "experienced" by a certain solute (see Fig. 3):

- Stage 1: Classical mode elution, during which the separation is run in As or Des mode.
- Stage 2: Sweep elution, the period beginning with the mobile phase switch during which a solute band continues to be subjected to classical mode conditions until overcome by the Stage 1 "stationary" phase front.
- Stage 3: Extrusion, beginning with the point at which the solute band has been overtaken by the Stage 1 "stationary" phase front, and chromatographic separation no longer occurs.

Following sample injection, separation with the "right" mobile phase is performed as in classical mode (Stage 1). This stage ends after pumping a volume V_{Stg1}^{EE}. At this point, the pumped phase is switched from the mobile phase to what was the stationary phase during Stage 1 without changing the flow direction or the column rotation. This begins the sweep elution stage (Stage 2) during which the pumped Stage 1 "stationary" phase, moving in the "wrong" flow direction, gradually displaces the Stage 1 mobile phase. Solute bands located ahead of the pumped "stationary" phase front continue to undergo chromatographic elution under classical mode conditions until overtaken by it. The Stage 2 duration experienced by each solute is solute-specific and dependent on K_i. The Stage 1 mobile phase continues to elute from the column outlet until a volume V_M of "stationary" phase has been pumped. At this point, the pumped stationary phase front has reached the outlet, and the entire column is filled with the Stage 1 "stationary" phase. All solutes remaining in the column are now undergoing extrusion (Stage 3). Extrusion begins for a solute when it has been surpassed by the Stage 1 "stationary" phase front. Due to the absence of the Stage 1 mobile phase, chromatographic partitioning no longer occurs, and the remaining solute bands move toward the column outlet at the same rate as the pumped "stationary" phase. All remaining solutes elute from the column after pumping a maximum additional stationary phase volume of V_S, meaning that the complete possible partition coefficient range from zero to infinity can be eluted with a total pumped volume of $V_{Stg1}^{EE} + V_C$.

The elution extrusion operating mode is simple to implement and does not require any equipment in addition to that needed for classical mode separations. With a single mobile phase pump and the mobile and stationary phases kept in the same reservoir, it is only necessary to move the mobile phase inlet tubing from one phase to the other to begin the extrusion step. At the end of an elution extrusion run, the sample and phase volumes present in the column at the start of the run have been completely eluted or displaced by the pumped stationary phase. This "clean" column, free of all highly retained solutes, is then ready for preparation by equilibration with the "right" mobile phase for the next injection. This is a preferable characteristic for, e.g., separations in which avoidance of cross-contamination between runs is important. Studies comparing the use of elution extrusion to classical mode have shown that elution extrusion can significantly reduce the run duration and therefore solvent consumption for a given separation [6,71,72].

Several applications of elution extrusion and their corresponding short-cut design approaches have been reported in the literature. These include the $2V_C$ method [69] for sample screening as well as selecting the Stage 1 elution volume, V_{Stg1}^{EE}, based on either a required resolution or the desired process stage during elution [70,73]. These short-cut models assume ideal extrusion conditions, i.e., the pumped stationary phase front exhibits a rectangular profile and the Stage 1 mobile phase is completely displaced from the column. It should however be pointed out that in practice a portion of the Stage 1 mobile phase may remain in the column (CCC or CPC) following the extrusion stage [68], negatively affecting short-cut model accuracy. A systematic study establishing guidelines for operating parameter selection that would ensure complete extrusion would be of interest to the field.

The $2V_C$ method was first suggested for rapid sample polarity range, i.e., K_i range, screening [69]. The name $2V_C$ refers to the

ability to use elution extrusion to elute an entire complex sample, i.e., solutes possessing partition coefficients from zero to infinity, using only two column volumes of pumped phases. It offers a quick approach for solvent system screening [11,72,74,75] as well as for sample fractionation prior to further separation [76,77] or high-throughput screening analysis for, e.g., drug discovery programs [69,78].

As previously mentioned, the maximum elution extrusion retention volume, corresponding to a solute partitioning exclusively in the stationary phase with $K_i = \infty$, is equivalent to $V_{Stg1}^{EE} + V_C$. In the $2V_C$ method, one column volume of mobile phase is pumped during Stage 1 ($V_{Stg1}^{EE} = V_C$), resulting in the elution of all components with a $K_i \leq 1$. A second column volume of the Stage 1 "stationary" phase is then pumped during Stages 2 and 3 to elute the remaining components with $K_i \geq 1$. When using the $2V_C$ elution extrusion as a screening method, the classical mode partition coefficient equation (Eq. (19)) can be used to determine K_i of solutes eluting with the mobile phase during Stages 1 and 2 while Eq. (24) [70] can be used to determine K_i for solutes eluting from the column with the pumped stationary phase while undergoing Stage 3

$$K_i = \frac{V_{Stg1}^{EE}}{V_{Stg1}^{EE} + V_C - V_{R,i}^{EE}} \tag{24}$$

where $V_{R,i}^{EE}$ is the retention volume of i with respect to the cumulative volume eluted from the column during all 3 elution extrusion stages. Of course, Eq. (24) is also valid for elution extrusion separations where $V_{Stg1}^{EE} \neq V_C$.

The $2V_C$ method offers a quick design approach when the entire chromatographic spectrum is of interest. However, for the targeted separation of a specific component, the optimal value of the Stage 1 elution volume, V_{Stg1}^{EE}, is not necessarily the column volume. Two different approaches for rational selection of the Stage 1 elution volume have been developed. In [73], V_{Stg1}^{EE} was chosen based on a required resolution. In elution extrusion, it is possible to take advantage of the fact that two solute bands may already be sufficiently resolved inside the column long before they reach the outlet. Under ideal conditions, the resolution between solute bands is not altered during the extrusion stage, although the widths of the bands as well as the volume distance between them are proportionally reduced by a factor of S_f [69]. Re-working the expression for resolution of two solutes inside the column first presented in [68], Eq. (25) was derived in [73] to determine t_{Stg1}^{EE}, the time at which a certain resolution is met inside the column under classical elution conditions

$$t_{Stg1}^{EE} = \frac{\left(2R_{S,col}^{EE} \Big/ \sqrt{\frac{1}{t_{R,1}^{CM}} - \sqrt{\frac{1}{t_{R,2}^{CM}}}}\right)^2}{N} \tag{25}$$

where $R_{S,col}^{EE}$ is the required resolution inside the column, $t_{R,i}^{CM}$ is the classical mode retention time Eqs. (13) and (18), and N is the theoretical stage number, here considered identical for both components 1 and 2, with $K_2 \geq K_1$. Multiplying t_{Stg1}^{EE} by the flow rate (Eq. (13)), gives the corresponding Stage 1 elution volume, V_{Stg1}^{EE}. The slight increase in resolution occurring during the sweep elution stage is not accounted for by Eq. (25), but as this further improves the separation, it is not critical for meeting the required resolution. After determination of V_{Stg1}^{EE}, the retention volumes can be calculated for components eluting during Stage 1 or 2 using the classical mode equation (Eq. (18)) or for those eluting during Stage 3 using Eq. (26), obtained by reworking Eq. (24).

$$V_{R,i}^{EE} = V_{Stg1}^{EE} + V_C - \frac{V_{Stg1}^{EE}}{K_i} \tag{26}$$

Eq. (26) does take the small distance travelled by the solute band during the sweep elution stage into consideration. The last solute to elute from the column with the mobile phase during sweep elution (Stage 2) has the partition coefficient value $K_i = V_{Stg1}^{EE}/V_S$ [70].

In the second approach, V_{Stg1}^{EE} is selected for the shortest run duration at the maximum resolution. Two solutes exhibit the highest resolution when eluting during the sweep elution stage (Stage 2) with the Stage 1 mobile phase, i.e., when they have undergone the chromatographic process for as long as possible and elute just before being subjected to the start of extrusion [70,79]. The resulting resolution is the same as that obtained during a simple classical mode separation under the same operating conditions, but the addition of the extrusion stage shortens the process duration. Therefore, for a target component possessing a known partition coefficient, the Stage 1 elution volume can be obtained using Eq. (27), adapted from [70]. In Eq. (27), i is the last-eluting solute of interest.

$$V_{Stg1}^{EE} = K_i V_S \tag{27}$$

It was found experimentally that sufficient resolution can generally be obtained with the elution extrusion operating mode for $0.25 < K_i < 16$, representing a marked improvement over the classical mode "sweet spot" range of $0.25 < K_i < 4$. However, these findings were specific to a single solvent system family [12]. In a single application study, elution extrusion was found to perform as well as dual mode (introduced in Section 3.3.1) for the quick elution of highly-retained solutes of interest [80]. For sample polarity range screening, dual mode is preferred over elution extrusion for accuracy [81]. One report of "overlapping elution extrusion" was made, in which a switch back to the Stage 1 mobile phase and injection of a new sample is made before all solutes from the preceding separation have been eluted from the column [79]. However, this method should be further evaluated for robustness and practicality, as only two consecutive injections were made.

3.2.2. Back extrusion

Similar to elution extrusion, the back extrusion operating mode can also be used to shorten the time needed for the complete elution of an injected sample containing components possessing a wide range of partition coefficients. However, in back extrusion, first thoroughly described in [82], it is not the change of the phase being pumped that leads to extrusion but rather the mobile phase flow direction. Hence, the same phase is used as the mobile phase throughout the run.

The following description of the back extrusion process is applicable for hydrodynamic CCC columns [82] and depicted in Fig. 4. Expected deviations when using hydrostatic CPC columns are addressed below. The back extrusion process can be split into three stages. Unlike in elution extrusion, all solutes are subjected to extrusion conditions at the same time, i.e., there is no analogous sweep elution stage.

- Stage 1: Classical mode elution, during which the separation is run in As or Des mode. Mobile phase elutes from the column outlet.
- Stage 2: Stationary phase extrusion, experienced by all solutes at the same time following the switch in mobile phase pumping direction. The Stage 1 stationary phase elutes from the column outlet.
- Stage 3: Echo peak elution, during which the solute band portions partitioned in the mobile phase at the start of Stage 2 elute from the column. The Stage 1 mobile phase again elutes from the column outlet.

In Stage 1, the separation is run in classical mode following sample injection with pumping of the mobile phase in the "right"

Back extrusion mode*

(1) Classical mode elution

As mode;
UP mobile

(2) Stationary phase extrusion
Reversal of mobile phase flow direction; interruption of chromatographic process
Stationary phase moves to column outlet and is extruded

Des mode;
UP mobile

(3) Echo peak elution
After complete extrusion of stationary phase, column completely filled with mobile phase
Possible "echo peak" elution

Des mode;
UP mobile

*depicted for hydrodynamic CCC columns

Fig. 4. Back extrusion mode, depicted for As elution mode and extrusion with upper phase. White shading: upper phase. Gray shading: lower phase.

direction for a volume V_{Stg1}^{BE}. During this time, solutes with $V_{R,i}^{CM} \leq V_{Stg1}^{BE}$ elute. At the end of Stage 1, the direction of the mobile phase flow is switched via the 4-port valve present on all standard LLC set-ups while keeping the rotational speed constant. This begins Stage 2, during which the stationary phase is extruded. The sudden change of flow in the "wrong" direction interrupts the hydrodynamic equilibrium between the phases and, therefore, the chromatographic process as well. Stationary phase retention is no longer possible and a complete splitting of the phases occurs, i.e., the lower phase moves to the column "tail" and the upper phase moves to the "head." The entire stationary phase volume is now located at the outlet end of the column. The portions of the solute bands located in the stationary phase at the time of the flow direction switch consequently move a factor S_f closer to the column outlet and become narrower by an equivalent proportion. The mobile phase then acts as a piston, extruding the stationary phase and the contained solute band portions. The solutes with the highest partition coefficients are closest to the outlet at the time of the flow direction switch and begin to elute first, i.e., the solute elution order is reversed with respect to Stage 1. Stage 2 begins when the stationary phase is completely extruded from the column after pumping a mobile phase volume equivalent to V_S, the stationary phase volume in the column at the start of the run.

Stage 3 begins when the column is completely filled with mobile phase. Mobile phase is again observed eluting from the column outlet. During Stage 3, the portions of the solute bands located in the mobile phase at the point of the flow direction switch, so-called echo peaks, leave the column. These solute band portions do not undergo the extrusion piston effect experienced by the stationary phase and are therefore subjected to a high degree of dispersion before eluting from the column as broad, diluted peaks. After pumping a maximal additional volume V_M of the mobile phase, all solutes have eluted from the column. Therefore, the maximum mobile phase volume required to ensure that all sample solutes have been eluted at the end of a back extrusion run is equivalent to $V_{Stg1}^{BE} + V_C$. As in elution extrusion, the separation run ends with a "clean" column. If it is desired to run the process semi-

continuously, the mobile phase in the column must first be exchanged with the stationary phase and then equilibrated with the mobile phase before a new injection can be made.

When a significant portion of a sample solute leaves the column in the form of an echo peak, its recovery can be reduced. For solutes with high partition coefficients, i.e., a high affinity for the stationary phase, the echo peak effect is less pronounced. To reduce the severity of the echo peak effect, it has been suggested to increase the duration of the classical mode stage (Stage 1) to the equivalent of the elution of two column volumes [82,83] rather than the single column volume often used in the $2V_C$ variation of the elution extrusion mode (see Section 3.2.1).

In the design of a back extrusion separation, the eluted mobile phase volume at which the flow direction switch occurs, V_{Stg1}^{BE}, must be selected. If this switch is to be made following the Stage 1 elution of a certain solute of known classical mode retention volume, $V_{R,i}^{CM}$ (Eq. (18)), V_{Stg1}^{BE} can be set to $V_{R,i}^{CM}$. The cumulative retention volume (Stage 1 and Stage 2) for a solute eluting during the stationary phase extrusion is given by Eq. (28) [82].

$$V_{R,i}^{BE} = V_{Stg1}^{BE}\left(1 + \frac{V_S}{V_{R,i}^{CM}}\right) \tag{28}$$

If back extrusion is used as a screening method, Eq. (29) can be used to determine the partition coefficients of solutes eluting during stationary phase extrusion in Stage 2 [82]. For solutes eluting during the classical elution stage (Stage 1), the classical mode retention volume equation (Eq. (18)) applies.

$$K_i = \frac{V_{Stg1}^{BE}}{V_{R,i}^{BE} - V_{Stg1}^{BE}} - \frac{V_M}{V_S} \tag{29}$$

A detailed description of the mechanism of the back extrusion process on hydrostatic CPC columns has yet to be reported in the literature. Due to the CPC column geometry, stationary phase retention within the individual chambers remains possible after the mobile phase flow direction switch. There would be no sudden movement of the stationary phase to one end of the column. Rather, it is expected that the mobile phase would sequentially

displace the stationary phase in each chamber, possibly with a sweep elution stage analogous to that observed in elution extrusion. The implications of this mechanism for the existence of the echo peak effect reported for CCC columns and for band broadening in general should be investigated. It should be noted that the existence of differences between predicted and experimental peak positions on hydrostatic CPC columns was briefly mentioned in [82] and postulated to be a result of incomplete extrusion of the stationary phase, as previously reported for CPC columns in [84].

Elution extrusion and back extrusion were experimentally compared for the screening [82] and separation [83] of complex natural product samples containing solutes spanning a wide range of polarities. In each comparative study, the same operating conditions and Stage 1 durations were used for both operating modes. Both elution extrusion and back extrusion were found to attain similar peak resolution, considerably shorten the process run time, and produce narrow, highly concentrated peaks for highly-retained solutes compared to classical mode. However, back extrusion was seen as less favorable due to the echo peak effect and the necessity of refilling the column with stationary phase before equilibration and a new injection can be performed.

3.2.3. Extractive back extrusion

Though it may not outperform elution extrusion, back extrusion can alternatively be used for the concentration and/or extraction of highly-retained target components often present at dilute concentrations in large volumes of feed. Such an approach, referred to here as extractive back extrusion and occasionally in the literature as centrifugal partition extraction, has been used on hydrostatic CPC columns for the recovery of non-polar target components from wastewater [85], algae cultivation broths containing viable cells [86–88], and pre-processed yeast fermentation biomass [89].

Contrary to typical LLC separations, in such extraction-type separations the solvent system, or, in the case of direct introduction of an aqueous feedstock as the mobile phase, the stationary phase solvent alone, is chosen for which the target component has a very high affinity, e.g., $K_i \approx 50$ [85]. The feed solution is continuously fed to the column, ideally until the stationary phase volume is saturated with the target component and the extraction has become inefficient [89]. The mobile phase flow direction is then switched to extrude the stationary phase, often using pure water instead in the place of the aqueous feed solution.

High throughput is given preference over chromatographic efficiency for such extractive back extrusion separations. CPC columns with larger cells and wider ducts tailored to this purpose have been developed, often referred to as centrifugal partition extraction (CPE) columns. Compared to conventional extraction techniques, target recovery using CPE columns can offer increased mass transfer and therefore higher yields as a result of the high interfacial area obtained between the two phases in the column cells [86,87].

A thorough theoretical study of extractive back extrusion addressing the determination of the optimal time point for the mobile phase flow reversal switch has yet to be reported in the literature. The classical mode retention volume equation (Eq. (18)) could be used to predict when the target component would elute during the initial classical mode stage. However, as a result of the low separation efficiency in CPE, significant band broadening would likely lead to a large deviation from the ideal predictions of Eq. (18), i.e., the dispersed solute band front would reach the column outlet earlier than predicted. The possible negative effects of high target component concentrations obtained in the stationary phase on the separation stability should also be further explored. Determination of the ideal target component partition coefficient range for such extractive back extrusion separations would also be of interest and could be used to guide solvent system selection.

3.3. Flow reversal modes

As described in Section 2.4, changing the elution mode results in a reversal of the mobile phase flow direction as well as of the elution order of the sample solutes. Proper selection of the number and duration of elution mode switches can shorten process run time and/or increase resolution when compared to classical mode. Flow reversal separations in LLC are similar to the backflush method in liquid–solid chromatography, in which the mobile phase flow direction is changed in order to elute highly retained components remaining near the column inlet at the time of elution of the target. However, a key difference in liquid–solid chromatography is that the adsorption behavior of the sample solutes is not affected by the mobile phase flow direction switch. In LLC, the partition coefficient is inversed (see Eq. (8)), since the roles of the mobile and stationary phases are also switched.

The simplest flow reversal mode, (single cycle) dual mode is presented first in Section 3.3.1. Further flow reversal mode developments for increased resolution (multiple dual mode, Section 3.3.2) and extension to ternary separations (trapping multiple dual mode, Section 3.3.3) are also discussed. A remark pertaining to all flow reversal modes described in this section as well as the continuous separation operating modes described in Section 3.4 should be made at this point. As the stationary phase fraction is a function of the operating parameters, including the elution mode, stationary phase loss may occur when switching from one elution mode to the other. By determining S_f as a function of flow rate in both elution modes through preliminary experiments, the mobile phase flow rate in each mode can be selected to ensure that no stationary phase loss occurs after the elution mode switch [90].

3.3.1. Dual mode

A dual mode separation consists of a single cycle of two steps in different elution modes (see Fig. 5). In the first step, the sample is injected and elution in As or Des mode is performed analog to a classical mode separation. At a certain point during the run, the second step is begun by switching the elution mode, i.e., As to Des or Des to As. The slowest-moving components during the first step now move the fastest to the opposite end of the column. In this second step, all remaining sample solutes not eluted from the column in the first step leave the column.

Dual mode lends itself to several different separation tasks. When target components possess very different partition coefficients, dual mode can be used as an alternative to classical mode to reduce run time and solvent consumption. Similar to closed-loop recycling, dual mode can also be used to improve resolution beyond that achieved in classical mode. As in elution extrusion and

Dual mode

(1) Classical mode elution

As mode;
UP mobile

(2) Elution mode reversal
Switch of mobile phase and flow direction
Reversal of solute elution order

Des mode;
LP mobile

Fig. 5. Dual mode, depicted for As elution mode in first step and Des elution mode in second step. White shading: upper phase. Gray shading: lower phase.

back extrusion, dual mode can also be used to elute the entire partition coefficient spectrum from zero to infinity, making it a suitable screening technique. These three applications are discussed below.

The use of dual mode to shorten the run time of a separation in which the target components possess both low and high partition coefficients is its most often reported application [91–97]. At least one target component is collected in the first step, while the remaining target(s) leave(s) the column in the second step as narrow, highly concentrated peaks. Assuming two target components of known partition coefficients and $K_1 < K_2$ in the elution mode of the first step, the elution mode switch should be made immediately following the elution of the earlier-eluting component 1. The eluted mobile phase volume in the first step, V_{Stp1}^{DM}, is therefore equivalent to $V_{R,1}^{CM}$ (see Eq. (18)). To determine the additional mobile phase volume needed to elute target component 2 in the second step, $V_{Stp2.2}^{DM}$, Eq. (30) can be used.

$$V_{Stp2.i}^{DM} = \frac{V_{Stp1}^{DM}}{K_i} \tag{30}$$

The cumulative retention volume in dual mode, $V_{R,i}^{DM}$, is therefore given by Eq. (31).

$$V_{R,i}^{DM} = V_{Stp1}^{DM} + V_{Stp2.i}^{DM} \tag{31}$$

It should be noted that Eqs. (30) and (31) give no indication of the degree of resolution between any additional solutes of interest.

When used as a method for increasing resolution, the two solutes of interest are both collected during the second step. In this way, they are subjected to a higher number of theoretical stages than if the separation had been run in classical mode in a single elution mode. A theoretical study determined which operating parameter relationships should be fulfilled in order for dual mode resolution to surpass that of classical mode [98]. However, the derived equations are based on equivalent separation durations in both operating modes, a restriction that does not allow for a thorough comparison. In a later theoretical study, the simpler and more general Eq. (32) was derived for determining dual mode resolution, R_S^{DM} [99].

$$R_S^{DM} = \sqrt{\frac{N V_{Stp1}^{DM}}{2}} \left(\sqrt{\frac{1}{V_{R,1}^{CM}}} - \sqrt{\frac{1}{V_{R,2}^{CM}}} \right) \tag{32}$$

Eq. (32) applies for two components of interest, 1 and 2, with $K_1 \leq K_2$ in the elution mode of the first step. $V_{R,i}^{CM}$ is the classical mode retention volume (Eq. (18)), also with respect to the elution mode of the first step. N is assumed to be the same for both components and in both elution modes. R_S^{DM} reaches its highest value when the elution mode switch is made just before the elution of component 1 at the outlet during the first step, i.e., $V_{Stp1}^{DM} = V_{R,1}^{CM}$. As mentioned in Section 3, in reality the peak width must be taken into account, meaning V_{Stp1}^{DM} should be slightly less than $V_{R,1}^{CM}$. A comparison with the resolution obtained in classical mode, R_S^{CM}, can be made using Eq. (20). Alternatively, by rearranging Eq. (32), the eluted mobile phase volume in the first step, V_{Stp1}^{DM}, can be determined for a required R_S^{DM}.

Dual mode can also be used as a screening technique [100,101]. As in the extrusion modes described in Section 3.2, the entire solute partition coefficient range from zero to infinity can be eluted from the column in a single run and with only 2 column volumes, $2V_C$. When one column volume of mobile phase is pumped in the first step ($V_{Stp1}^{DM} = V_C$), all solutes with $K_i \leq 1$ with respect to the first step elution mode will leave the column. All remaining solutes possessing $K_i \geq 1$ (or, with respect to the current elution mode after the switch, $K_i \leq 1$) will elute from the column during the second step after pumping an additional column volume of the corresponding mobile phase. In theory, any value of V_{Stp1}^{DM} may be used.

The corresponding dual mode retention volume needed to ensure elution of the entire partition coefficient spectrum, $V_{R,\infty}^{DM}$, equivalent to the cumulative mobile phase pumped during both steps is given by Eq. (33) [98].

$$V_{R,\infty}^{DM} = \frac{V_{Stp1}^{DM} - V_M + V_S}{V_{Stp1}^{DM} - V_M} V_{Stp1}^{DM} \tag{33}$$

As can be seen by setting $V_{Stp1}^{DM} = V_C$ in Eq. (33), $V_{R,\infty}^{DM}$ becomes $2V_C$, in accordance with the statement above. A minimum value of $V_{R,\infty}^{DM}$ (Eq. (34)) is obtained when Eq. (35) is fulfilled [98].

$$V_{R,\infty}^{DM} = V_S + V_M + 2\sqrt{V_S V_M} \tag{34}$$

$$V_{Stp1}^{DM} = V_S + \sqrt{V_S V_M} \tag{35}$$

To determine partition coefficients from the resulting dual mode chromatograms, the classical mode equation (Eq. (19)) can be applied for all solutes eluting from the column during the first step. For those solutes leaving the column during the second step, Eq. (36) can be used [102,103]

$$K_i = \frac{V_{Stp1}^{DM}}{V_{Stp2.i}^{DM}} \tag{36}$$

where $V_{Stp2.i}^{DM}$ is the retention volume of component i with respect to the second step only. The cumulative retention volume for the entire process is therefore given by Eq. (37).

$$V_{R,i}^{DM} = V_{Stp1}^{DM} + V_{Stp2.i}^{DM} \tag{37}$$

As previously mentioned, dual mode is preferred to elution extrusion for partition coefficient determination [81]. Dual mode also has the added benefit that, a "clean," equilibrated column is obtained at the end of a separation run when eluting the entire partition coefficient spectrum. There is then no need for new preparation of the column before beginning the next separation; only the elution mode must be switched.

3.3.2. Multiple dual mode

The improvement in resolution achieved in dual mode can be further extended by performing multiple cycles of elution mode switches (see Fig. 6) in multiple dual mode, first reported in [104]. Higher sample loadings can also be obtained. However, similar to closed-loop recycling mode (Section 3.1.3), the increase in resolution gained with additional cycles is limited by the competing increase in band broadening [104].

A variety of multiple dual mode process variations have been described in the literature. They differ in the location, duration, and frequency of sample injection, as well as in the manner of fraction collection. The sample is generally prepared in the mobile phase corresponding to the elution mode(s) it will be injected in. The site of injection may be at one end of the column (as depicted in Fig. 6) [99,104–111] or at an intermediate point along the

Multiple dual mode

Multiple consecutive dual mode cycles

As mode;
UP mobile

Des mode;
LP mobile
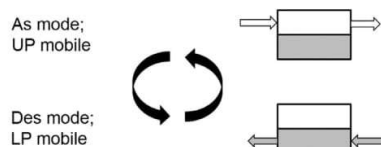
Fig. 6. Multiple dual mode, depicted for a single-column set-up. White shading: upper phase. Gray shading: lower phase.

set-up [112,113], located along the column itself or between two columns connected in series. When the injection is made from one end of the column, the sample can only be introduced in one elution mode. By performing the injection at an intermediate point along the set-up, the sample can be introduced in one or both elution modes. A single injection may be made at the start of the run [99,104–108,110,112,113], or injections can be repeated periodically during the process [104,109,111], generally at the start of each new cycle. The choice of injection type depends on the amount of feed to be processed and the solubility of the sample in the mobile phase(s). When only a small sample volume is to be treated, the simplest option is a single sample injection. On the other hand, when a large volume of feed should be processed or the feed components have low solubility in the mobile phase, periodically repeated injections may be preferred.

Different fraction collection schemes can also be implemented. When a single injection is performed, the solutes of interest may be subjected to multiple cycles without allowing their elution from the column to improve their resolution. They may then be collected in their entirety in a single step [99,106–108,110], or elute from the column split between the two steps of a cycle [109], resulting in recovery in two different mobile phases. This process variation is best combined with low injection volumes, leaving enough target solute-free volume inside the column to allow for sufficiently long step durations while avoiding target elution before the collection cycle. Alternatively, fractions of the solutes of interest may be collected alternately in one or both elution mode steps over multiple cycles [104,105,109–113]. The elution mode is switched before either stream becomes impure. This product collection strategy may be preferred at high column loadings, where attempting to prevent the solutes from eluting from the column as described above would result in very short step durations.

When injections are periodically repeated, the sample solutes from a single injection may be completely eluted in a single cycle, or fractions may be collected in both elution modes during in each cycle. In both cases, a cyclic steady-state (CSS) can be achieved. However, in the latter, several cycles are needed until CSS is reached.

Depending on the multiple dual mode variation selected, LLC set-ups of varying complexity are required. As previously mentioned, a single column or two columns connected in series may be used. The feed may be introduced over an injection valve or by pump at the corresponding inlet location. As in dual mode, the switch between the two elution modes is performed with a switching valve.

Several general guidelines for operating parameter selection in flow reversal modes have been given in the literature. These recommendations are also applicable for the continuous separation modes discussed in Section 3.4. In general, it is preferable to find a solvent system in which the solutes of interest have partition coefficients close to 1. This way, the duration of the As and Des steps will be similar, leading to similar solvent consumption in both elution modes [90,114]. When possible, preparing the column with a pre-set upper phase/lower phase ratio of 50/50 is also desirable, as this leads to the same S_f [115] and similar column efficiency in both modes when the flow rate is kept constant [90]. Additionally, step durations in both elution modes should be selected to be as long as possible to prevent excessive wear on the valves and to subject the solutes of interest to the maximum number of theoretical stages per cycle [90].

The step durations in multiple dual mode must be chosen to ensure that only the desired products elute from the column in each step. In [104,106–108] preliminary classical mode and/or single dual mode runs were performed to determine the elution step durations. Alternatively, step durations can be selected with the help of short-cut models, such as that appearing in [99]. This mul-

tiple dual mode short-cut model is an extension of that developed for single cycle dual mode operation in the same publication. The derived model is applicable to the full peak elution collection technique, where the solutes of interest are subjected to multiple cycles and do not elute from the column until satisfactory resolution is achieved. The solute bands leave the column in their entirety during a single step. The model is valid for the following specific case: two solutes, 1 and 2, with 1 having a lower partition coefficient in the first step elution mode; single injection at one end of the column; the second step of a cycle always returns component 2 to the initial injection site; both solutes eventually elute from the column during the second step of a cycle.

The eluted volume during the first step of any cycle, V_{Stp1}^{MDM}, is determined with Eq. (38) by defining a value $f > 1$, so that V_{Stp1}^{MDM} corresponds to a fraction $1/f$ of the classical mode retention volume of solute 1, $V_{R,1}^{CM}$ (see Eq. (18)). This ensures that neither solute elutes during the first step of the first cycle.

$$V_{Stp1}^{MDM} = \frac{V_{R,1}^{CM}}{f} \tag{38}$$

The selection of f represents a compromise between step durations and number of cycles. The higher the value of f, the shorter the step durations and the greater the number of cycles needed to reach a certain resolution.

To fulfill the requirement that solute 2 is returned to the site of injection at the end of the second step of each cycle, the eluted volume in the second step of every cycle is determined from Eq. (39)

$$V_{Stp2}^{MDM} = \frac{V_{R,1}^{CM}}{K_2} \tag{39}$$

where K_2 corresponds to the partition coefficient of solute 2 in the elution mode of the first step.

The total number of steps, m, needed to have solute 1 located at the column outlet at the end of the first step of a cycle can be calculated using Eq. (40).

$$m = \frac{2(f-1)K_2}{K_2 - K_1} + 1 \tag{40}$$

Having determined the total number of steps, m, the resolution of the two solutes at the time of their elution can be calculated by determining the peak variances as a function of the absolute cumulative distance traveled by each solute during the process, X_1 and X_2 Eqs. (41) and (42). The column length, L, appearing in the original equations has been eliminated by defining a dimensionless column length of 1.

$$X_1 = \frac{1}{f}\left(\frac{m-1}{2} + 1 + \frac{m-1}{2}\frac{V_{R,1}}{V_{R,2}}\right) \tag{41}$$

$$X_2 = m\frac{1}{f}\frac{V_{R,1}}{V_{R,2}} \tag{42}$$

The variance corresponding to Gaussian-shaped peaks with a width at base of 4σ can be expressed as Eq. (43).

$$\sigma_i = \sqrt{\frac{X_i}{N_i}} \tag{43}$$

The resolution for this variation of multiple dual mode, R_S^{MDM}, can then be predicted using Eq. (44).

$$R_S^{MDM} = \frac{1 - \frac{V_{R,1}}{fV_{R,2}}}{2(\sigma_1 + \sigma_2)} \tag{44}$$

A different set of short-cut model equations would be necessary for each possible multiple dual mode variation. Equations were derived for a second variation, namely sample injection at an intermediate point along the set-up, splitting it into two equal volumes

with the same phase ratio in each [107]. The model predicts in which elution mode a solute will elute under the given operating parameters using the net velocity in both modes, $v_{net,i}$, calculated with Eq. (45)

$$v_{net,i} = \frac{(1 + \beta)(F_{Des}t_{Des} - F_{As}t_{As}K_{Des,i})}{(1 + K_{Des,i}\beta)(t_{Des} + t_{As})} \quad (45)$$

where $t_{Des/As}$ is the step duration and $\beta = V_U/V_L$. The column cross-sectional area appearing in the original equations, A_C, has been eliminated by assigning it the dimensionless value of 1. The resulting sign of $v_{net,i}$ determines in which elution mode solute i will elute. When $v_{net,i} < 0$, i elutes in As mode, while $v_{net,i} > 0$ indicates elution in Des mode. A value of $v_{net,i} = 0$ signifies that i travels the same distance in each elution mode, resulting in a net movement of zero toward either end of the column and an infinite multiple dual mode retention time. When $v_{net,i} \neq 0$ the multiple dual mode retention time can be calculated using Eq. (46)

$$t_{R,i}^{MDM} = \frac{V_C}{2|v_{net,i}|} \quad (46)$$

where V_C is the total volume of the two columns in series. By dividing $t_{R,i}^{MDM}$ by the cycle time, equivalent to $t_{Des} + t_{As}$, the number of cycles until elution of i from the column can be estimated.

A generalized short-cut model approach that can be easily adapted to the different multiple dual mode variations is lacking in the literature. Ideally, this short-cut model would be able to predict step durations allowing for elution of the solutes in a desired elution mode and point during the run for a given set of operating parameters. Adaptable resolution equations would be helpful as well.

Several investigations further explored modeling of the multiple dual mode process [109–111,113], providing analytical solutions to the equilibrium cell model describing the peak concentration profiles for a wide range of process variations. Although the derived equations present a simple approach to modeling of multiple dual mode processes, they generally must be implemented in a coding environment. In [111], the possibility to use varying step durations from cycle to cycle to compensate for increasing band broadening during the process was demonstrated by simulations.

3.3.3. Trapping multiple dual mode

A variation of the multiple dual mode process, trapping multiple dual mode allows the separation of a sample mixture into three product streams and facilitates the isolation of intermediately-eluting target components, i.e., components possessing intermediate partition coefficients with respect to the rest of the sample solutes. Such a sample mixture can be most simply represented by three solutes of interest A, B, and C with $K_{Des,A} < K_{Des,B} < K_{Des,C}$ in Des mode and $K_{As,A} > K_{As,B} > K_{As,C}$ in As mode, with B as the intermediately-eluting target component. The alphabetical solute-naming convention is used here instead of the numerical one used previously in order to have an elution-mode specific description of the partition coefficients. By proper selection of the As and Des step durations, the intermediately-eluting component B remains "trapped" on the column while A and C are eluted from opposite column ends over multiple cycles. This strategy was first reported in [112] as a variation of intermittent countercurrent extraction (ICcE), described in Section 3.4.1. The trapping multiple dual mode process can be broken down into three stages:

- Stage 1: Column loading, during which the sample mixture is fed onto the column.
- Stage 2: Separation, consisting of multiple cycles of As and Des steps, during which components A and C are eluted from opposite ends of the column while the intermediately-eluting target remains "trapped" on the column.

- Stage 3: Recovery, during which the intermediately-eluting target B is collected. Stage 3 is started after sufficient elution of A and C from the column.

As in the multiple dual mode separations described in Section 3.3.2, feed introduction in trapping multiple dual mode can take place at the beginning of the process during a single dual mode cycle [116–118], periodically at the start of each cycle [114], or continuously over several cycles [112]. During the recovery stage, the target component may be obtained during an extended step in one elution mode [114,116–118] or, when working with CCC columns, by extruding the column contents using compressed air [112]. Extrusion by pumping the "wrong" mobile phase as in elution extrusion would also be an option. Although all reports of trapping multiple dual mode report the use of a set-up consisting of two columns connected in series with sample injection between them [112,114,116–118], use of a single column with sample injection from one end would also be possible. A schematic diagram for the two-column trapping multiple dual mode process with injection during a single dual mode cycle and target collection during a single extended elution step is found in Fig. 7. The general flow reversal mode process recommendations described in Section 3.3.2 are applicable to trapping multiple dual mode as well.

The selection of the As and Des step durations during the loading and separation stages is not trivial, as they are intrinsically linked to each other and determine the ability to effectively "trap" the intermediately-eluting target component B. In [116], short-cut model equations were derived for selection of the step durations as well as the number of cycles. The short-cut model is valid for the following set-up and process: single loading cycle with feed introduction between two-columns connected in series; during the loading cycle, only the feed solution is introduced without accompanying elution of pure mobile phase. The term L_C appearing in the equations in the original publication has been eliminated by defining a dimensionless column length of 1.

For use of the short-cut model equations, the position of the intermediately-eluting component B band front at the end of the loading, $x_{Des,B}^{load}$ and $x_{As,B}^{load}$, and separation steps, $x_{Des,B}^{sep}$ and $x_{As,B}^{sep}$, must be specified. The dimensionless position x_B is a fraction of the "length" of each column, with the inlet as the reference position $x_B = 0$ and all positions between the inlet and either outlet possessing a positive sign, with each of the outlets defined as position $x_B = 1$. Complete separation of components A and C from the target B is achieved when the following constraints on x_B Eqs. (47)–(49) are fulfilled in both elution modes. To simplify the initial process design, identical values for the band positions in the loading and separation stages may be selected, i.e., $x_{Des,B}^{load} = x_{As,B}^{load} = x_B^{load}$; $x_{Des,B}^{sep} = x_{As,B}^{sep} = x_B^{sep}$.

- During the column loading stage, B remains inside the columns.
$$0 \leq x_B^{load} \leq 1 \quad (47)$$

- During the separation stage, B remains inside the columns.
$$x_B^{load} \leq x_B^{sep} \leq 1 \quad (48)$$

- During the separation stage, B travels a net distance of zero during each cycle. (Exception: Cycle 1)
$$\Delta x_{B,Des}^{sep} - \Delta x_{B,As}^{sep} = 0 \quad (49)$$

Having defined values for x_B^{load} and x_B^{sep} in both elution modes, the step durations in the loading stage, t_{Des}^{load} and t_{As}^{load} (Eqs. (50) and (51)), and separation stage, t_{Des}^{sep} and t_{As}^{sep} (Eqs. (54)–(55)), can be calculated. For the duration of the first step of the first separation stage cycle, $t_{Des}^{sep,1st}$ or $t_{As}^{sep,1st}$, depending on the elution mode, Eq. (52) or (53) should be used, respectively. This first step is shorter in duration than all subsequent steps in the same elution

Trapping multiple dual mode

(1) Loading
Feed introduced during a single cycle
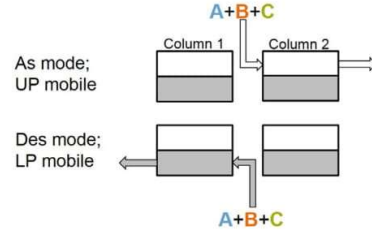
(2) Separation
Multiple cycles of As and Des steps
A elutes in Des mode, C in As mode
B remains trapped in columns
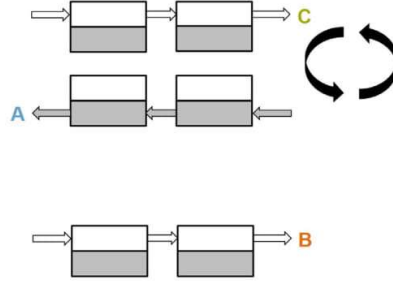
(3) Recovery
Collection of target B in a single step (As or Des)
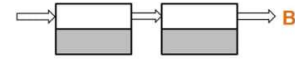
Fig. 7. Trapping multiple dual mode, depicted for a two-column set-up with loading between the columns during one cycle and recovery of the intermediately-eluting target B in As elution mode. $K_{As, A} > K_{As, B} > K_{As, C}$ and $K_{Des, A} < K_{Des, B} < K_{Des, C}$. White shading: upper phase. Gray shading: lower phase.

mode as a result of the injection of the sample in the middle of the two column set-up.

$$t_{Des}^{load} = x_{Des,B}^{load} \frac{V_L + K_{Des,B}V_U}{F_{Des}} \tag{50}$$

$$t_{As}^{load} = x_{As,B}^{load} \frac{V_U + K_{As,B}V_L}{F_{As}} \tag{51}$$

$$t_{Des}^{sep,1st} = \left(x_{Des,B}^{sep} - x_{Des,B}^{load}\right) \frac{V_L + K_{Des,B}V_U}{F_{Des}} \tag{52}$$

$$t_{As}^{sep,1st} = \left(x_{As,\ B}^{sep} - x_{As,B}^{load}\right) \frac{V_U + K_{As,B}V_L}{F_{As}} \tag{53}$$

$$t_{Des}^{sep} = \left[\left(x_{Des,B}^{sep} - x_{Des,B}^{load}\right) + \left(x_{As,B}^{sep} - x_{As,B}^{load}\right)\right] \frac{V_L + K_{Des,B}V_U}{F_{Des}} \tag{54}$$

$$t_{As}^{sep} = \left[\left(x_{Des,B}^{sep} - x_{Des,B}^{load}\right) + \left(x_{As,B}^{sep} - x_{As,B}^{load}\right)\right] \frac{V_U + K_{As,B}V_L}{F_{As}} \tag{55}$$

The short-cut model presented in [116] also provides equations for prediction of the number of Stage 2 (separation) cycles needed to completely elute components A and C from the column to obtain pure B in the recovery stage, n_A^{sep} and n_C^{sep}. The equations vary slightly depending on the first elution mode in each cycle. When the first elution mode is Des, Eqs. (56) and (58) are valid for components A and C, respectively. Eqs. (57) and (59) are valid when the first elution mode is As. n_A^{sep} and n_C^{sep} should be rounded up to the nearest integer. $v_{Des,i} = \frac{F_L}{V_L + K_{Des,i}V_U}$ is the velocity of component i in Des mode and $v_{As,i} = \frac{F_U}{V_U + K_{As,i}V_L}$ its corresponding velocity in As mode.

$$n_A^{sep} = \frac{\left(t_{Des}^{load} - t_{Des}^{sep,1st}\right)v_{Des,A} + t_{As}^{sep}v_{As,A} + 1}{t_{Des}^{sep}v_{Des,A} - t_{As}^{sep}v_{As,A}} + 1 \tag{56}$$

$$n_A^{sep} = \frac{\left(t_{Des}^{load} - t_{Des}^{sep}\right)v_{Des,A} + t_{As}^{sep,1st}v_{As,A} + 1}{t_{Des}^{sep}v_{Des,A} - t_{As}^{sep}v_{As,A}} + 1 \tag{57}$$

$$n_C^{sep} = \frac{\left(t_{As}^{load} + t_{As}^{sep}\right)v_{As,C} - t_{Des}^{sep,1st}v_{Des,C} + 1}{t_{As}^{sep}v_{As,C} - t_{Des}^{sep}v_{Des,C}} + 1 \tag{58}$$

$$n_C^{sep} = \frac{\left(t_{As}^{load} + t_{As}^{sep,1st}\right)v_{As,C} - t_{Des}^{sep}v_{Des,C} + 1}{t_{As}^{sep}v_{As,C} - t_{Des}^{sep}v_{Des,C}} + 1 \tag{59}$$

In [114], the trapping multiple dual mode step durations were selected by adaptation of the short-cut equations presented in [99] for multiple dual mode (addressed in Section 3.3.2). However, unlike Eqs. (50)–(59), those derived in [99] do not take into account the wide solute bands often encountered at high volume loadings, a condition under which the description of a solute band only by its retention volume and without regard for its width can in practice lead to incorrect estimates of step durations and impure product streams. Therefore, use of the short-cut equations from [116] is recommended, as the entire solute bands are considered.

Trapping multiple dual mode was found in [117] and [80,112] to outperform classical mode with respect to throughput for specific applications. A more thorough comparison of trapping multiple dual mode and classical mode was made with respect to productivity and for a wide range of separation factors and purity and yield requirements of B [118]. It was found that trapping multiple dual mode can extend the use of LLC methods down to separation factors as low as 1.1, with its use being most advantageous for separation factors between the target B and the components A and C around 1.3. At separation factors of 1.5, classical mode resulted in higher productivities with the exception of the highest purity and yield requirements (≥95%). For separation factors above 1.5, the simpler classical mode is preferred.

3.4. Continuous modes

Although batch mode separations are often the norm in industrial settings, continuous processes are preferred in the treatment of large feed volumes for their higher productivity and lower solvent consumption. As in the multi-column simulated moving bed (SMB) mode of liquid–solid chromatography, continuous separations can be achieved with LLC techniques as well. The continuous LLC separations are a further extension of the flow reversal modes described in Section 3.3. The concept for the LLC separation of a continuous feed stream into two or three (or more) product streams first appeared in a patent [119]. These binary and ternary (and higher) continuous separations are described in Sections 3.4.1 and 3.4.2, respectively.

3.4.1. Continuous binary separations

Continuous binary separation processes can be used to split a large feed volume into two product streams, foregoing the need for multiple batch separations. The separation is performed on a

Continuous binary separation (ICcE/sCPC)

Continuous cyclic process
Simultaneous introduction of feed and mobile phase
Collection of A in Des mode, B in As mode
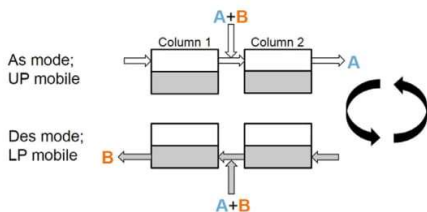
Fig. 8. Continuous binary separation (ICcE/sCPC), depicted for two-column set-up with loading between the columns. $K_{As,\,A} > K_{As,\,B}$ and $K_{Des,\,A} < K_{Des,\,B}$. White shading: upper phase. Gray shading: lower phase.

LLC set-up consisting of two columns connected in series with feed introduction between them. Two mobile phase pumps as well as two feed pumps are generally required. As in multiple dual mode (Section 3.3.2), multiple cycles each consisting of two steps in different elution modes are performed, one in As mode and the other in Des mode. The feed mixture is continuously introduced dissolved in the mobile phase corresponding to the current elution mode. Meanwhile, the corresponding pure mobile phase is introduced at the column inlet appropriate for the flow direction. The net flow rate in the column downstream of the feed introduction point is therefore the combined flow rates of the pure mobile phase and the feed stream. The target component should possess the highest or lowest partition coefficient relative to the other solutes of the feed mixture, allowing it to elute fastest from the column in one of the two elution modes and be collected in pure form. The As and Des step durations must therefore be selected so that the elution mode switches are made before the target product stream becomes impure. A schematic diagram of the process is found in Fig. 8 for the simplest case of a binary feed mixture of components A and B with $K_{Des,\,A} < K_{Des,\,B}$ and $K_{As,\,A} > K_{As,\,B}$. A is collected in Des mode, and B is collected from the opposite end of the set-up in As mode.

As is characteristic of such cyclic continuous processes, a cyclic steady-state (CSS) is eventually reached following an initial start-up phase. Under CSS conditions, the elution profiles obtained during the As and Des steps are identical from one cycle to the next. Continuous binary LLC separations have been reported for CCC columns, first mentioned in [112] and referred to as intermittent countercurrent extraction (ICcE), as well as for CPC columns, first described in a patent [119] and later referred to in a publication as sequential centrifugal partition chromatography (sCPC) [90]. However, only in the sCPC publications were CSS conditions achieved [20,90,120,121]. Those reports utilizing ICcE columns did not continuously introduce the feed for the entirety of the separation run [107,112,115,122–125]. With the exception of possibly [125], CSS was not reached, rendering these separations to be closer to resembling quasi-continuous multiple dual mode batch processes. Nonetheless, it was recognized by that prolonged introduction of the feed would eventually lead to CSS conditions [125].

To maintain operation at CSS conditions for the prolonged process durations demanded by continuous separations, the ICcE/sCPC operating parameters must be selected to ensure process stability, namely maintenance of a constant phase ratio. The general flow reversal mode design guidelines presented in Section 3.3.2 for multiple dual mode should be followed, i.e., solvent system providing target partition coefficients close to 1, pre-set phase ratio of 50/50, and long step durations. Additionally, it is recommended to operate

at the maximum net flow rate allowing maintenance of the pre-set phase ratio in order to have a high column efficiency as well as to allow the use of a higher feed flow rate [116].

For selection of the step durations, t_{Des} and t_{As}, and the flow rates of the mobile phase, F_{Des} and F_{As}, and feed, $F_{Des,\,feed}$ and $F_{As,\,feed}$, that satisfy the limits of the maximum allowable net flow rate in the As and Des modes, two short-cut model approaches have been presented in the literature. In the first [107], equation Eq. (45) was derived to determine from which end of the column, i.e., in which elution mode, a given component will elute according to the sign of its net velocity in the two elution modes. This equation was previously presented in the discussion of multiple dual mode (Section 3.3.2) but is also applicable to continuous binary separations. When two components have velocities with opposite signs, they will be completely separated and elute from opposite ends of the column. A drawback of this approach is that it requires the As and Des step durations as input values. From a design perspective, it would be preferable to first fix the flow rates instead, as they are subject to the physical limitations of the system, and then afterward determine the step duration combinations resulting in a complete binary separation. This was the approach taken in [126].

The second short-cut model presented in [126] provides a systematic approach to the selection of the ICcE/sCPC operating parameters and can be considered analogous to triangle theory used for the design of continuous binary liquid–solid chromatography separations with SMB technology. To obtain complete separation of components A and B, the following process restrictions represented by Eqs. (60)–(63) must be fulfilled:

- At the end of each Des step, B has not eluted from Column 1

$$t_{Des} < \frac{V_L + K_{Des,B}V_U}{F_{Des} + F_{Des,\,feed}} \qquad (60)$$

- At the end of each As step, B is completely eluted from Column 1

$$\frac{t_{Des}}{t_{As}} < \frac{F_{As}}{F_{Des} + F_{Des,\,feed}}K_{Des,B} \qquad (61)$$

- At the end of the As step, A has not eluted from Column 2

$$t_{As} < \frac{V_U + K_{As,A}V_L}{F_{As} + F_{As,\,feed}} \qquad (62)$$

- At the end of the Des step, A is completely eluted from Column 2

$$\frac{t_{Des}}{t_{As}} < \frac{F_{As} + F_{As,\,feed}}{F_{Des}}K_{Des,A} \qquad (63)$$

For certain parameter combinations (K, V, F), plotting the constraining equations Eqs. (60)–(63) in a t_{As} vs. t_{Des} diagram results in a region of complete separation (see example in Fig. 9). Under the ideal assumptions applicable for all short-cut models described in Section 3, all t_{Des}, t_{As} pairs found within this region will result in two pure product streams and complete recovery of A and B. The existence of a region of complete separation for a certain set of flow rates and partition coefficients can be confirmed using Eq. (64), obtained from Eqs. (61) and (63) [126]. The effects of values of the mobile phase and feed flow rates on the size and shape of the region of complete separation are demonstrated and discussed in [121].

$$\frac{\left(F_{As} + F_{As,\,feed}\right)\left(F_{Des} + F_{Des,\,feed}\right)}{F_{Des}F_{As}} \leq \frac{K_{Des,B}}{K_{Des,A}} \qquad (64)$$

After the existence of a region of complete separation has been established, a t_{Des}, t_{As} pair is selected. It is recommended that the

146
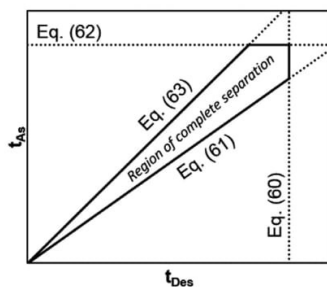
Fig. 9. Plot of constraining equations, continuous binary separation (ICcE/sCPC) short-cut model. Region of t_{Des}, t_{As} pairs resulting in complete separation of components A and B under ideal conditions.

point be located far from the origin and not too close to the region borders, accounting for the fact that band broadening effects shrink the effective area of the region of complete separation under non-ideal conditions and that fluctuations in the operating parameters, e.g., flow rates, phase ratio, as well as inaccuracies in measured partition coefficients shift the region borders [121].

Successful implementation of the short-cut model presented in [126] (Eqs. (60)–(63)) has been demonstrated experimentally in [90,120,121] for binary mixtures of model solutes with separation factors as low as 1.3 [121]. A further study demonstrated the ability to use the short-cut model for the fractionation of a mixture of four model solutes (A, B, C, and D) in three different ways: A and B, C, D; A, B and C, D; and A, B, C and D [116]. Each was viewed as

a pseudo-binary separation, demonstrating the applicability of the short-cut method for the separation of complex multi-component mixtures into two product streams at a desired split point. This same study addressed throughput maximization and presented a detailed approach for identification of the maximum feed concentration.

A thorough comparison of ICcE/sCPC continuous binary separations with alternative semi-continuous operating modes, e.g., stacked batch injections or multiple dual mode, is currently lacking in the literature, but would be helpful in assisting the user in which operating mode to select with respect to the properties of the feed mixture and the amount of feed to be processed. Such a study would also assist in determining if the investment in the more complex equipment needed for ICcE/sCPC separations is economically sound. Additionally, it has been acknowledged that preset phase ratios other than 50/50 may be used, corresponding to different stationary phase fractions in the two elution modes, provided that the flow rates for maintaining this constant phase ratio are selected in both modes [126]. However, the cases for which this would provide an advantage for the process have yet to be identified.

### 3.4.2. Cascades for multi-component separations

As previously mentioned, target components are often present in complex multi-component mixtures and possess intermediate partition coefficient values. For such targets, continuous separation with a single binary separation step is not possible without pre-treatment of the feed. For the continuous production of three product streams, it has been suggested to connect two continuous


Fig. 10. Continuous cascade for ternary separation, depicted for separation of A from B and C in first stage and B from C in second stage. $K_{As, A} > K_{As, B} > K_{As, C}$ and $K_{Des, A} < K_{Des, B} < K_{Des, C}$. White shading: upper phase. Gray shading: lower phase.
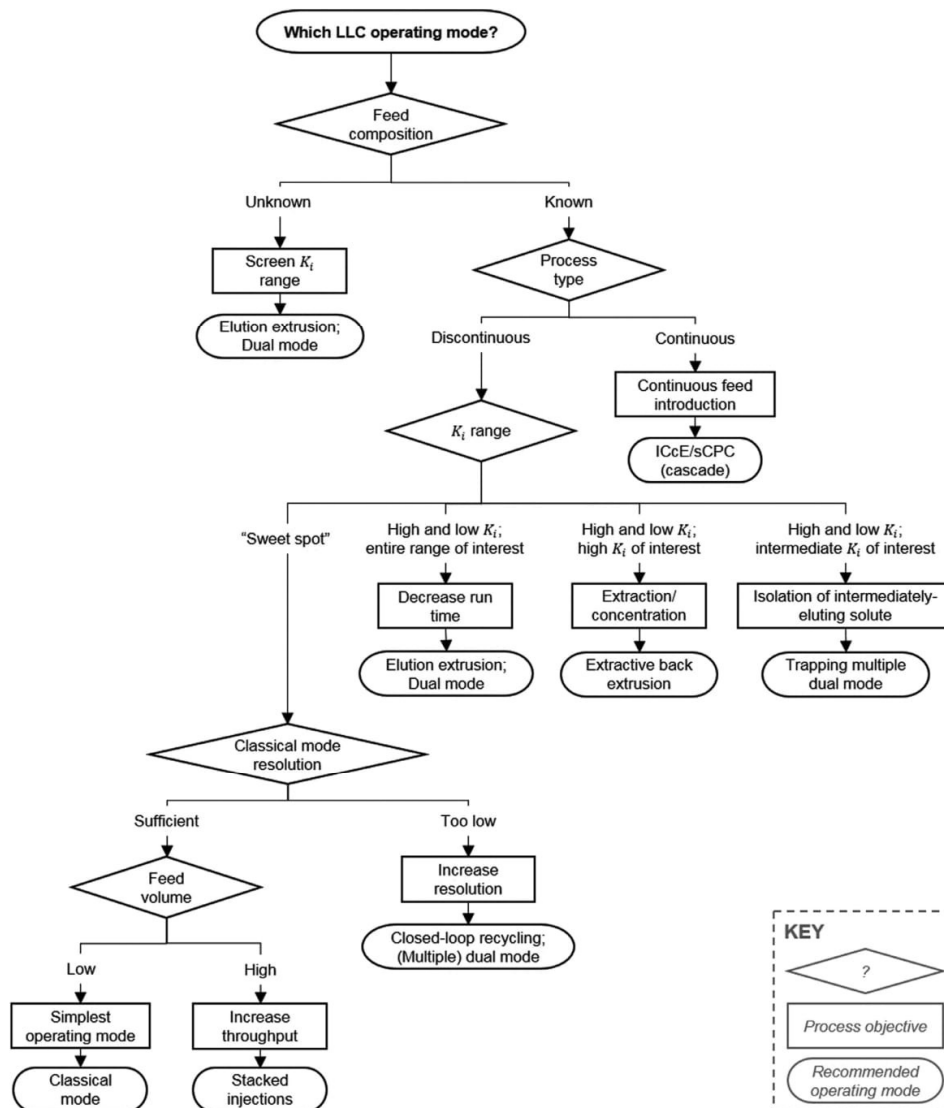
Fig. 11. Flow diagram for LLC operating mode selection.

binary ICcE/sCPC separations in series. One product stream from the first unit is used as the feed for the second, further fractionating it into two more product streams [119]. A schematic diagram of the process is depicted in Fig. 10. This cascade approach can be applied to higher separations of k components by using $k-1$ continuous binary separation units. Continuous multi-component separations using LLC technology have yet to be reported in the literature.

The inclusion of additional binary separation units quickly increases the complexity of the design of the overall process. In addition to the interdependent operating parameters described in Section 3.4.1 that must be chosen for each stage of the cascade, a number of other design challenges must also be addressed. For example, as one product stream from the first stage becomes the feed stream for the second separation stage, it would be necessary to take into account the step durations in both stages to ensure a

steady flow of feed to the second stage. The use of a buffer tank between the stages should be considered. Additionally, the product concentration should be taken into account, as the unavoidable dilution of the feed solution by the mobile phase at the point of feed introduction would become further pronounced during the second separation stage. This may necessitate the use of a concentration step before the second separation stage with, e.g., an organic solvent nanofiltration membrane process. The development of such separations would be especially interesting for industrial applications

4. Conclusion

As the result of the presence of a liquid stationary phase, LLC exhibits very high process flexibility. In addition to several operating modes with analogous implementations in liquid–solid

chromatography (Section 3.1 Classical mode and variations), LLC also possesses a wide variety of additional operating modes unique to the technology. These are based on the ability to extrude one phase from the column with the other (Section 3.2 Extrusion modes) or the possibility of switching the roles of the mobile and stationary phases during operating (Section 3.3 Flow reversal modes, Section 3.4 Continuous separation modes).

Simple classical mode separations are best-suited to mixtures with solutes possessing partition coefficients in the "sweet spot" range and separation factors greater than 1.5. The classical mode variations of stacked injections and closed-loop recycling can be used to increase feed throughput and increase resolution, respectively. Both are most effective for mixtures consisting of a few solutes with similar partition coefficients.

Extrusion modes are useful when working with sample mixtures possessing a wide range of partition coefficients. Both elution extrusion and back extrusion can be used to elute the entire partition coefficient spectrum from zero to infinity, making them useful as both a screening method and a means of reducing separation run duration. Elution extrusion is generally preferable, due to the absence of the echo peak effect encountered in back extrusion and the fact that the column is completely filled with stationary phase at the end of the run, ready for the next equilibration and injection. Extractive back extrusion can alternatively be used for the separation of highly retained components from large feed volumes. The target solute partitions nearly exclusively in the stationary phase, which is then extruded from the column for recovery.

The flow reversal modes create a virtual lengthening of the column. Single cycle dual mode separations can be used to improve resolution as well as perform sample screening. Similar to the extrusion modes, the entire partition coefficient spectrum can be quickly eluted from the column. Compared to single cycle dual mode, multiple dual mode makes it possible to further improve resolution and/or treat larger sample volumes. An intermediately-eluting component can be isolated using trapping multiple dual mode. Continuous separations based on flow reversal can be applied for the separation of large volumes of binary feed mixtures. By connecting two (or more) binary separation units in series, ternary (or higher) continuous separations also become possible. Multi-component continuous separations have yet to be explored in the literature.

The available short-cut models and simple equations for preliminary operating parameter selection have been presented and critiqued. A flow diagram for LLC operating mode selection summarizing key characteristics and areas of application is found in Fig. 11. The information contained in this review will hopefully help serve as a preliminary guide to operating mode and operating parameter selection in LLC. Various gaps in the available LLC literature have been identified and show that there is a clear need for thorough operating mode comparison studies performed for a wide range of different separation tasks and operating parameter ranges. Detailed simulation studies and numerical optimization methods will likely play a key role in achieving this.

Declaration of Competing Interest

The authors declare that they have no known competing financial interests or personal relationships that could have appeared to influence the work reported in this paper.

References

[1] Y. Ito, Golden rules and pitfalls in selecting optimum conditions for high-speed counter-current chromatography, J. Chromatogr. A 1065 (2005) 145–168.

[2] A. Berthod, Countercurrent chromatography and the journal of liquid chromatography: a love story, J. Liq. Chromatogr. Related Technol. 30 (2007) 1447–1463.

[3] G.F. Pauli, S.M. Pro, J.B. Friesen, Countercurrent separation of natural products, J. Nat. Prod. 71 (2008) 1489–1508.

[4] J.B. Friesen, J.B. McAlpine, S.N. Chen, G.F. Pauli, Countercurrent separation of natural products: an update, J. Nat. Prod. 78 (2015) 1765–1796.

[5] A. Marston, I. Slacanin, K. Hostettmann, Some new developments in centrifugal partition chromatography and applications in the separation of natural-products, J. Liq. Chromatogr. 13 (1990) 3615–3624.

[6] D.P. Ward, P. Hewitson, M. Cardenas-Fernandez, C. Hamley-Bennett, A. Diaz-Rodriguez, N. Douillet, J.P. Adams, D.J. Leak, S. Ignatova, G.J. Lye, Centrifugal partition chromatography in a biorefinery context: optimisation and scale-up of monosaccharide fractionation from hydrolysed sugar beet pulp, J. Chromatogr. A 1497 (2017) 56–63.

[7] D. Thornton, X. Yang, L. Hsu, Automated countercurrent chromatography method development and process scale-up at GlaxoSmithKline, J. Chromatogr. A 1487 (2017) 129–138.

[8] I. Sutherland, C. Thickitt, N. Douillet, K. Freebairn, D. Johns, C. Mountain, P. Wood, N. Edwards, D. Rooke, G. Harris, D. Keay, B. Mathews, R. Brown, I. Garrard, P. Hewitson, S. Ignatova, Scalable technology for the extraction of pharmaceutics: outcomes from a 3 year collaborative industry/academia research programme, J. Chromatogr. A 1282 (2013) 84–94.

[9] I.A. Sutherland, Recent progress on the industrial scale-up of counter-current chromatography, J. Chromatogr. A 1151 (2007) 6–13.

[10] J.B. Friesen, G.F. Pauli, GUESS - A generally useful estimate of solvent systems in CCC, J. Liq. Chromatogr. Related Technol 28 (2005) 2777–2806.

[11] Y.B. Lu, A. Berthod, R.L. Hu, W.Y. Ma, Y.J. Pan, Screening of complex natural extracts by countercurrent chromatography using a parallel protocol, Anal. Chem. 81 (2009) 4048–4059.

[12] J.B. Friesen, G.F. Pauli, Performance characteristics of countercurrent separation in analysis of natural products of agricultural significance, J. Agric. Food Chem. 56 (2008) 19–28.

[13] Y.J. Liu, P.Q. Kuang, S.F. Guo, Q. Sun, T. Xue, H.G. Li, An overview of recent progress in solvent systems, additives and modifiers of counter current chromatography, New J. Chem. 42 (2018) 6584–6600.

[14] A. Frey, E. Hopmann, M. Minceva, Selection of biphasic liquid systems in liquid-liquid chromatography using predictive thermodynamic models, Chem. Eng. Technol. 37 (2014) 1663–1674.

[15] E. Hopmann, W. Arlt, M. Minceva, Solvent system selection in counter-current chromatography using conductor-like screening model for real solvents, J. Chromatogr. A 1218 (2011) 242–250.

[16] E. Hopmann, A. Frey, M. Minceva, A priori selection of the mobile and stationary phase in centrifugal partition chromatography and counter-current chromatography, J. Chromatogr. A 1238 (2012) 68–76.

[17] Z.C. Li, Y.J. Zhou, F.M. Chen, L. Zhang, Y. Yang, Property calculation and prediction for selecting solvent systems in CCC, J. Liq. Chromatogr. Related Technol. 26 (2003) 1397–1415.

[18] L. Marchal, O. Intes, A. Foucault, J. Legrand, J.M. Nuzillard, J.H. Renault, Rational improvement of centrifugal partition chromatographic settings for the production of 5-n-alkylresorcinols from wheat bran lipid extract. I. Flooding conditions-optimizing the injection step, J. Chromatogr. A 1005 (2003) 51–62.

[19] A.H. Peng, P. Hewitson, H.Y. Ye, L.S. Zu, I. Garrard, I. Sutherland, L.J. Chen, S. Ignatova, Sample injection injection strategy to increase throughput in counter-current chromatography: case study of Honokiol purification, J. Chromatogr. A 1476 (2016) 19–24.

[20] J. Goll, M. Minceva, Continuous fractionation of multicomponent mixtures with sequential centrifugal partition chromatography, AIChE J. 63 (2017) 1659–1673.

[21] A. Berthod, Separation with a liquid stationary-phase – the countercurrent chromatography technique, Instrum. Sci. Technol. 23 (1995) 75–89.

[22] W.D. Conway, Y. Ito, Resolution in countercurrent chromatography, J. Liq. Chromatogr. 8 (1985) 2195–2207.

[23] O. Bousquet, A.P. Foucault, F. Legoffic, Efficiency and resolution in countercurrent chromatography, J. Liq. Chromatogr. 14 (1991) 3343–3363.

[24] A.P. Foucault, O. Bousquet, F. Legoffic, Importance of the parameter Vm/Vc in countercurrent chromatography – tentative comparison between instrument designs, J. Liq. Chromatogr. 15 (1992) 2691–2706.

[25] A. Berthod, B. Billardello, Test to evaluate countercurrent chromatographs-liquid stationary phase retention and chromatographic resolution, J. Chromatogr. A 902 (2000) 323–335.

[26] L. Marchal, A. Foucault, G. Patissier, J.M. Rosant, J. Legrand, Influence of flow patterns on chromatographic efficiency in centrifugal partition chromatography, J. Chromatogr. A 869 (2000) 339–352.

[27] L. Marchal, J. Legrand, A. Foucault, Mass transport and flow regimes in centrifugal partition chromatography, AIChE J. 48 (2002) 1692–1704.

[28] S. Adelmann, G. Schembecker, Influence of physical properties and operating parameters on hydrodynamics in centrifugal partition chromatography, J. Chromatogr. A 1218 (2011) 5401–5413.

[29] S. Chollet, L. Marchal, J. Meucci, J.H. Renault, J. Legrand, A. Foucault, Methodology for optimally sized centrifugal partition chromatography columns, J. Chromatogr. A 1388 (2015) 174–183.

[30] N. Fumat, A. Berthod, K. Faure, Effect of operating parameters on a centrifugal partition chromatography separation, J. Chromatogr. A 1474 (2016) 47–58.

[31] B.A. Bidlingmeyer, F.V. Warren, Column efficiency measurement, Anal. Chem. 56 (1984) A583.

[32] Preparative Chromatography, 2nd ed., Wiley-VCH Verlag & Co., Germany, 2012.

[33] J.B. Friesen, G.F. Pauli, Binary concepts and standardization in counter-current separation technology, J. Chromatogr. A 1216 (2009) 4237–4244.

[34] A. Berthod, D.W. Armstrong, Centrifugal partition chromatography. 1. General features, J. Liq. Chromatogr. 11 (1988) 547–566.

[35] A. Berthod, D.W. Armstrong, Centrifugal partition chromatography. 2. Selectivity and efficiency, J. Liq. Chromatogr. 11 (1988) 567–583.

[36] E. Bouju, A. Berthod, K. Faure, Scale-up in centrifugal partition chromatography: the "free-space between peaks" method, J. Chromatogr. A 1409 (2015) 70–78.

[37] K. Hostettmann, A. Marston, Countercurrent chromatography in the preparative separation of plant-derived natural products, J. Liq. Chromatogr. Related Technol. 24 (2001) 1711–1721.

[38] J.S. Jeon, C.L. Park, A.S. Syed, Y.M. Kim, I.J. Cho, C.Y. Kim, Preparative separation of sesamin and sesamolin from defatted sesame meal via centrifugal partition chromatography with consecutive sample injection, J. Chromatogr. B 1011 (2016) 108–113.

[39] Y.F. He, C.X. Ding, X.Y. Wang, H.L. Wang, Y.R. Suo, Using response surface methodology to optimize countercurrent chromatographic separation of polyphenol compounds from Fenugreek (*Trigonella foenum-graecum* L.) seeds, J. Liq. Chromatogr. Related Technol. 38 (2015) 29–35.

[40] Y.H. Guan, P. Hewitson, R.N.A.M. van den Heuvel, Y. Zhao, R.P.G. Siebers, Y.P. Zhuang, I. Sutherland, Scale-up protein separation on stainless steel wide bore toroidal columns in the type-J counter-current chromatography, J. Chromatogr. A 1424 (2015) 102–110.

[41] X. Tong, T. Zhou, X.H. Xiao, G.K. Li, A consecutive preparation method based upon accelerated solvent extraction and high-speed counter-current chromatography for isolation of aesculin from *Cortex fraxinus*, J. Sep. Sci. 35 (2012) 3609–3614.

[42] K. He, X.L. Ye, X.G. Li, H.Y. Chen, L.J. Yuan, Y.F. Deng, X. Chen, X.D. Li, Separation of two constituents from purple sweet potato by combination of silica gel column and high-speed counter-current chromatography, J. Chromatogr. B 881–882 (2012) 49–54.

[43] X.L. Cao, Y. Tian, T.Y. Zhang, Y. Ito, Semi-preparative separation and purification of taxol analogs by high-speed countercurrent chromatography, Prep. Biochem. Biotech. 28 (1998) 79–87.

[44] J.-Y. Zhou, Q.-C. Fang, Y.-W. Lee, The application of high-speed counter-current chromatography to the semipreparative separation of vincamine and vincine, Phytochem. Anal. 1 (1990) 74–76.

[45] A.E. Kostanyan, On influence of sample loading conditions on peak shape and separation efficiency in preparative isocratic counter-current chromatography, J. Chromatogr. A 1254 (2012) 71–77.

[46] C.X. Zhao, C.H. He, Sample capacity in preparative high-speed counter-current chromatography, J. Chromatogr. A 1146 (2007) 186–192.

[47] J. Meng, Z. Yang, J.L. Liang, M.Z. Guo, S.H. Wu, Multi-channel recycling counter-current chromatography for natural product isolation: tanshinones as examples, J. Chromatogr. A 1327 (2014) 27–38.

[48] Q. Bin Han, J.Z. Song, C.F. Qiao, L. Wong, H.X. Xu, Preparative separation of gambogic acid and its C-2 epimer using recycling high-speed counter-current chromatography, J. Chromatogr. A 1127 (2006) 298–301.

[49] S.Q. Tong, Y.X. Guan, J.Z. Yan, B. Zheng, L.Y. Zhao, Enantiomeric separation of (R, S)-naproxen by recycling high speed counter-current chromatography with hydroxypropyl-beta-cyclodextrin as chiral selector, J. Chromatogr. A 1218 (2011) 5434–5440.

[50] A.E. Kostanyan, Modeling of closed-loop recycling liquid-liquid chromatography: analytical solutions and model analysis, J. Chromatogr. A 1406 (2015) 156–164.

[51] A.E. Kostanyan, Simple equations to simulate closed-loop recycling liquid-liquid chromatography: ideal and non-ideal recycling models, J. Chromatogr. A 1423 (2015) 71–78.

[52] A.E. Kostanyan, Modeling of preparative closed-loop recycling liquid-liquid chromatography with specified duration of sample loading, J. Chromatogr. A 1471 (2016) 94–101.

[53] A.E. Kostanyan, A.A. Erastov, Theoretical study of closed-loop recycling liquid-liquid chromatography and experimental verification of the theory, J. Chromatogr. A 1462 (2016) 55–62.

[54] A.E. Kostanyan, Theoretical study of separation and concentration of solutes by closed-loop recycling liquid chromatography with multiple sample injection, J. Chromatogr. A 1506 (2017) 82–92.

[55] A. Kostanyan, M. Martynova, A. Erastov, V. Belova, Simultaneous concentration and separation of target compounds from multicomponent mixtures by closed-loop recycling countercurrent chromatography, J. Chromatogr. A 1560 (2018) 26–34.

[56] A.E. Kostanyan, V.V. Belova, Closed-loop recycling dual-mode counter-current chromatography. a theoretical study, J. Chromatogr. A 1588 (2019) 174–179.

[57] Q.Z. Du, C.Q. Ke, Y. Ito, Recycling high-speed countercurrent chromatography for separation of taxol and cephalomannine, J. Liq. Chromatogr. Related Technol. 21 (1998) 157–162.

[58] M. Martin, F. Verillon, C. Eon, G. Guiochon, Theoretical and experimental-study of recycling in high-performance liquid-chromatography, J. Chromatogr. 125 (1976) 17–41.

[59] B. Coq, G. Cretier, J.L. Rocca, J. Vialle, Recycling technique in preparative liquid-chromatography, J. Liq. Chromatogr. 4 (1981) 237–249.

[60] P. Scherpian, G. Schembecker, Scaling-up recycling chromatography, Chem. Eng. Sci. 64 (2009) 4068–4080.

[61] A. Seidel-Morgenstern, G. Guiochon, Theoretical-study of recycling in preparative chromatography, AIChE J. 39 (1993) 809–819.

[62] J. Xie, J. Deng, F. Tan, J. Su, Separation and purification of echinacoside from *Penstemon barbatus* (Can.) Roth by recycling high-speed counter-current chromatography, J. Chromatogr. B 878 (2010) 2665–2668.

[63] S.Y. Shi, Y.J. Ma, Y.P. Zhang, L.L. Liu, Q. Liu, M.J. Peng, X. Xiong, Systematic separation and purification of 18 antioxidants from *Pueraria lobata* flower using HSCCC target-guided by DPPH-HPLC experiment, Sep. Purif. Technol. 89 (2012) 225–233.

[64] J.H. Yang, H.Y. Ye, H.J. Lai, S.C. Li, S.C. He, S.J. Zhong, L.J. Chen, A.H. Peng, Separation of anthraquinone compounds from the seed of *Cassia obtusifolia* L. using recycling counter-current chromatography, J. Sep. Sci. 35 (2012) 256–262.

[65] Q. Liu, H.L. Zeng, S.J. Jiang, L. Zhang, F.Z. Yang, X.Q. Chen, H. Yang, Separation of polyphenols from leaves of *Malus hupehensis* (Pamp.) Rehder by off-line two-dimensional high speed counter-current chromatography combined with recycling elution mode, Food Chem. 186 (2015) 139–145.

[66] J.M. He, S.Y. Zhang, Q. Mu, Online-storage recycling counter-current chromatography for preparative isolation of naphthaquinones from *Arnebia euchroma* (Royle) Johnst, J. Chromatogr. A 1464 (2016) 79–86.

[67] V. Belova, Separation and concentration of rare earths by recycling liquid-liquid chromatography with multiple sample injection: a computational study, Russ. J. Inorg. Chem. 63 (2018) 473–478.

[68] A. Berthod, M.J. Ruiz-Angel, S. Carda-Broch, Elution-extrusion countercurrent chromatography. Use of the liquid nature of the stationary phase to extend the hydrophobicity window, Anal. Chem. 75 (2003) 5886–5894.

[69] A. Berthod, M. Hassoun, G. Harris, Using the liquid nature of the stationary phase: the elution-extrusion method, J. Liq. Chromatogr. Related Technol. 28 (2005) 1851–1866.

[70] A. Berthod, J.B. Friesen, T. Inui, G.F. Pauli, Elution-extrusion countercurrent chromatography: theory and concepts in metabolic analysis, Anal. Chem. 79 (2007) 3371–3382.

[71] A. Berthod, Band broadening inside the chromatographic column: the interest of a liquid stationary phase, J. Chromatogr. A 1126 (2006) 347–356.

[72] Y.B. Lu, R. Liu, A. Berthod, Y.J. Pan, Rapid screening of bioactive components from *Zingiber cassumunar* using elution-extrusion counter-current chromatography, J. Chromatogr. A 1181 (2008) 33–44.

[73] S.C. Li, S.C. He, S.J. Zhong, X.M. Duan, H.Y. Ye, J. Shi, A.H. Peng, L.J. Chen, Elution-extrusion counter-current chromatography separation of five bioactive compounds from *Dendrobium chrysototxum* Lindl, J. Chromatogr. A 1218 (2011) 3124–3128.

[74] R.L. Hu, Y.B. Lu, X.J. Dai, Y.J. Pan, Screening of antioxidant phenolic compounds in Chinese Rhubarb combining fast counter-current chromatography fractionation and liquid chromatography/mass spectrometry analysis, J. Sep. Sci. 33 (2010) 1595–1603.

[75] J. Bradow, F. Riley, L. Philippe, Q. Yan, B. Schuff, G.H. Harris, Automated solvent system screening for the preparative countercurrent chromatography of pharmaceutical discovery compounds, J. Sep. Sci. 38 (2015) 3983–3991.

[76] Z. Chen, J.B. Wu, W. Shen, P. Liu, Y. Cao, Y.B. Lu, Counter-current chromatographic method for preparative scale isolation of picrosides from traditional Chinese medicine *Picrorhiza scrophulariiflora*, J. Sep. Sci. 34 (2011) 1910–1916.

[77] D.B. Ren, Y.H. Qin, Y.H. Yun, H.M. Lu, X.Q. Chen, Y.Z. Liang, Separation of nine compounds from *Salvia plebeia* R.Br. using two-step high-speed counter-current chromatography with different elution modes, J. Sep. Sci. 37 (2014) 2118–2125.

[78] C. Napolitano, M. Wismer, E. Furlano, G. Harris, B. Uhrig, K. Blake, G. Kath, C. Dufresne, An in-house built semiautomated countercurrent chromatography workstation, JALA-J. Assoc. Lab. Aut. 14 (2009) 27–35.

[79] D.F. Wu, X.J. Cao, S.H. Wu, Overlapping elution-extrusion counter-current chromatography: a novel method for efficient purification of natural cytotoxic andrographolides from *Andrographis paniculata*, J. Chromatogr. A 1223 (2012) 53–63.

[80] H.Y. Ye, S. Ignatova, H.D. Luo, Y.F. Li, A.H. Peng, L.J. Chen, I. Sutherland, Preparative separation of a terpenoid and alkaloids from *Tripterygium wilfordii* Hook. f. using high-performance counter-current chromatography comparison of various elution and operating strategies, J. Chromatogr. A 1213 (2008) 145–153.

[81] A. Berthod, S. Carda-Broch, Determination of liquid-liquid partition coefficients by separation methods, J. Chromatogr. A 1037 (2004) 3–14.

[82] Y.B. Lu, Y.J. Pan, A. Berthod, Using the liquid nature of the stationary phase in counter-current chromatography. V. The back-extrusion method, J. Chromatogr. A 1189 (2008) 10–18.

[83] Y.B. Lu, W.Y. Ma, R.L. Hu, A. Berthod, Y.J. Pan, Rapid and preparative separation of traditional Chinese medicine *Evodia rutaecarpa* employing elution-extrusion and back-extrusion counter-current chromatography: comparative study, J. Chromatogr. A 1216 (2009) 4140–4146.

[84] A. Berthod, Y.I. Han, D.W. Armstrong, Centrifugal partition chromatography. 5. Octanol-water partition-coefficients, direct and indirect determination, J. Liq. Chromatogr. 11 (1988) 1441–1456.

[85] R.A. Menges, T.S. Menges, G.L. Bertrand, D.W. Armstrong, L.A. Spino, Extraction of nonionic surfactans from waste-water using centrifugal partition chromatography, J. Liq. Chromatogr. 15 (1992) 2909–2925.

[86] J. Pruvost, J. Legrand, A. Foucault, Method for the intensive extraction of cellular compounds from micro-organisms by continuous culture and extraction, and corresponding device, United States, 2014.

[31] B.A. Bidlingmeyer, F.V. Warren, Column efficiency measurement, Anal. Chem. 56 (1984) A583.

[32] Preparative Chromatography, 2nd ed., Wiley-VCH Verlag & Co., Germany, 2012.

[33] J.B. Friesen, G.F. Pauli, Binary concepts and standardization in counter-current separation technology, J. Chromatogr. A 1216 (2009) 4237–4244.

[34] A. Berthod, D.W. Armstrong, Centrifugal partition chromatography. 1. General features, J. Liq. Chromatogr. 11 (1988) 547–566.

[35] A. Berthod, D.W. Armstrong, Centrifugal partition chromatography. 2. Selectivity and efficiency, J. Liq. Chromatogr. 11 (1988) 567–583.

[36] E. Bouju, A. Berthod, K. Faure, Scale-up in centrifugal partition chromatography: the "free-space between peaks" method, J. Chromatogr. A 1409 (2015) 70–78.

[37] K. Hostettmann, A. Marston, Countercurrent chromatography in the preparative separation of plant-derived natural products, J. Liq. Chromatogr. Related Technol. 24 (2001) 1711–1721.

[38] J.S. Jeon, C.L. Park, A.S. Syed, Y.M. Kim, I.J. Cho, C.Y. Kim, Preparative separation of sesamin and sesamolin from defatted sesame meal via centrifugal partition chromatography with consecutive sample injection, J. Chromatogr. B 1011 (2016) 108–113.

[39] Y.F. He, C.X. Ding, X.Y. Wang, H.L. Wang, Y.R. Suo, Using response surface methodology to optimize countercurrent chromatographic separation of polyphenol compounds from Fenugreek (Trigonella foenum-graecum L.) seeds, J. Liq. Chromatogr. Related Technol. 38 (2015) 29–35.

[40] Y.H. Guan, P. Hewitson, R.N.A.M. van den Heuvel, Y. Zhao, R.P.G. Siebers, Y.P. Zhuang, I. Sutherland, Scale-up protein separation on stainless steel wide bore toroidal columns in the type-J counter-current chromatography, J. Chromatogr. A 1424 (2015) 102–110.

[41] X. Tong, T. Zhou, X.H. Xiao, G.K. Li, A consecutive preparation method based upon accelerated solvent extraction and high-speed counter-current chromatography for isolation of aesculin from Cortex fraxinus, J. Sep. Sci. 35 (2012) 3609–3614.

[42] K. He, X.L. Ye, X.G. Li, H.Y. Chen, L.J. Yuan, Y.F. Deng, X. Chen, X.D. Li, Separation of two constituents from purple sweet potato by combination of silica gel column and high-speed counter-current chromatography, J. Chromatogr. B 881–882 (2012) 49–54.

[43] X.L. Cao, Y. Tian, T.Y. Zhang, Y. Ito, Semi-preparative separation and purification of taxol analogs by high-speed countercurrent chromatography, Prep. Biochem. Biotech. 28 (1998) 79–87.

[44] J.-Y. Zhou, Q.-C. Fang, Y.-W. Lee, The application of high-speed counter-current chromatography to the semipreparative separation of vincamine and vincine, Phytochem. Anal. 1 (1990) 74–76.

[45] A.E. Kostanyan, On influence of sample loading conditions on peak shape and separation efficiency in preparative isocratic counter-current chromatography, J. Chromatogr. A 1254 (2012) 71–77.

[46] C.X. Zhao, C.H. He, Sample capacity in preparative high-speed counter-current chromatography, J. Chromatogr. A 1146 (2007) 186–192.

[47] J. Meng, Z. Yang, J.L. Liang, M.Z. Guo, S.H. Wu, Multi-channel recycling counter-current chromatography for natural product isolation: tanshinones as examples, J. Chromatogr. A 1327 (2014) 27–38.

[48] Q. Bin Han, J.Z. Song, C.F. Qiao, L. Wong, H.X. Xu, Preparative separation of gambogic acid and its C-2 epimer using recycling high-speed counter-current chromatography, J. Chromatogr. A 1127 (2006) 298–301.

[49] S.Q. Tong, Y.X. Guan, J.Z. Yan, B. Zheng, L.Y. Zhao, Enantiomeric separation of (R, S)-naproxen by recycling high speed counter-current chromatography with hydroxypropyl-beta-cyclodextrin as chiral selector, J. Chromatogr. A 1218 (2011) 5434–5440.

[50] A.E. Kostanyan, Modeling of closed-loop recycling liquid-liquid chromatography: analytical solutions and model analysis, J. Chromatogr. A 1406 (2015) 156–164.

[51] A.E. Kostanyan, Simple equations to simulate closed-loop recycling liquid-liquid chromatography: ideal and non-ideal recycling models, J. Chromatogr. A 1423 (2015) 71–78.

[52] A.E. Kostanyan, Modeling of preparative closed-loop recycling liquid-liquid chromatography with specified duration of sample loading, J. Chromatogr. A 1471 (2016) 94–101.

[53] A.E. Kostanyan, A.A. Erastov, Theoretical study of closed-loop recycling liquid-liquid chromatography and experimental verification of the theory, J. Chromatogr. A 1462 (2016) 55–62.

[54] A.E. Kostanyan, Theoretical study of separation and concentration of solutes by closed-loop recycling liquid chromatography with multiple sample injection, J. Chromatogr. A 1506 (2017) 82–92.

[55] A. Kostanyan, M. Martynova, A. Erastov, V. Belova, Simultaneous concentration and separation of target compounds from multicomponent mixtures by closed-loop recycling countercurrent chromatography, J. Chromatogr. A 1560 (2018) 26–34.

[56] A.E. Kostanyan, V.V. Belova, Closed-loop recycling dual-mode counter-current chromatography. a theoretical study, J. Chromatogr. A 1588 (2019) 174–179.

[57] Q.Z. Du, C.Q. Ke, Y. Ito, Recycling high-speed countercurrent chromatography for separation of taxol and cephalomannine, J. Liq. Chromatogr. Related Technol. 21 (1998) 157–162.

[58] M. Martin, F. Verillon, C. Eon, G. Guiochon, Theoretical and experimental-study of recycling in high-performance liquid-chromatography, J. Chromatogr. 125 (1976) 17–41.

[59] B. Coq, G. Cretier, J.L. Rocca, J. Vialle, Recycling technique in preparative liquid-chromatography, J. Liq. Chromatogr. 4 (1981) 237–249.

[60] P. Scherpian, G. Schembecker, Scaling-up recycling chromatography, Chem. Eng. Sci. 64 (2009) 4068–4080.

[61] A. Seidel-Morgenstern, G. Guiochon, Theoretical-study of recycling in preparative chromatography, AIChE J. 39 (1993) 809–819.

[62] J. Xie, J. Deng, F. Tan, J. Su, Separation and purification of echinacoside from Pentemon barbatus (Can.) Roth by recycling high-speed counter-current chromatography, J. Chromatogr. B 878 (2010) 2665–2668.

[63] S.Y. Shi, Y.J. Ma, Y.P. Zhang, L.L. Liu, Q. Liu, M.J. Peng, X. Xiong, Systematic separation and purification of 18 antioxidants from Pueraria lobata flower using HSCCC target-guided by DPPH-HPLC experiment, Sep. Purif. Technol. 89 (2012) 225–233.

[64] J.H. Yang, H.Y. Ye, H.J. Lai, S.C. Li, S.C. He, S.J. Zhong, L.J. Chen, A.H. Peng, Separation of anthraquinone compounds from the seed of Cassia obtusifolia L. using recycling counter-current chromatography, J. Sep. Sci. 35 (2012) 256–262.

[65] Q. Liu, H.L. Zeng, S.J. Jiang, L. Zhang, F.Z. Yang, X.Q. Chen, H. Yang, Separation of polyphenols from leaves of Malus hupehensis (Pamp.) Rehder by off-line two-dimensional high speed counter-current chromatography combined with recycling elution mode, Food Chem. 186 (2015) 139–145.

[66] J.M. He, S.Y. Zhang, Q. Mu, Online-storage recycling counter-current chromatography for preparative isolation of naphthaquinones from Arnebia euchroma (Royle) Johnst, J. Chromatogr. A 1464 (2016) 79–86.

[67] V. Belova, Separation and concentration of rare earths by recycling liquid-liquid chromatography with multiple sample injection: a computational study, Russ. J. Inorg. Chem. 63 (2018) 473–478.

[68] A. Berthod, M.J. Ruiz-Angel, S. Carda-Broch, Elution-extrusion countercurrent chromatography. Use of the liquid nature of the stationary phase to extend the hydrophobicity window, Anal. Chem. 75 (2003) 5886–5894.

[69] A. Berthod, M. Hassoun, G. Harris, Using the liquid nature of the stationary phase: the elution-extrusion method, J. Liq. Chromatogr. Related Technol. 28 (2005) 1851–1866.

[70] A. Berthod, J.B. Friesen, T. Inui, G.F. Pauli, Elution-extrusion countercurrent chromatography: theory and concepts in metabolic analysis, Anal. Chem. 79 (2007) 3371–3382.

[71] A. Berthod, Band broadening inside the chromatographic column: the interest of a liquid stationary phase, J. Chromatogr. A 1126 (2006) 347–356.

[72] Y.B. Lu, R. Liu, A. Berthod, Y.J. Pan, Rapid screening of bioactive components from Zingiber cassumunar using elution-extrusion counter-current chromatography, J. Chromatogr. A 1181 (2008) 33–44.

[73] S.C. Li, S.C. He, S.J. Zhong, X.M. Duan, H.Y. Ye, J. Shi, A.H. Peng, L.J. Chen, Elution-extrusion counter-current chromatography separation of five bioactive compounds from Dendrobium chrysototxum Lindl, J. Chromatogr. A 1218 (2011) 3124–3128.

[74] R.L. Hu, Y.B. Lu, X.J. Dai, Y.J. Pan, Screening of antioxidant phenolic compounds in Chinese Rhubarb combining fast counter-current chromatography fractionation and liquid chromatography/mass spectrometry analysis, J. Sep. Sci. 33 (2010) 1595–1603.

[75] J. Bradow, F. Riley, L. Philippe, Q. Yan, B. Schuff, G.H. Harris, Automated solvent system screening for the preparative countercurrent chromatography of pharmaceutical discovery compounds, J. Sep. Sci. 38 (2015) 3983–3991.

[76] Z. Chen, J.B. Wu, W. Shen, P. Liu, Y. Cao, Y.B. Lu, Counter-current chromatographic method for preparative scale isolation of picrosides from traditional Chinese medicine Picrorhiza scrophulariiflora, J. Sep. Sci. 34 (2011) 1910–1916.

[77] D.B. Ren, Y.H. Qin, Y.H. Yun, H.M. Lu, X.Q. Chen, Y.Z. Liang, Separation of nine compounds from Salvia plebeia R.Br. using two-step high-speed counter-current chromatography with different elution modes, J. Sep. Sci. 37 (2014) 2118–2125.

[78] C. Napolitano, M. Wismer, E. Furlano, G. Harris, B. Uhrig, K. Blake, G. Kath, C. Dufresne, An in-house built semiautomated countercurrent chromatography workstation, JALA-J. Assoc. Lab. Aut. 14 (2009) 27–35.

[79] D.F. Wu, X.J. Cao, S.H. Wu, Overlapping elution-extrusion counter-current chromatography: a novel method for efficient purification of natural cytotoxic andrographolides from Andrographis paniculata, J. Chromatogr. A 1223 (2012) 53–63.

[80] H.Y. Ye, S. Ignatova, H.D. Luo, Y.F. Li, A.H. Peng, L.J. Chen, I. Sutherland, Preparative separation of a terpenoid and alkaloids from Tripterygium wilfordii Hook. f. using high-performance counter-current chromatography comparison of various elution and operating strategies, J. Chromatogr. A 1213 (2008) 145–153.

[81] A. Berthod, S. Carda-Broch, Determination of liquid-liquid partition coefficients by separation methods, J. Chromatogr. A 1037 (2004) 3–14.

[82] Y.B. Lu, Y.J. Pan, A. Berthod, Using the liquid nature of the stationary phase in counter-current chromatography. V. The back-extrusion method, J. Chromatogr. A 1189 (2008) 10–18.

[83] Y.B. Lu, W.Y. Ma, R.L. Hu, A. Berthod, Y.J. Pan, Rapid and preparative separation of traditional Chinese medicine Evodia rutaecarpa employing elution-extrusion and back-extrusion counter-current chromatography: comparative study, J. Chromatogr. A 1216 (2009) 4140–4146.

[84] A. Berthod, Y.I. Han, D.W. Armstrong, Centrifugal partition chromatography. 5. Octanol-water partition-coefficients, direct and indirect determination, J. Liq. Chromatogr. 11 (1988) 1441–1456.

[85] R.A. Menges, T.S. Menges, G.L. Bertrand, D.W. Armstrong, L.A. Spino, Extraction of nonionic surfactants from waste-water using centrifugal partition chromatography, J. Liq. Chromatogr. 15 (1992) 2909–2925.

[86] J. Pruvost, J. Legrand, A. Foucault, Method for the intensive extraction of cellular compounds from micro-organisms by continuous culture and extraction, and corresponding device, United States, 2014.

[87] L. Marchal, M. Mojaat-Guemir, A. Foucault, J. Pruvost, Centrifugal partition extraction of beta-carotene from *Dunaliella salina* for efficient and biocompatible recovery of metabolites, Bioresource Technol. 134 (2013) 396–400.

[88] A. Bauer, M. Minceva, Direct extraction of astaxanthin from the microalgae *Haematococcus pluvialis* using liquid-liquid chromatography, RSC Adv. 9 (2019) 22779–22789.

[89] C. Ungureanu, L. Marchal, A.A. Chirvase, A. Foucault, Centrifugal partition extraction, a new method for direct metabolites recovery from culture broth: case study of torularhodin recovery from *Rhodotorula rubra*, Bioresource Technol. 132 (2013) 406–409.

[90] E. Hopmann, J. Goll, M. Minceva, Sequential centrifugal partition chromatography: a new continuous chromatographic technology, Chem. Eng. Technol. 35 (2012) 72–82.

[91] M. Englert, S. Hammann, W. Vetter, Isolation of beta-carotene, alpha-carotene and lutein from carrots by countercurrent chromatography with the solvent system modifier benzotrifluoride, J. Chromatogr. A 1388 (2015) 119–125.

[92] J. Li, X.Y. Zhang, Q. Yu, X.H. Fu, W.N. Wang, One-Step separation of four flavonoids from Herba Salviae Plbeiae by HSCCC, J. Chromatogr. Sci. 52 (2014) 1288–1293.

[93] J.S. Jeon, C.Y. Kim, Preparative separation and purification of flavonoids and stilbenoids from *Parthenocissus tricuspidata* stems by dual-mode centrifugal partition chromatography, Sep. Purif. Technol. 105 (2013) 1–7.

[94] A. Angelis, A. Urbain, M. Halabalaki, N. Aligiannis, A.L. Skaltsounis, One-step isolation of gamma-oryzanol from rice bran oil by non-aqueous hydrostatic countercurrent chromatography, J. Sep. Sci. 34 (2011) 2528–2537.

[95] H.B. Li, F. Chen, Separation and purification of Epimedin A, B, C, and Icariin from the medicinal herb *Epimedium brevicornum* maxim by dual-mode HSCCC, J. Chromatogr. Sci. 47 (2009) 337–340.

[96] C.X. Zhao, C.H. He, Preparative isolation and purification of atractylon and atractylenolide III from the Chinese medicinal plant *Atractylodes macrocephala* by high-speed counter-current chromatography, J. Sep. Sci. 29 (2006) 1630–1636.

[97] A. Berthod, B. Billardello, S. Geoffroy, Polyphenols in countercurrent chromatography. An example of large scale separation, Analusis 27 (1999) 750–757.

[98] M. Agnely, D. Thiebaut, Dual-mode high-speed counter-current chromatography: retention, resolution and examples, J. Chromatogr. A 790 (1997) 17–30.

[99] N. Mekaoui, A. Berthod, Using the liquid nature of the stationary phase. VI. Theoretical study of multi-dual mode countercurrent chromatography, J. Chromatogr. A 1218 (2011) 6061–6071.

[100] M.J. Ruiz-Angel, V. Pino, S. Carda-Broch, A. Berthod, Solvent systems for countercurrent chromatography: an aqueous two phase liquid system based on a room temperature ionic liquid, J. Chromatogr. A 1151 (2007) 65–73.

[101] K.A. Alvi, Screening natural products: bioassay-directed isolation of active components by dual-mode CCC, J. Liq. Chromatogr. Related Technol. 24 (2001) 1765–1773.

[102] R.A. Menges, G.L. Bertrand, D.W. Armstrong, Direct measurement of octanol-water partition-coefficients using centrifugal partition chromatography with a back-flushing technique, J. Liq. Chromatogr. 13 (1990) 3061–3077.

[103] S.J. Gluck, E.J. Martin, Extended octanol-water partition-coefficient determination by dual-mode centrifugal partition chromatography, J. Liq. Chromatogr. 13 (1990) 3559–3570.

[104] E. Delannay, A. Toribio, L. Boudesocque, J.M. Nuzillard, M. Zeches-Hanrot, E. Dardennes, G. Le Dour, J. Sapi, J.H. Renault, Multiple dual-mode centrifugal partition chromatography, a semi-continuous development mode for routine laboratory-scale purifications, J. Chromatogr. A 1127 (2006) 45–51.

[105] C. Roullier, M. Chollet-Krugler, A. Bernard, J. Boustie, Multiple dual-mode centrifugal partition chromatography as an efficient method for the purification of a mycosporine from a crude methanolic extract of *Lichina pygmaea*, J. Chromatogr. B 877 (2009) 2067–2073.

[106] N. Rubio, S. Ignatova, C. Minguillon, I.A. Sutherland, Multiple dual–mode countercurrent chromatography applied to chiral separations using a (S)-naproxen derivative as chiral selector, J. Chromatogr. A 1216 (2009) 8505–8511.

[107] Y. Yang, H.A. Aisa, Y. Ito, Mathematical model of computer-programmed intermittent dual countercurrent chromatography applied to hydrostatic and hydrodynamic equilibrium systems, J. Chromatogr. A 1216 (2009) 6310–6318.

[108] S.Q. Tong, Y. Zheng, J.Z. Yan, Enantioseparation of chiral aromatic acids by multiple dual mode counter-current chromatography using hydroxypropyl—cyclodextrin as chiral selector, J. Sep. Sci. 36 (2013) 2035–2042.

[109] A.E. Kostanyan, Multiple dual mode counter-current chromatography with periodic sample injection: steady-state and non-steady-state operation, J. Chromatogr. A 1373 (2014) 81–89.

[110] A.E. Kostanyan, A.A. Erastov, O.N. Shishilov, Multiple dual mode counter-current chromatography with variable duration of alternating phase elution steps, J. Chromatogr. A 1347 (2014) 87–95.

[111] A.E. Kostanyan, A.A. Erastov, Steady state preparative multiple dual mode counter-current chromatography: productivity and selectivity. Theory and experimental verification, J. Chromatogr. A 1406 (2015) 118–128.

[112] P. Hewitson, S. Ignatova, H.Y. Ye, L.J. Chen, I. Sutherland, Intermittent counter-current extraction as an alternative approach to purification of Chinese herbal medicine, J. Chromatogr. A 1216 (2009) 4187–4192.

[113] A.E. Kostanyan, S.N. Ignatova, I.A. Sutherland, P. Hewitson, Y.A. Zakhodjaeva, A.A. Erastov, Steady-state and non-steady state operation of counter-current chromatography devices, J. Chromatogr. A 1314 (2013) 94–105.

[114] N. Mekaoui, J. Chamieh, V. Dugas, C. Demesmay, A. Berthod, Purification of Coomassie Brilliant Blue G-250 by multiple dual mode countercurrent chromatography, J. Chromatogr. A 1232 (2012) 134–141.

[115] S. Ignatova, P. Hewitson, B. Mathews, I. Sutherland, Evaluation of dual flow counter-current chromatography and intermittent counter-current extraction, J. Chromatogr. A 1218 (2011) 6102–6106.

[116] J. Goll, R. Morley, M. Minceva, Trapping multiple dual mode centrifugal partition chromatography for the separation of intermediately-eluting components: operating parameter selection, J. Chromatogr. A 1496 (2017) 68–79.

[117] R. Morley, M. Minceva, Trapping multiple dual mode centrifugal partition chromatography for the separation of intermediately-eluting components: throughput maximization strategy, J. Chromatogr. A 1501 (2017) 26–38.

[118] R.M. Morley, M. Minceva, Operating mode selection for the separation of intermediately-eluting components with countercurrent and centrifugal partition chromatography, J. Chromatogr. A (2019).

[119] F. Couillard, A. Foucault, D. Durand, Method and Device for Separating Constituents of a Liquid Charge By Means of Liquid-Liquid Centrifuge Chromatography, U.S.P.a.T. Office (Ed.), Institut Francais du Petrole Couillard, F., USA, 2008.

[120] E. Hopmann, M. Minceva, Separation of a binary mixture by sequential centrifugal partition chromatography, J. Chromatogr. A 1229 (2012) 140–147.

[121] J. Goll, A. Frey, M. Minceva, Study of the separation limits of continuous solid support free liquid-liquid chromatography: separation of capsaicin and dihydrocapsaicin by centrifugal partition chromatography, J. Chromatogr. A 1284 (2013) 59–68.

[122] I. Sutherland, P. Hewitson, S. Ignatova, Scale-up of counter-current chromatography: demonstration of predictable isocratic and quasi-continuous operating modes from the test tube to pilot/process scale, J. Chromatogr. A 1216 (2009) 8787–8792.

[123] A.H. Peng, H.Y. Ye, J. Shi, S.C. He, S.J. Zhong, S.C. Li, L.J. Chen, Separation of honokiol and magnolol by intermittent counter-current extraction, J. Chromatogr. A 1217 (2010) 5935–5939.

[124] P. Hewitson, S. Ignatova, I. Sutherland, Intermittent counter-current extraction—effect of the key operating parameters on selectivity and throughput, J. Chromatogr. A 1218 (2011) 6072–6078.

[125] P. Hewitson, I. Sutherland, A.E. Kostanyan, A.A. Voshkin, S. Ignatova, Intermittent counter-current extraction—equilibrium cell model, scaling and an improved bobbin design, J. Chromatogr. A 1303 (2013) 18–27.

[126] J. Volkl, W. Arlt, M. Minceva, Theoretical study of sequential centrifugal partition chromatography, AlchE J. 59 (2013) 241–249.

152

Appendix D. Assumptions, boundary and initial conditions, equilibrium stage model

Model assumptions [71]:

- The two columns are identical

- The off-column volume is negligible

- The volumes of the two liquid phases is equal in all stages in both columns (same S_f)

- The phase volumes of the upper and lower phases remain independent of the current elution mode and constant (no stationary phase loss); the phase roles are instantaneously reversed when switching from one elution mode to the next

- The partition coefficients are independent of the solute concentration (linear chromatography assumption)

- The theoretical stage numbers are equivalent in the As and Des elution modes $(N_{As,k} = N_{Des,k} = N_k)$

Table D1. Initial and boundary conditions for the equilibrium stage model (batch injection).

Process stage	Ascending mode (As)	Descending mode (Des)
All	$F^L = 0$	$F^U = 0$
Before injection $t = 0$	$c_{k,i} = 0$	$c_{k,i} = 0$
During injection $t \in [0, t_{inj}]$	$F^U = F$ $c_{k,in}^U = c_k^{U,feed}$	$F^L = F$ $c_{k,in}^L = c_k^{L,feed}$
During elution $t \in [t_{inj}, t_{end}]$	$F^U = F$ $c_{k,in}^U = 0$	$F^L = F$ $c_{k,in}^L = 0$

References

[1] Y. Ito, Countercurrent chromatography, Journal of biochemical and biophysical methods, 5 (1981) 105-129.

[2] A. Berthod, Countercurrent chromatography and the Journal of Liquid Chromatography: a love story, Journal of liquid chromatography & related technologies, 30 (2007) 1447-1463.

[3] A. Berthod, M.J. Ruiz-Angel, S. Carda-Broch, Elution− extrusion countercurrent chromatography. Use of the liquid nature of the stationary phase to extend the hydrophobicity window, Analytical chemistry, 75 (2003) 5886-5894.

[4] M. Agnely, D. Thiebaut, Dual-mode high-speed counter-current chromatography: retention, resolution and examples, J. Chromatogr. A, 790 (1997) 17-30.

[5] N. Mekaoui, A. Berthod, Using the liquid nature of the stationary phase. VI. Theoretical study of multi-dual mode countercurrent chromatography, J. Chromatogr. A, 1218 (2011) 6061-6071.

[6] P. Hewitson, S. Ignatova, H. Ye, L. Chen, I. Sutherland, Intermittent counter-current extraction as an alternative approach to purification of Chinese herbal medicine, J. Chromatogr. A, 1216 (2009) 4187-4192.

[7] S. Adelmann, G. Schembecker, Influence of physical properties and operating parameters on hydrodynamics in Centrifugal Partition Chromatography, J. Chromatogr. A, 1218 (2011) 5401-5413.

[8] A. Fromme, F. Funke, J. Merz, G. Schembecker, Correlating physical properties of aqueous-organic solvent systems and stationary phase retention in a centrifugal partition chromatograph in descending mode, J. Chromatogr. A, 1615 (2020) 460742.

[9] S. Adelmann, C. Schwienheer, G. Schembecker, Multiphase flow modeling in centrifugal partition chromatography, J. Chromatogr. A, 1218 (2011) 6092-6101.

[10] J. Goll, G. Audo, M. Minceva, Comparison of twin-cell centrifugal partition chromatographic columns with different cell volume, J. Chromatogr. A, 1406 (2015) 129-135.

[11] S. Roehrer, M. Minceva, Influence of temperature on the separation performance in solid support-free liquid-liquid chromatography, J. Chromatogr. A, 1594 (2019) 129-139.

[12] A. Berthod, B. Billardello, S. Geoffroy, Polyphenols in countercurrent chromatography. An example of large scale separation, Analusis, 27 (1999) 750-757.

[13] A. Peng, P. Hewitson, H. Ye, L. Zu, I. Garrard, I. Sutherland, L. Chen, S. Ignatova, Sample injection strategy to increase throughput in counter-current chromatography: Case study of Honokiol purification, J. Chromatogr. A, 1476 (2016) 19-24.

[14] L. Marchal, O. Intes, A. Foucault, J. Legrand, J.-M. Nuzillard, J.-H. Renault, Rational improvement of centrifugal partition chromatographic settings for the production of 5-n-alkylresorcinols from wheat bran lipid extract: I. Flooding conditions—optimizing the injection step, J. Chromatogr. A, 1005 (2003) 51-62.

[15] N. Amarouche, L. Boudesocque, C. Sayagh, M. Giraud, J. McGarrity, A. Butte, L. Marchal, A. Foucault, J.-H. Renault, Purification of a modified cyclosporine A by co-current centrifugal partition chromatography: Process development and intensification, J. Chromatogr. A, 1311 (2013) 72-78.

[16] J.B. Friesen, J.B. McAlpine, S.-N. Chen, G.F. Pauli, Countercurrent separation of natural products: an update, Journal of natural products, 78 (2015) 1765-1796.

[17] G.F. Pauli, S.M. Pro, J.B. Friesen, Countercurrent separation of natural products, Journal of natural products, 71 (2008) 1489-1508.

[18] E. Hopmann, M. Minceva, Separation of a binary mixture by sequential centrifugal partition chromatography, J. Chromatogr. A, 1229 (2012) 140-147.

[19] E. Hopmann, J. Goll, M. Minceva, Sequential centrifugal partition chromatography: a new continuous chromatographic technology, Chemical engineering & technology, 35 (2012) 72-82.

[20] J. Goll, M. Minceva, Continuous fractionation of multicomponent mixtures with sequential centrifugal partition chromatography, AIChE Journal, 63 (2017) 1659-1673.

[21] F. Wang, Y. Ito, Y. Wei, Recent progress on countercurrent chromatography modeling, Journal of liquid chromatography & related technologies, 38 (2015) 415-421.

[22] J. Brent Friesen, G.F. Pauli, GUESS—a generally useful estimate of solvent systems for CCC, Journal of liquid chromatography & related technologies, 28 (2005) 2777-2806.

[23] A.P. Foucault, Centrifugal Partition Chromatography, Taylor & Francis, 1994.

[24] Y. Ito, Golden rules and pitfalls in selecting optimum conditions for high-speed counter-current chromatography, J. Chromatogr. A, 1065 (2005) 145-168.

[25] J.M. Prausnitz, R.N. Lichtenthaler, E.G. De Azevedo, Molecular thermodynamics of fluid-phase equilibria, Pearson Education, 1998.

[26] A. Berthod, Separation with a liquid stationary phase: the countercurrent chromatography technique, Instrumentation science & technology, 23 (1995) 75-89.

[27] H. Schmidt-Traub, M. Schulte, A. Seidel-Morgenstern, Preparative chromatography, Wiley Online Library, 2012.

[28] W. Murayama, T. Kobayashi, Y. Kosuge, H. Yano, Y. Nunogaki, K. Nunogaki, A new centrifugal counter-current chromatograph and its application, J. Chromatogr. A, 239 (1982) 643-649.

[29] Kromaton - Fast Centrifugal Partition Chromatography, in, 2020.

[30] Product Guide, in: G. Corporation (Ed.), 2020.

[31] RotaChrom - Perpetual Innovation, in, 2020.

[32] A. Berthod, J.B. Friesen, T. Inui, G.F. Pauli, Elution− extrusion countercurrent chromatography: theory and concepts in metabolic analysis, Analytical chemistry, 79 (2007) 3371-3382.

[33] Z. Chen, J. Wu, W. Shen, P. Liu, Y. Cao, Y. Lu, Counter-current chromatographic method for preparative scale isolation of picrosides from traditional Chinese medicine Picrorhiza scrophulariiflora, Journal of separation science, 34 (2011) 1910-1916.

[34] S. Li, S. He, S. Zhong, X. Duan, H. Ye, J. Shi, A. Peng, L. Chen, Elution–extrusion counter-current chromatography separation of five bioactive compounds from Dendrobium chrysototxum Lindl, J. Chromatogr. A, 1218 (2011) 3124-3128.

[35] X. Cao, Y. Tian, T.Y. Zhang, Y. Ito, Semi-preparative separation and purification of taxol analogs by high-speed countercurrent chromatography, Preparative biochemistry & biotechnology, 28 (1998) 79-87.

[36] J.-S. Jeon, C.L. Park, A.S. Syed, Y.-M. Kim, I.J. Cho, C.Y. Kim, Preparative separation of sesamin and sesamolin from defatted sesame meal via centrifugal partition chromatography with consecutive sample injection, Journal of Chromatography B, 1011 (2016) 108-113.

[37] J.Y. Zhou, Q.C. Fang, Y.W. Lee, The application of high-speed countercurrent chromatography to the semipreparative separation of vincamine and vincine, Phytochemical Analysis, 1 (1990) 74-76.

[38] S. Tong, Y.-X. Guan, J. Yan, B. Zheng, L. Zhao, Enantiomeric separation of (R, S)-naproxen by recycling high speed counter-current chromatography with hydroxypropyl-β-cyclodextrin as chiral selector, J. Chromatogr. A, 1218 (2011) 5434-5440.

[39] J. Xie, J. Deng, F. Tan, J. Su, Separation and purification of echinacoside from Penstemon barbatus (Can.) Roth by recycling high-speed counter-current chromatography, Journal of Chromatography B, 878 (2010) 2665-2668.

[40] J. Yang, H. Ye, H. Lai, S. Li, S. He, S. Zhong, L. Chen, A. Peng, Separation of anthraquinone compounds from the seed of Cassia obtusifolia L. using recycling counter-current chromatography, Journal of separation science, 35 (2012) 256-262.

[41] F. Yang, J. Quan, T.Y. Zhang, Y. Ito, Multidimensional counter-current chromatographic system and its application, J. Chromatogr. A, 803 (1998) 298-301.

[42] Q. Liu, H. Zeng, S. Jiang, L. Zhang, F. Yang, X. Chen, H. Yang, Separation of polyphenols from leaves of Malus hupehensis (Pamp.) Rehder by off-line two-dimensional High Speed Counter-Current Chromatography combined with recycling elution mode, Food Chemistry, 186 (2015) 139-145.

[43] M. Müller, M. Murić, L. Glanz, W. Vetter, Improving the resolution of overlapping peaks by heartcut two-dimensional countercurrent chromatography with the same solvent system in both dimensions, J. Chromatogr. A, 1596 (2019) 142-151.

[44] G. Tian, T. Zhang, Y. Zhang, Y. Ito, Separation of tanshinones from Salvia miltiorrhiza Bunge by multidimensional counter-current chromatography, J. Chromatogr. A, 945 (2002) 281-285.

[45] Y. Wei, Y. Ito, Preparative isolation of imperatorin, oxypeucedanin and isoimperatorin from traditional Chinese herb "bai zhi" Angelica dahurica (Fisch. ex Hoffm) Benth. et Hook using multidimensional high-speed counter-current chromatography, J. Chromatogr. A, 1115 (2006) 112-117.

[46] M. Englert, L. Brown, W. Vetter, Heart-cut two-dimensional countercurrent chromatography with a single instrument, Analytical chemistry, 87 (2015) 10172-10177.

[47] N. Mekaoui, J. Chamieh, V. Dugas, C. Demesmay, A. Berthod, Purification of Coomassie Brilliant Blue G-250 by multiple dual mode countercurrent chromatography, J. Chromatogr. A, 1232 (2012) 134-141.

[48] S. Ignatova, P. Hewitson, B. Mathews, I. Sutherland, Evaluation of dual flow counter-current chromatography and intermittent counter-current extraction, J. Chromatogr. A, 1218 (2011) 6102-6106.

[49] J.C. Dearden, G.M. Bresnen, The measurement of partition coefficients, Quantitative Structure-Activity Relationships, 7 (1988) 133-144.

[50] A. Berthod, D.W. Armstrong, Centrifugal partition chromatography. VI. Temperature effects, Journal of liquid chromatography, 11 (1988) 1457-1474.

[51] Y. Wei, F. Wang, S. Wang, Y. Zhang, Modelling counter-current chromatography using a temperature dependence plate model, Journal of Chromatography B, 933 (2013) 30-36.

[52] S. Adelmann, T. Baldhoff, B. Koepcke, G. Schembecker, Selection of operating parameters on the basis of hydrodynamics in centrifugal partition chromatography for the purification of nybomycin derivatives, J. Chromatogr. A, 1274 (2013) 54-64.

[53] A.J. Martin, R.L. Synge, A new form of chromatogram employing two liquid phases: A theory of chromatography. 2. Application to the micro-determination of the higher monoamino-acids in proteins, Biochemical Journal, 35 (1941) 1358-1368.

[54] R.-M. Nicoud, Chromatographic Processes, Cambridge University Press, 2015.

[55] Y. Ito, Toroidal coil planet centrifuge for counter-current chromatography, J. Chromatogr. A, 192 (1980) 75-87.

[56] C.-X. Zhao, C.-H. He, Sample capacity in preparative high-speed counter-current chromatography, J. Chromatogr. A, 1146 (2007) 186-192.

[57] A. Weisz, A.J. Langowski, M.B. Meyers, M.A. Thieken, Y. Ito, Preparative purification of tetrabromotetrachlorofluorescein and phloxine B by centrifugal counter-current chromatography, J. Chromatogr. A, 538 (1991) 157-164.

[58] A. Fromme, C. Fischer, D. Klump, G. Schembecker, Correlating the phase settling behavior of aqueous-organic solvent systems in a centrifugal partition chromatograph, J. Chromatogr. A, (2020) 461005.

[59] C. Schwienheer, J. Merz, G. Schembecker, Investigation, comparison and design of chambers used in centrifugal partition chromatography on the basis of flow pattern and separation experiments, J. Chromatogr. A, 1390 (2015) 39-49.

[60] A. Berthod, Countercurrent chromatography, Elsevier, 2002.

[61] L. Marchal, J. Legrand, A. Foucault, Mass transport and flow regimes in centrifugal partition chromatography, AIChE journal, 48 (2002) 1692-1704.

[62] M. Van Buel, L. Van der Wielen, K.C.A. Luyben, Effluent concentration profiles in centrifugal partition chromatography, AIChE journal, 43 (1997) 693-702.

[63] C. Schwienheer, J. Krause, G. Schembecker, J. Merz, Modelling centrifugal partition chromatography separation behavior to characterize influencing hydrodynamic effects on separation efficiency, J. Chromatogr. A, 1492 (2017) 27-40.

[64] M. Van Buel, F. Van Halsema, L. Van der Wielen, K.C.A. Luyben, Flow regimes in centrifugal partition chromatography, AIChE journal, 44 (1998) 1356-1362.

[65] S. Roehrer, M. Minceva, Characterization of a centrifugal partition chromatographic column with spherical cell design, Chemical Engineering Research and Design, 143 (2019) 180-189.

[66] D.W. Armstrong, G.L. Bertrand, A. Berthod, Study of the origin and mechanism of band broadening and pressure drop in centrifugal countercurrent chromatography, Analytical chemistry, 60 (1988) 2513-2519.

[67] M.J. van Buel, L.A. van der Wielen, K.C.A. Luyben, Pressure drop in centrifugal partition chromatography, J. Chromatogr. A, 773 (1997) 1-12.

[68] T. Maryutina, S. Ignatova, B.Y. Spivakov, I. Sutherland, The efficiency of substance separation in countercurrent liquid chromatography, Journal of Analytical Chemistry, 58 (2003) 762-767.

[69] N. Fumat, A. Berthod, K. Faure, Effect of operating parameters on a centrifugal partition chromatography separation, J. Chromatogr. A, 1474 (2016) 47-58.

[70] A. Foucault, E.C. Frias, C. Bordier, F.L. Goffic, Centrifugal Partition Chromatography: Stability of Various Biphasic Systems and Pertinence of the "Stoke's Model" to Describe the Influence of the Centrifugal Field Upon the Efficiency, Journal of Liquid Chromatography & Related Technologies, 17 (1994) 1-17.

[71] J. Völkl, W. Arlt, M. Minceva, Theoretical study of sequential centrifugal partition chromatography, AIChE Journal, 59 (2013) 241-249.

[72] A. Kostanian, Modelling counter-current chromatography: a chemical engineering perspective, J. Chromatogr. A, 973 (2002) 39-46.

[73] A. Kostanyan, General regularities of liquid chromatography and countercurrent extraction, Theoretical Foundations of Chemical Engineering, 40 (2006).

[74] A.E. Kostanyan, Modeling of preparative closed-loop recycling liquid-liquid chromatography with specified duration of sample loading, J. Chromatogr. A, 1471 (2016) 94-101.

[75] A.E. Kostanyan, Multiple dual mode counter-current chromatography with periodic sample injection: Steady-state and non-steady-state operation, J. Chromatogr. A, 1373 (2014) 81-89.

[76] G. Storti, R. Baciocchi, M. Mazzotti, M. Morbidelli, Design of optimal operating conditions of simulated moving bed adsorptive separation units, Industrial & engineering chemistry research, 34 (1995) 288-301.

[77] A. Rajendran, G. Paredes, M. Mazzotti, Simulated moving bed chromatography for the separation of enantiomers, J. Chromatogr. A, 1216 (2009) 709-738.

[78] C. Migliorini, M. Mazzotti, M. Morbidelli, Continuous chromatographic separation through simulated moving beds under linear and nonlinear conditions, J. Chromatogr. A, 827 (1998) 161-173.

[79] G. Guiochon, A. Felinger, D.G. Shirazi, Fundamentals of preparative and nonlinear chromatography, Elsevier, 2006.

[80] P. Hewitson, I. Sutherland, A.E. Kostanyan, A.A. Voshkin, S. Ignatova, Intermittent counter-current extraction—equilibrium cell model, scaling and an improved bobbin design, J. Chromatogr. A, 1303 (2013) 18-27.

[81] A.E. Kostanyan, On influence of sample loading conditions on peak shape and separation efficiency in preparative isocratic counter-current chromatography, J. Chromatogr. A, 1254 (2012) 71-77.

[82] A. Fromme, C. Fischer, K. Keine, G. Schembecker, Characterization and correlation of mobile phase dispersion of aqueous-organic solvent systems in centrifugal partition chromatography, J. Chromatogr. A, (2020) 460990.

[83] E. Bouju, A. Berthod, K. Faure, Scale-up in centrifugal partition chromatography: The "free-space between peaks" method, J. Chromatogr. A, 1409 (2015) 70-78.

[84] Y. Lu, A. Berthod, R. Hu, W. Ma, Y. Pan, Screening of complex natural extracts by countercurrent chromatography using a parallel protocol, Analytical chemistry, 81 (2009) 4048-4059.

[85] J.B. Friesen, G.F. Pauli, Performance characteristics of countercurrent separation in analysis of natural products of agricultural significance, Journal of agricultural and food chemistry, 56 (2008) 19-28.

[86] J. Liang, J. Meng, D. Wu, M. Guo, S. Wu, A novel 9× 9 map-based solvent selection strategy for targeted counter-current chromatography isolation of natural products, J. Chromatogr. A, 1400 (2015) 27-39.

[87] A. Frey, E. Hopmann, M. Minceva, Selection of Biphasic Liquid Systems in Liquid-Liquid Chromatography Using Predictive Thermodynamic Models, Chemical Engineering & Technology, 37 (2014) 1663-1674.

[88] E. Hopmann, W. Arlt, M. Minceva, Solvent system selection in counter-current chromatography using conductor-like screening model for real solvents, J. Chromatogr. A, 1218 (2011) 242-250.

[89] Z. Li, Y. Zhou, F. Chen, L. Zhang, Y. Yang, Property calculation and prediction for selecting solvent systems in CCC, Journal of liquid chromatography & related technologies, 26 (2003) 1397-1415.

[90] F. Oka, H. Oka, Y. Ito, Systematic search for suitable two-phase solvent systems for high-speed counter-current chromatography, J. Chromatogr. A, 538 (1991) 99-108.

[91] M. Henschke, L.H. Schlieper, A. Pfennig, Determination of a coalescence parameter from batch-settling experiments, Chemical Engineering Journal, 85 (2002) 369-378.

[92] W. Aleem, N. Mellon, Experimental study on the effect of parameters on sedimentation and coalescing profiles in liquid-liquid batch settler, Procedia engineering, 148 (2016) 887-895.

[93] Y. Shan, A. Seidel-Morgenstern, Analysis of the isolation of a target component using multicomponent isocratic preparative elution chromatography, J. Chromatogr. A, 1041 (2004) 53-62.

[94] L. Marchal, A. Foucault, G. Patissier, J. Rosant, J. Legrand, Influence of flow patterns on chromatographic efficiency in centrifugal partition chromatography, J. Chromatogr. A, 869 (2000) 339-352.

[95] E. Rundquist, C. Pink, E. Vilminot, A. Livingston, Facilitating the use of counter-current chromatography in pharmaceutical purification through use of organic solvent nanofiltration, J. Chromatogr. A, 1229 (2012) 156-163.

[96] P. Marchetti, M.F. Jimenez Solomon, G. Szekely, A.G. Livingston, Molecular separation with organic solvent nanofiltration: a critical review, Chemical reviews, 114 (2014) 10735-10806.

[97] M.N. Sovilj, B.G. Nikolovski, M.Đ. Spasojević, Hydrodynamics in spray and packed liquid-liquid extraction columns: A review, Macedonian Journal of Chemistry and Chemical Engineering, 38 (2019) 267-282.

[98] O. Weinstein, R. Semiat, D. Lewin, Modeling, simulation and control of liquid-liquid extraction columns, Chemical Engineering Science, 53 (1998) 325-339.

[99] J. Joshi, K. Nandakumar, Computational modeling of multiphase reactors, (2015).

[100] G.F. Pauli, S.M. Pro, L.R. Chadwick, T. Burdick, L. Pro, W. Friedl, N. Novak, J. Maltby, F. Qiu, J.B. Friesen, Real-time volumetric phase monitoring: advancing chemical analysis by countercurrent separation, Analytical chemistry, 87 (2015) 7418-7425.

[101] T. Michel, E. Destandau, C. Elfakir, New advances in countercurrent chromatography and centrifugal partition chromatography: focus on coupling strategy, Analytical and bioanalytical chemistry, 406 (2014) 957-969.

[102] K. Binnemans, P.T. Jones, B. Blanpain, T. Van Gerven, Y. Pontikes, Towards zero-waste valorisation of rare-earth-containing industrial process residues: a critical review, Journal of Cleaner Production, 99 (2015) 17-38.

[103] V. Belova, On rare metal separation by counter-current extraction in chromatography mode, Russian Journal of Inorganic Chemistry, 61 (2016) 1601-1608.

[104] P.S. Fedotov, UNTRADITIONAL APPLICATIONS OF COUNTERCURRENT CHROMATOGRAPHY, Journal of Liquid Chromatography & Related Technologies, 25 (2002) 2065-2078.

[105] K. Hennebrüder, W. Engewald, H.-J. Stärk, R. Wennrich, Enrichment of rare-earth elements (REE) and Gd-DTPA in surface water samples by means of countercurrent chromatography (CCC), Analytica chimica acta, 542 (2005) 216-221.

[106] E. Kitazume, M. Bhatnagar, Y. Ito, Separation of rare earth elements by high-speed counter-current chromatography, J. Chromatogr. A, 538 (1991) 133-140.

[107] N. Mirabella, V. Castellani, S. Sala, Current options for the valorization of food manufacturing waste: a review, Journal of Cleaner Production, 65 (2014) 28-41.

[108] R.C. Fierascu, I. Fierascu, S.M. Avramescu, E. Sieniawska, Recovery of natural antioxidants from agro-industrial side streams through advanced extraction techniques, Molecules, 24 (2019) 4212.